TE
662
.A3
no.
FHWA-
RD-
76-180

Report No. FHWA-RD-76-180

SELECTED WIND AND BRIDGE MOTION DATA RECORDED AT LONG-SPAN BRIDGE SITES

Dept. of Transportation
MAR 10 1977
Library

August 1976
Annual Report

This document is available to the public through the National Technical Information Service, Springfield, Virginia 22161

Prepared for
FEDERAL HIGHWAY ADMINISTRATION
Offices of Research & Development
Washington, D.C. 20590

DISCLAIMER NOTICE

This document is disseminated under the sponsorship of the Department of Transportation in the interest of information exchange. The United States Government assumes no liability for its contents or use thereof.

The contents of this report reflect the views of the authors, who are responsible for the facts and the accuracy of the data presented herein. The contents do not necessarily reflect the official views or policy of the Department of Transportation.

This report does not constitute a standard, specification, or regulation.

FHWA DISTRIBUTION NOTICE

A limited number of copies of this report describing research methodology and preliminary findings are being distributed by memorandum to appropriate members of the research community.

E 662 A3 no. FHWA-RD-76-180

TECHNICAL REPORT STANDARD TITLE PAGE

1. Report No.	2. Government Accession No.	3. Recipient's Cotolog No.
FHWA-RD-76-180		

4. Title ond Subtitle	5. Report Dote
SELECTED WIND AND BRIDGE MOTION DATA RECORDED AT LONG-SPAN BRIDGE SITES	August 1976
	6. Performing Orgonizotion Code
7. Author(s)	8. Performing Organizotion Report No.
C.L. Gerhardt, D.D. Nelson, and D.M. Greene	
9. Performing Organizotion Nome ond Address	10. Work Unit No.
Systems Technology Associates, Inc. 2990 Telestar Court Falls Church, VA 22042	FCP 35A1012
	11. Contract or Grant No.
	DOT-FH-11-7769
	13. Type of Report ond Period Covered
12. Sponsoring Agency Nome ond Address	Annual Report July 1975 through June 1976
Offices of Research and Development Federal Highway Administration U.S. Department of Transportation Washington, D.C. 20590	14. Sponsoring Agency Code
	S0585

15. Supplementary Notes

FHWA contract manager: R.H. Gade (HRS-11)

16. Abstract

Wind velocity and bridge motion data recorded at two long-span bridge sites are presented. Methods of data reduction are specified, and detailed and summary data are included. Wind velocity spectra are compared to theoretical models. Bridge motion data are shown as acceleration spectra and acceleration time histories. A project chronology and data base summary are also included.

Dept. of Transportation
MAR 10 1977
Library

17. Key Words	18. Distribution Stotement
Wind, Bridge motion, Long-span bridge, Data reduction, Frequency spectrum	No restrictions. This document is available to the public through the National Technical Information Service, Springfield, VA 22161

19. Security Classif. (of this report)	20. Security Classif. (of this poge)	21. No. of Pages	22. Price
Unclassified	Unclassified	151	

Form DOT F 1700.7 (8-69)

TABLE OF CONTENTS

		Page
1.	INTRODUCTION	1
	1.1 DATA ACQUISITION SYSTEM	1
	1.2 DATA REDUCTION	6
2.	WIND DATA	9
	2.1 PROCESSING APPROACH	12
	2.1.1 Interpolation of Discontinuous Data	14
	2.1.2 Correction for Anemometer Response Characteristics	16
	2.1.3 Correlation of Data with Theoretical Models	19
	2.2 NEWPORT - AUGUST 1971	23
	2.3 NEWPORT - JANUARY 1972	32
	2.4 SITKA - NOVEMBER 1975	37
	2.5 SITKA - MAY 1976	39
3.	BRIDGE MOTION DATA	41
	3.1 PROCESSING APPROACH	41
	3.1.1 Calculation of Damping Factors	43
	3.2 SITKA - DECEMBER 1975	44
4.	SUMMARY AND PLANS	48
REFERENCES		53
APPENDICES:		
	A. CHRONOLOGY OF SIGNIFICANT PROJECT EVENTS	55
	B. DATA BASE SUMMARY	59
	C. INDIVIDUAL CHANNEL WIND SPECTRA: NEWPORT, AUGUST 1971	66

TABLE OF CONTENTS (continued)

		Page
D.	INDIVIDUAL CHANNEL WIND SPECTRA: NEWPORT, JANUARY 1972	99
E.	INDIVIDUAL CHANNEL WIND SPECTRA: SITKA, NOVEMBER 1975	116
F.	INDIVIDUAL CHANNEL WIND SPECTRA: SITKA, MAY 1975	121
G.	INDIVIDUAL CHANNEL ACCELERATION SPECTRA: SITKA, DECEMBER 1975	126

LIST OF ILLUSTRATIONS

Figure		Page
1.	Geographic locations of bridge sites	2
2.	Narragansett Bay bridge, Newport, Rhode Island	3
3.	Sitka Harbor bridge, Sitka, Alaska	3
4.	Instrumentation configuration - Newport	4
5.	Instrumentation configuration - Sitka	5
6.	Data acquisition system block diagram	7
7.	Example tape summary program statistical summary	10
8.	Example MODE3D program display	11
9.	Functional processing sequence for wind data	13
10.	Example plot format of wind spectrum	14
11.	Recording system data discontinuities	15
12.	Anemometer response vs. wind angle (15 cm propeller)	18
13.	Angle of attack vs. wind velocity at individual sensor locations (Newport, August 1971)	23
14.	Five-channel average horizontal and vertical wind spectra for 20 mph wind (Newport, August 1971)	24
15.	Five-channel average horizontal and vertical wind spectra for 35 mph wind (Newport, August 1971)	26
16.	Five-channel average horizontal and vertical wind spectra for 50 mph wind (Newport, August 1971)	28
17.	Five-channel average horizontal and vertical wind spectra for 60 mph wind (Newport, August 1971)	30
18.	Angle of attack vs. wind velocity at individual sensor locations (Newport, January 1972)	32
19.	Five-channel average horizontal and vertical wind spectra for 40 mph wind (Newport, January 1972)	33

LIST OF ILLUSTRATIONS (continued)

Figure		Page
20.	Five-channel average horizontal and vertical wind spectra for 50 mph wind (Newport, January 1972) .	35
21.	Angle of attack vs. wind velocity at individual sensor locations (Sitka, November 1975)	37
22.	Four-channel average horizontal and vertical wind spectra for 30 mph wind (Sitka, November 1975) . .	38
23.	Angle of attack vs. wind velocity at individual sensor locations (Sitka, May 1976)	39
24.	Four-channel average horizontal and vertical wind spectra for 25 mph wind (Sitka, May, 1976)	40
25.	Functional processing sequence for acceleration data	42
26.	Example plot format of acceleration spectrum . . .	43
27.	Damping factor calculations for a typical acceleration spectrum frequency component	44
28.	Time history of acceleration data (Sitka, December 1975)	45
29.	Simplified individual, sum and difference spectra for first bridge motion event	49
30.	Simplified individual, sum and difference spectra for second bridge motion event	50
31.	Simplified individual, sum and difference spectra for third bridge motion event	51
32.	Individual channel horizontal and vertical wind spectra for 20 mph wind (Newport, August 1971) . .	67
33.	Individual channel horizontal and vertical wind spectra for 35 mph wind (Newport, August 1971) . .	75
34.	Individual channel horizontal and vertical wind spectra for 50 mph wind (Newport, August 1971) . .	83

LIST OF ILLUSTRATIONS (continued)

Figure		Page
35.	Individual channel horizontal and vertical wind spectra for 60 mph wind (Newport, August 1971) . .	91
36.	Individual channel horizontal and vertical wind spectra for 40 mph wind (Newport, January 1972) .	100
37.	Individual channel horizontal and vertical wind spectra for 50 mph wind (Newport, January 1972) .	108
38.	Individual channel horizontal resultant and vertical wind spectra for 30 mph wind (Sitka, November 1975)	117
39.	Individual channel horizontal resultant and vertical wind spectra for 25 mph wind (Sitka, May 1976)	122
40.	Individual channel acceleration spectra during first bridge motion event	127
41.	Individual channel acceleration spectra during second bridge motion event	133
42.	Individual channel acceleration spectra during third bridge motion event	139

LIST OF TABLES

Table		Page
1.	Significant project computer programs	8
2.	Expected errors for various combinations of interpolated data points	16
3.	Corrected anemometer responses and remaining errors at selected wind angles	19
4.	Statistical and implied physical characteristics of selected wind data samples	22
5.	Summary of predominant spectral components during bridge motion events	52

1. INTRODUCTION

This report is prepared in accordance with U.S. Department of Transportation contract DOT-FH-11-7769. Under this contract, Systems Technology Associates, Inc. provides field calibration services for a data acquisition system and reduces data from the system to investigate wind velocities, directions and effects at long-span bridge sites. The data acquisition system has been installed on the Narragansett Narrows bridge in Newport, Rhode Island, and on the Sitka Harbor bridge in Sitka, Alaska. The geographic locations and photographs of these sites are shown in Figures 1 through 3. Selected data recorded at Newport and Sitka are presented in this report.

Section 2 presents wind velocity spectra from data recorded on four separate occasions between 1971 and 1976. Data were selected to show the most significant wind conditions at the two bridge sites with respect to mean wind velocity, data variance, and wind angle. Section 3 presents bridge motion data in the form of acceleration spectra. These show predominant frequencies of bridge motions during a single event recorded at the Sitka site. No bridge motion data was recorded at the Newport site due to instrumentation difficulties.

Section 4 contains a summary of activities during the reporting period and describes future project plans. The appendices include a chronology of significant project events since the inception of the project, a summary of data collected and maintained during the project, and detailed data associated with Sections 2 and 3. The remaining paragraphs of this section briefly introduce the data acquisition system and the computer programs used to process project data.

1.1 DATA ACQUISITION SYSTEM

Data is acquired using instrumentation and a special-purpose data recording system which can be installed in various configurations at selected bridge sites. Figures 4 and 5 show the installation configurations at the Newport and Sitka sites.

Instrumentation basically consists of anemometers to measure wind velocities and directions, and accelerometers to measure bridge motions. Anemometers measure three orthogonal wind component velocities - along, across and vertical to the bridge deck. Resultant velocities and directions are derived from these measurements. Instruments are located at several stations along the windward side of the bridge on mountings which extend from the edge of the structure near roadbed level. Servo accelerometers measure vertical roadbed accelerations with

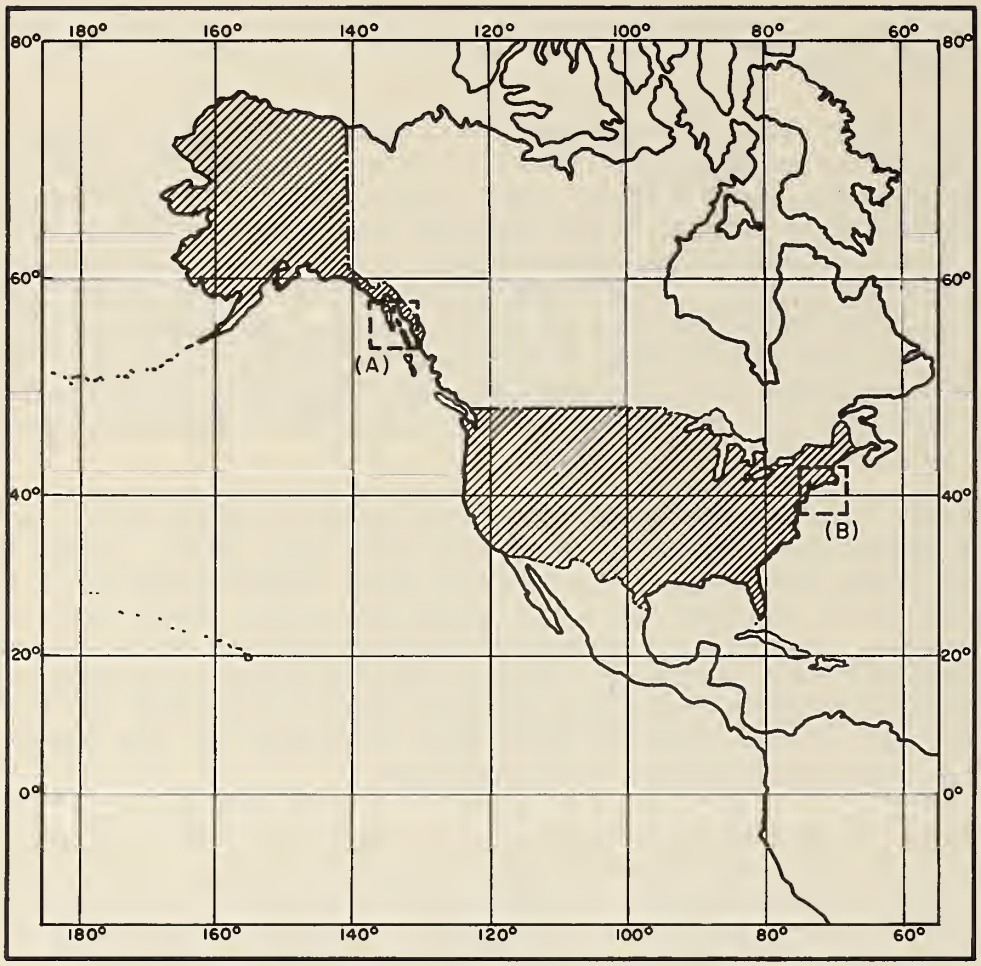

INSET (A)

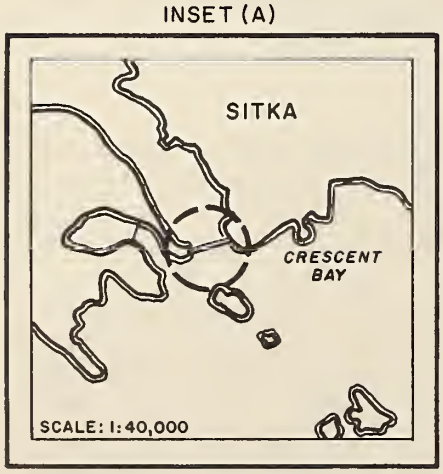

SITKA HARBOR BRIDGE

INSET (B)

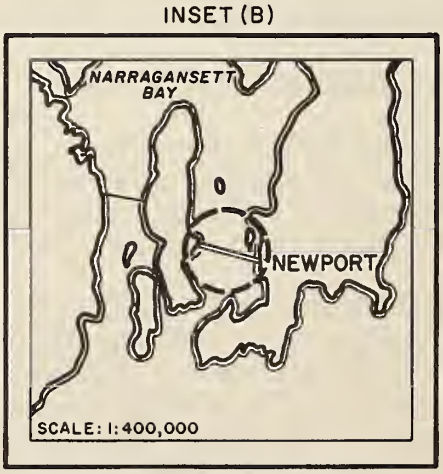

NARRAGANSETT BAY BRIDGE

Figure 1. Geographic locations of bridge sites.

Figure 2. Narragansett Bay bridge, Newport, Rhode Island.

Figure 3. Sitka Harbor bridge, Sitka, Alaska.

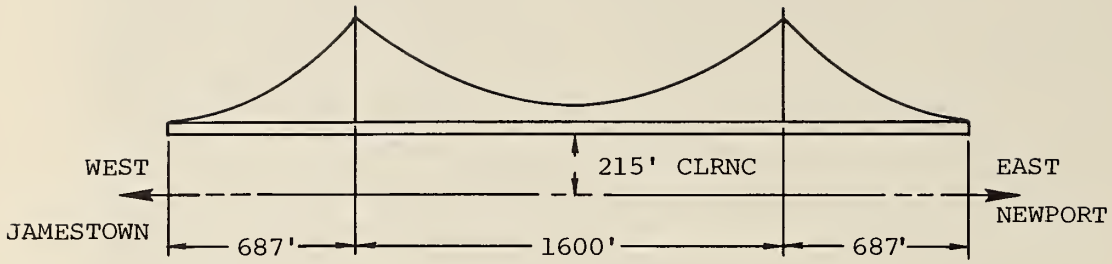

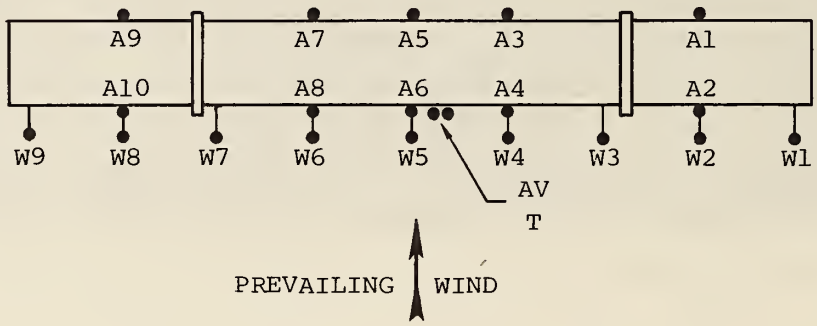

INSTRUMENTATION

A1-A10	ACCELEROMETERS (VERTICAL MOTION)
W1-W5	3-D ANEMOMETERS (SEE INSET A)
AV	AEROVANE
T	TEMPERATURE

INSET A

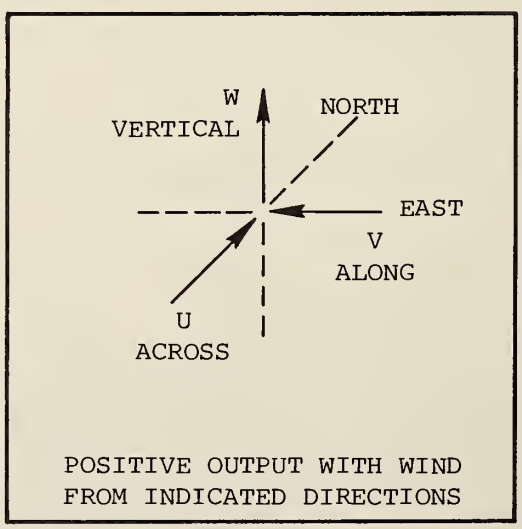

Figure 4. Instrumentation configuration - Newport.

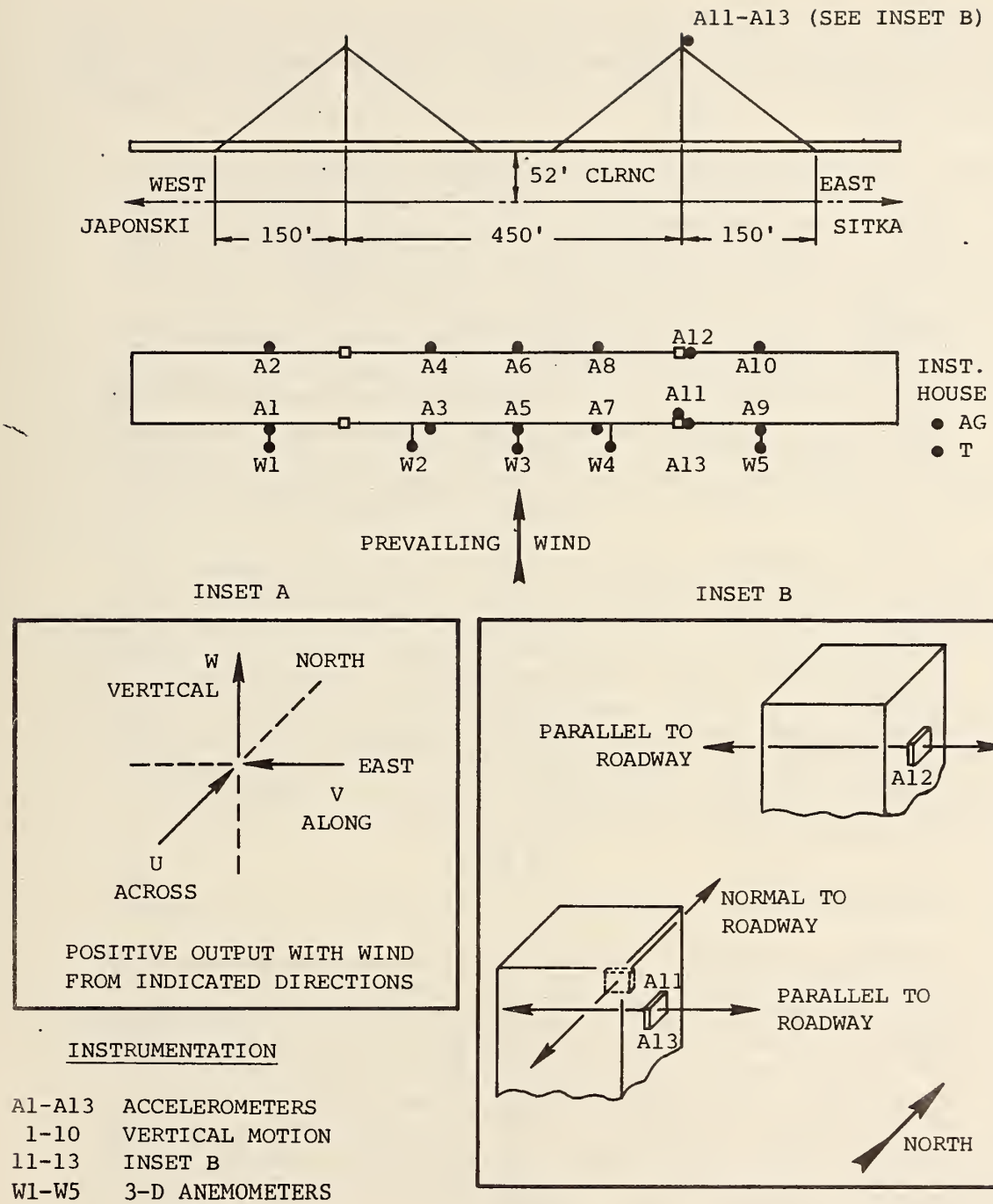

INSTRUMENTATION

A1-A13	ACCELEROMETERS
1-10	VERTICAL MOTION
11-13	INSET B
W1-W5	3-D ANEMOMETERS
	INSET A
AG	ACCELEROGRAPH
T	TEMPERATURE

Figure 5. Instrumentation configuration - Sitka.

respect to time. The instruments are hard-mounted on both sides of the bridge structure at roadbed level. Acceleration data are numerically converted to provide vertical and torsional roadbed displacement data.

A block diagram of the data recording system is shown in Figure 6. Analog signals from the anemometers, accelerometers and other sensors are continuously input, multiplexed and converted to digital levels. These levels are compared to preset levels selected on the control panel, and if greater for a selected time interval, automatically activate data recording. When the system is active, continuous scans of all sensors are input and recorded along with coded time information on digital magnetic tapes. The system has two recorders which switch over at the end of a tape to provide nearly thirty hours of recording capacity. Tapes are standard nine-track, 800 bpi NRZI format and data are recorded in binary (uncoded) form. Details of the record formats are included in the data recording system manuals.

While overall system sampling occurs at 500 samples per second, effective channel sample rates are dependant upon multiplexer channel assignments. At the Newport site, anemometer data were sampled at 14.3 Hz and accelerometer data were sampled at 7.1 Hz. At the Sitka site, both anemometer and accelerometer data were sampled at 14.3 Hz. Eight-bit analog-to-digital conversion and signal conditioning provided accelerometer resolution of .0389 g at Newport, and .0031 g at Sitka. Anemometer resolution at each site was .934 mph (.418 m/s). Further details of the data acquisition system are contained in other publications (6,7,8,10,12).

1.2 DATA REDUCTION

Data recorded on digital magnetic tapes are subsequently processed using FHWA computer facilities. Table 1 lists many of the production oriented computer programs used to reduce the data. Production software is distinguished from developmental software in that the former category includes programs which require little set-up, are seldom modified and which are typically used in processing project data. Developmental programs are used for special data reduction requirements, and are relatively complex and inefficient. If a continuing need exists for a developmental program, the routine is revised to facilitate production usage.

The data presented in this report were processed using the spectral analysis programs. These programs and their output are described in detail in Sections 2 and 3. The output from two

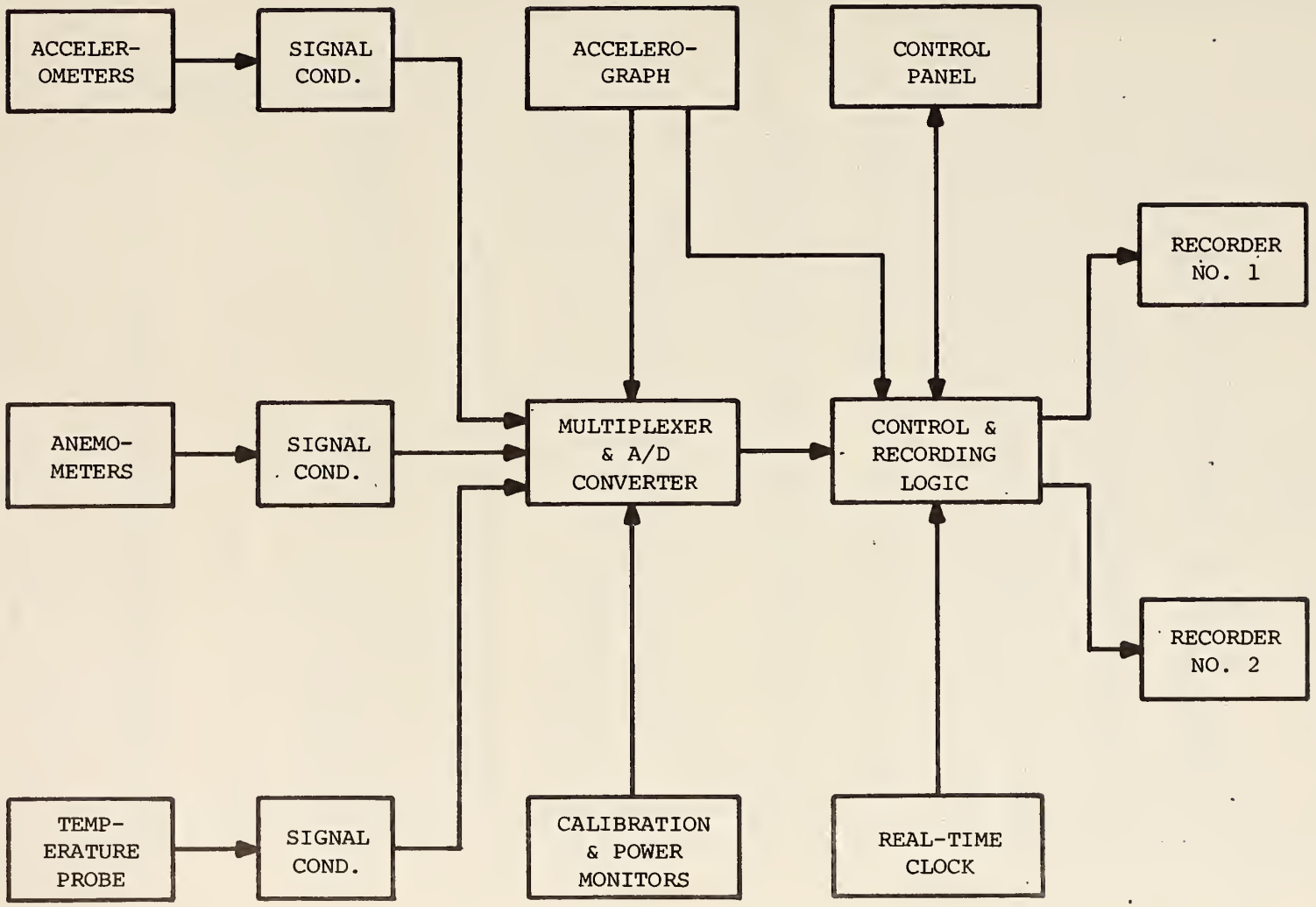

Figure 6. Data acquisition system block diagram.

Table 1. Significant project computer programs.

Name	Purpose
ACCPLT	Generates side-by-side plots of data from all accelerometers for selected data records.
ACCSPC	Calculates and plots power spectral density for selected accelerometer data.
CALFIL	Updates and maintains instrumentation system channel calibration file.
COPY	Copies selected records from data base to work tape.
INTERP	A subroutine to generate missing data points through interpolation.
MODE3D	Plots three-dimensional views of geometrical bridge configuration at sequential instants of time.
NEWPRT	A subroutine to read Newport data tapes, and demultiplex and calibrate sensor data.
RBMAX	Generates table of record-by-record accelerometer maxima, and average wind directions and velocities.
SITKA	A subroutine to read Sitka data tapes, and demultiplex and calibrate sensor data.
TAPSUM	Generates index and 10-minute statistical summaries for all data recorded on field data tapes.
UVCAL	A subroutine to calculate anemometer propeller response correction factors.
WINDOW	A subroutine to apply 10% cosine^2 taper to data samples.
WNDSPC	Calculates and plots power spectral density for selected anemometer data.

other programs provide unique insight to the project from the aspects of data collection and data presentation. These programs are briefly described in the following paragraphs.

The data acquisition system is activated automatically when wind velocities or bridge motions exceed certain thresholds. Likewise, the system stops recording when the data falls below these levels. The obvious question then arises "What data were recorded?" The tape summary programs, one for Newport tapes and one for Sitka tapes, were designed to process entire tapes and to summarize the events, conditions and data recorded. Figure 7 is an example of a statistical data summary output by these programs. One such summary is generated for every ten minutes of data recorded within a recording event. The start, stop and duration times for each summary are indicated and the minimum, maximum, mean and standard deviation of all samples for each instrument are listed. With this output, it is possible to determine when the system was recording, what activated the system, the worst case and general wind and bridge motion activities, the similarity of activities between instruments, and the integrity of the instruments and data recording system. Foremost, however, the output permits the isolation of data of particular interest, which is a unique problem when voluminous data is automatically recorded at remote, unattended locations.

MODE3D is a computer program which presents data of interest in a form strictly for visual interpretation. The output from this program can be displayed on paper or photographic film. Figure 8 shows several frames of output which represents in three-dimensional perspective the geometrical configuration of the Sitka bridge at several instants of time. One frame is produced for each scan of the accelerometers. When viewed sequentially, these frames present an animated reconstruction of the behavior of the bridge. Output to film is effected using a Stromberg Carlson Data Graphics SC4020 camera system at Johns Hopkins University Applied Physics Laboratory. Standard 16mm film is used which can be prepared and projected at speeds to simulate real-time or slow motion bridge behavior. Viewing these films provides unique insight into the composition of complex bridge bending modes.

2. WIND DATA

The wind data selected for analyses were recorded on four separate occasions at Newport and Sitka. The most significant data were recorded at Newport in August, 1971 during the passage of Tropical Storm DORIA. Gusts up to 80 mph accompanied the storm and mean winds of nearly 60 mph were recorded across the bridge deck. Ten-minute data samples at various wind veloc-

TAPE NO. 010431 START 129:23:29:53
EVENT NO. 1 STOP 129:23:39:49
INTERVAL SUMMARY 1- 5 DURATION 0: 9:56

SENSOR	MINIMUM	MAXIMUM	MEAN	STD.DEV.
A1	-0.003	0.016	0.0053	0.0018
A2	-0.006	0.006	0.0000	0.0008
A3	-0.013	0.019	0.0043	0.0017
A4	-0.009	0.016	0.0018	0.0017
A5	-0.006	0.016	0.0035	0.0012
A6	-0.009	0.009	0.0002	0.0009
A7	-0.013	0.009	0.0009	0.0015
A8	-0.009	0.009	0.0005	0.0012
A9	-0.009	0.003	-0.0037	0.0014
A10	-0.006	0.006	0.0001	0.0008
A11	-0.399	0.402	-0.0243	0.1335
A12	-0.031	0.028	-0.0004	0.0052
A13	-0.022	0.028	-0.0024	0.0035
1U	-10.275	17.748	1.9835	3.0811
2U	-5.605	10.275	1.5476	2.2460
3U	-17.748	10.275	1.6762	2.6651
4U	-14.012	10.275	0.5507	3.2004
5U	-12.144	10.275	0.8639	2.8536
1V	0.0	39.233	17.9534	6.7865
2V	2.802	35.497	18.2446	5.2424
3V	3.736	39.233	20.3352	5.4311
4V	1.868	31.760	15.7992	4.7510
5V	2.802	36.431	19.9670	5.9127
1W	-7.473	14.012	0.0645	2.3799
2W	-6.539	11.209	2.0944	2.4378
3W	-3.736	9.341	2.0527	2.1225
4W	-10.275	13.078	0.6234	2.4798
5W	-3.736	14.012	2.3521	2.1214
SEIS	0.156	0.156	0.1563	0.0000
SPAR	-1.484	0.0	-0.5642	0.1837
SPAR	-2.109	-0.625	-1.1971	0.1989
TEMP	5.800	6.525	6.2922	0.1782
CL:F	9.922	9.922	9.9219	0.0000
CL:Z	0.0	0.0	0.0	0.0000
CL:M	5.000	5.000	5.0000	0.0000
LVM	-8.594	-8.359	-8.4808	0.0568
PUM	0.078	0.078	0.0781	0.0000
IRG	0.0	0.0	0.0	0.0000

Figure 7. Example tape summary program statistical summary.

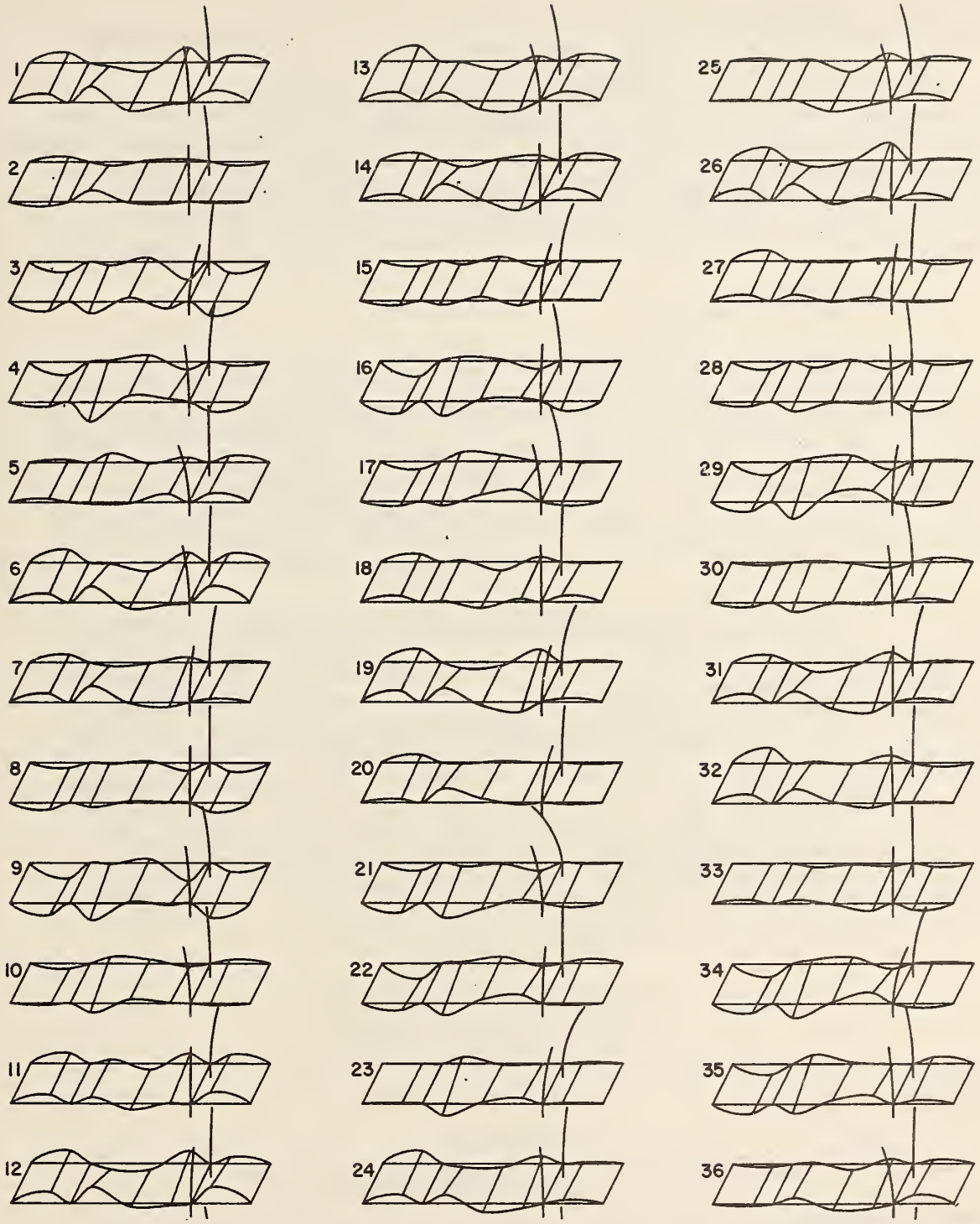

Figure 8. Example MODE3D program display.

ities were processed to derive spectra which show the general amplitude and frequency of wind gusts.

Spectra for both horizontal and vertical winds were derived using time-to-frequency domain transform techniques. This section discusses the methods used to condition and transform the data, and presents in separate subsections, the average horizontal and vertical wind spectra for each of the four recording events. Additional detailed spectra are included in Appendices C-F.

2.1 PROCESSING APPROACH

Alternative processing methods were tested and discussed in a previous report (3). The processing approach presented in this section was adopted in consonance with the previous investigation. Two additional considerations in conditioning data samples were investigated and the results are discussed in Sections 2.1.1 and 2.1.2. Section 2.1.3 describes the method used to correlate project data with theoretical models of wind spectra, and lists the results of the comparisons.

Figure 9 shows the sequence of processing the recorded wind data. Ten-minute data samples of U-, V-, and W- component winds for all sensor stations are first isolated and corrected for propeller response errors. Data sets are then decimated to obtain a reasonable number of data points and an acceptable sample rate. The previously recommended factor of four is used in this study to obtain 2048 data points at an effective sample rate of approximately 3.6 Hz. The mean and linear ramp trend, if any, are then removed and a 10% cosine^2 taper is applied prior to transforming the data. The IBM subroutine RHARM is used to calculate Fourier series coefficients (5). These are converted to amplitude and used in the calculation of reduced power density, RPD, as follows:

$$RPD_i = \frac{\text{frequency}_i \times \text{amplitude}_i^2}{\text{data sample variance}}$$

As a matter of convention, spectral frequency is converted to wave number, WN, by:

$$WN_i = \frac{\text{frequency}_i}{\text{data sample mean horizontal velocity}}$$

Nineteen point data averaging is used in the final processing step to reduce "spiky" fluctuations in the spectra and to better display the spectral power density.

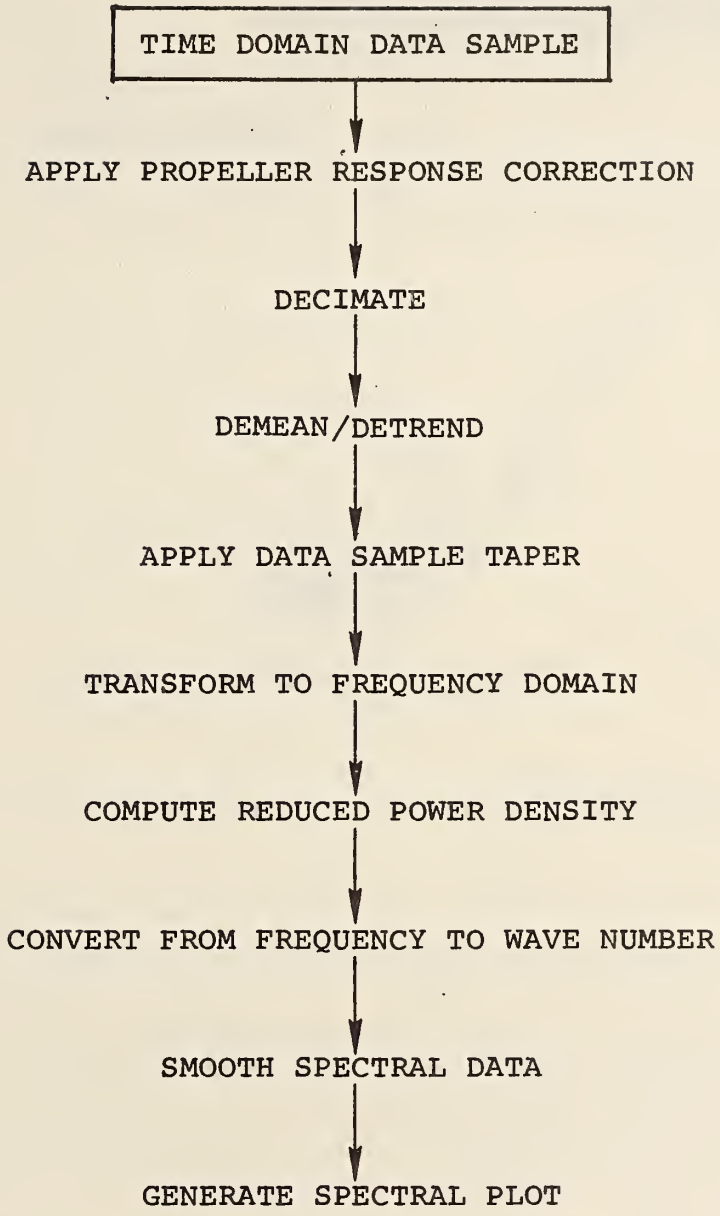

Figure 9. Functional processing sequence for wind data.

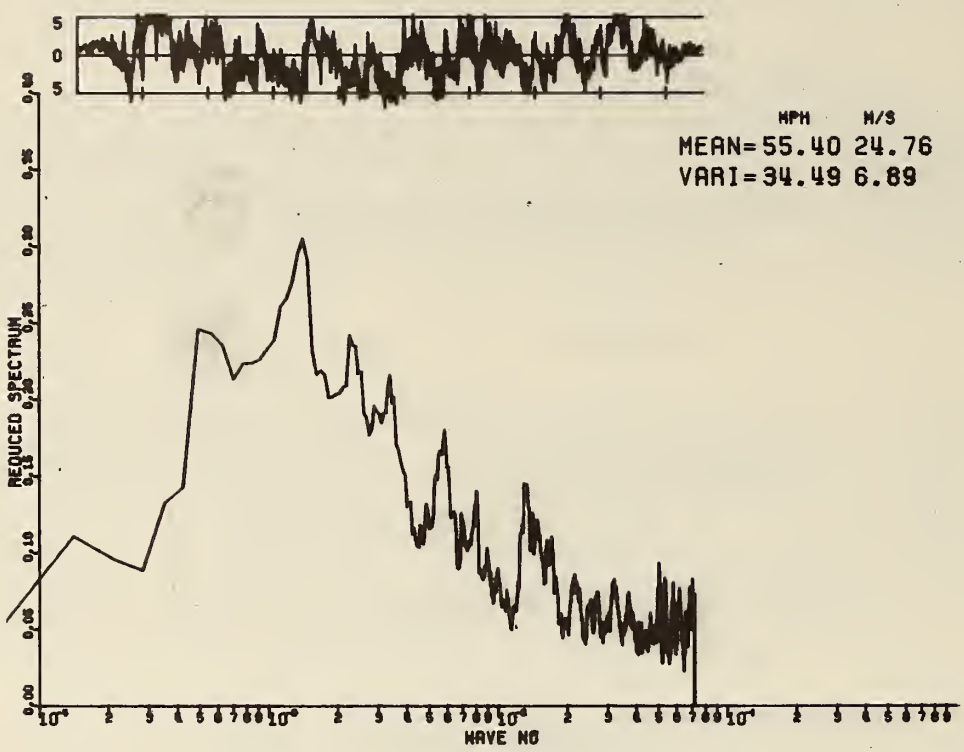

Figure 10. Example plot format of wind spectrum.

To simplify interpretation, all wind spectra are displayed in a common format. Figure 10 is an example of the plot format. The abscissa is a three decade logarithmic scale of wind wave number expressed in cycles per meter. The linear vertical scale is reduced power density expressed in non-dimensional units. Individual channel plots have an inset listing the mean and variance of the data sample in miles per hour and meters per second. These plots also include time-traces of the tapered data samples used to derive the adjoining spectra. The abscissa on these traces is time in 4.48 sec steps, and the ordinate is wind velocity in m/s from the mean.

2.1.1 Interpolation of Discontinuous Data

The data acquisition system installed at the Newport and Sitka sites from October 1970 to August 1975 used incremental tape drives for data recording. These instruments transferred measurements to magnetic tape as they were taken. When inter-

record gaps were recorded, however, measurements could not be transferred and were lost. To allow sufficient time for recording interrecord gaps, two complete multiplexor scans were skipped at the end of each record. This resulted in data recording discontinuities of .28 sec after every record (4.48 sec). Figure 11 illustrates the effect of these discontinuities. In September, 1975, the incremental tape drives were replaced with fully buffered, synchronous tape recorders which eliminate data discontinuities.

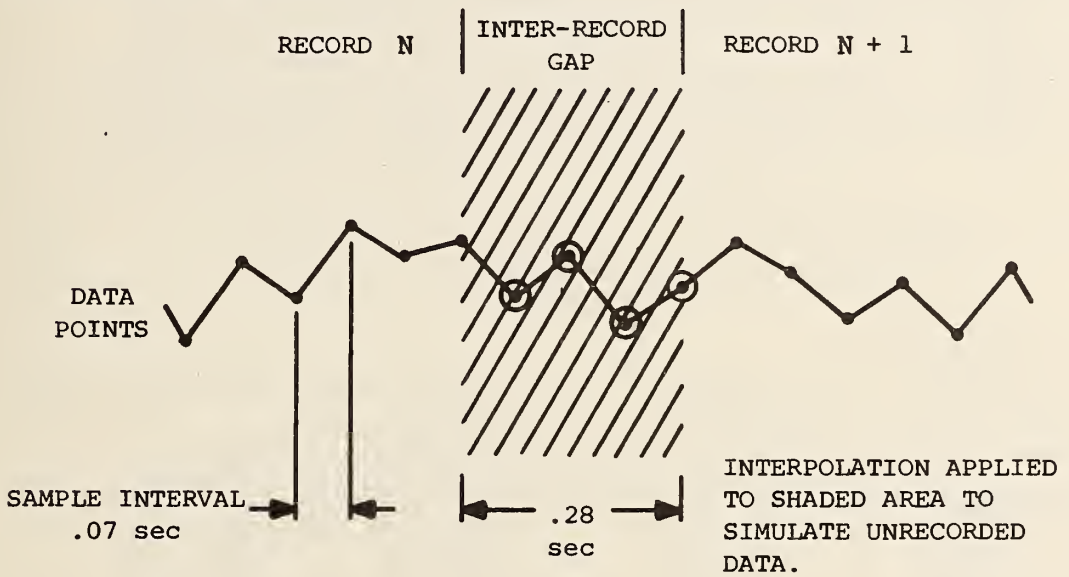

Figure 11. Recording system data discontinuities.

To process previously recorded data, interpolation is used to replace lost data measurements. For Newport recordings, four anemometer values and two accelerometer values are interpolated. For early Sitka recordings, four values are interpolated for both anemometers and accelerometers. Aitken's method of interpolation (1) is used to construct a polynomial of n-1 degrees through n given data points which symetrically bound m missing data points. The algorithm uses iterative determinant solutions of a polynomial to calculate individual data points. Each resulting interpolated value has positional significance equal to all other points in the data stream.

To test the accuracy of the technique, two data sets were generated to simulate real data. One set approximates bridge motion data with a .73 Hz sine wave. The other data is a set of uniformly distributed random numbers with a mean of 33.5 and a

standard deviation of 5.6, which simulates wind velocity data. Multiple data records were created within each set and four interpolated data points were calculated to correspond with four data points between adjacent records. The simulated data points from the test data and the interpolated points were then separately averaged and compared. These statistics are listed in Table 2 and show the relative accuracy of the interpolation technique as the number of given data points is varied.

Since interpolated values are determined by an approximation of the behavior of surrounding points, accuracy is dependant upon the repeatability and continuity of the given data. As expected, the errors associated with the sine wave test data are small compared to the random data. Based on these tests, interpolation using six given data points (three on each side of the data discontinuity) provides maximum accuracy for both data types.

Table 2. Expected errors for various combinations of interpolated data points.

a) Sine wave test data.

No. Points	Average Test Value	Average Interp Value	Average Difference	Error
4	.218140	.215128	.003012	1.3%
6	.218140	.217952	.000188	.09%
8	.218140	.218133	.000007	.0032%
10	.218140	.218140	0.0	0%

b) Random test data.

No. Points	Average Test Value	Average Interp Value	Average Difference	Error
4	33.786865	33.559189	.227676	.67%
6	33.786865	33.639175	.147690	.43%
8	33.786865	33.156097	.630768	1.8%
10	33.786865	30.647079	3.139786	9.3%

2.1.2 Correction for Anemometer Response Characteristics

An anemometer signal results from the wind driving a polystyrene propeller which is coupled to a miniature d.c. voltage generator. The voltage is proportional to propeller speed and

its polarity indicates the direction of propeller rotation. The propeller responds only to that component of the wind which is parallel to its axis of rotation. Propeller response to angular winds is a function of the cosine of the wind angle.

Figure 12 compares the theoretical and the manufacturer's measured response data for the four-bladed propeller used in the data acquisition system. By correcting for the differences between the calibration data and the cosine function, correction factors can be derived based on the following relationships:

$$\theta = \arctan \frac{v}{u}$$

$$U = \frac{u \cos \theta}{y_\theta}$$

$$V = \frac{v \cos (90-\theta)}{y_{90-\theta}}$$

$$R = \sqrt{U^2 + V^2}$$

where:

θ is the wind angle relative to the U-component axis
u and v are recorded orthogonal component velocities
U, V, and R are corrected component and resultant velocities, and
y is the calculated response for a given wind angle.

An eight degree polynomial was fitted to data points consisting of propeller responses and corresponding wind angles between 2° and 88°. This limited data set was used since the propeller response is symetrical for all positive direction winds and since negative direction winds are not considered in project analyses. Wind angles less then 2° give 100% response and wind angles greater than 88° result in propeller stall.

The form of the polynomial and the derived coefficients are:

$$y = a_0 + a_1x + a_2x^2 + a_3x^3 \ldots a_7x^7$$

where:

y is percent response,
x is wind angle in radians,

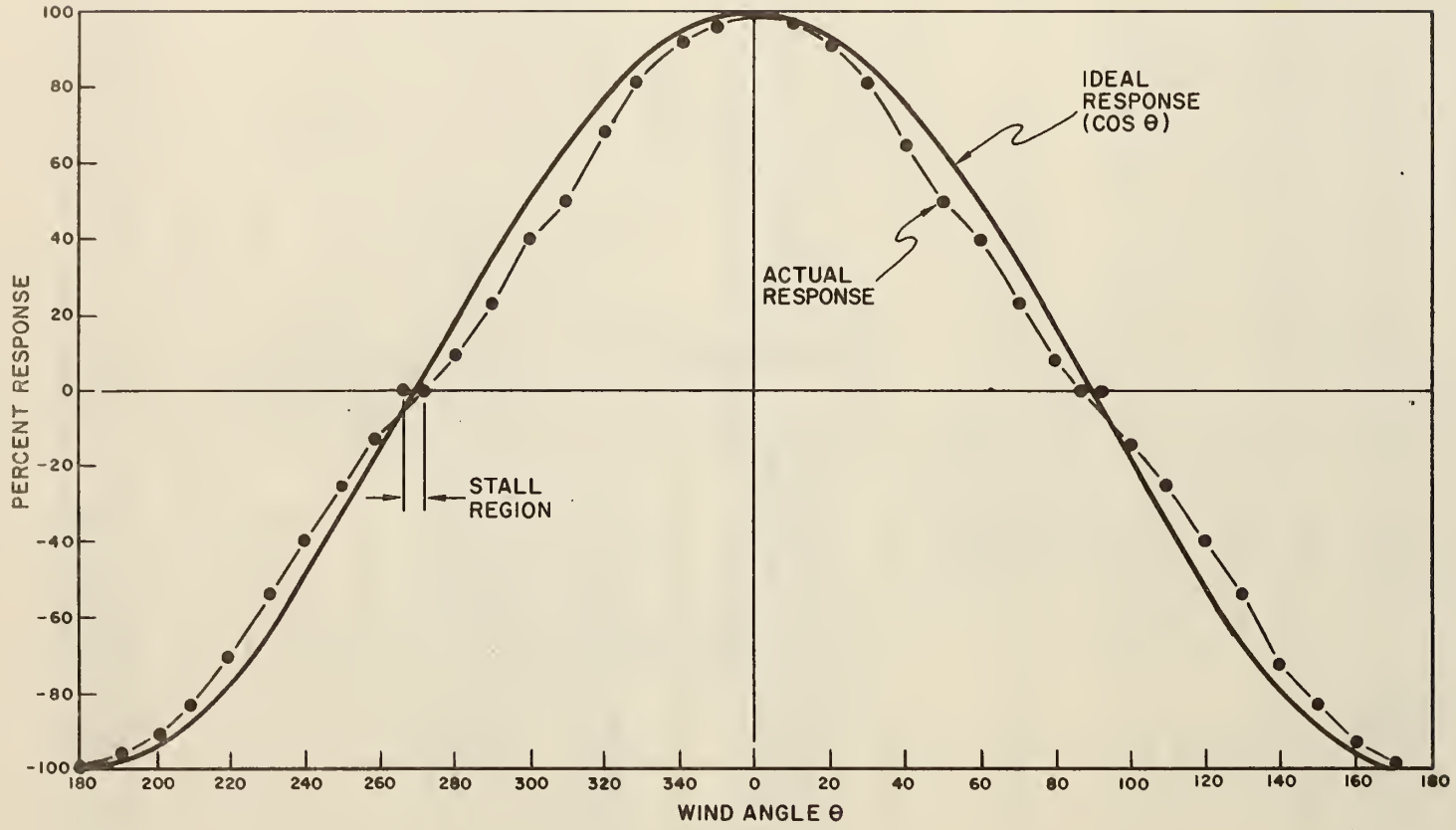

Figure 12. Anemometer response vs. wind angle (15 cm propeller).

and the following coefficients are given:

$a_0 = 99.70563$ $\quad a_4 = 85.19067$

$a_1 = 5.49133$ $\quad a_5 = 25.50650$

$a_2 = 64.69608$ $\quad a_6 = 56.69714$

$a_3 = 69.52574$ $\quad a_7 = 17.33202$

Table 3 lists the results of propeller response correction for various wind angles. All figures are percent of response to resultant wind velocity.

Table 3. Corrected anemometer responses and remaining errors at selected wind angles.

Wind Angle (degrees)	Ideal Response (%)	Actual Response (%) (a)	Corrected Response (%) (b)	Remaining Error (%) (a-b)
0	100.0	100.0	100.0	0.0
10	98.5	98.0	98.1	0.4
20	94.0	92.0	93.9	0.1
30	86.6	82.0	87.4	-0.8
40	76.6	68.0	77.0	-0.4
50	64.3	51.0	61.9	2.4
60	50.0	40.0	52.1	-2.0
70	34.2	24.0	34.0	-0.2
80	17.4	10.0	16.8	-0.6
90	0.0	0.0	0.0	0.0

As an example, given a 50 mph wind at an angle of 30° from the U-axis, the ideal U-component velocity should be 86.6% x 50 = 43.3 mph. However, the measured velocity after correction will be 87.4% x 50 = 43.7 mph, resulting in an error of 0.8% x 50 = .4 mph. The mean error over all angles is 0.05% with a standard deviation of 1.05%.

2.1.3 Correlation of Data with Theoretical Models

The plots in Sections 2.2 and 2.5 show the combined spectral results for all transducers for each particular data sample. Average horizontal and vertical spectra are included for each selected nominal wind velocity. An approach to superimpose the curves of theoretical models on these spectra was described in a paper coauthored by the FHWA contract manager, Mr. R.H. Gade (2). An extract from this paper is included below:

For horizontal spectra a comparative plot is based on the following Harris - Von Karman formula: (4)

$$\frac{nS_U(n)}{\kappa \bar{U}^2(10)} = \frac{4N}{(2+N^2)^{5/6}}$$

where κ is the surface drag coefficient, and $\bar{U}(10)$ is the mean velocity, both referred to 10-meter height, and

$$N = \frac{nL}{\bar{U}(10)}$$, L being a peak wavelength "constant".

This formula is converted for comparative purposes to the desired form as follows:

$$\frac{nS_U(n)}{\sigma_U^2} = \frac{4K^2\bar{U}^2(z)}{\sigma_U^2 \ln\frac{10}{z_0} \ln\frac{62.7}{z_0}} \cdot \left[\frac{L\frac{1}{\lambda(z)}}{\left[2 + \left(\frac{1}{\lambda(z)} L \frac{\ln\frac{62.7}{z_0}}{\ln\frac{10}{z_0}}\right)^2\right]^{5/6}} \right]$$

where K, Karman's constant, is taken as 0.4, $\bar{U}(z)$ is averaged mean wind velocity at bridge height and $1/\lambda(z) = n/\bar{U}(z)$; z_0, the surface roughness length, is related to κ by the formula:

$$\kappa = \frac{K^2}{\left(\ln\frac{10}{z_0}\right)^2}$$

The peaks of the sample and reference spectra were arbitrarily equated to obtain the values of κ and L. The resulting relations are:

$$1.812\ \kappa\bar{U}^2(10) = \left[n\ S_U(n)\right]_{max}$$

$$L = \frac{\sqrt{3}\ \ln\left(10/z_0\right)}{\frac{1}{\lambda(z)} \ln\frac{62.7}{z_0}}$$

For vertical spectra an empirical spectrum is derived from the following Panofsky formula: (9)

$$\frac{nS_W(n)}{\kappa\bar{U}^2(10)} = \frac{6f}{(1 + 4f)^2}$$

where $f = nz/\bar{U}$, z being the height of the transducer, and $\bar{U}$ being the mean horizontal velocity at that height.

This formula is converted for comparative purposes to the desired form as follows:

$$\frac{nS_W(n)}{\sigma_W^2} = \frac{K^2\,\bar{U}^2(z)\,(1/\lambda(z))\,6z}{\sigma_W^2\left(\ln\frac{62.7}{z_0}\right)^2\left(1 + 4z/\lambda(z)\right)^2}$$

The surface drag coefficient is similarly obtained by

$$0.375\ \kappa\bar{U}^2(10) = \left[nS_W(n)\right]_{max}$$

and z_0 as above.

Peak values from sample spectra were identified manually and a computer program was used to generate smooth curves and calculate implied model parameters based upon these values. The peak values, model parameters and sample identification information are listed in Table 4.

Table 4. Statistical and implied physical characteristics of selected wind data samples.

a) Using U-Component wind.

Sample ID		Horizontal Wind Data							Vertical Wind Data					
Tape	Rec	Mean m/s	Var $(m/s)^2$	Peak Ht	Peak Freq	Rough Leng m	Drag Coeff	Leng Const m	Mean m/s	Var $(m/s)^2$	Peak Ht	Peak Freq	Rough Leng m	Drag Coeff
WIND01	2380	10.8	3.4	.29	.056	.1794	.0099	229	5.2	.92	.37	.167	.6855	.0223
WIND01	2920	16.9	7.8	.27	.052	.1186	.0081	398	5.1	1.60	.38	.105	.3037	.0131
WIND01	3460	22.4	8.9	.20	.049	.0074	.0031	631	4.7	2.23	.40	.085	.1880	.0101
WIND01	3580	25.3	6.7	.23	.045	.0011	.0019	811	4.2	2.00	.34	.108	.0342	.0050
WIND04	3627	18.4	3.0	.24	.045	.0005	.0017	597	4.0	.83	.35	.153	.0146	.0038
WIND04	4136	21.0	5.3	.26	.051	.0041	.0026	577	4.2	1.86	.37	.100	.1272	.0084

b) Using resultant horizontal wind.

WIND01	2380	19.2	4.1	.24	.043	.0019	.0022	637	5.2	.92	.37	.167	.0204	.0042
WIND01	2920	20.2	5.2	.25	.030	.0045	.0027	942	5.1	1.60	.38	.105	.1073	.0078
WIND01	3460	23.6	6.7	.19	.043	.0008	.0018	796	4.7	2.23	.40	.085	.1377	.0087
WIND01	3580	25.5	6.7	.24	.045	.0012	.0020	815	4.2	2.00	.34	.108	.0342	.0050
WIND04	3627	18.5	2.9	.24	.045	.0004	.0016	603	4.0	.83	.35	.153	.0140	.0037
WIND04	4136	21.4	4.3	.27	.047	.0014	.0020	653	4.2	1.86	.37	.100	.1130	.0080
010419	2209	14.1	2.7	.30	.011	.0035	.0025	2096	3.7	.75	.34	.091	.0165	.0089
010431	3053	11.8	1.6	.29	.012	.0014	.0020	1618	3.6	.35	.27	.057	.0013	.0020

2.2 NEWPORT - AUGUST 1971

This section presents data recorded at the Newport bridge site on August 28, 1971. The specific start and stop times associated with the data are unknown due to recorded time inaccuracies. The data are from Tropical Storm DORIA, which passed near the bridge, with mean wind velocities to 60 mph and gusts to 80 mph. Data from five wind sensors were processed at mean wind velocities of 20, 35, 50, and 60 mph.

Figure 13 compares the average vertical wind angles of attack at the mean U-component wind velocities experienced at each sensor station. Figures 14 through 17 show five-sensor, ensemble average wind spectra at the four selected wind velocities. Each figure includes separate plots of the U-component spectrum, the resultant horizontal spectrum, the vertical spectrum adjusted to the U-component velocity, and the vertical spectrum adjusted to the resultant horizontal velocity. Individual channel spectra for this recording event are included in Appendix C.

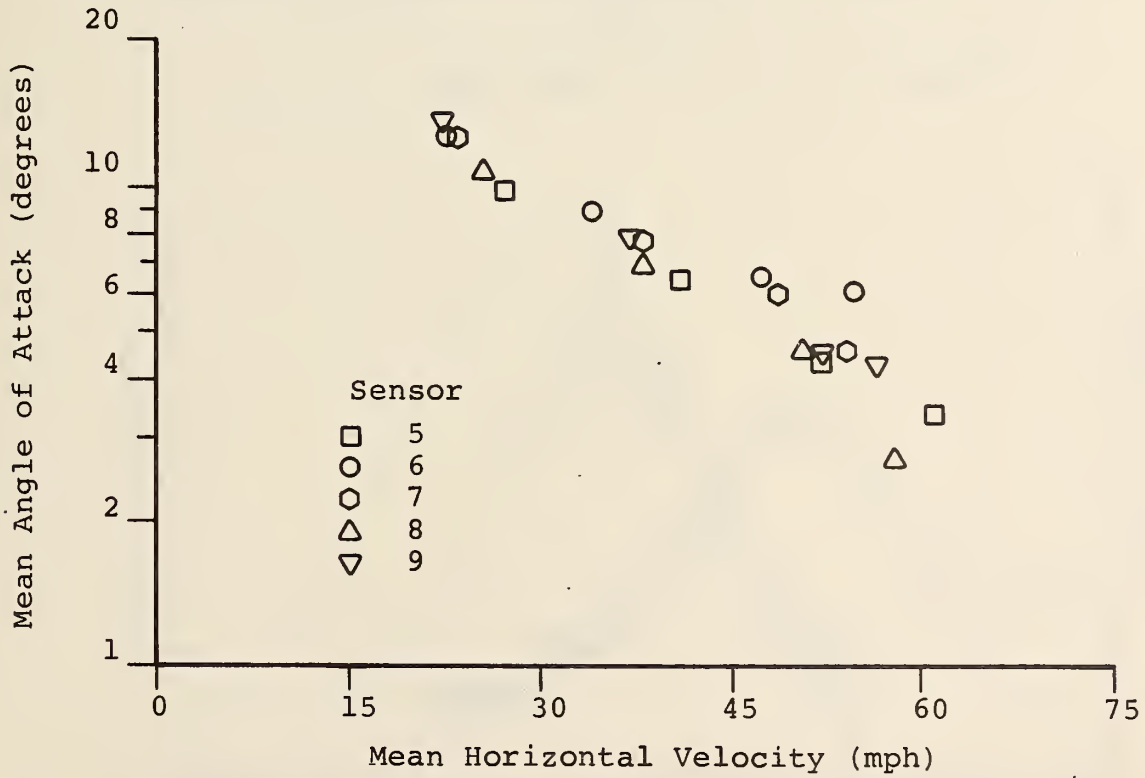

Figure 13. Angle of attack vs. wind velocity at individual sensor locations (Newport, August 1971).

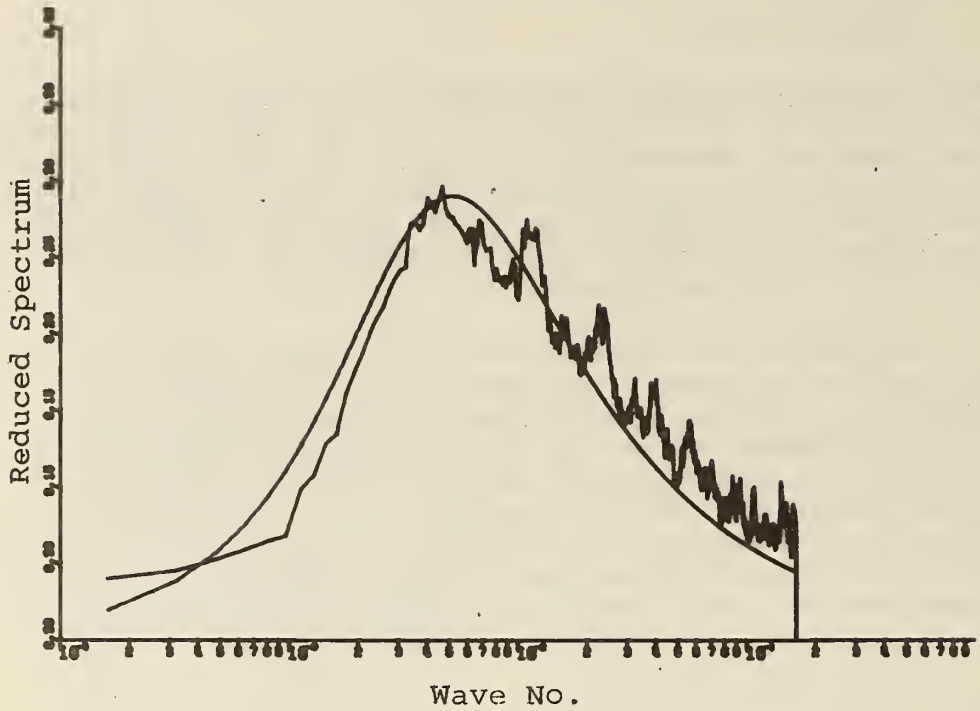

a) U-component - 5U, 6U, 7U, 8U, 9U.

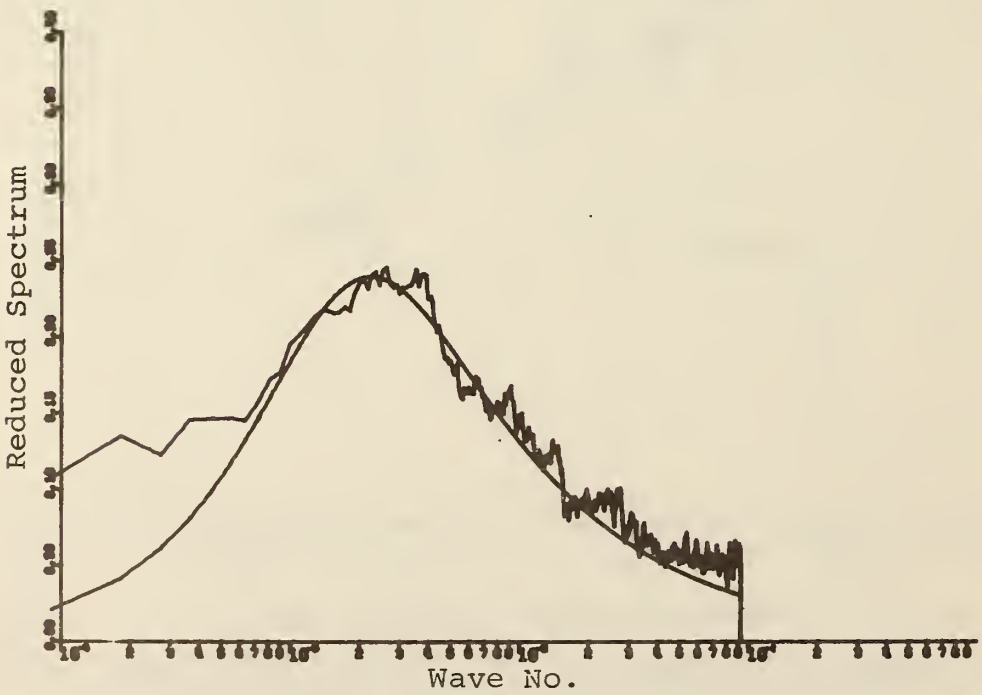

b) Resultant horizontal - 5R, 6R, 7R, 8R, 9R.

Figure 14. Five-channel average horizontal and vertical wind spectra for 20 mph wind (Newport, August 1971).

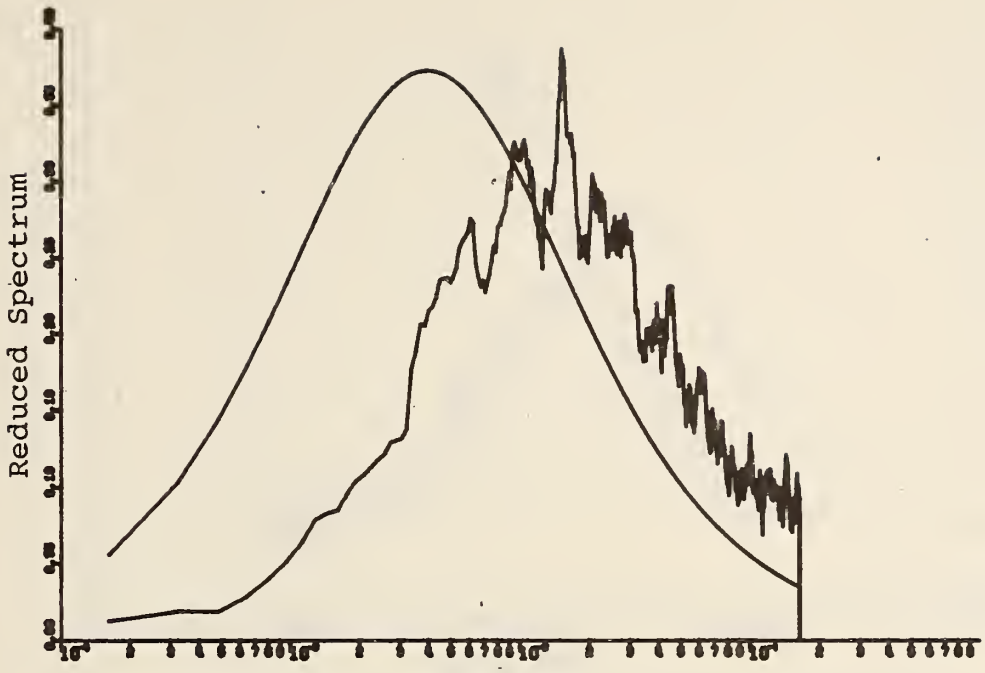

c) Vertical - 5W/U, 6W/U, 7W/U, 8W/U, 9W/U.

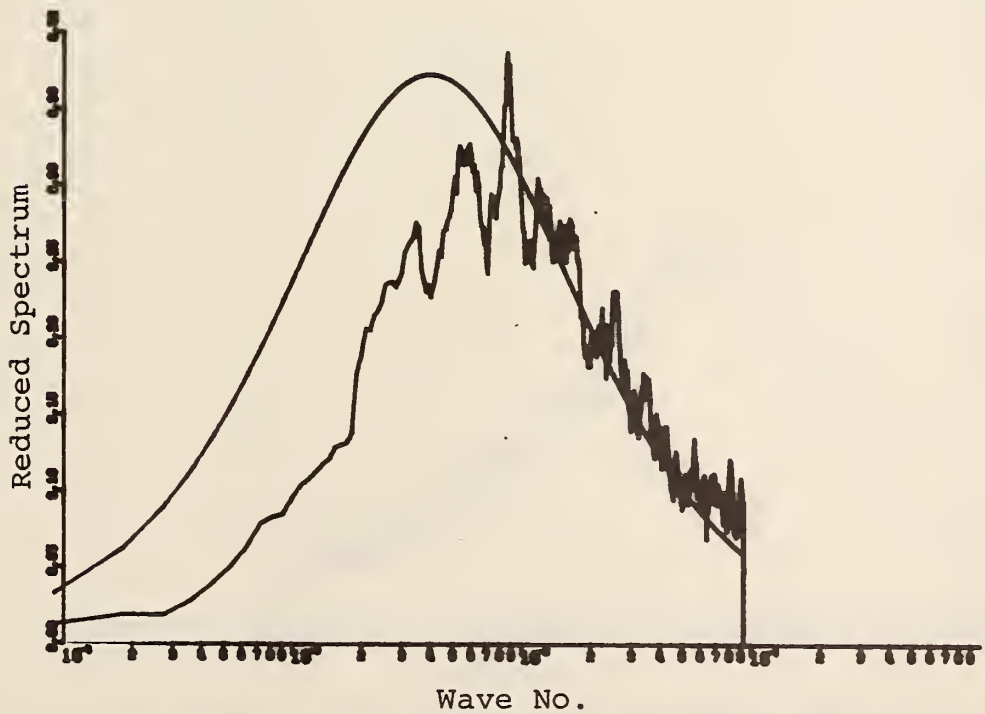

d) Vertical - 5W/R, 6W/R, 7W/R, 8W/R, 9W/R.

Figure 14. Five-channel average horizontal and vertical wind spectra for 20 mph wind (Newport, August 1971)(continued).

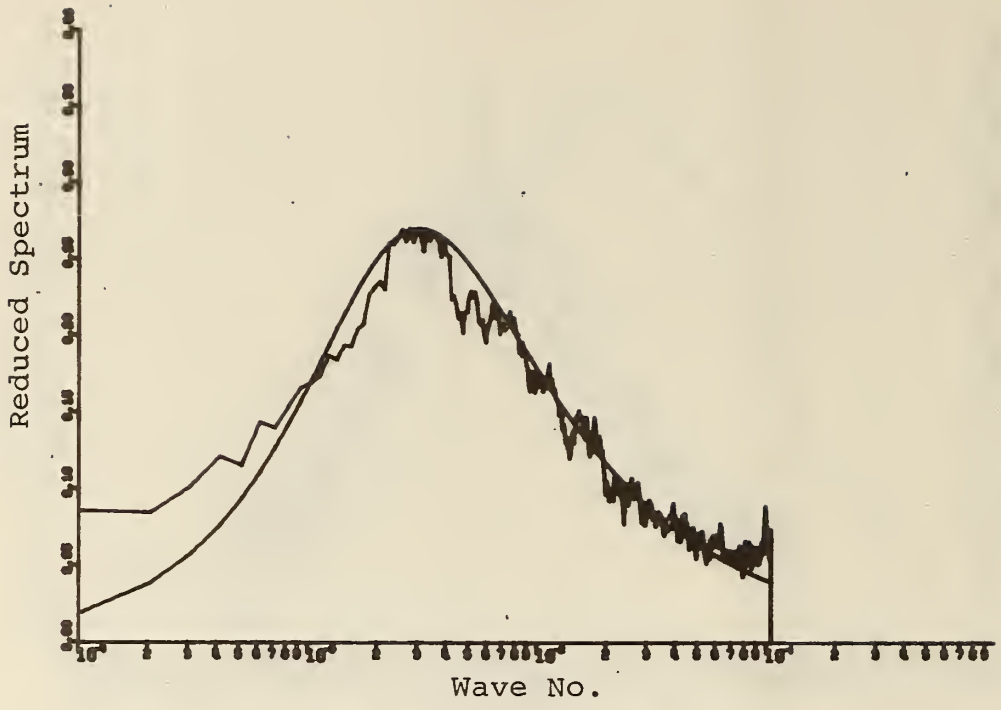

a) U-component - 5U, 6U, 7U, 8U, 9U.

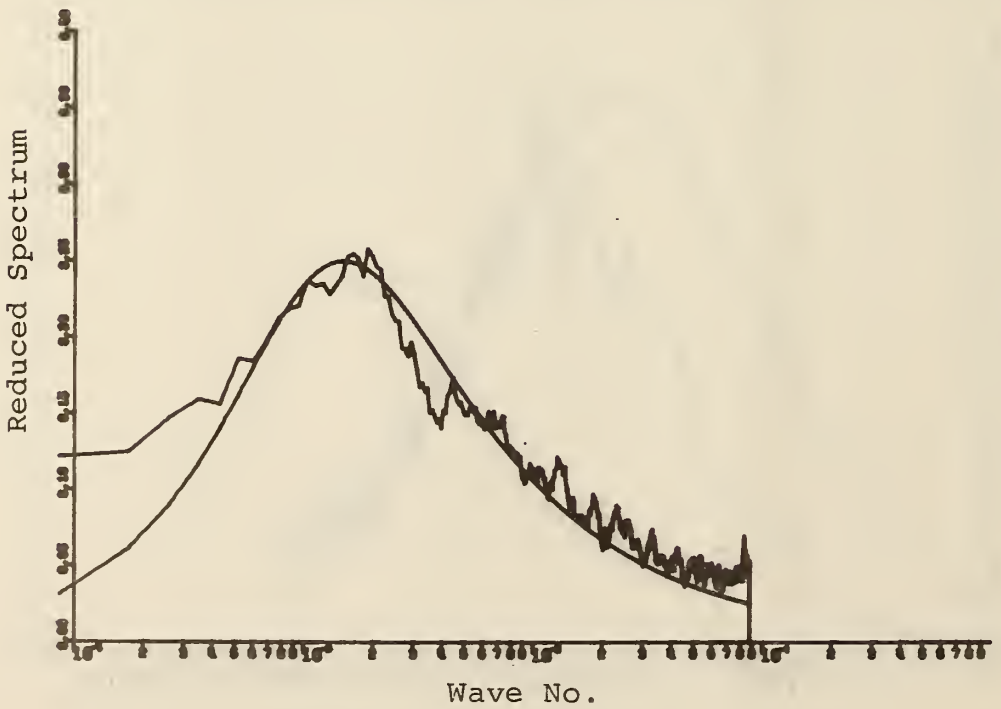

b) Resultant horizontal - 5R, 6R, 7R, 8R, 9R.

Figure 15. Five-channel average horizontal and vertical wind spectra for 35 mph wind (Newport, August 1971).

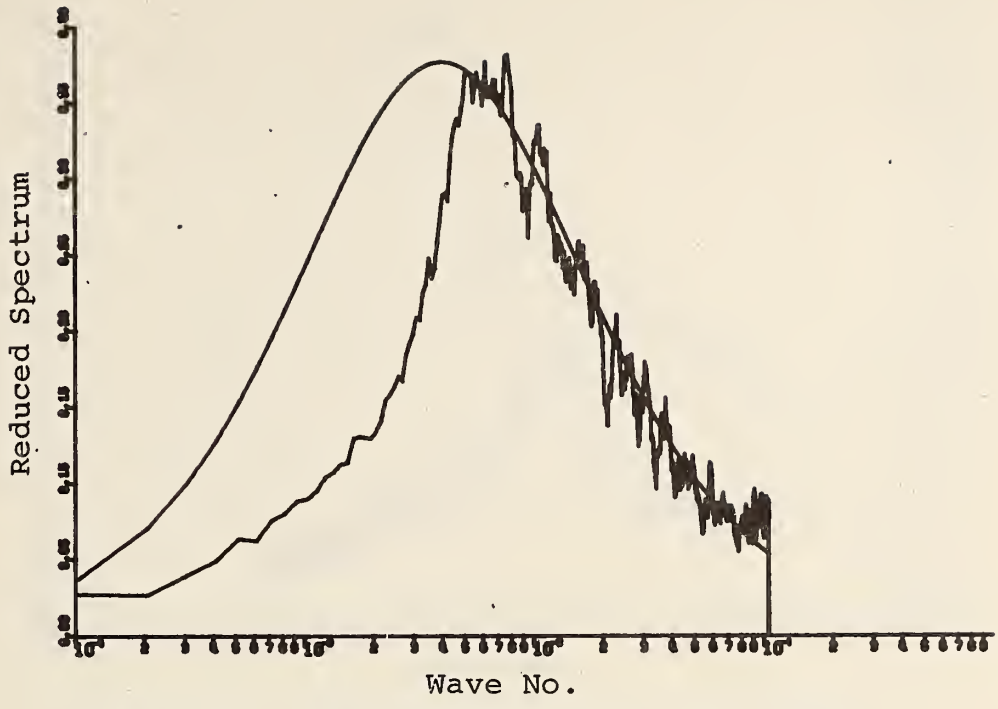

c) Vertical - 5W/U, 6W/U, 7W/U, 8W/U, 9W/U.

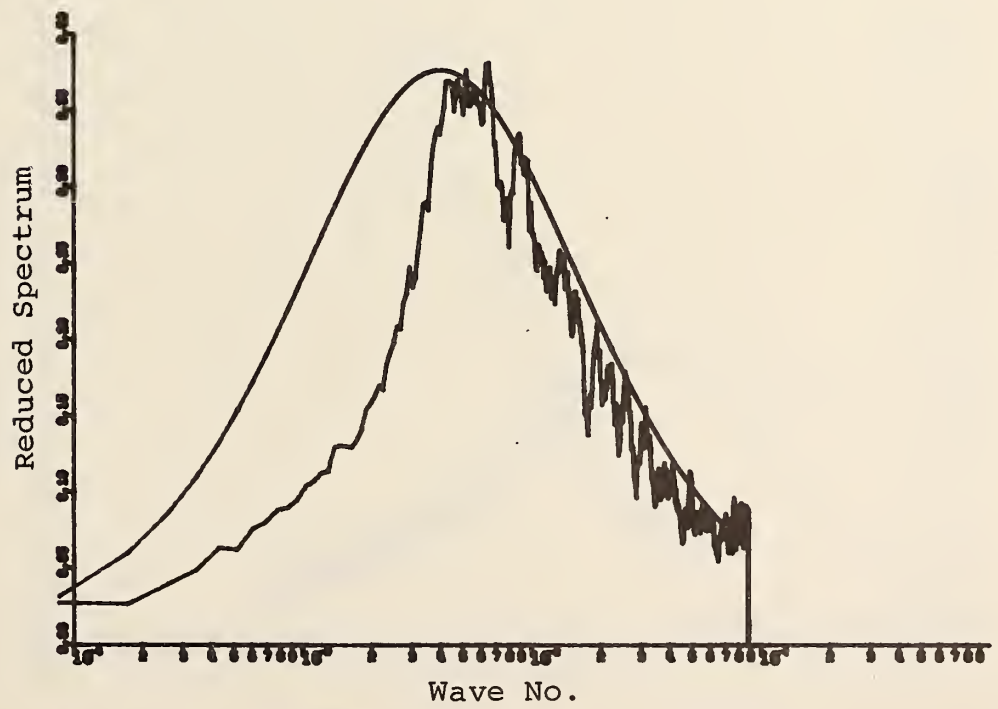

d) Vertical - 5W/R, 6W/R, 7W/R, 8W/R, 9W/R.

Figure 15. Five-channel average horizontal and vertical wind spectra for 35 mph wind (Newport, August 1971)(continued).

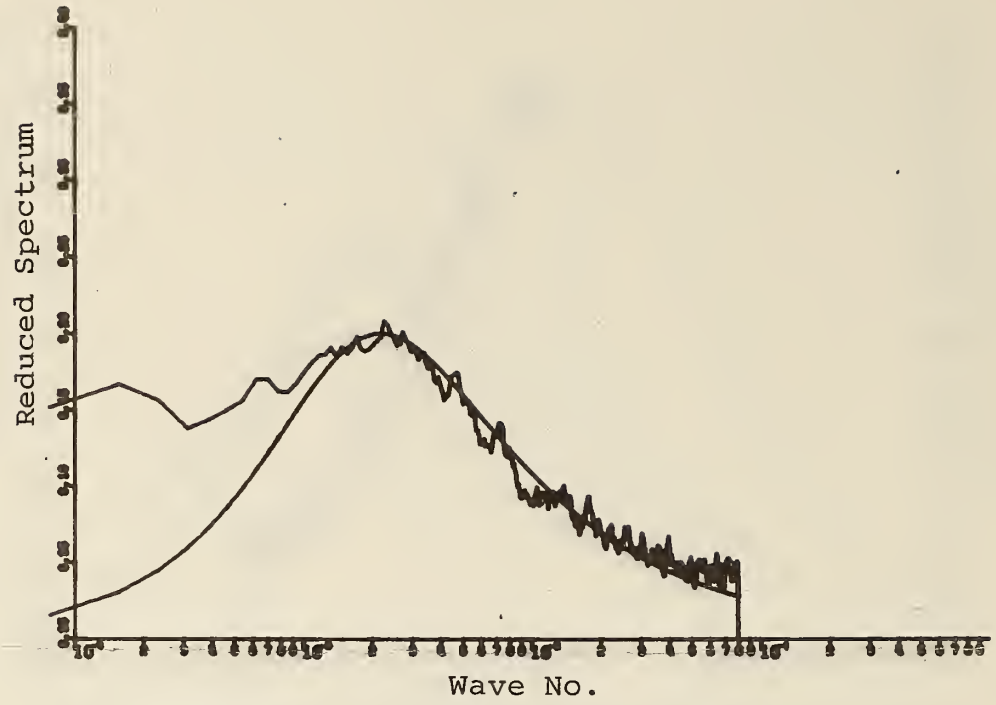

a) U-component - 5U, 6U, 7U, 8U, 9U.

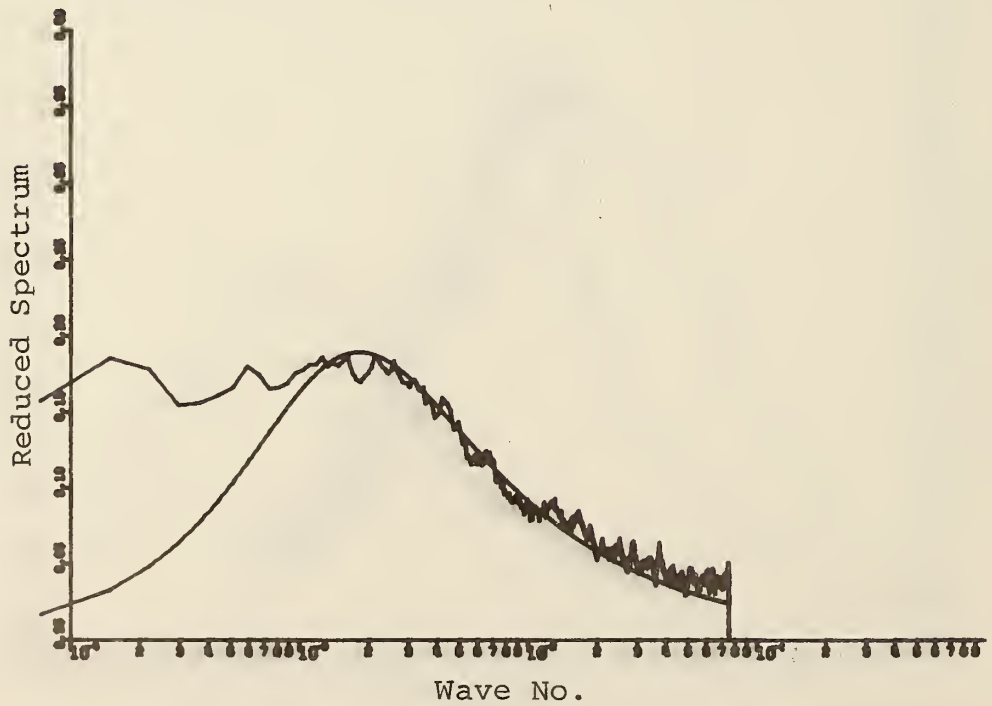

b) Resultant horizontal - 5R, 6R, 7R, 8R, 9R.

Figure 16. Five-channel average horizontal and vertical wind spectra for 50 mph wind (Newport, August 1971).

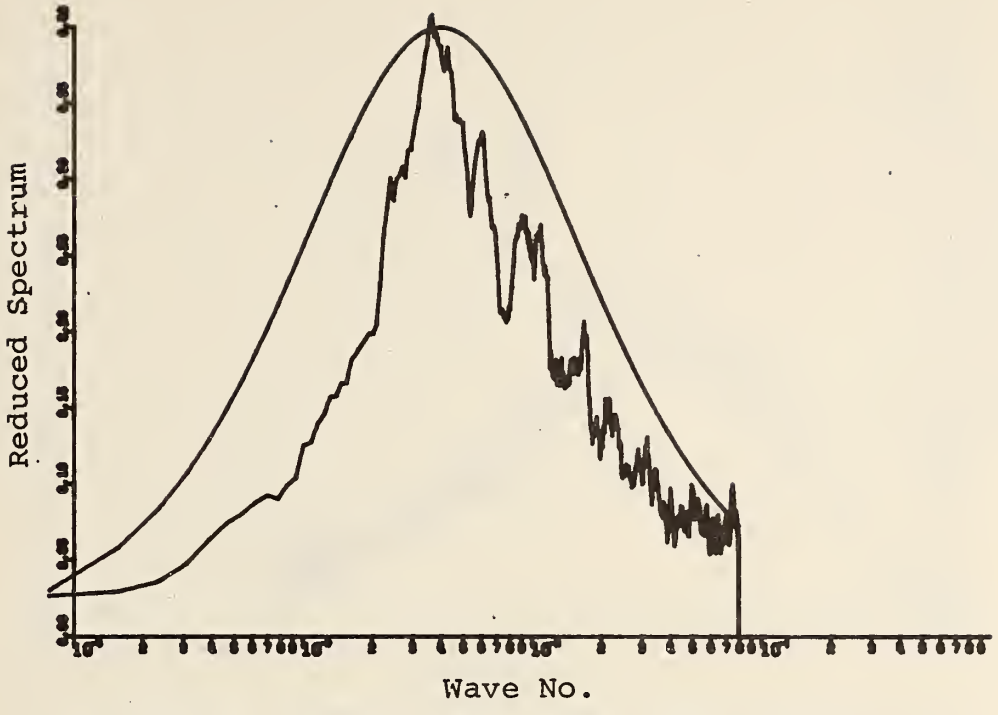

c) Vertical - 5W/U, 6W/U, 7W/U, 8W/U, 9W/U.

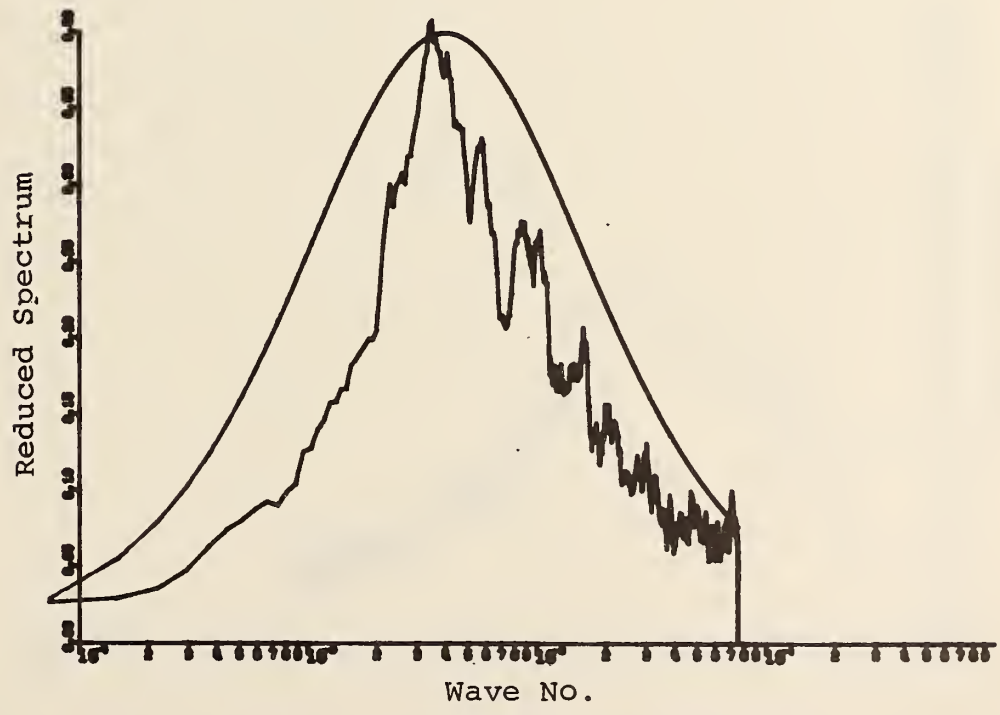

d) Vertical - 5W/R, 6W/R, 7W/R, 8W/R, 9W/R.

Figure 16. Five-channel average horizontal and vertical wind spectra for 50 mph wind (Newport, August 1971)(continued).

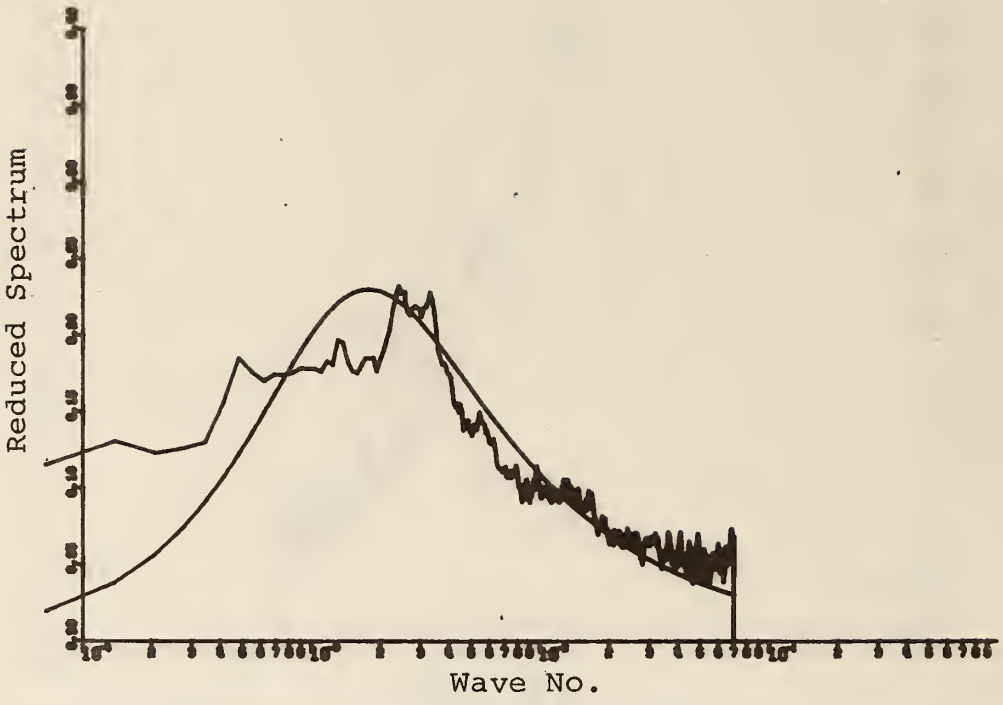

a) U-component - 5U, 6U, 7U, 8U, 9U.

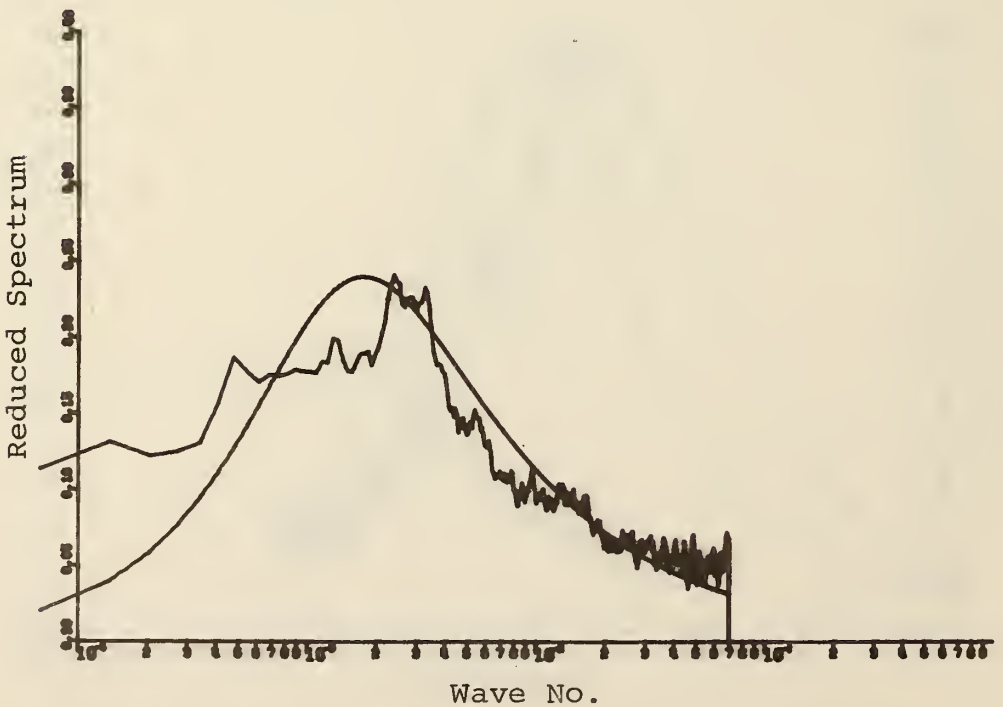

b) Resultant horizontal - 5R, 6R, 7R, 8R, 9R.

Figure 17. Five-channel average horizontal and vertical wind spectra for 60 mph wind (Newport, August 1971).

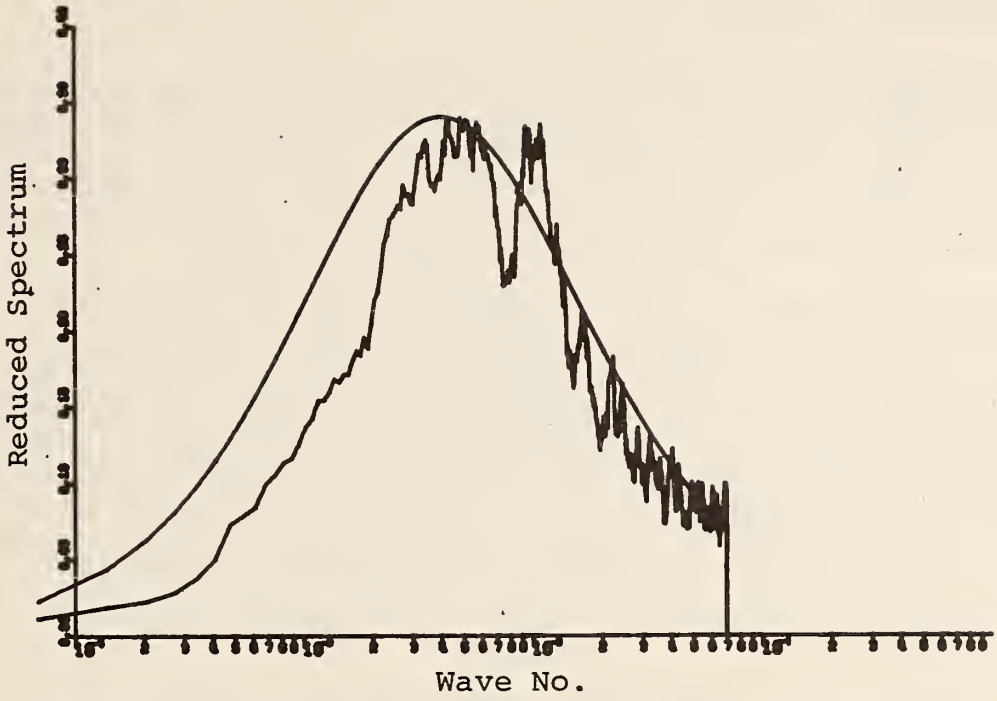

c) Vertical - 5W/U, 6W/U, 7W/U, 8W/U, 9W/U.

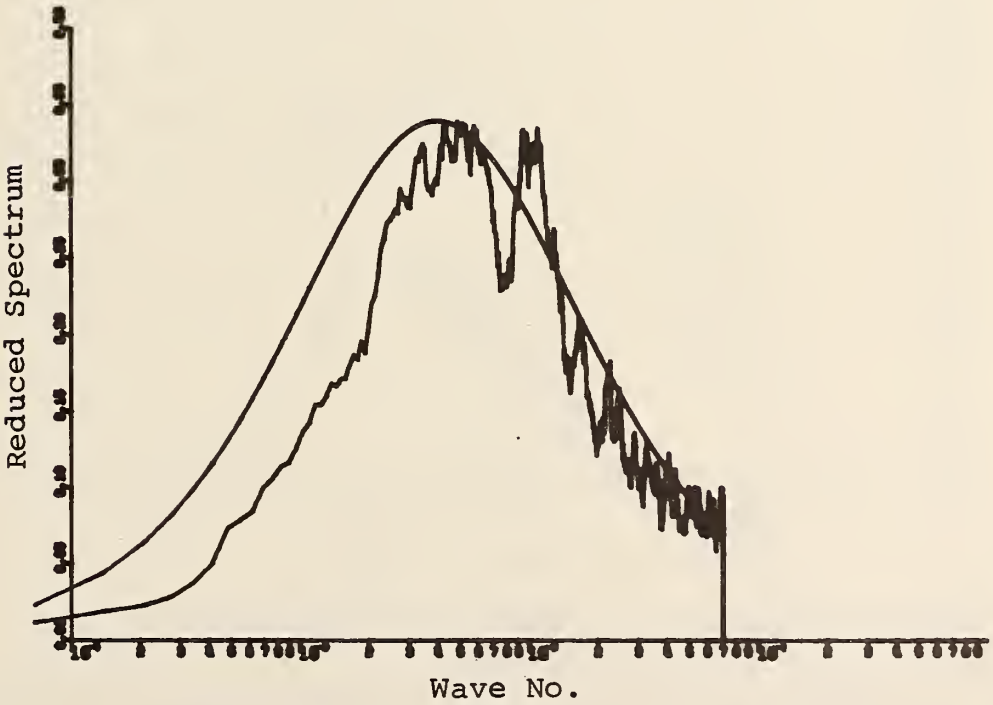

d) Vertical - 5W/R, 6W/R, 7W/R, 8W/R, 9W/R.

Figure 17. Five-channel average horizontal and vertical wind spectra for 60 mph wind (Newport, August 1971)(continued).

2.3 NEWPORT - JANUARY 1972

This section presents data recorded at the Newport bridge site in January 1972. The specific date, start and stop times associated with the data are unknown due to recorded time inaccuracies. The data are from a storm with mean wind velocities to 50 mph and gusts to 70 mph. Data from five wind sensors were processed at mean wind velocities of 40 and 50 mph.

Figure 18 compares the average vertical wind angles of attack at the mean U-component wind velocities experienced at each sensor station. Figures 19 and 20 show five-sensor, ensemble average wind spectra at the two selected wind velocities. Each figure includes separate plots of the U-component spectrum, the resultant horizontal spectrum, the vertical spectrum adjusted to the U-component velocity, and the vertical spectrum adjusted to the resultant horizontal velocity. Individual channel spectra for this recording event are included in Appendix D.

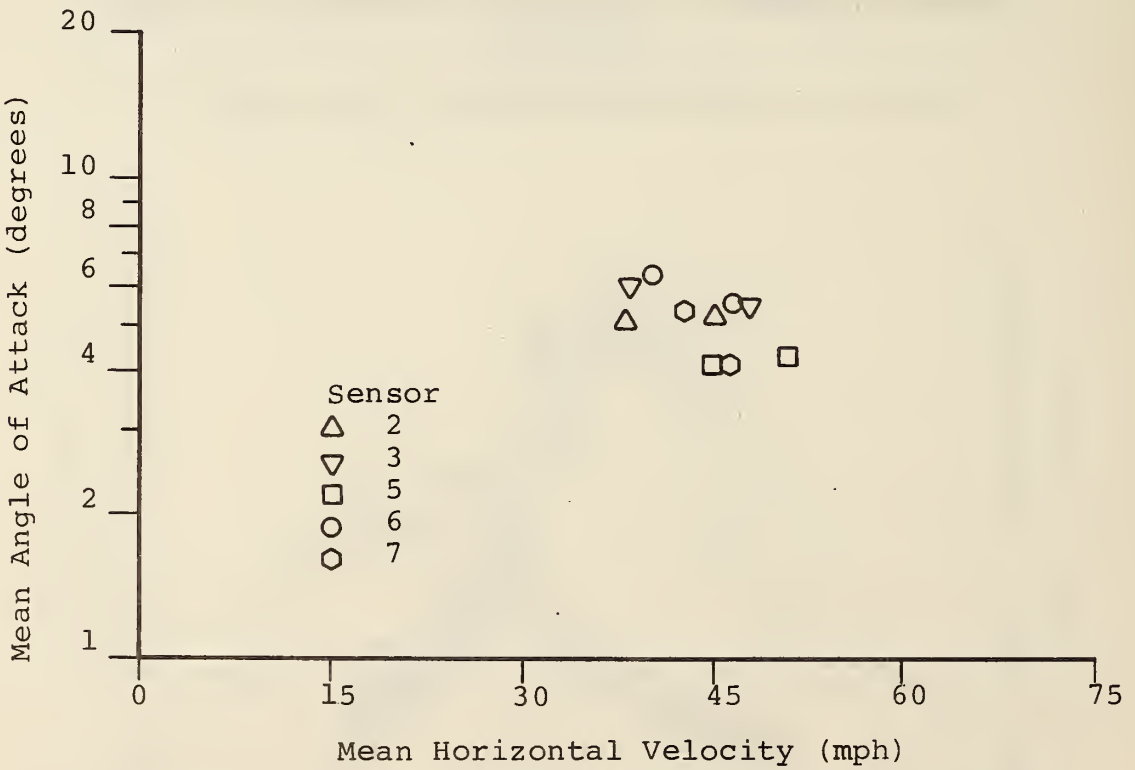

Figure 18. Angle of attack vs. wind velocity at individual sensor locations (Newport, January 1972).

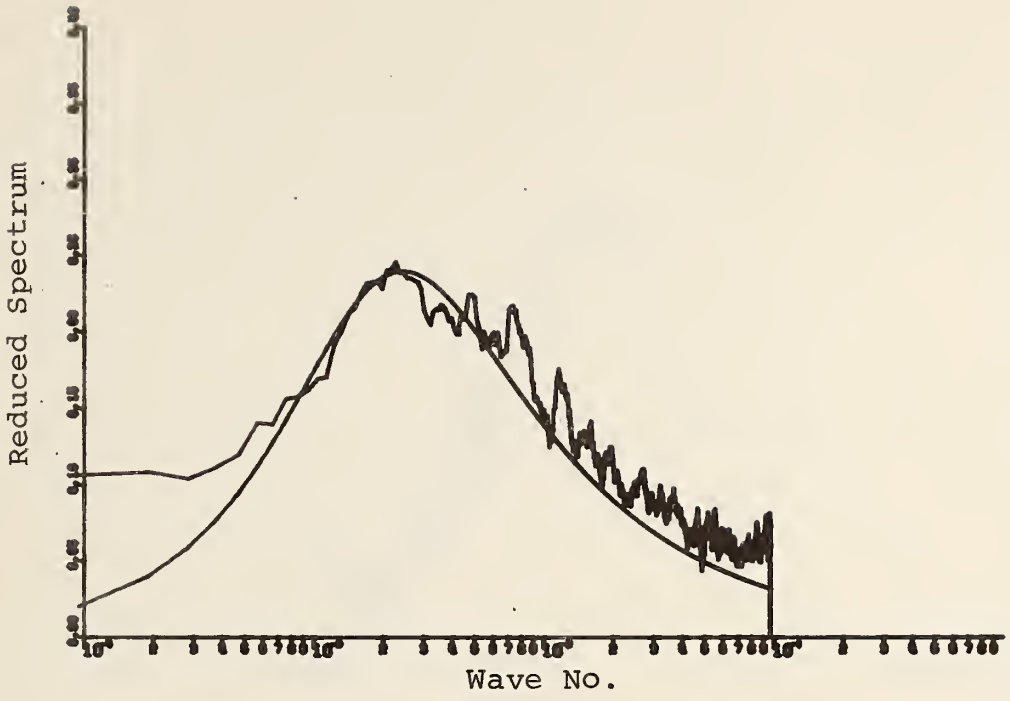

a) U-component - 2U, 3U, 5U, 6U, 7U.

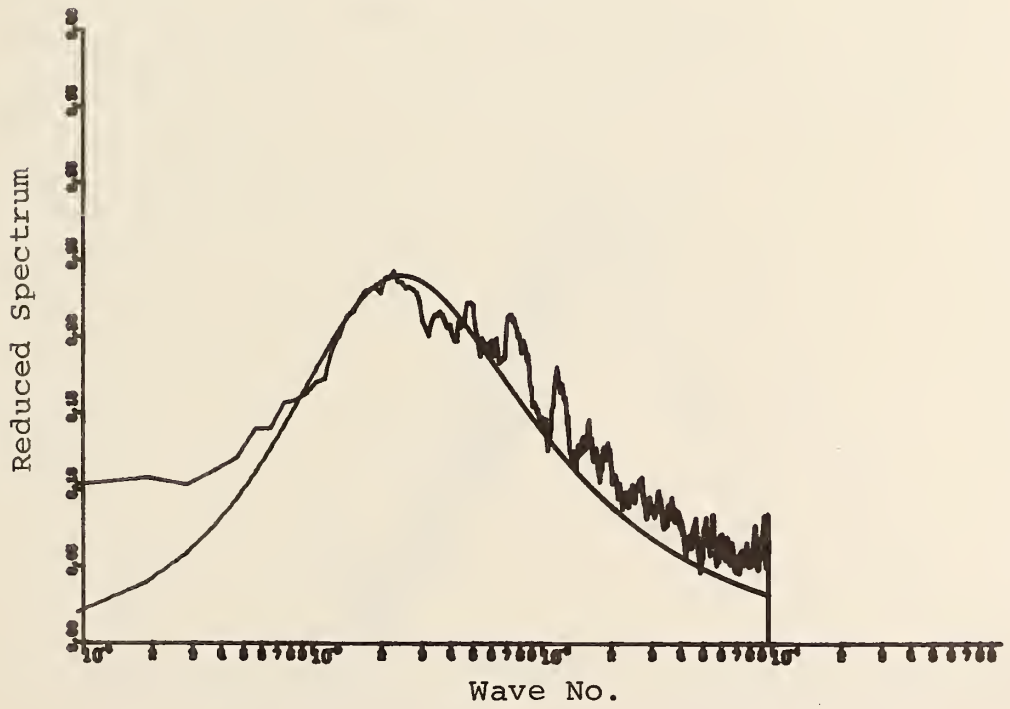

b) Resultant horizontal - 2R, 3R, 5R, 6R, 7R.

Figure 19. Five-channel average horizontal and vertical wind spectra for 40 mph wind (Newport, January 1972).

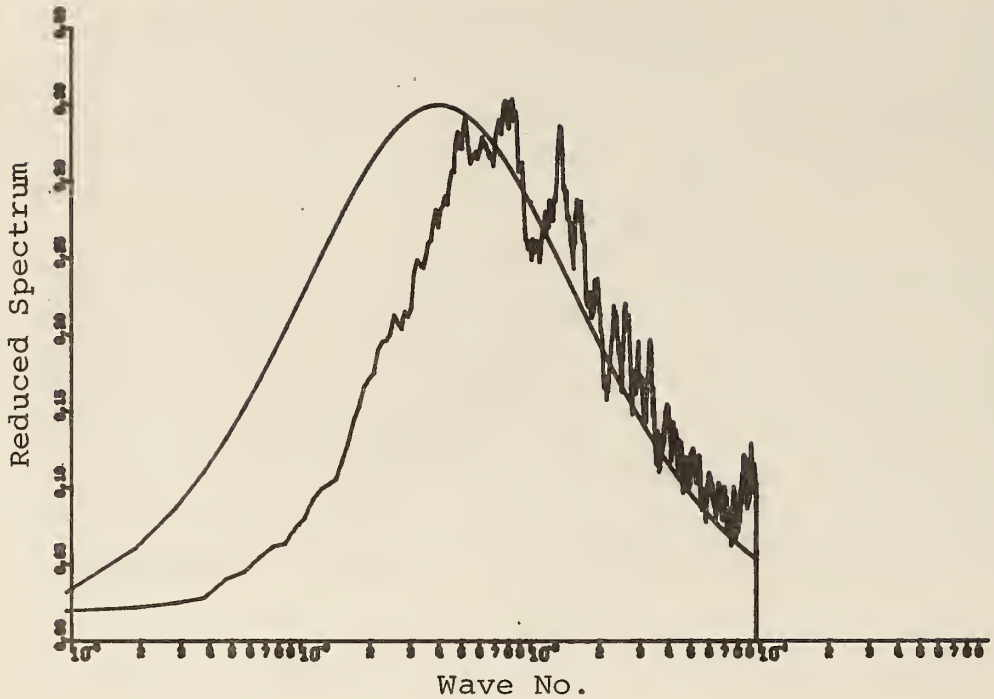

c) Vertical - 2W/U, 3W/U, 5W/U, 6W/U, 7W/U.

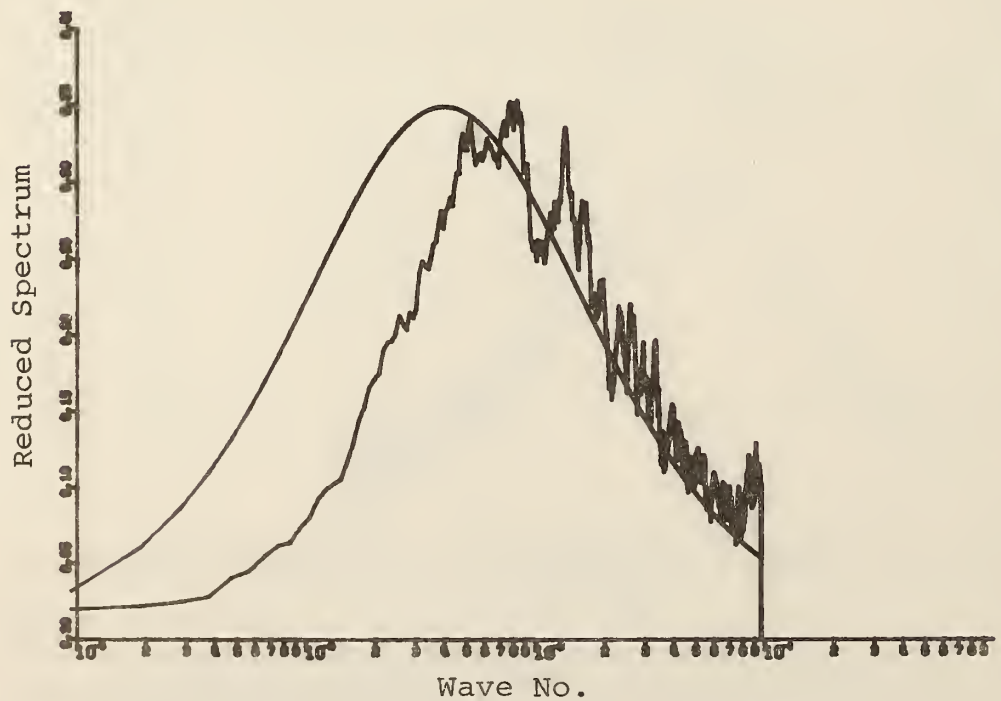

d) Vertical - 2W/R, 3W/R, 5W/R, 6W/R, 7W/R.

Figure 19. Five-channel average horizontal and vertical wind spectra for 40 mph wind (Newport, January 1972)(continued).

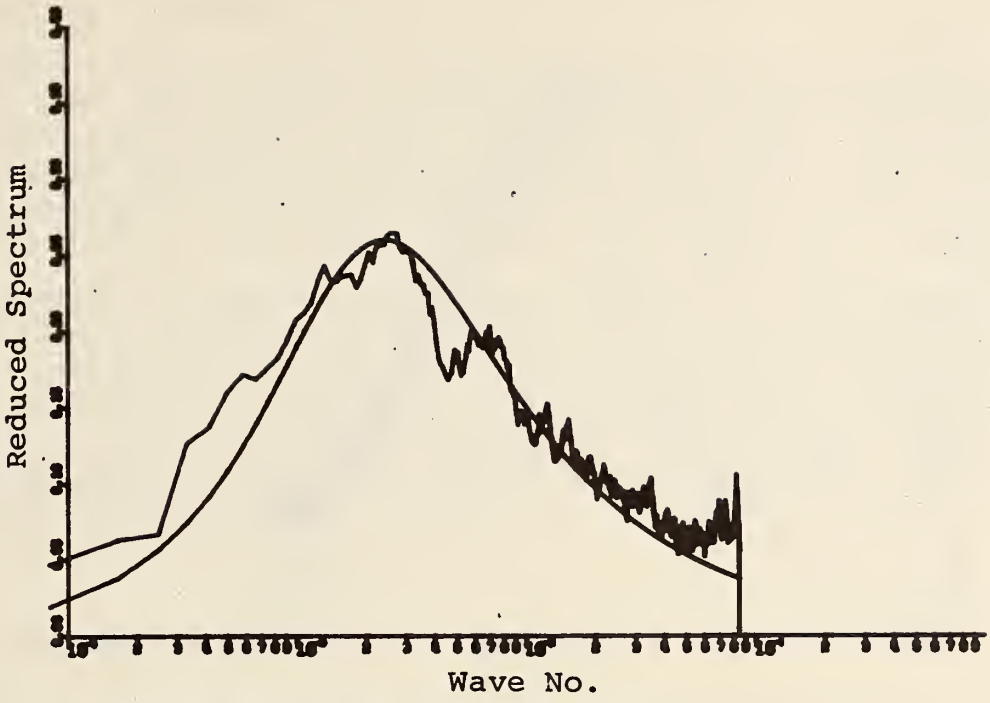

a) U-component - 2U, 3U, 5U, 6U, 7U.

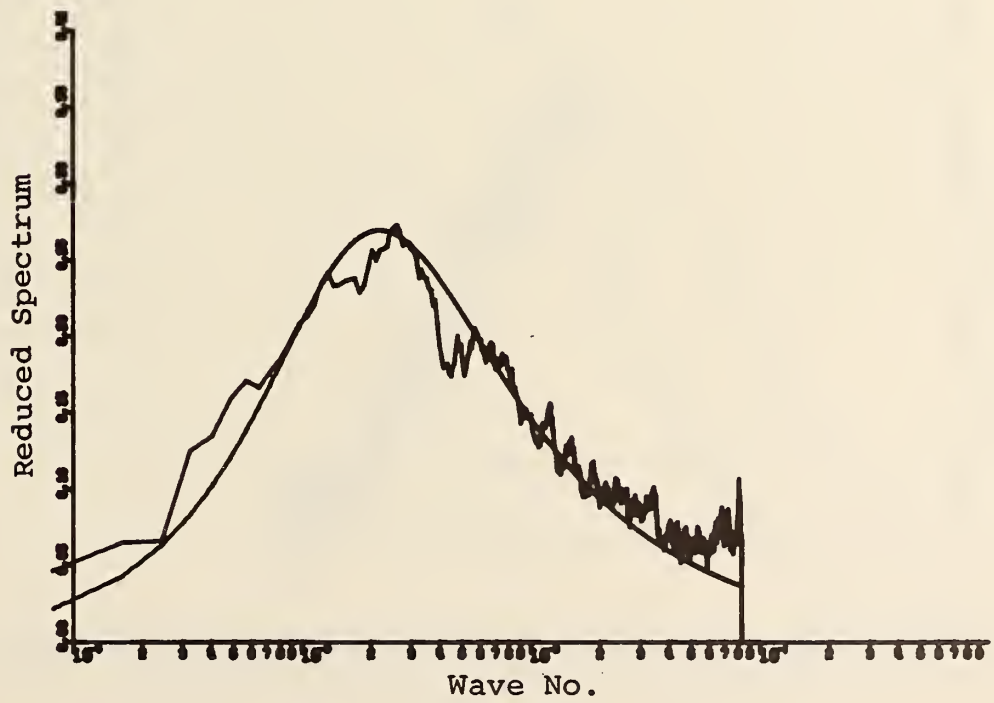

b) Resultant horizontal - 2R, 3R, 5R, 6R, 7R.

Figure 20. Five-channel average horizontal and vertical wind spectra for 50 mph wind (Newport, January 1972).

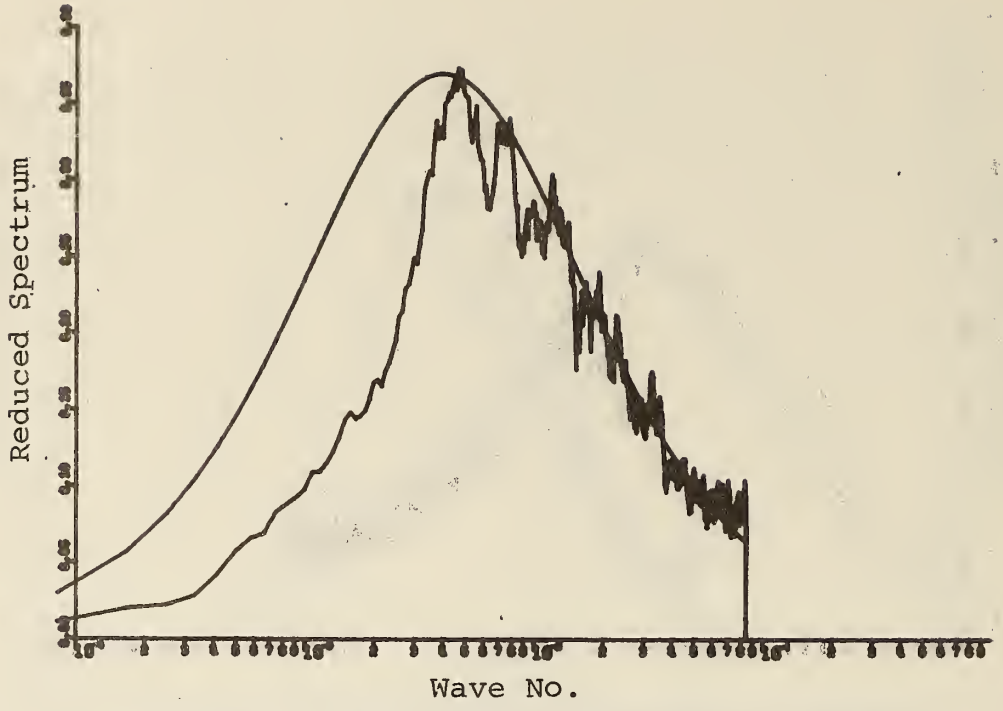

c) Vertical - 2W/U, 3W/U, 5W/U, 6W/U, 7W/U.

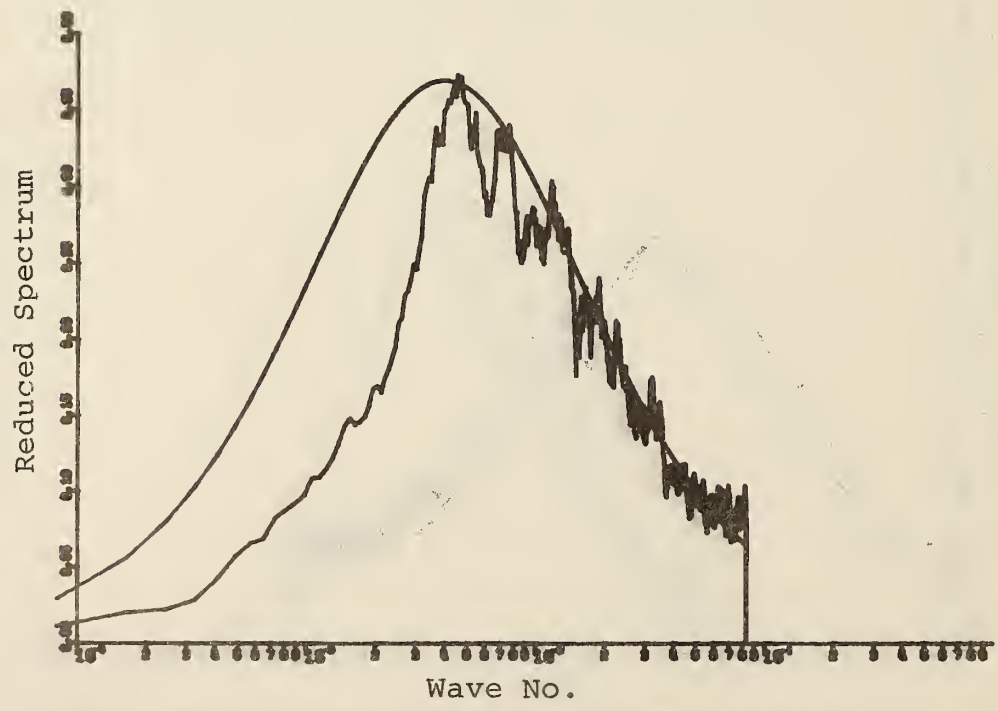

d) Vertical - 2W/R, 3W/R, 5W/R, 6W/R, 7W/R.

Figure 20. Five-channel average horizontal and vertical wind spectra for 50 mph wind (Newport, January 1972)(continued).

2.4 SITKA - NOVEMBER 1975

This section presents data recorded at the Sitka bridge site at 2218 on November 10, 1975. The processed data have a mean wind velocity of 30 mph and gusts to 50 mph. Data from four wind sensors were processed, Since the wind direction was nearly parallel to the bridge, only the resultant horizontal wind was used. U-component winds were not separately displayed.

Figure 21 compares the average vertical wind angles of attack at the mean resultant horizontal wind velocities experienced at each sensor station. Figure 22 shows four-sensor, ensemble average wind spectra at the selected wind velocity. The plot at the top of the figure is the resultant horizontal wind spectrum and the plot at the bottom is the vertical wind spectrum. Individual channel spectra for this recording event are included in Appendix E.

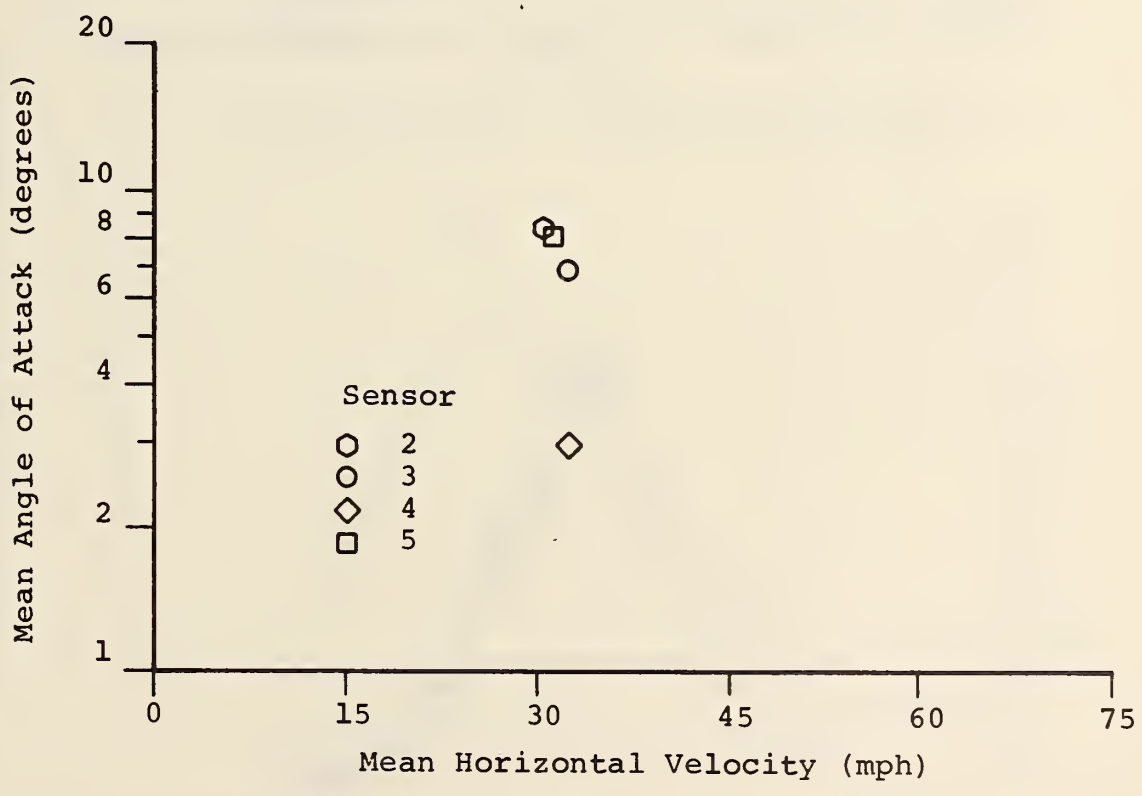

Figure 21. Angle of attack vs. wind velocity at individual sensor locations (Sitka, November 1975).

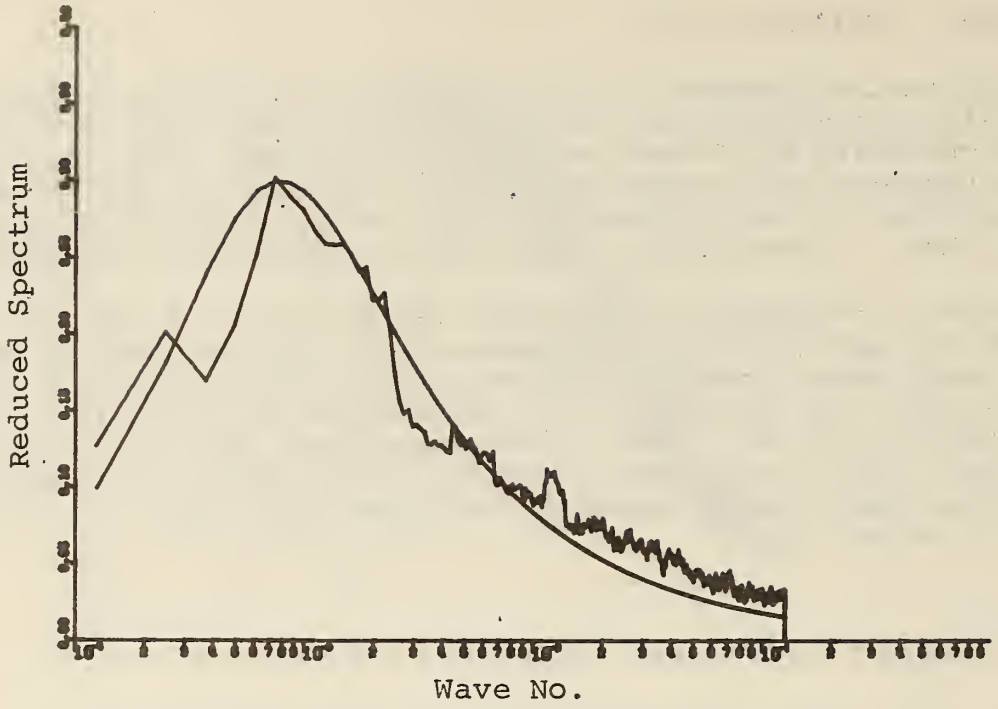

a) Resultant horizontal - 2R, 3R, 4R, 5R.

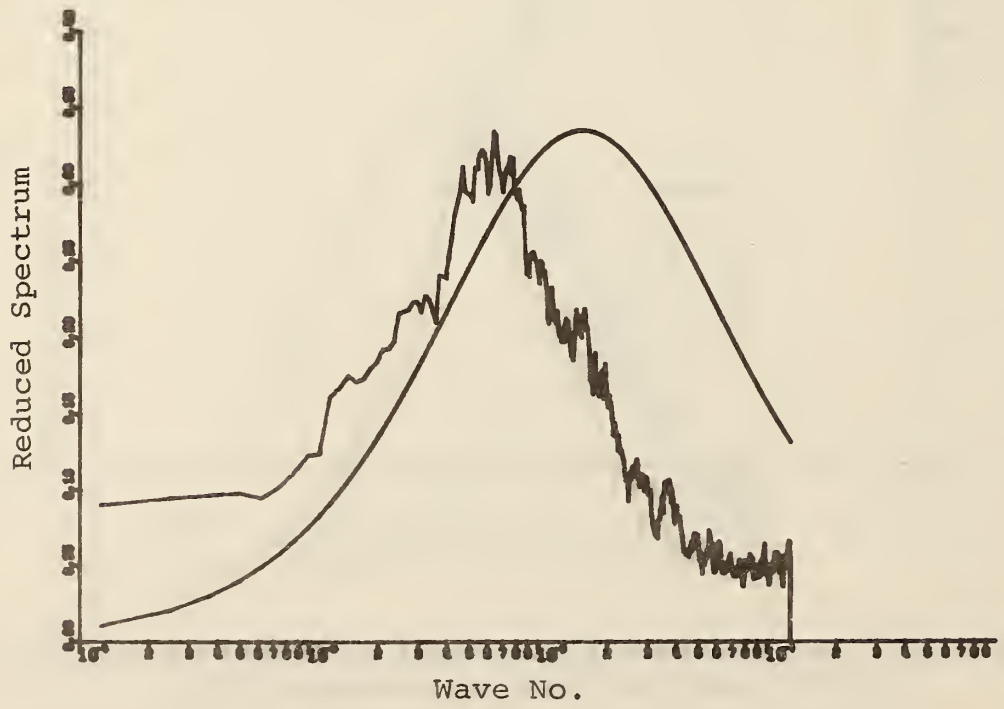

b) Vertical - 2W/R, 3W/R, 4W/R, 5W/R.

Figure 22. Four-channel average horizontal and vertical wind spectra for 30 mph wind (Sitka, November 1975).

2.5 SITKA - MAY 1976

This section presents data recorded at the Sitka bridge site at 0536 on May 9, 1976. The processed data have a mean wind velocity of 25 mph and gusts to 35 mph. Data from four wind sensors were processed. Since the wind direction was nearly parallel to the bridge, only the resultant horizontal wind was used. U-component winds were not separately displayed.

Figure 23 compares the average vertical wind angles of attack at the mean resultant horizontal wind velocities experienced at each sensor station. Figure 24 shows four-sensor ensemble average wind spectra at the selected wind velocity. The plot at the top of the figure is the resultant horizontal wind spectrum, and the plot at the bottom is the vertical wind spectrum. Individual channel spectra for this recording event are included in Appendix F.

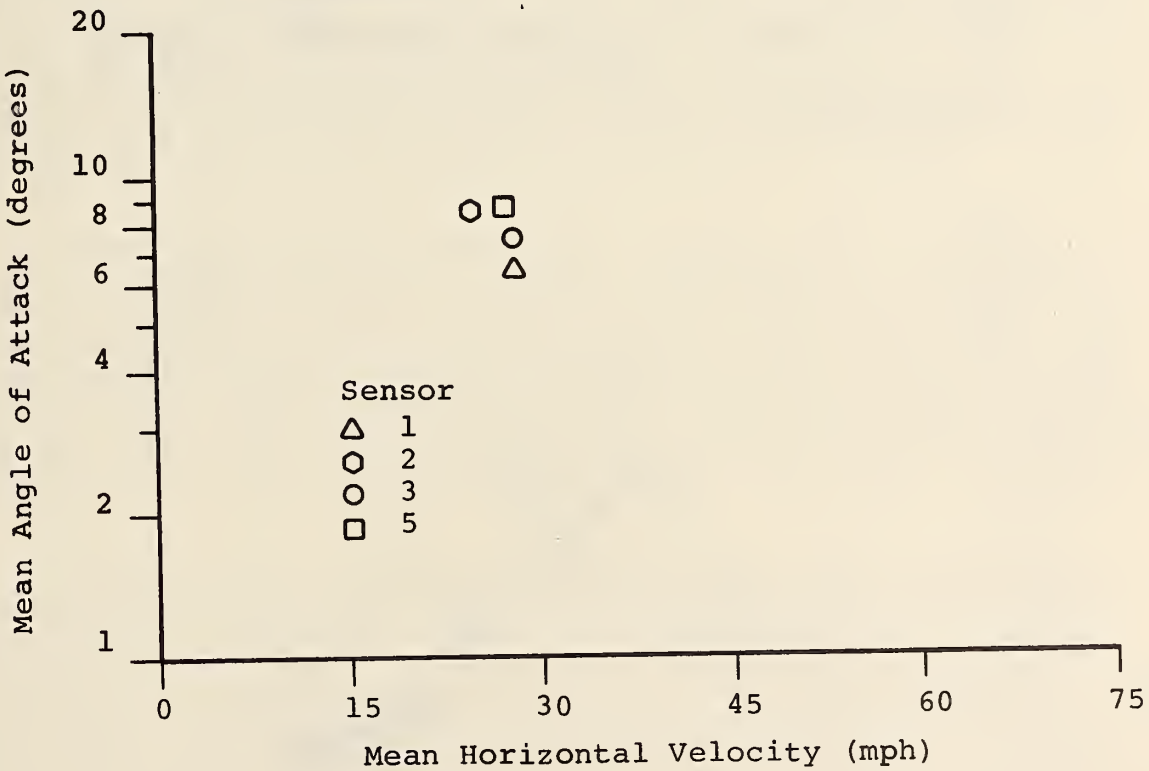

Figure 23. Angle of attack vs. wind velocity at individual sensor locations (Sitka, May 1976).

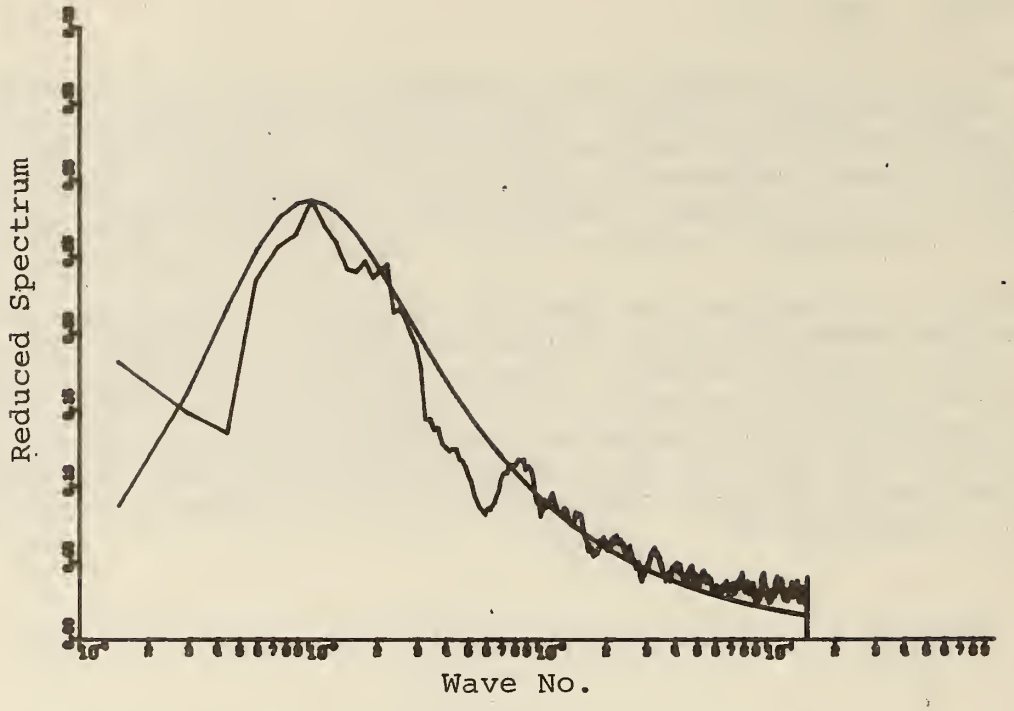

a) Horizontal - 1R, 2R, 3R, 5R.

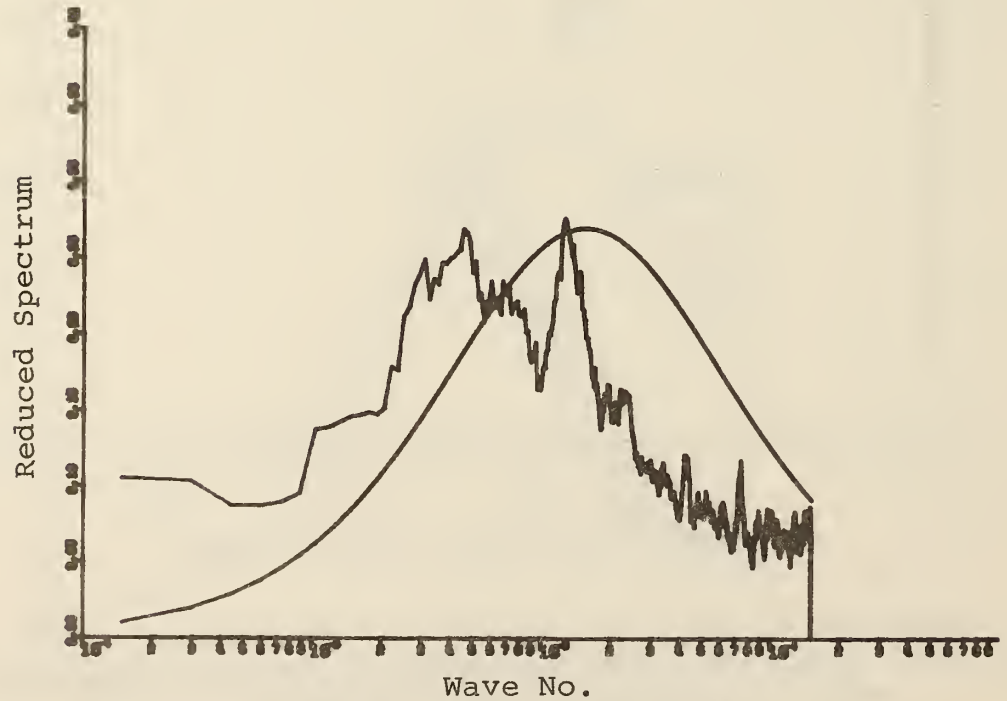

b) Vertical - 1W/R, 2W/R, 3W/R, 5W/R.

Figure 24. Four-channel average horizontal and vertical wind spectra for 25 mph wind (Sitka, May 1976).

3. BRIDGE MOTION DATA

The bridge motion data selected for analyses were recorded at Sitka on a single occasion. No other bridge motion data are available due to either instrumentation problems or to lack of significant bridge motion activity.

In this section, acceleration data are presented in the form of time history traces and spectral plots. The methods used to process the data and the results of processing are discussed. Detailed spectral plots are included in Appendix G.

3.1 PROCESSING APPROACH

Figure 25 indicates the sequence of steps used to process accelerometer data. This sequence is the same as that used to process anemometer data except for sample preparation and the conversion of terms for data presentation. Continuous 512-point data samples are used to obtain maximum discrete frequency information in distinct bridge motion events. Samples are demeaned and detrended to eliminate bias and linear drift errors, and are then tapered and transformed into the frequency domain. Conventional power density values are derived from Fourier series coefficients and the data are plotted with respect to frequency.

An example plot is shown in Figure 26. The vertical axis is power density in units of g^2/sec. The range of this axis varies from plot to plot to show the relative amplitude of frequency components within the data sample. The horizontal axis is expressed in Hertz. A time history of the tapered data sample is shown in the inset plot accompanying individual channel spectra. The ordinate is expressed in g's and the abscissa shows relative time where each mark represents 4.48 seconds (one data record).

To distinguish between frequency components representing vertical and torsional bending modes, acceleration data from instruments on opposite sides of the bridge are arithmetically summed and differenced, and spectra are produced to indicate whether the outputs of the accelerometer pairs are in-phase. The hypothesis is that in-phase data implies vertical bridge motion and out-of-phase data implies torsional bridge motion. Since frequency components in spectra of in-phase paired accelerometer data will be of greater amplitude than frequency components in spectra of individual accelerometer data, those frequencies with greater amplitudes must represent vertical bridge motion. Similarly, frequency components related to torsional bridge motion will be of lower amplitudes in spectra of paired accelerometer

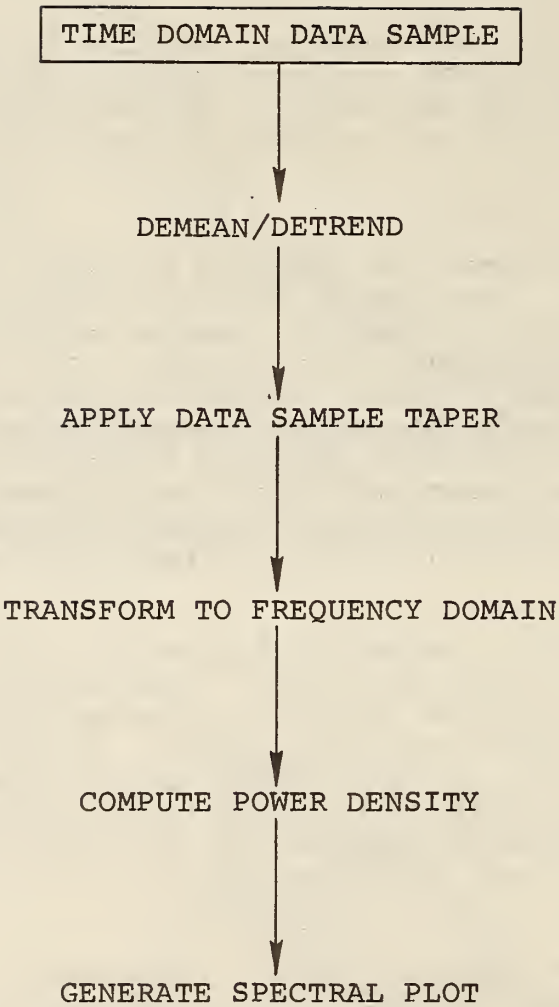

Figure 25. Functional processing sequence for acceleration data.

data, compared to spectra of individual accelerometer data. The latter components are shown by producing spectra of the arithmetic difference data between accelerometer pairs. This causes torsional frequency components to increase rather than decrease in amplitude and simplifies comparisons of spectra.

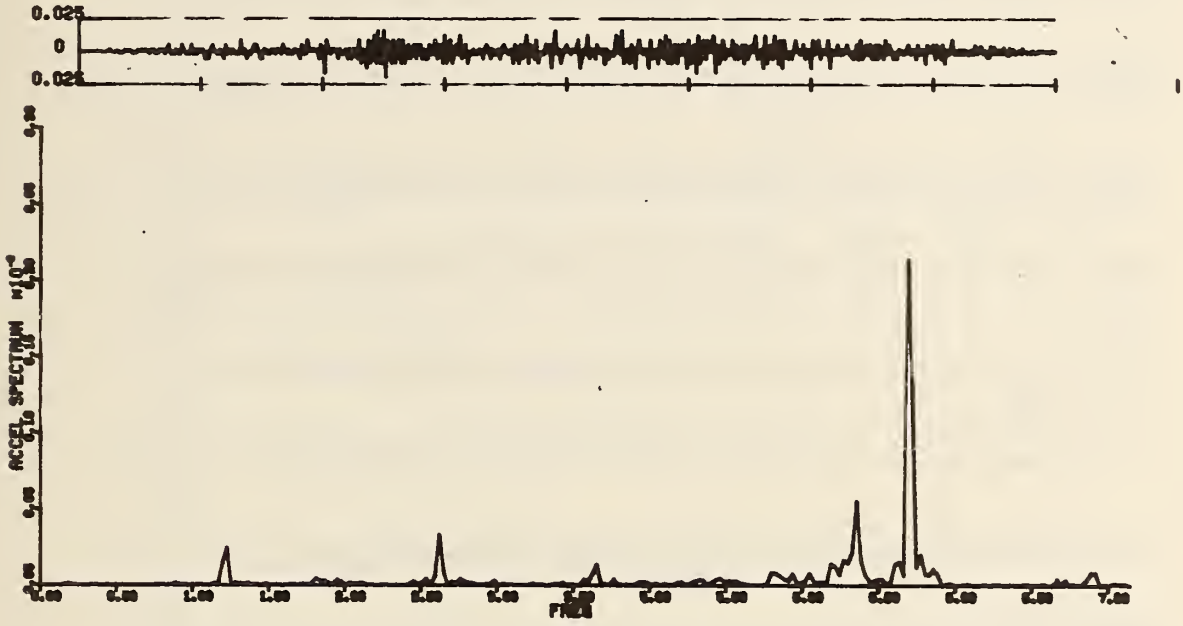

Figure 26. Example plot format of acceleration spectrum.

3.1.1 Calculation of Damping Factors

Attempts to calculate bridge structure damping factors using direct measurements of the decaying time history amplitudes proved inadequate. The calculated values were simply too low to be believable. An alternate method, however, provides factors which are both believable and consistent. This approach involves the measurement of the bandwidth, $\Delta\omega$, at the half-power points of a discrete frequency component, ω_n. These measurements are used to calculate the system damping factor, ζ, by:

$$\zeta = \frac{1}{2} \frac{\Delta\omega}{\omega_n}$$

Acceleration spectral data values are plotted and measurements are taken manually. Figure 27 is a typical plot of the discrete data points used to define a frequency component at approximately 2.65 Hz. The bandwidth of this component, .06 Hz, is measured at the indicated half-amplitude point and results in a damping factor of .011.

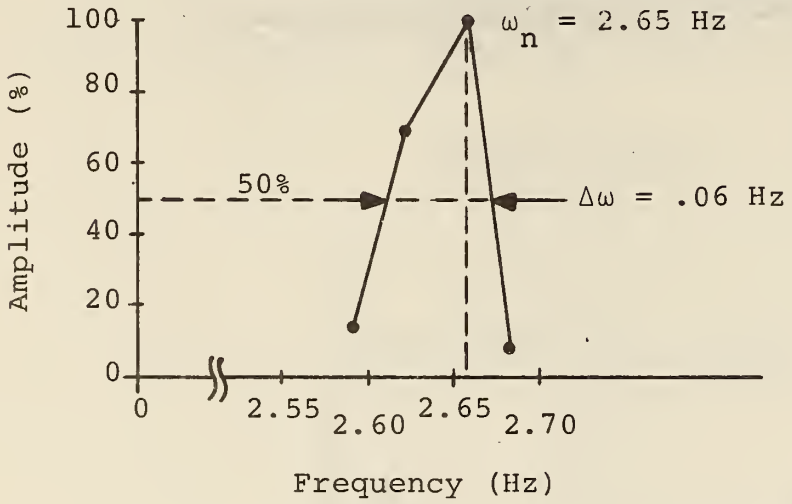

$$\zeta = 1/2 \frac{\Delta\omega}{\omega_n}$$

$$= 1/2 \times \frac{.06}{2.65}$$

$$= 0.11$$

Figure 27. Damping factor calculations for a typical acceleration spectrum frequency component.

Application of this method results in calculated damping factors between .006 and .011 for torsional vibrations and .009 to .013 for vertical vibrations. These preliminary results are based on limited acceleration data; further investigations will be based upon derived displacement data.

3.2 SITKA - DECEMBER 1975

Significant bridge motion activity occurred during a recording event on December 6, 1975. The recording system was activated by winds which reached a peak velocity of 38 mph. The system was active from 1426 to 1432. Several other recording events had occurred during the day with similar winds but lower amplitude bridge vibrations. The cause of the bridge vibrations has not been determined. Figure 28 shows a time history of data from all accelerometers during the recording event. The ordinate for the thirteen accelerometer traces is amplitude in g's

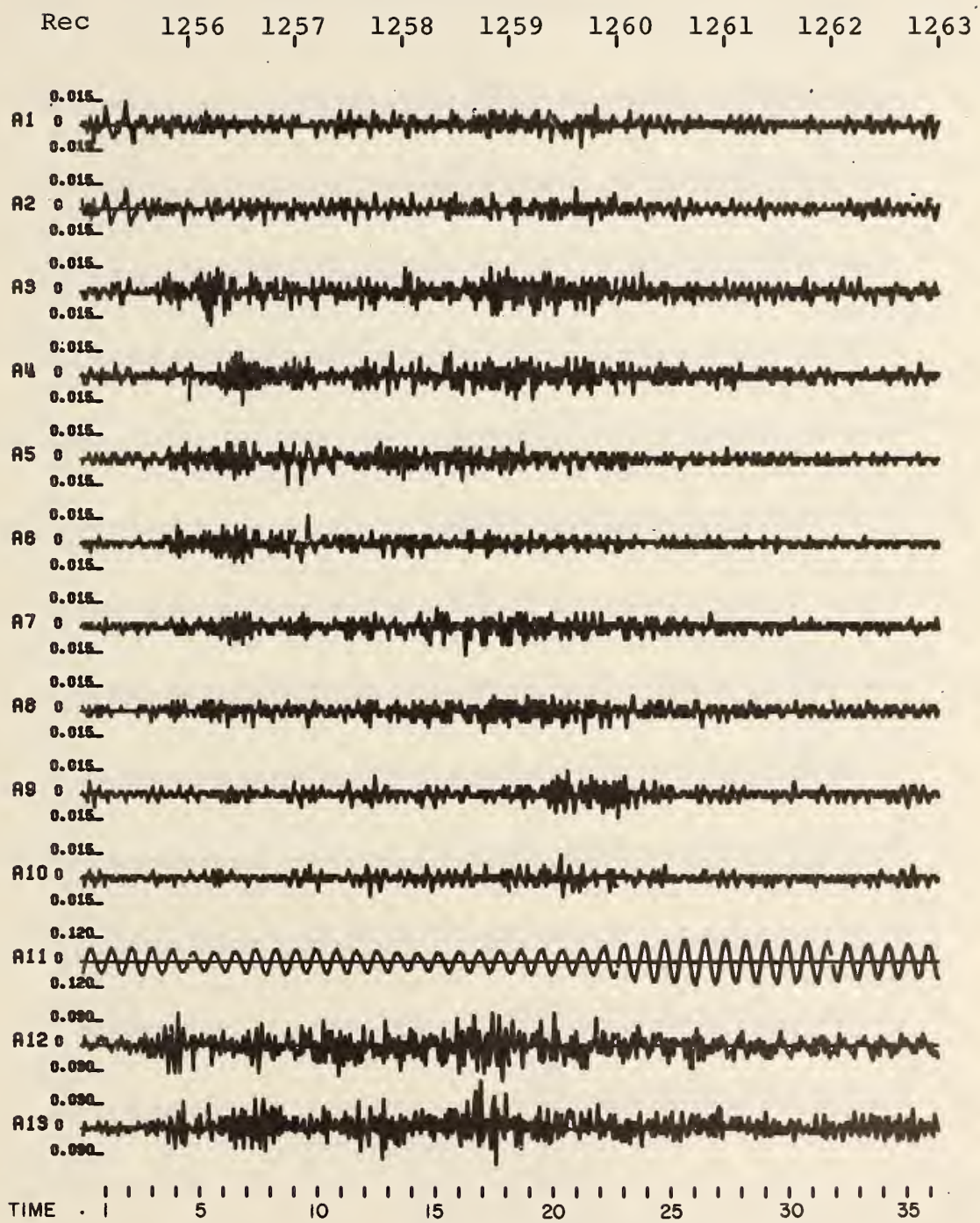

a) First bridge motion event.

Figure 28. Time history of acceleration data (Sitka, December 1975).

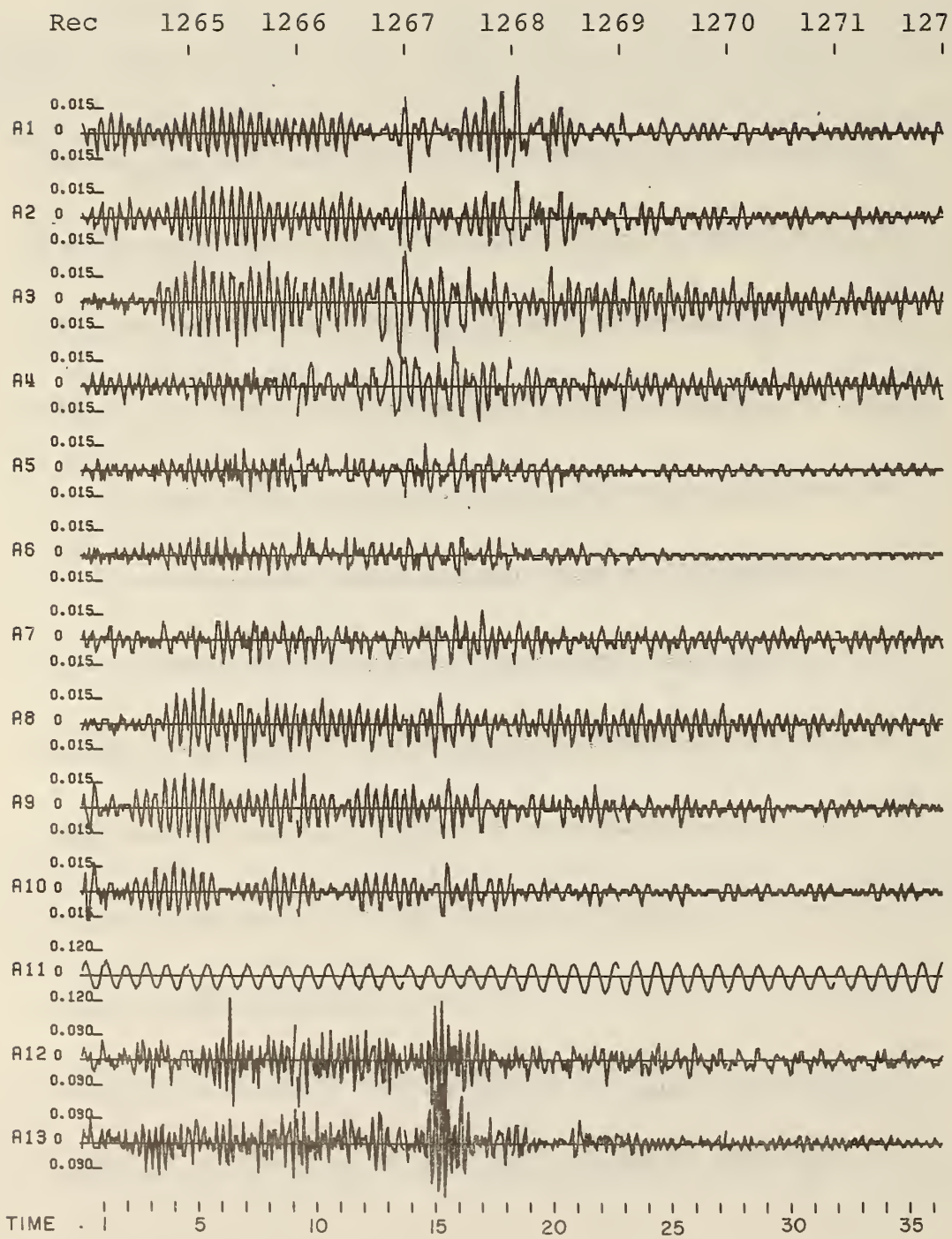

b) Second bridge motion event.

Figure 28. Time history of acceleration data (Sitka, December 1975)(continued).

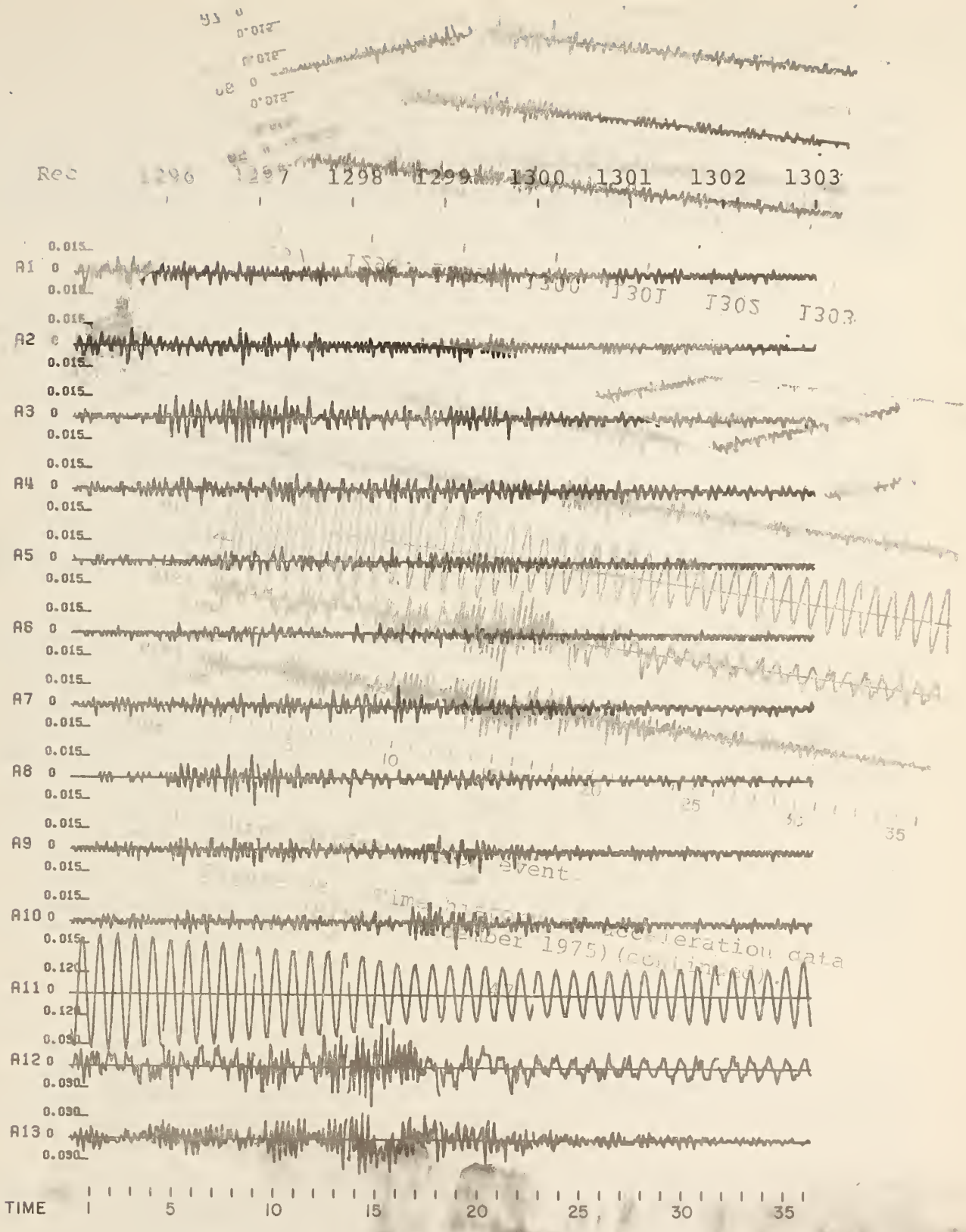

c) Third bridge motion event.

Figure 28. Time history of acceleration data (Sitka, December 1975)(continued).

and the abscissa is time. The marks at the top of the plots indicate records and the marks at the bottom of the plots indicate seconds. Three separate vibration events were defined within distinct eight record (36 seconds) intervals. Data from each of these events were processed separately because each shows somewhat different vibrational activity.

Frequency data for the events are illustrated in Figures 29 through 31. Each row of four plots shows simplified spectra for the two accelerometers on opposite sides of the bridge at a particular station; the difference or out-of-phase spectrum which corresponds to torsional bending modes; and the sum or in-phase spectrum which corresponds to vertical bending modes. The plots show the predominant frequency components for each spectrum. The detailed spectra for the accelerometers are included in Appendix G. Note that the ordinate range which is expressed in $g^2/sec \times 10^{-6}$ is constant for each row but varies from row to row and from event to event. Variation in the scale permits display of predominant frequency components while retaining a measure of absolute amplitudes.

In spectra for the three events, some frequency components increase and some decrease in both relative and absolute amplitude. Also, in comparing events, there is some variability in spectral frequency content and implied bending modes. However, based upon the hypothesis of correlation between data from the two sides of the bridge, the predominant roadbed torsional mode frequencies are 2.65 and 5.7 Hz. The predominant roadbed vertical mode frequency is 2.65 Hz. Several strong in-phase tower acceleration frequencies were present near 3.5 and 4.2 Hz and a strong out-of-phase frequency occurred at 5.7 Hz. Table 5 presents a more complete list of predominant frequencies. Note that all frequency information is based on acceleration data. Utilization of displacement data may yield slightly different results.

4. SUMMARY AND PLANS

During this reporting period, three trips were made to Sitka, Alaska, to calibrate the instrumentation. During one trip, the incremental drive tape recorders were replaced with buffered, synchronous drive recorders. The performance of the instrumentation of the new recorders has been excellent and subsequent data recordings have been virtually error free. While substantial data have been recorded, most winds have been from the southeast at moderate speeds. Since the bridge has an east-west alignment, large wind angles have been experienced rather than the anticipated zero-angle, across-deck winds. Only one bridge motion event was recorded and it may have been

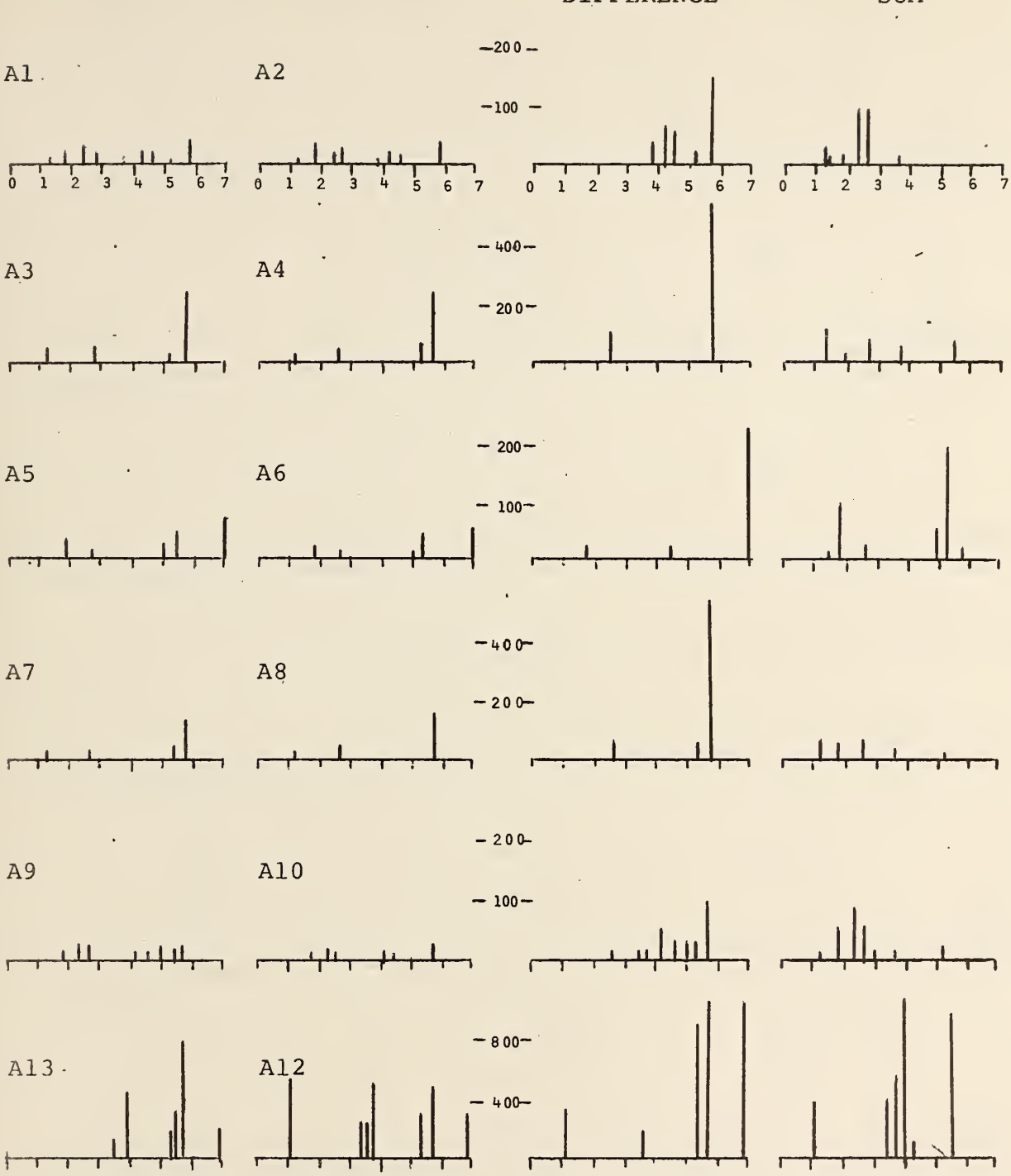

Figure 29. Simplified individual, sum and difference spectra for first bridge motion event.

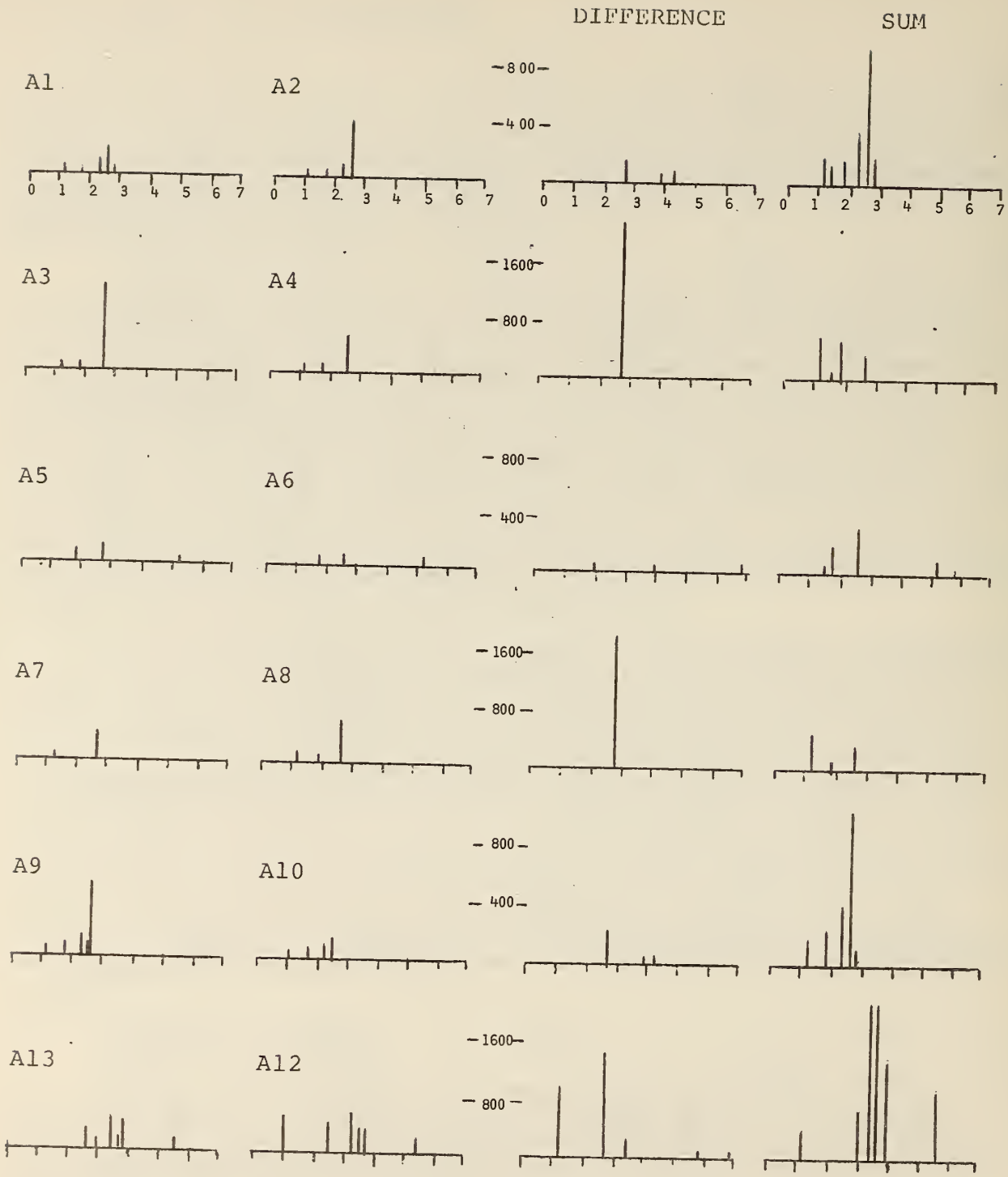

Figure 30. Simplified individual, sum and difference spectra for second bridge motion event.

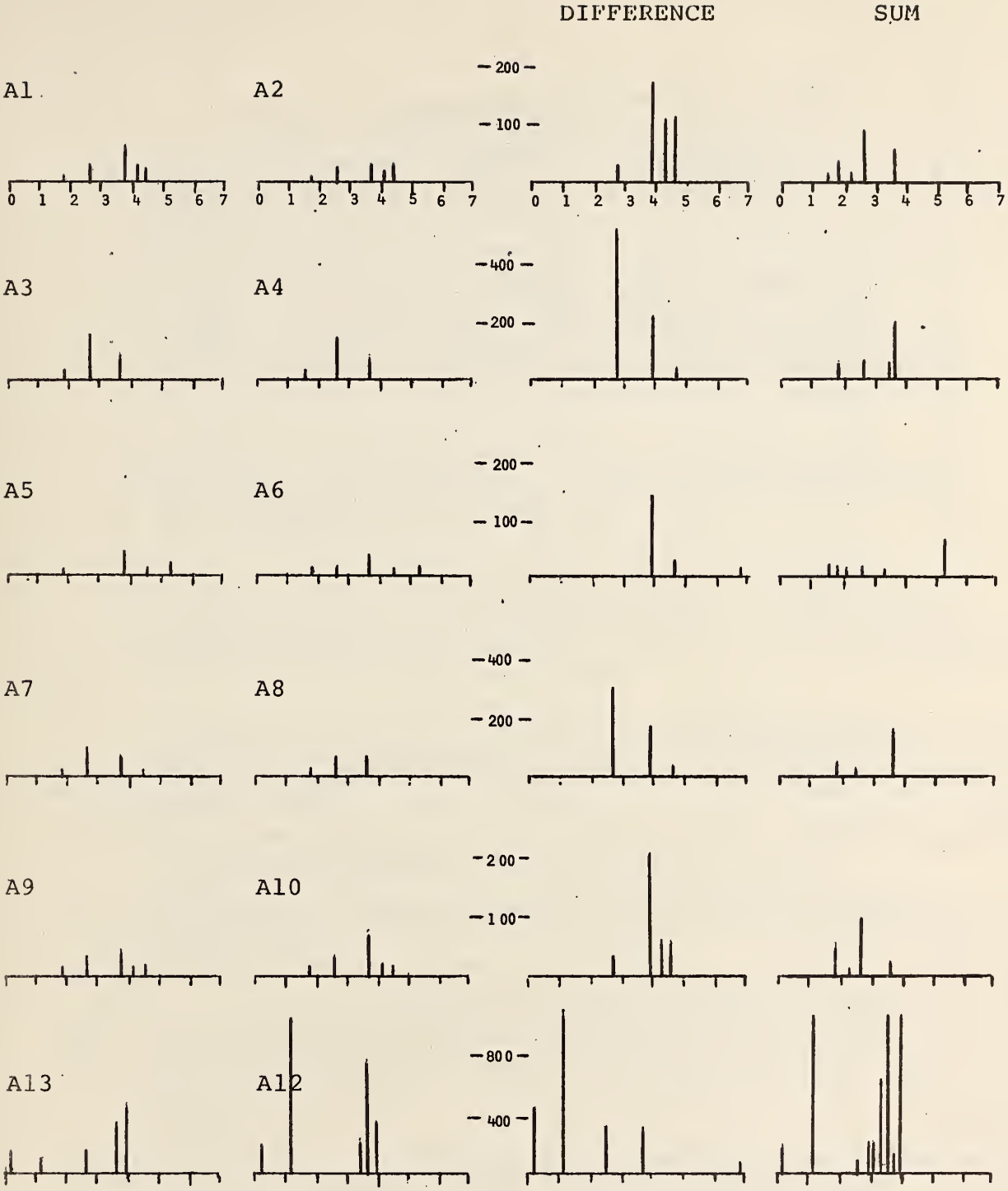

Figure 31. Simplified individual, sum and difference spectra for third bridge motion event.

Table 5. Summary of predominant spectral components during bridge motion events.

Event	Roadbed				Towers	
	Vertical	Span	Torsion	Span	In-Phase	Out-Phase
1	5.3	Mid	5.7 6.9	Qtr Mid	3.9 5.7	5.4 5.7 6.9
2	2.5	End	2.6	Qtr	3.4 3.6 3.8	2.6
3	2.6	End	2.6 3.9 3.9	Qtr Mid End	3.6 3.9	

All frequency values expressed in Hertz.

caused by vehicular traffic. Current plans are to remove the system from the Sitka Harbor bridge in the Spring, 1977, and return it for overhaul at the Federal Highway Research Station in McLean, Virginia. Other bridge sites are under evaluation as candidates for future instrumentation installations.

All data recorded at the Newport site, and data recorded at the Sitka site since the installation of the new recorders, have been cataloged. A summary of the data base is included in Appendix B. This report has presented selected data from the data base, indicative of wind and bridge motion activity at the two instrumented, long-span bridge sites. Frequency spectra of wind data have been generated to show the statistical characteristics of winds at various velocities at the two sites. Frequency spectra of bridge motion data show the predominant vibratory frequencies and bending modes of the Sitka bridge. Future efforts will involve the calculation of bridge displacement data from acceleration data. Corresponding frequency spectra will be compared. Future motion pictures of bridge motion will also be based on displacement data. Should a seismic event or significant winds initiate bridge activity at Sitka, all efforts will be directed towards the detailed analysis and correlation of bridge motions and the initiating force.

REFERENCES

1. Conte, S.D. and C. deBoor, Elementary Numerical Analysis, McGraw - Hill Book Company, New York: 1972.

2. Gade, R.H. and R.H. Scanlan, "Aspects of Hurricane Winds as Recorded at an Instrumented Suspension Bridge", Dynamic Response of Structures: Instrumentation, Testing Methods and System Identification, Proceedings of the ASCE/EMD Specialty Conference, University of California, Los Angeles: March, 1976.

3. Gerhardt, C.L. and D.D. Nelson, Monitoring and Recording Wind Velocities, Directions, and Effects at Long-Span Bridge Sites. Report No. FHWA-RD-76-10, Washington, D.C. : August, 1975.

4. Harris, R.I. "The Nature of the Wind", Modern Design of Wind Sensitive Structures. Proceedings of the Seminar held 18 June 1970 at the Institution of Civil Engineers. London: 1971

5. International Business Machines Corporation, System/360 Scientific Subroutine Package, Version III. GH20-0205-4. White Plains, New York: August 1970.

6. Melpar, Inc. Technical Proposal for an Instrumentation System to Monitor and Record Wind Velocities, Directions and Effects at Suspension Bridge Sites (A90447.602). Falls Church, Virginia: June, 1969.

7. _____. Installation and Operation Manual for an Instrumentation System to Monitor and Record Wind Velocities, Directions and Effects at Suspension Bridge Sites. Falls Church, Virginia: Undated.

8. _____. Final Report for an Instrumentation System to Monitor and Record Wind Velocities, Directions and Effects at Suspension Bridge Sites. Falls Church, Virginia: March, 1971.

9. Panofsky, H.A. and R.A. McCormick, "The Spectrum of Vertical Velocity Near the Surface," Quarterly Journal of the Royal Meteorological Society, Vol. 86, 1960.

10. Systems Technology Associates, Inc. Final Report for an Instrumentation System to Monitor and Record Wind, Seismic and Bridge Activities at Bridge Sites. Report No. STA-031-001. Falls Church, Virginia: July, 1973

11. _____. Final Report for a Software System to Analyze Wind Sensor and Accelerometer Data Acquired at Bridge Sites. Report No. STA-031-002. Falls Church, Virginia: July 1973

12. _____. Final Report for an Instrumentation System to Monitor and Record Wind, Seismic and Bridge Activities at Bridge Sites. Report No. STA-031-010. Falls Church, Virginia: July, 1974.

13. _____. Final Report for a Software System to Analyze Wind Sensor and Accelerometer Data Acquired at Bridge Sites. Report No. STA-031-020. Falls Church, Virginia: July, 1974.

APPENDIX A

CHRONOLOGY OF SIGNIFICANT PROJECT EVENTS

APPENDIX A

CHRONOLOGY OF SIGNIFICANT PROJECT EVENTS

06/30/69	Contract awarded to Melpar (American Standard, Inc.) to design, fabricate, and install the instrumentation system.
09/20/69	Survey of Newport, Rhode Island, bridge site.
10/26/70	System installed on Newport Bridge.
12/28/70	Calibration and maintenance trip.
01/28/71	Accelerometers removed and returned to manufacturer for repair.
05/19/71	Sensor cables removed from bridge due to unscheduled painting of bridge.
07/01/71	Contract awarded to Systems Technology Associates, Inc. to process data and service instrumentation system.
08/16/71	Reinstall instrumentation on west half of bridge.
08/28/71	Tropical Storm DORIA.
08/31/71	Trip to Newport bridge to retrieve data tapes.
01/16/72	Reinstall instrumentation on east half of bridge.
02/09/72	Trip to bridge to retrieve data tapes.
02/24/72	Calibration and maintenance trip. Shelter constructed for instrumentation.
03/20/72	Calibration and maintenance trip.

04/24/72 Sensors disconnected and system shut down for bridge repainting.

06/04/72 System removed from Newport bridge site, and returned to FHRS for refurbishment.

09/30/72 System installed on Sitka, Alaska bridge.

11/09/72 Alaska Department of Highways replaced accelerometer A10.

02/12/73 Calibration and maintenance trip. Recorder #1 removed and returned to manufacturer for repair.

07/09/73 Calibration and maintenance trip. Recorder #1 reinstalled.

09/18/73 Presentation on project given at annual conference on Federally Coordinated Program of R&D in Highway Transportation, San Francisco.

10/09/73 Trip to bridge site. Tower motion study.

04/15/74 Calibration and maintenance trip. Installed line-voltage and power-up monitors.

08/15/74 Calibration and maintenance trip. Replaced accelerometers A3, A4.

11/--/74 Automobile accident on bridge damaged sensor cables.

12/16/74 Calibration and maintenance trip. Repaired cables from automobile accident. Replaced accelerometers A1, A2.

05/11/75 Calibration and maintenance trip. Refurbished anemometers, relocated accelerograph, replaced accelerometer A9.

08/24/75 Calibration and maintenance trip. Installed new tape recorders. Replaced accelerometers A2, A4, A8, A11. Replaced anemometers at W3, W4, W5.

09/19/75 Presentation on project given at annual conference on Federally Coordinated Program of R&D in Highway Transportation, Minneapolis.

10/29/75 Calibration and maintenance trip. Repaired tape recorder #1 and faulty sensor cables. Replaced anemometers at W2.

03/19/76 Calibration and maintenance trip.

APPENDIX B

DATA BASE SUMMARY

NEWPORT DATA

Tape	Event	Date	Begin	End	Duration (Hr:Min)	Type	Wind Azm/Vel (°/mph)	Max Gust (mph)	Comments
WIND01	1	08/28/71	-	-	8:10	Wind	200/50	83	T/S DORIA
WIND04	1	01/26/72	-	-	10:59	Wind	200/45	73	
WIND05	1	01/--/72	-	-	6:55	Wind	260/39	36	
WIND06	1	02/--/72	-	-	5:54	Wind	110/46	68	
WIND06	2	02/13/72	-	-	0:46	Wind	210/28	42	
WIND06	3	02/15/72	-	-	2:08	Wind	290/24	45	
WIND11	2	04/06/72	-	-	0:52	Wind	220/27	38	
WIND11	3	04/--/72	-	-	8:03	Test	200/26	35	
WIND12	1	04/--/72	-	-	11:10	Test	245/18	25	
WIND13	1	04/--/72	-	-	4:50	Test	160/22	40	

SITKA DATA

Tape	Event	Date	Begin	End	Duration (Hr:Min)	Type	Wind Azm/Vel (°/mph)	Max Gust (mph)	Comments
010419	4	11/10/75	1811	1815	0:04	Wind	098/25	37	
010419	5	11/10/75	1905	1909	0:04	Wind	103/26	35	
010419	6	11/10/75	1916	1931	0:15	Wind	100/28	43	
010419	7	11/10/75	1936	2158	2:22	Wind	105/30	48	
010419	8	11/10/75	2219	2242	0:23	Wind	104/31	51	
010419	9	11/10/75	2254	2348	0:54	Wind	100/31	50	
010419	10	11/10/75	2357	0027	0:30	Wind	113/27	51	
010419	11	11/11/75	0036	0139	1:02	Wind	099/32	60	
010419	12	11/11/75	0158	0204	0:05	Wind	103/25	40	
010420	3	11/18/75	0454	0458	0:04	Wind	094/24	36	
010420	4	11/18/75	0520	0526	0:06	Wind	098/27	37	
010420	5	11/18/75	0931	0946	0:14	Wind	094/28	40	
010420	6	11/18/75	1011	1016	0:05	Wind	096/25	34	
010420	7	11/18/75	1948	2005	0:17	Wind	097/29	45	
010420	8	11/18/75	2045	2104	0:20	Wind	098/27	44	
010420	9	11/20/75	2136	2140	0:04	Wind	102/24	36	
010426	1	11/22/75	1859	1910	0:11	Wind	100/27	42	

SITKA DATA (continued)

Tape	Event	Date	Begin	End	Duration (Hr:Min)	Type	Wind Azm/Vel (°/mph)	Max Gust (mph)	Comments
010426	1	11/22/75	1859	1910	0:11	Wind	100/27	42	
010426	2	11/22/75	2101	2114	0:13	Wind	093/28	44	
010426	3	11/23/75	0519	0535	0:16	Wind	098/28	45	
010426	4	11/23/75	0553	0611	0:18	Wind	094/26	44	
010426	5	11/23/75	0624	0628	0:04	Wind	098/23	42	
010426	6	12/01/75	1117	1229	1:12	Wind	100/31	45	
010426	7	12/01/75	1236	1248	0:12	Wind	104/28	36	
010426	8	12/01/75	1309	1313	0:04	Wind	100/27	36	
010421	1	12/05/75	0108	0115	0:07	Wind	097/28	37	
010424	2	12/06/76	1212	1243	0:31	Wind	093/27	44	Tower motion
010424	3	12/06/75	1245	1252	0:07	Wind	095/27	47	
010424	4	12/06/75	1253	1316	0:23	Wind	095/28	46	Deck motion
010424	5	12/06/75	1321	1332	0:11	Wind	091/25	42	
010424	6	12/06/75	1409	1419	0:09	Wind	092/29	45	
010424	7	12/06/75	1427	1433	0:06	Wind	092/25	38	Deck motion
010424	8	12/06/75	1527	1546	0:19	Wind	093/27	49	
010424	9	12/06/75	1550	1554	0:04	Wind	095/27	39	Deck motion
010424	10	12/13/75	1557	1607	0:11	Wind	097/28	50	

SITKA DATA (continued)

Tape	Event	Date	Begin	End	Duration (Hr:Min)	Type	Wind Azm/Vel (°/mph)	Max Gust (mph)	Comments
010424	11	12/13/75	1621	1707	0:46	Wind	097/30	50	
010424	12	12/13/75	1711	1930	2:19	Wind	095/33	54	
010424	13	12/13/75	1934	1947	0:13	Wind	095/28	45	
010424	14	12/14/75	0034	0044	0:10	Wind	258/23	50	Unusual wind direction
010422	1	12/16/75	1457	1514	0:17	Wind	097/29	43	
010422	2	12/16/75	1550	1554	0:04	Wind	104/28	37	
010422	3	12/16/75	1555	1612	0:16	Wind	101/28	39	
010422	4	12/18/75	2144	2148	0:05	Wind	094/26	44	
010422	5	12/18/75	2156	2207	0:11	Wind	093/27	48	
010422	6	12/18/75	2242	2247	0:05	Wind	096/26	43	
010422	7	12/18/75	2311	2328	0:17	Wind	099/29	45	
010422	8	12/19/75	1346	1350	0:04	Wind	192/18	34	Power failed. Wind direction
010422	10	(12/19/75)	(0010)	(0013)	0:03	Wind	193/13	24	Power restored
010423	4	12/24/75	1929	1933	0:04	Wind	100/28	36	
010423	5	12/26/75	0744	0749	0:06	Wind	089/26	50	Unusual wind on 1V
010405	2	01/14/76	0112	0116	0:04	Wind	095/28	38	1V inoperative
010404	1	01/20/76	1741	1745	0:04	Wind	117/25	49	1V inoperative
010404	2	01/20/76	1809	1848	0:39	Wind	101/33	48	1V inoperative
010404	3	01/20/76	1931	1958	0:27	Wind	096/31	53	1V inoperative

SITKA DATA (continued)

Tape	Event	Date	Begin	End	Duration (Hr:Min)	Type	Wind Azm/Vel (°/mph)	Max Gust (mph)	Comments
010404	4	01/20/76	2200	2205	0:05	Wind	100/28	45	1V inoperative
010404	5	01/25/76	2220	2257	0:37	Wind	096/32	47	1V inoperative
010404	6	01/26/76	1332	1349	0:16	Wind	102/28	50	1V inoperative
010404	7	01/26/76	1457	1503	0:06	Wind	107/32	47	1V inoperative
010404	8	02/01/76	0918	0925	0:06	Wind	101/32	50	1V inoperative
010431	1	05/08/76	2250	0016	1:27	Wind	098/22	50	
010431	2	05/09/76	0139	0200	0:21	Wind	098/22	39	
010431	3	05/09/76	0212	0220	0:08	Wind	096/21	32	
010431	4	05/09/76	0222	0231	0:09	Wind	098/22	36	
010431	5	05/09/76	0233	0248	0:14	Wind	094/19	32	
010431	6	05/09/76	0250	0307	0:17	Wind	090/22	36	
010431	7	05/09/76	0313	0330	0:16	Wind	097/24	36	
010431	8	05/09/76	0331	0335	0:04	Wind	098/18	28	
010431	9	05/09/76	0436	0530	0:55	Wind	105/23	37	
010431	10	05/09/76	0539	0559	0:22	Wind	105/23	33	
010431	11	05/09/76	0606	0629	0:23	Wind	100/23	34	
010431	12	05/09/76	0633	0652	0:20	Wind	099/25	32	
010431	13	05/09/76	0654	0736	0:42	Wind	104/24	38	
010431	14	05/09/76	0730	0743	0:05	Wind	103/22	36	

SITKA DATA (continued)

Tape	Event	Date	Begin	End	Duration (Hr:Min)	Type	Wind Azm/Vel (°/mph)	Max Gust (mph)	Comments
010431	15	05/09/76	1139	1227	0:48	Wind	114/25	45	
010431	16	05/09/76	1229	1254	0:25	Wind	105/27	44	
010431	17	05/24/76	1219	1225	0:06	Wind	101/22	32	1V biased
010431	18	05/24/76	1318	1327	0:09	Wind	091/18	30	1V biased
010431	19	05/24/76	1429	1437	0:08	Wind	095/17	31	1V biased
010431	20	05/24/76	1547	1558	0:11	Wind	100/20	28	1V biased

APPENDIX C

INDIVIDUAL CHANNEL WIND SPECTRA: NEWPORT, AUGUST 1971

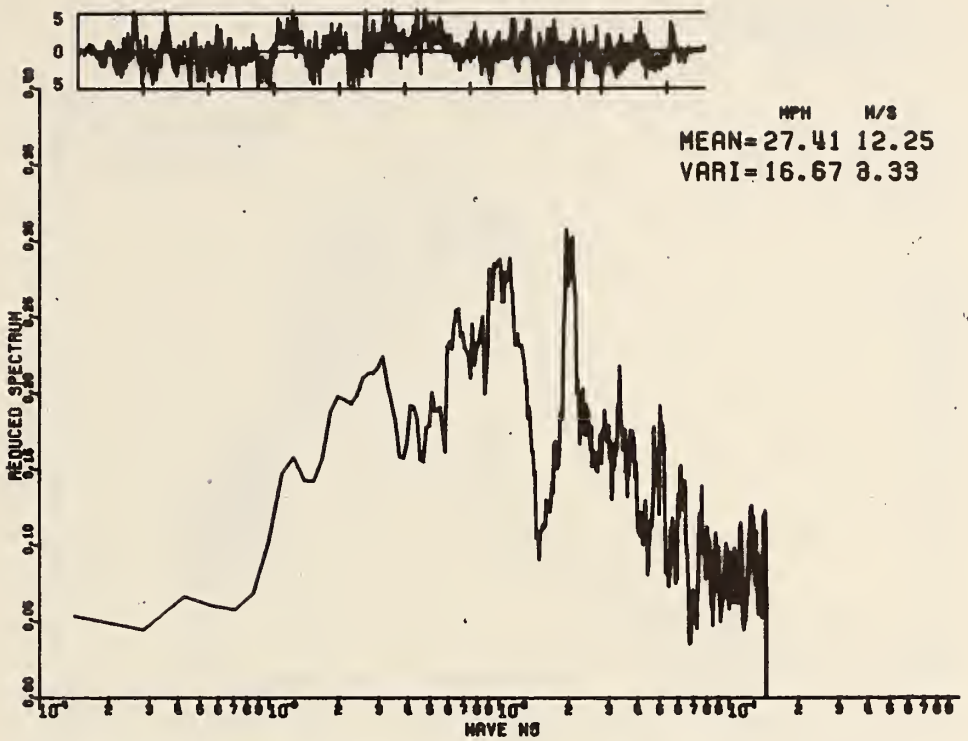

a) U-component - 5U.

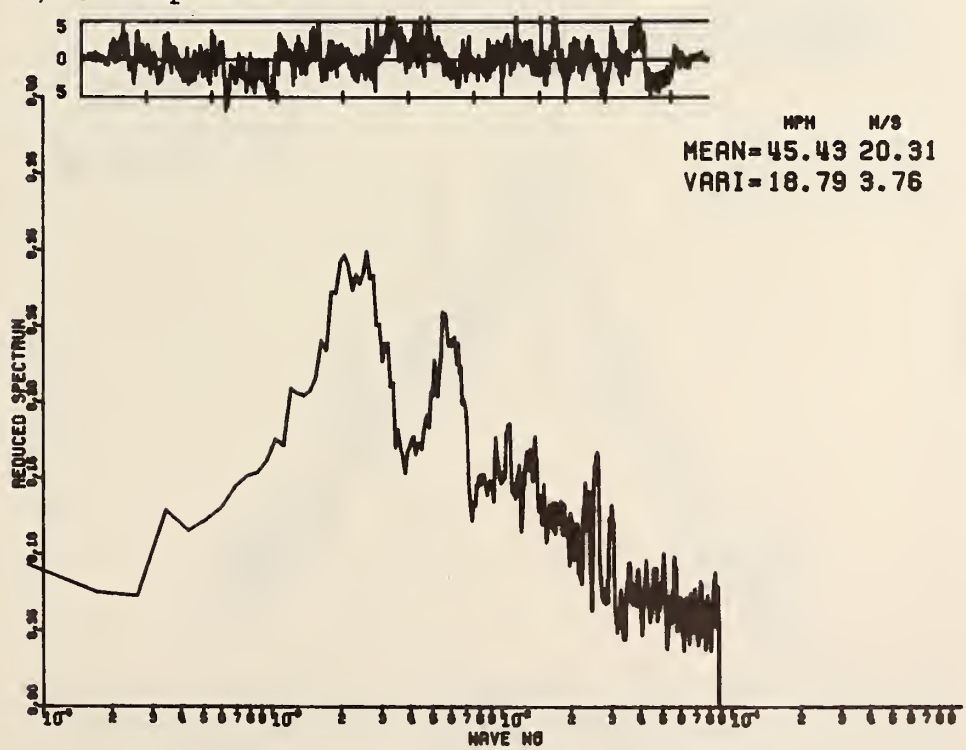

b) Resultant horizontal - 5R.

Figure 32. Individual channel horizontal and vertical wind spectra for 20 mph wind (Newport, August 1971).

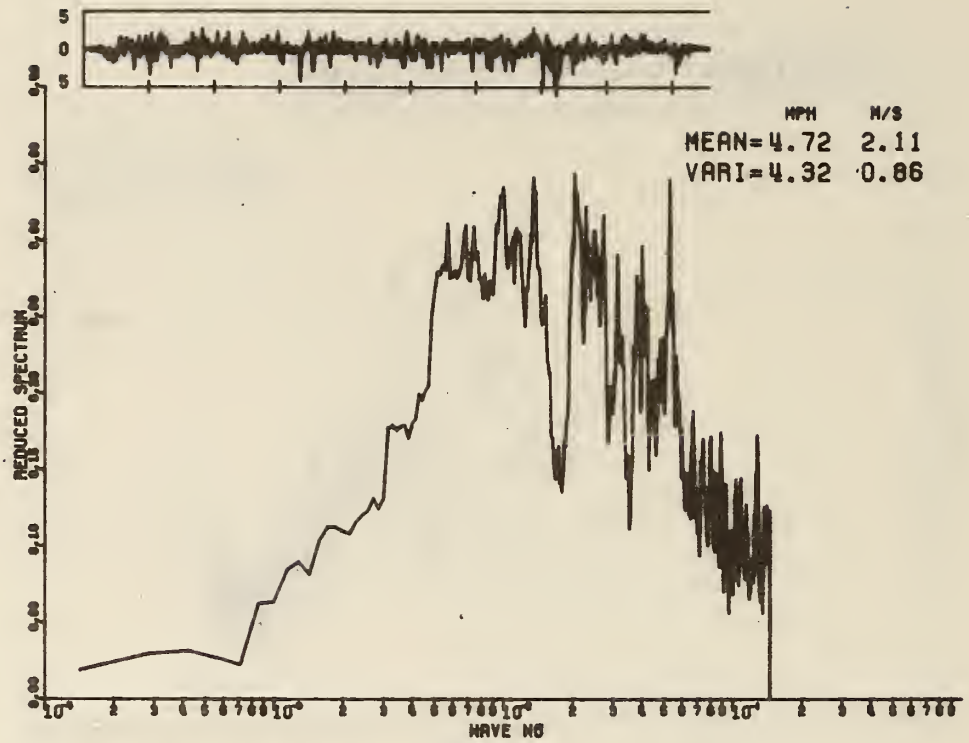

c) Vertical - 5W/U.

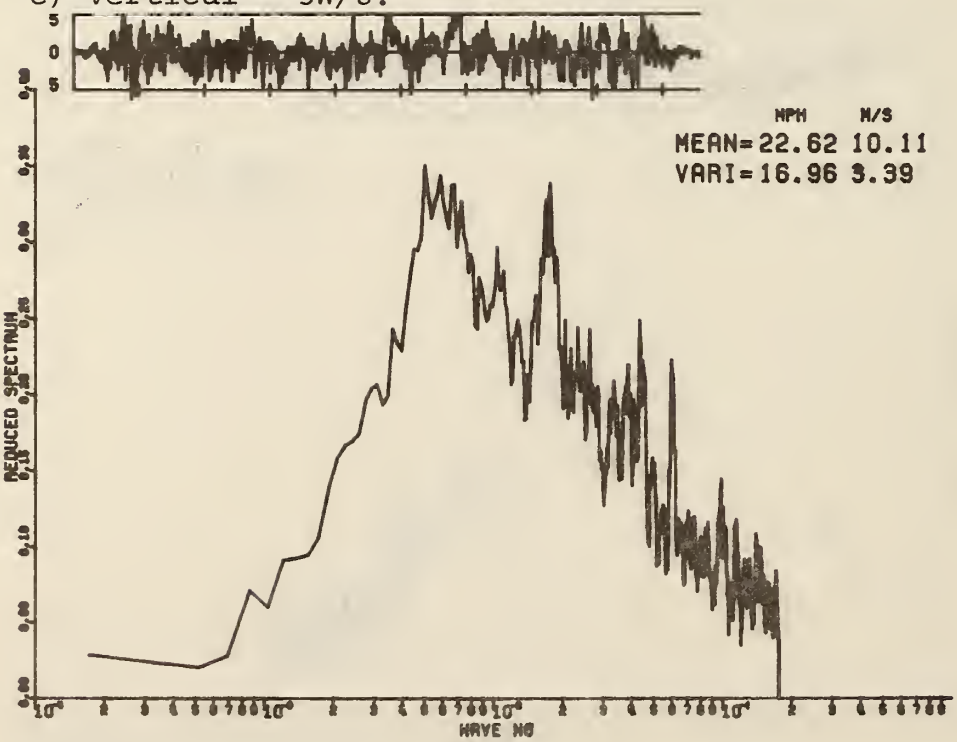

d) U-component - 6U.

Figure 32. Individual channel horizontal and vertical wind spectra for 20 mph wind (Newport, August 1971)(continued).

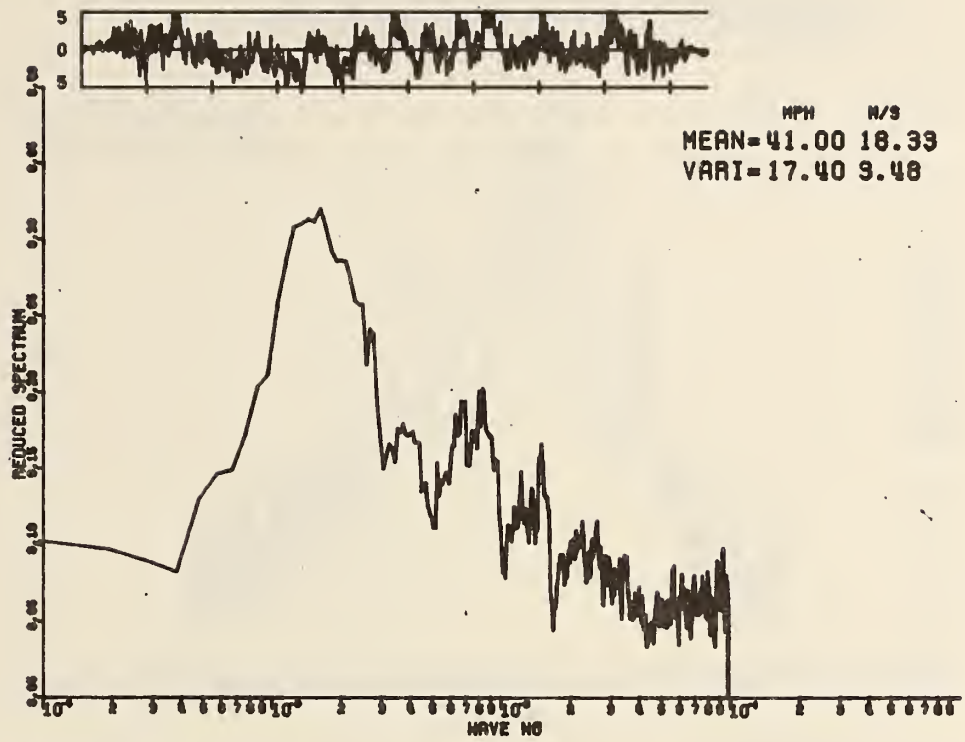

e) Resultant horizontal - 6R.

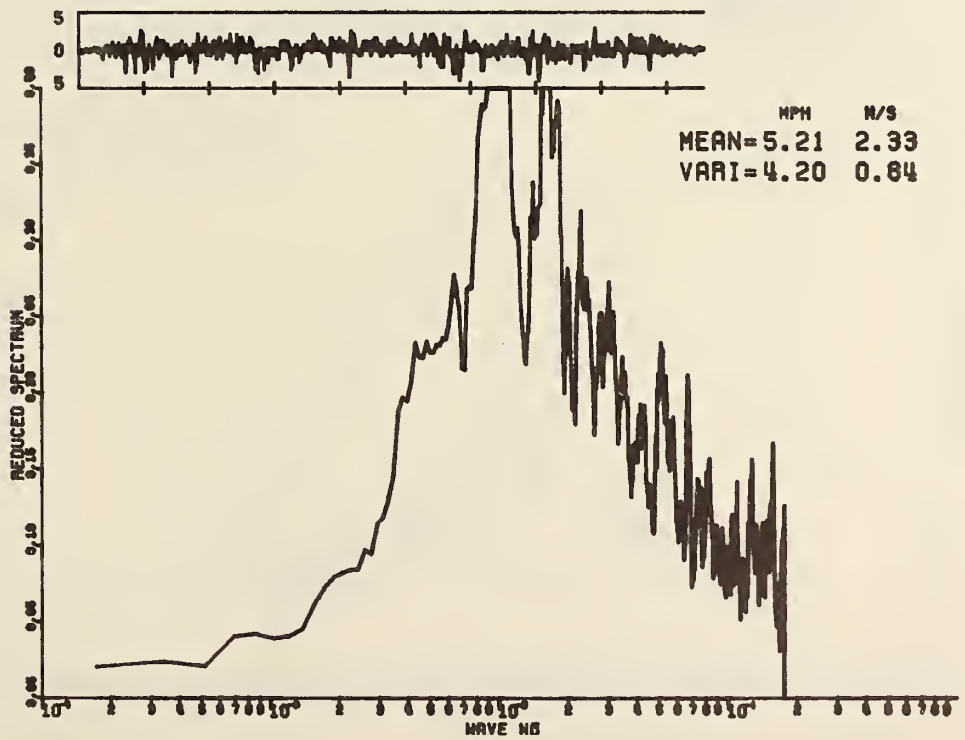

f) Vertical - 6W/U.

Figure 32. Individual channel horizontal and vertical wind spectra for 20 mph wind (Newport, August 1971)(continued).

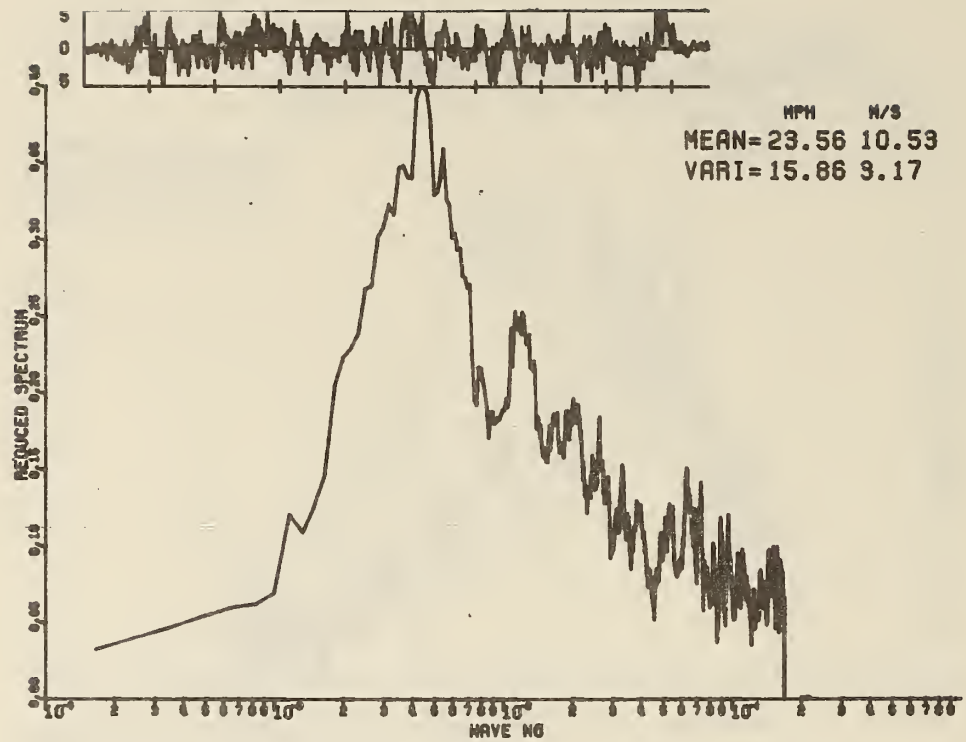

g) U-component - 7U.

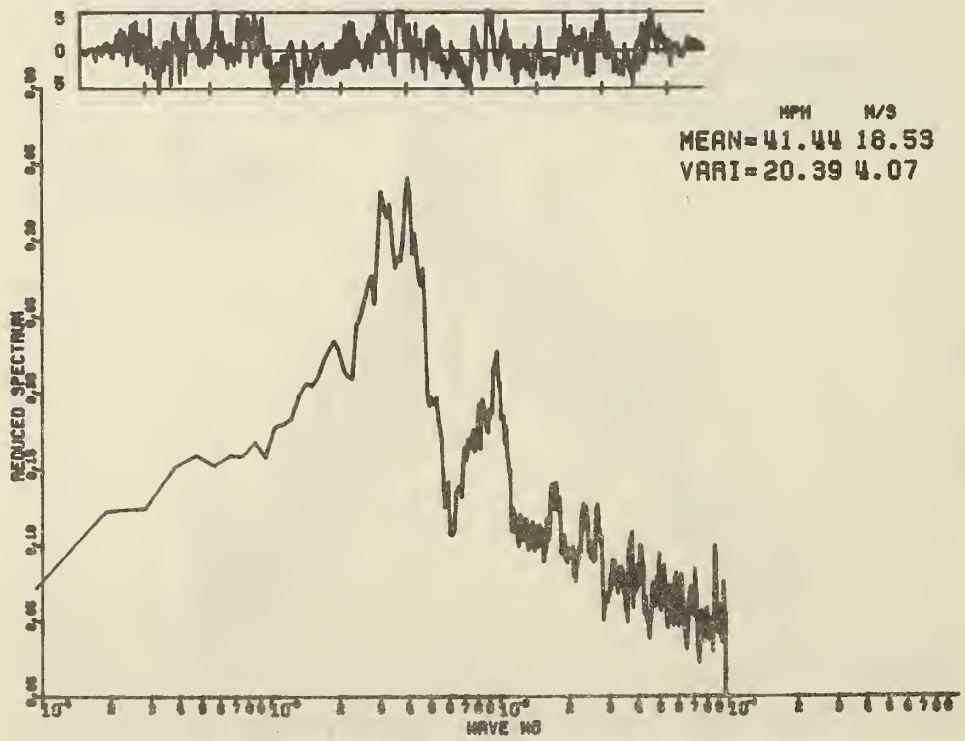

b) Resultant horizontal - 7R.

Figure 32. Individual channel horizontal and vertical wind spectra for 20 mph wind (Newport, August 1971)(continued).

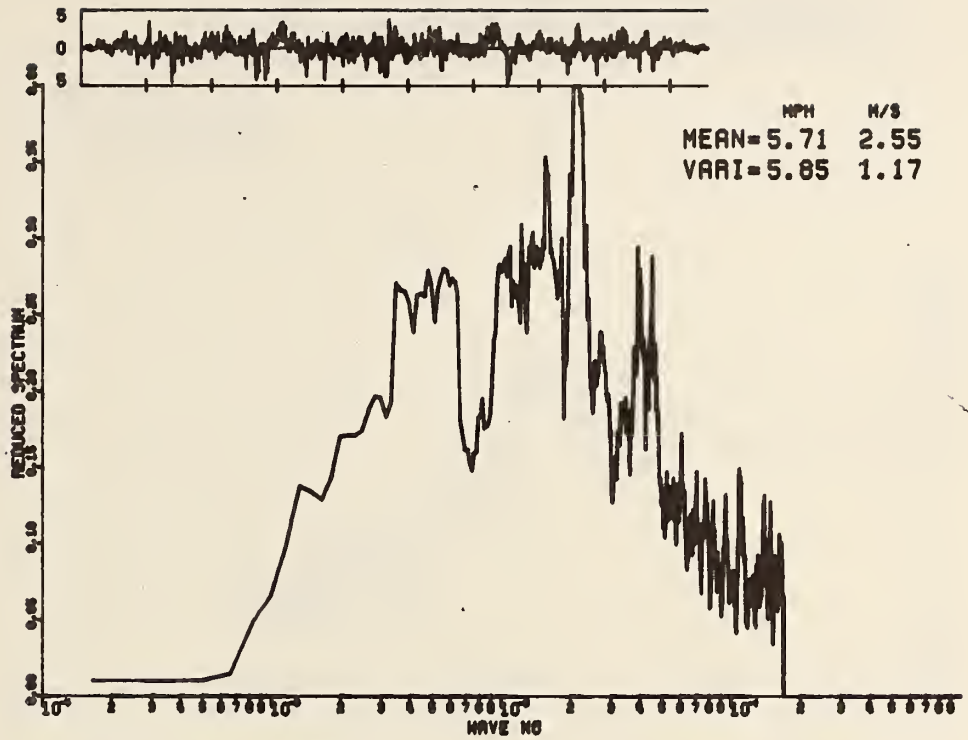

i) Vertical - 7W/U.

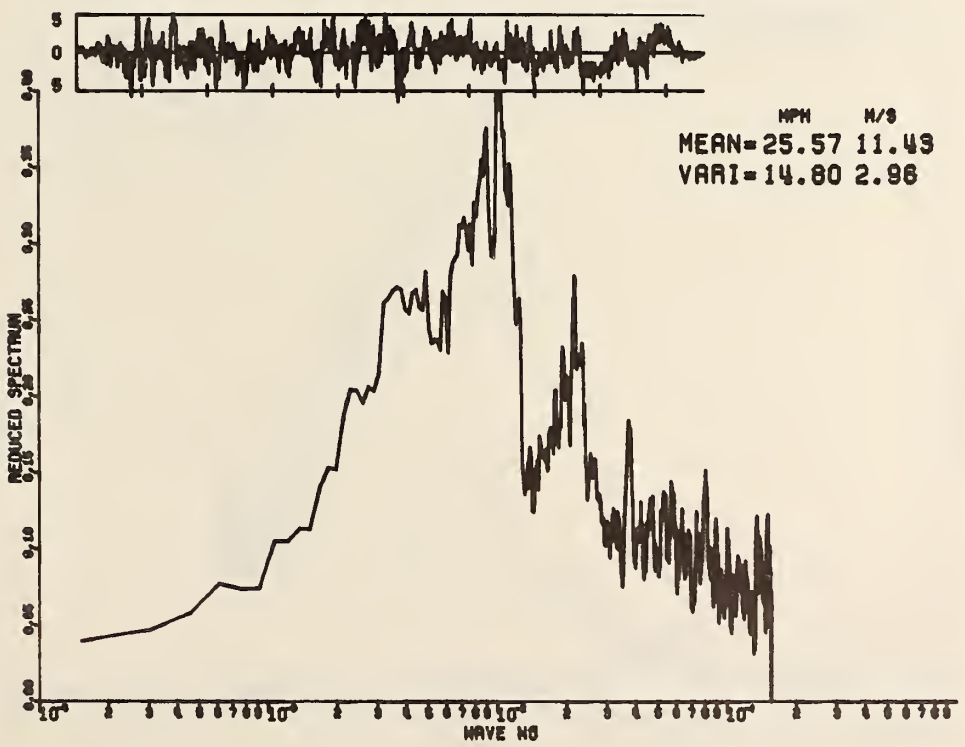

j) U-component - 8U.

Figure 32. Individual channel horizontal and vertical wind spectra for 20 mph wind (Newport, August 1971)(continued).

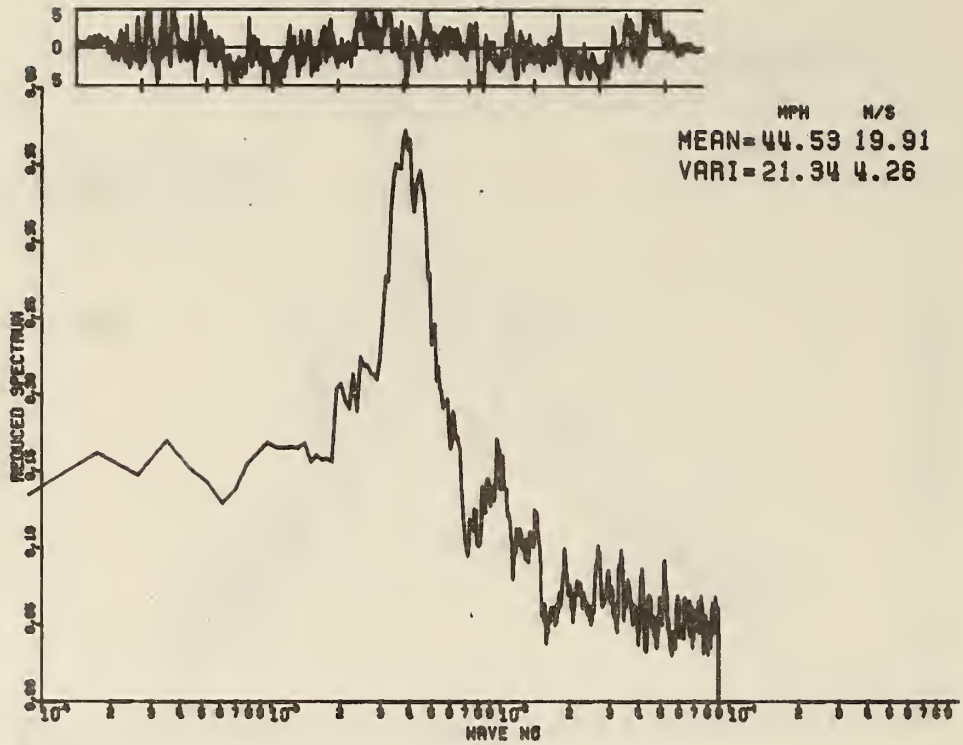

k) Resultant horizontal - 8R.

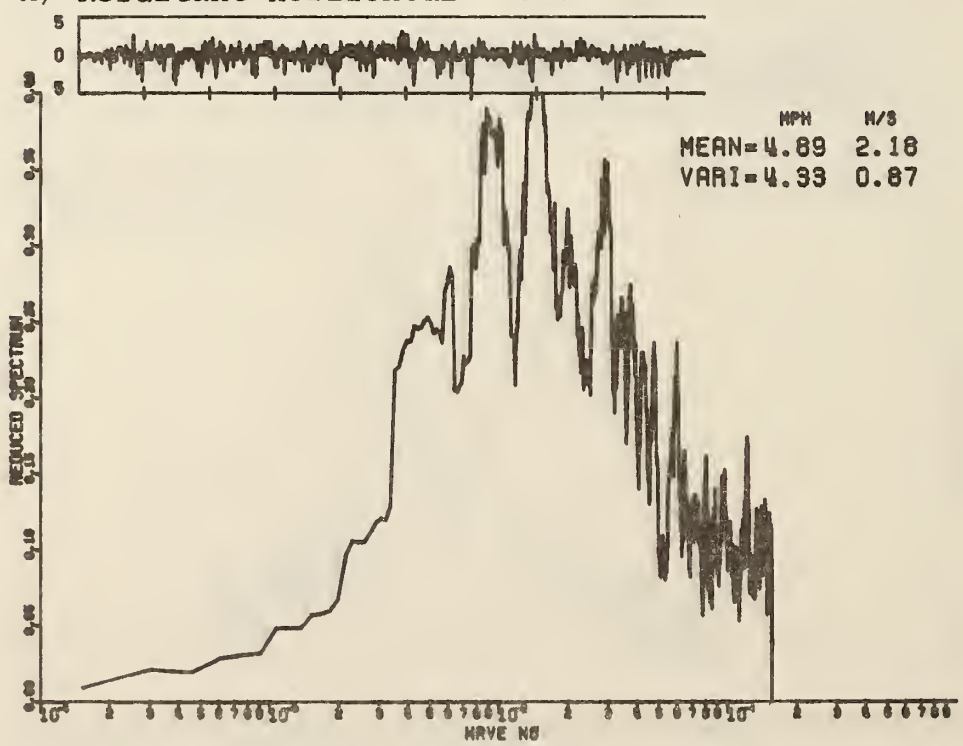

l) Vertical - 8W/U.

Figure 32. Individual channel horizontal and vertical wind spectra for 20 mph wind (Newport, August 1971)(continued).

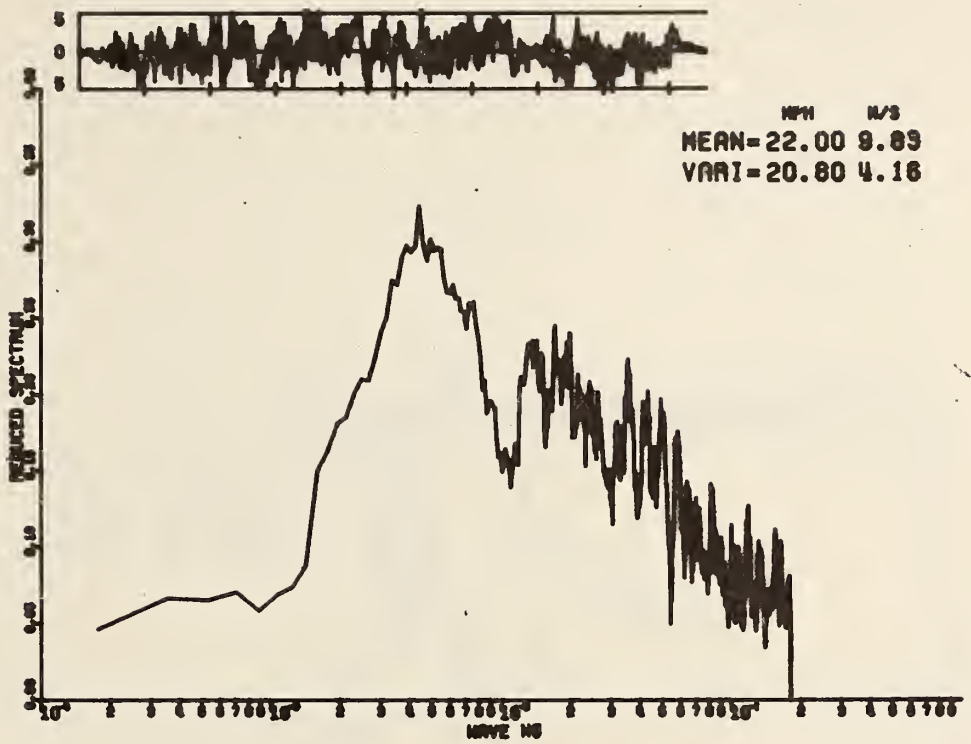

m) U-component - 9U.

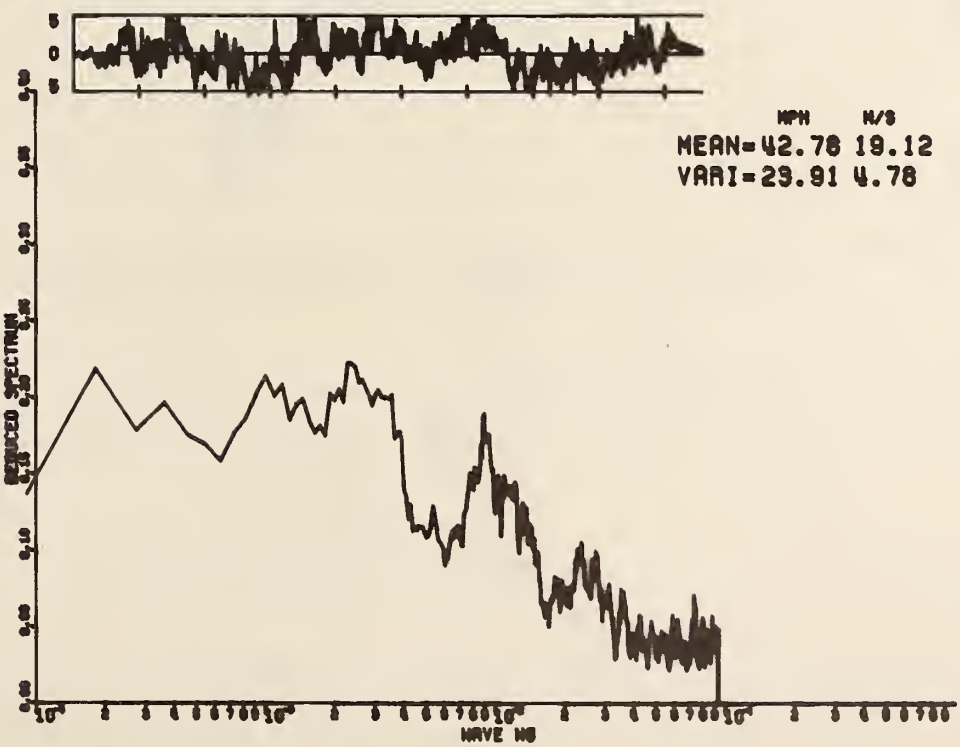

n) Resultant horizontal - 9R.

Figure 32. Individual channel horizontal and vertical wind spectra for 20 mph wind (Newport, August 1971)(continued).

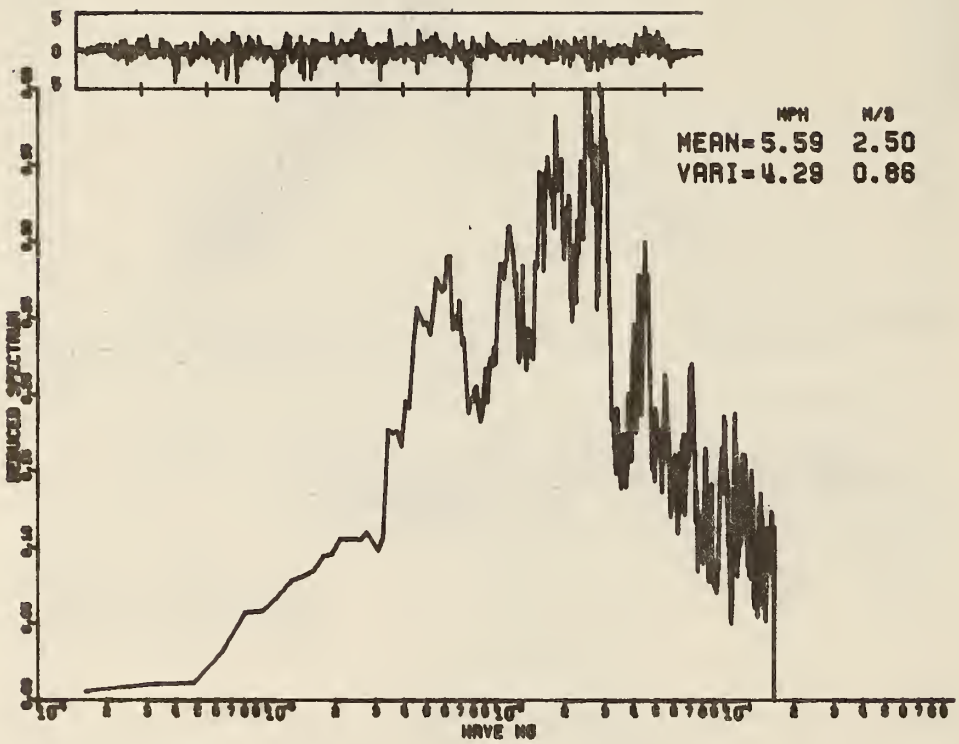

o) Vertical - 9W/U.

Figure 32. Individual channel horizontal and vertical wind spectra for 20 mph wind (Newport, August 1971)(continued).

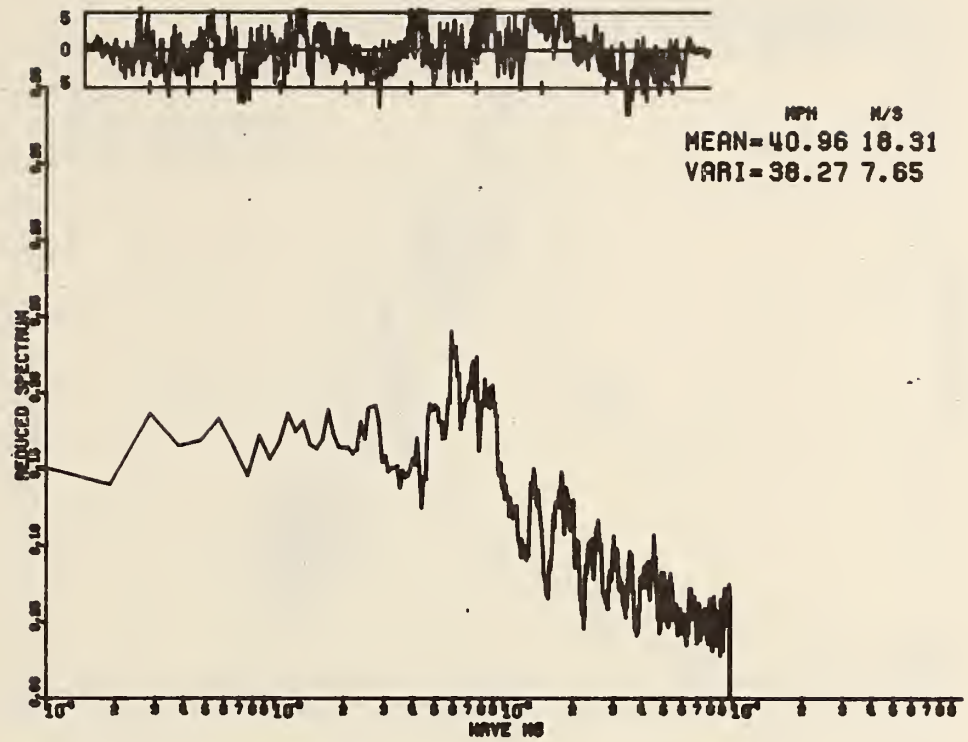

a) U-component - 5U.

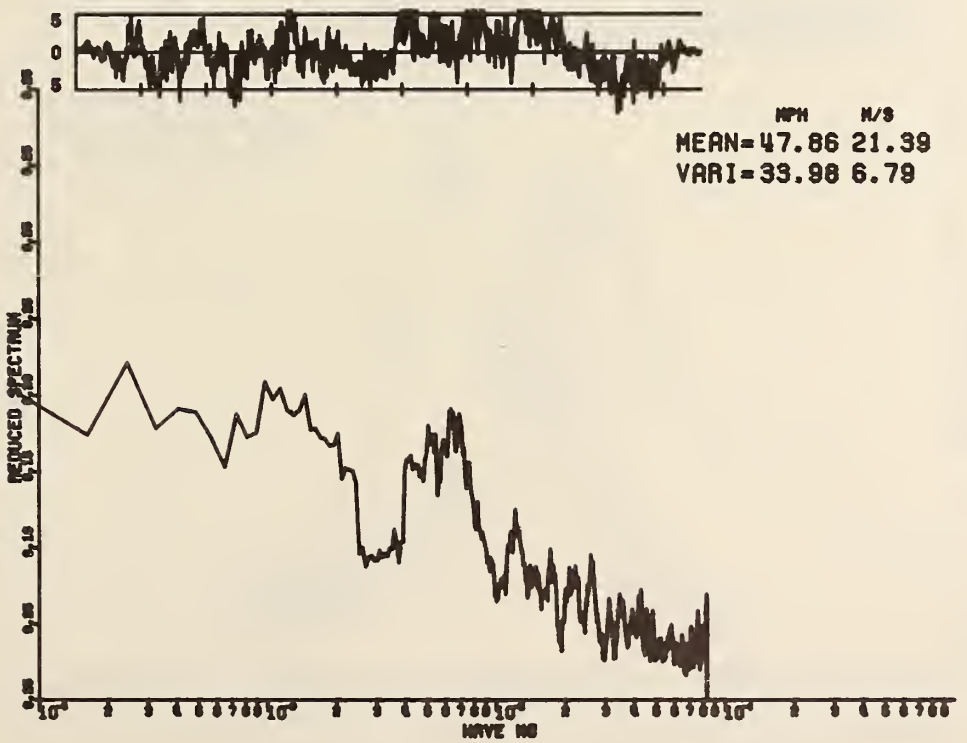

b) Resultant horizontal - 5R.

Figure 33. Individual channel horizontal and vertical wind spectra for 35 mph wind (Newport, August 1971).

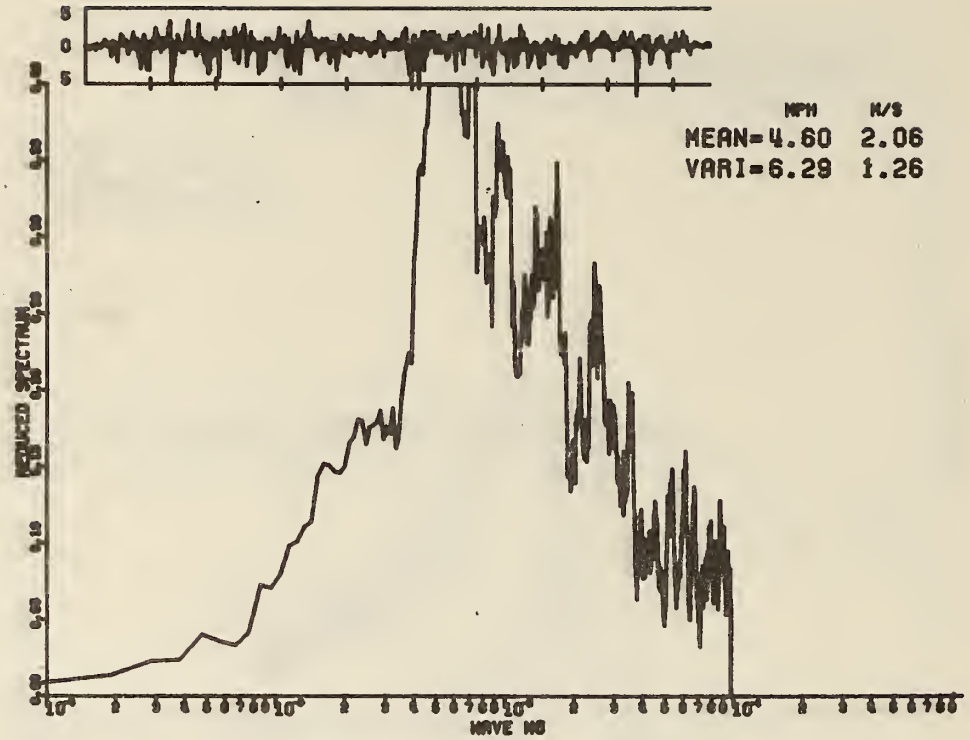

c) Vertical - 5W/U.

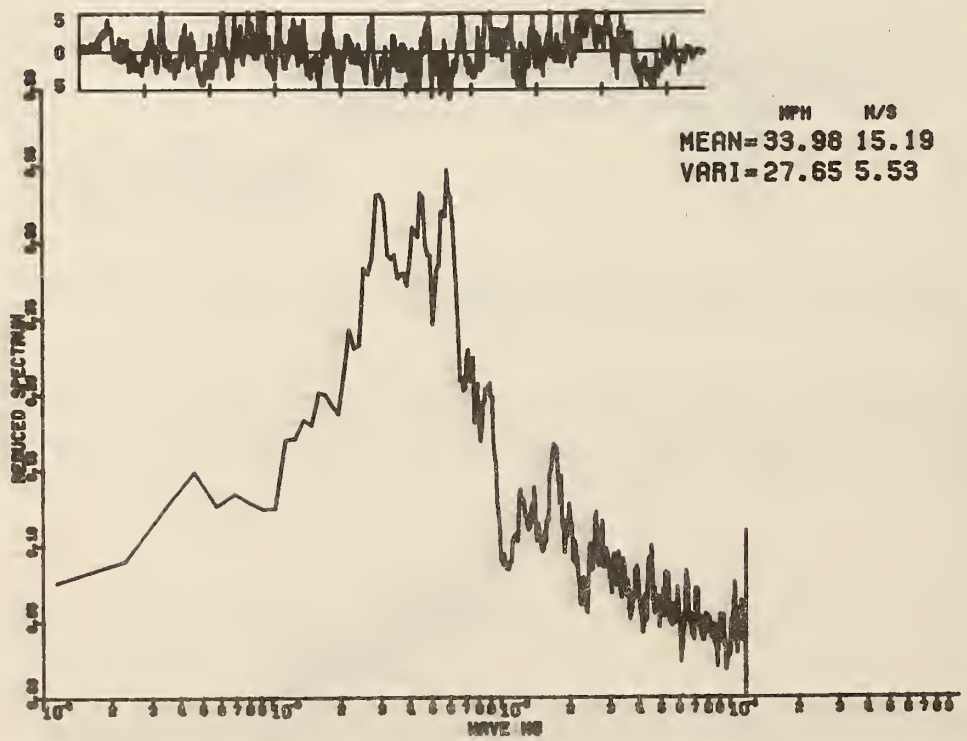

d) U-component - 6U.

Figure 33. Individual channel horizontal and vertical wind spectra for 35 mph wind (Newport, August 1971)(continued).

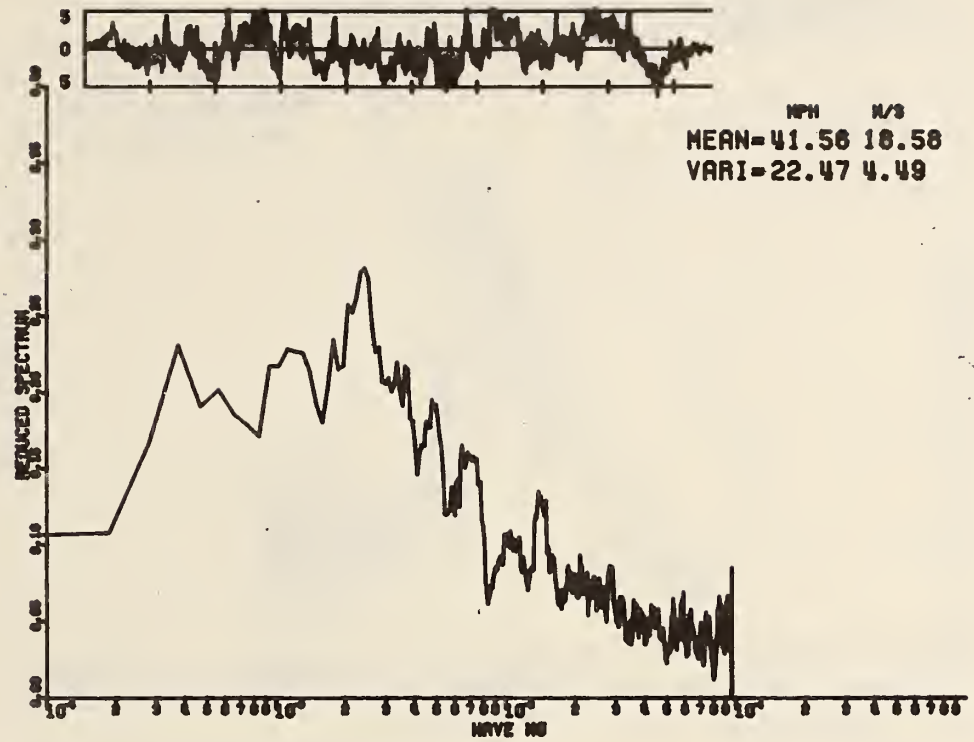

e) Resultant horizontal - 6R.

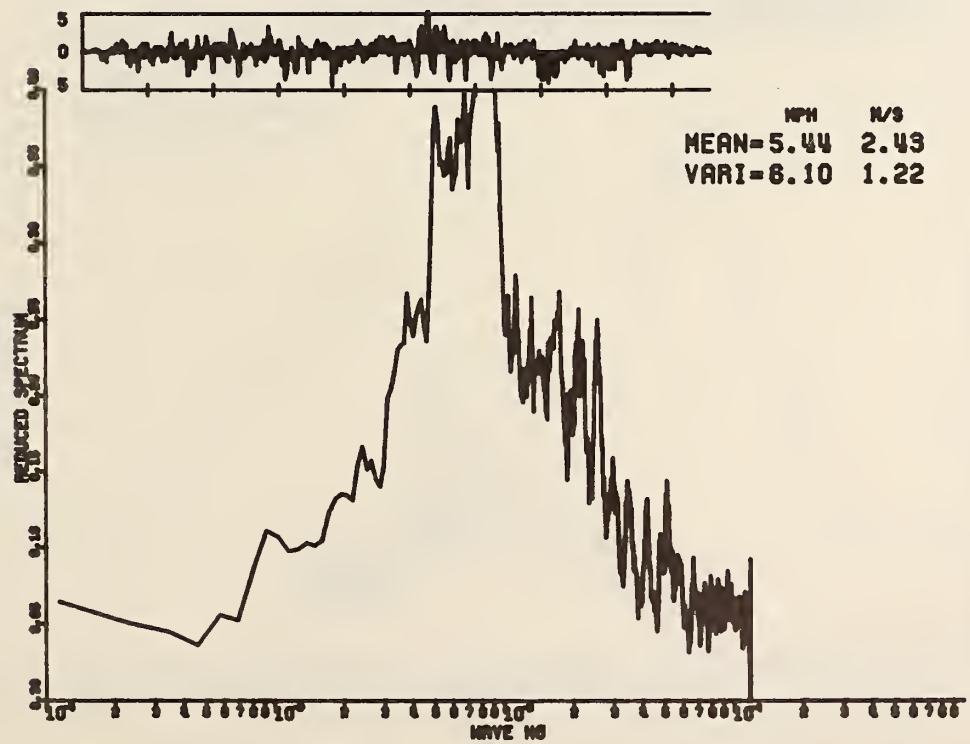

f) Vertical - 6W/U.

Figure 33. Individual channel horizontal and vertical wind spectra for 35 mph wind (Newport, August 1971)(continued).

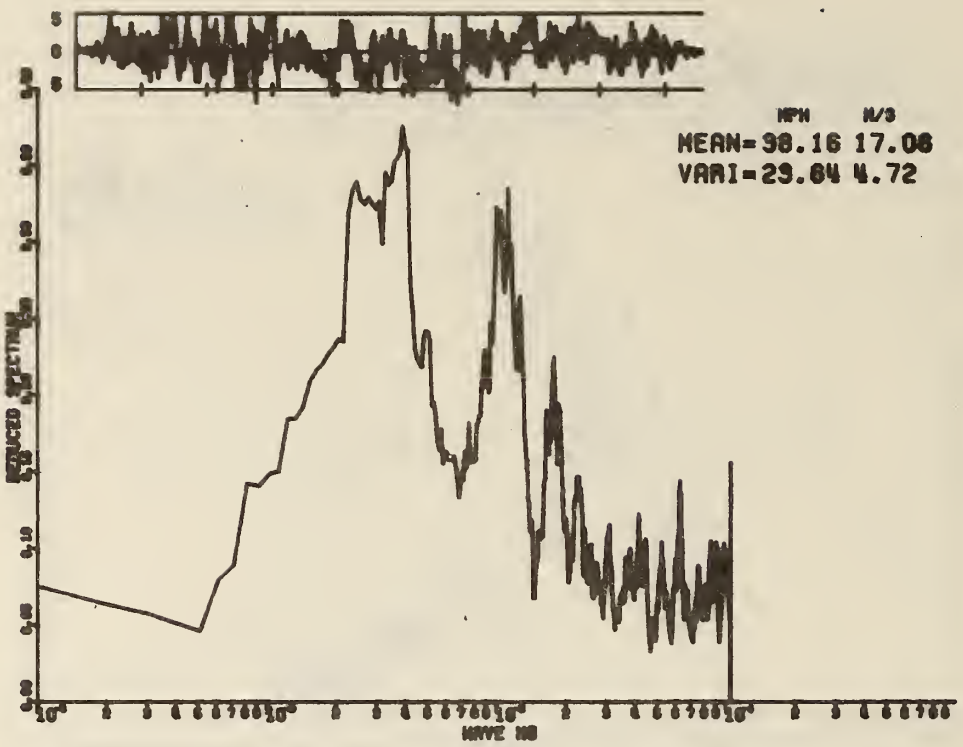

g) U-component - 7U.

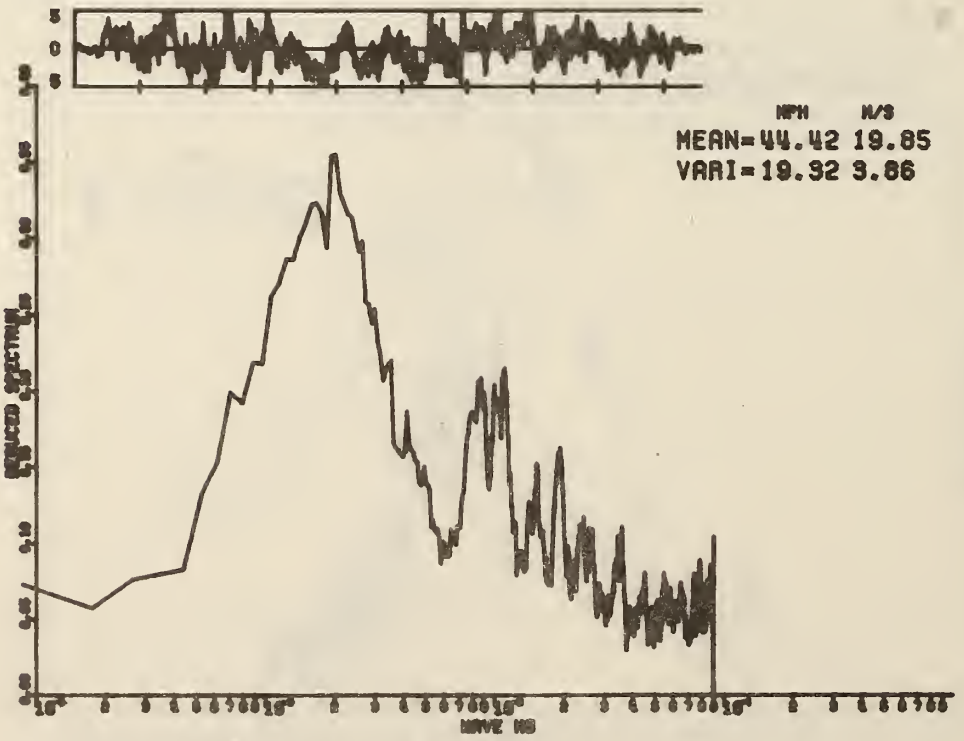

h) Resultant horizontal - 7R.

Figure 33. Individual channel horizontal and vertical wind spectra for 35 mph wind (Newport, August 1971)(continued).

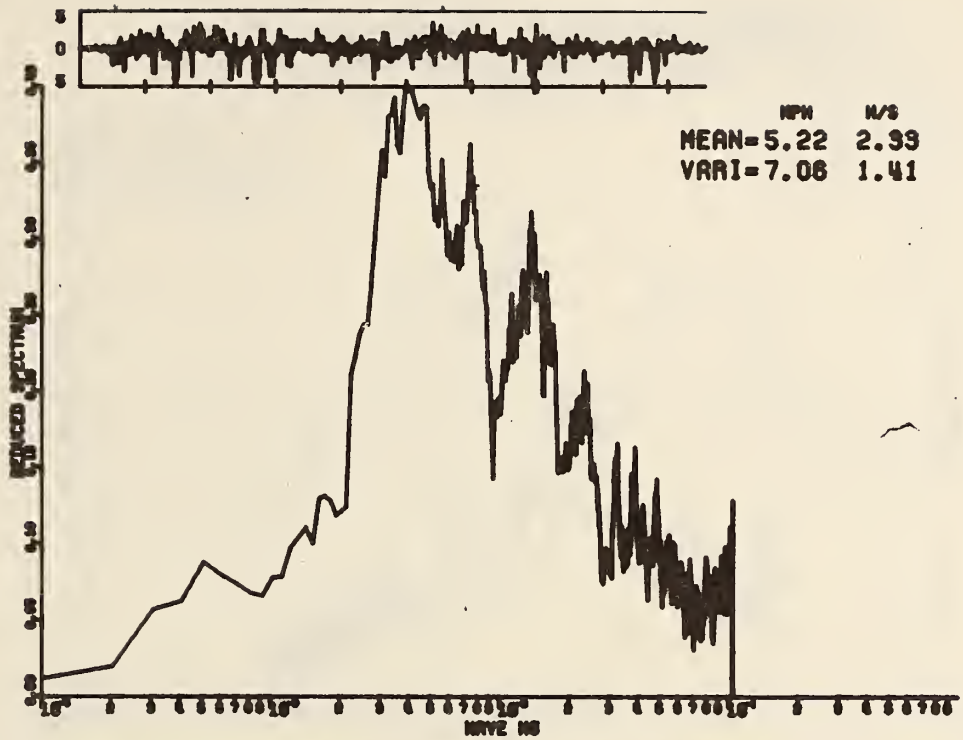

i) Vertical - 7W/U.

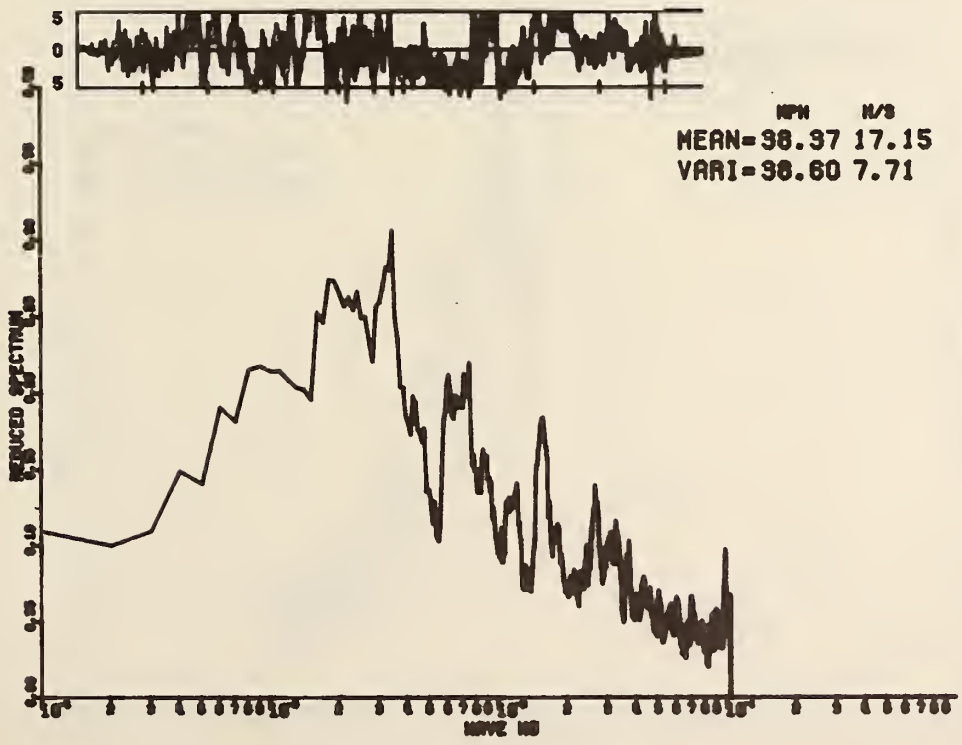

j) U-component - 8U.

Figure 33. Individual channel horizontal and vertical wind spectra for 35 mph wind (Newport, August 1971)(continued).

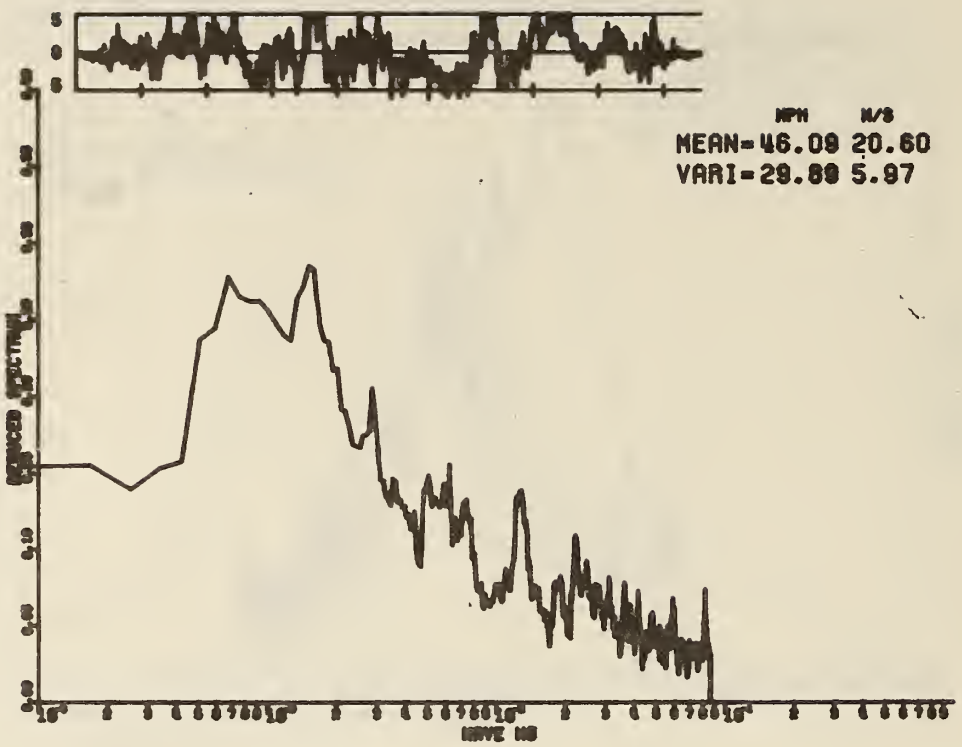

k) Resultant horizontal - 8R.

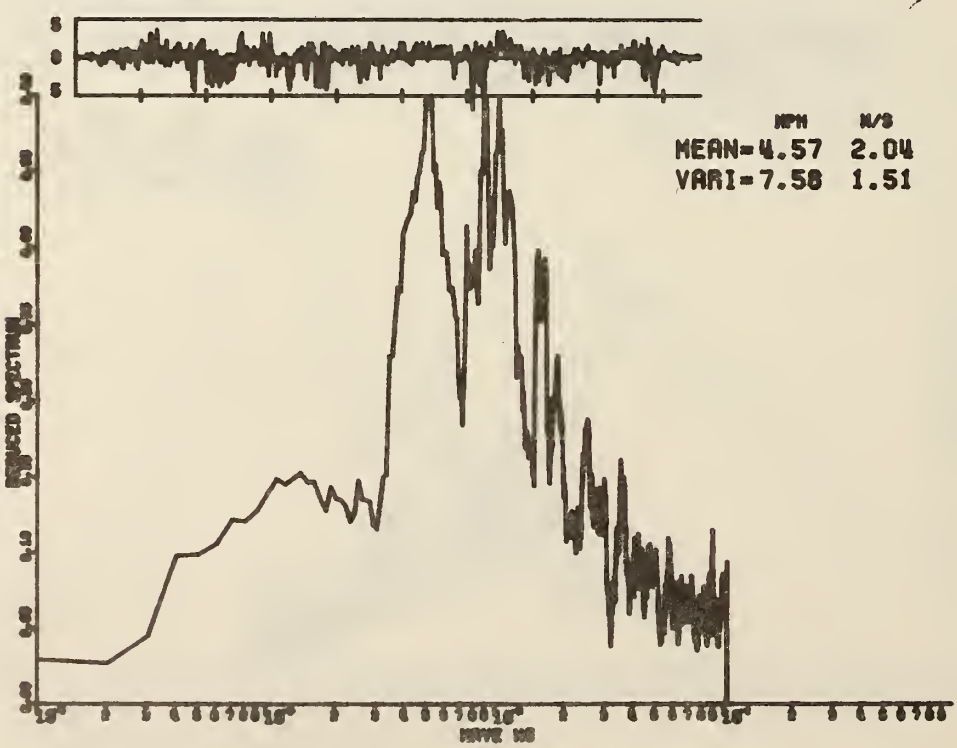

l) Vertical - 8W/U.

Figure 33. Individual channel horizontal and vertical wind spectra for 35 mph wind (Newport, August 1971)(continued).

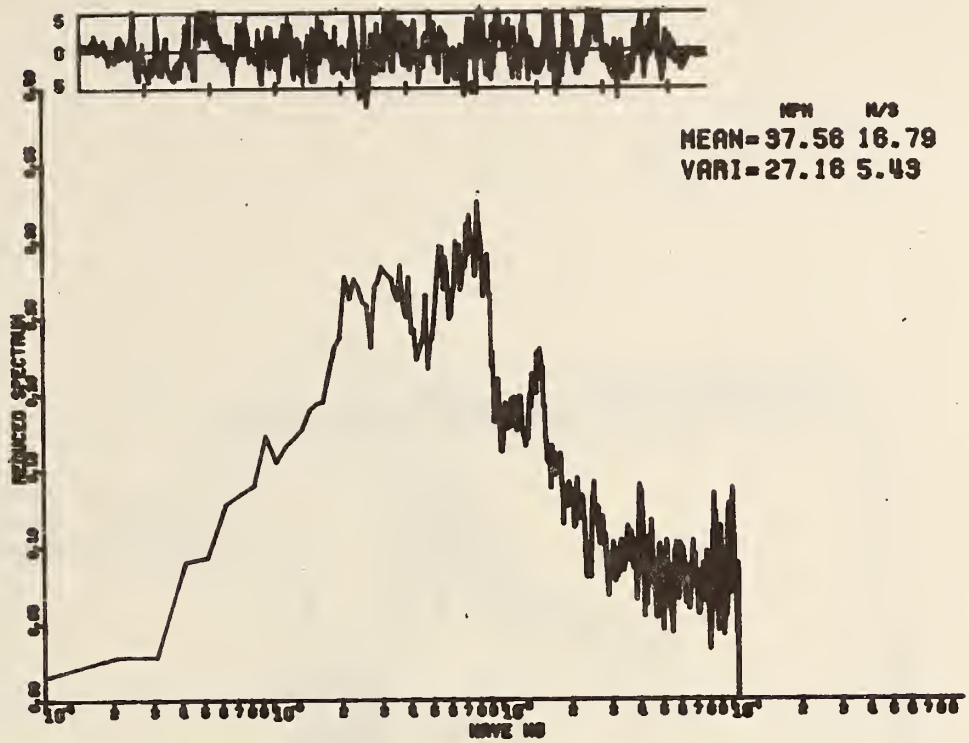

m) U-component - 9U.

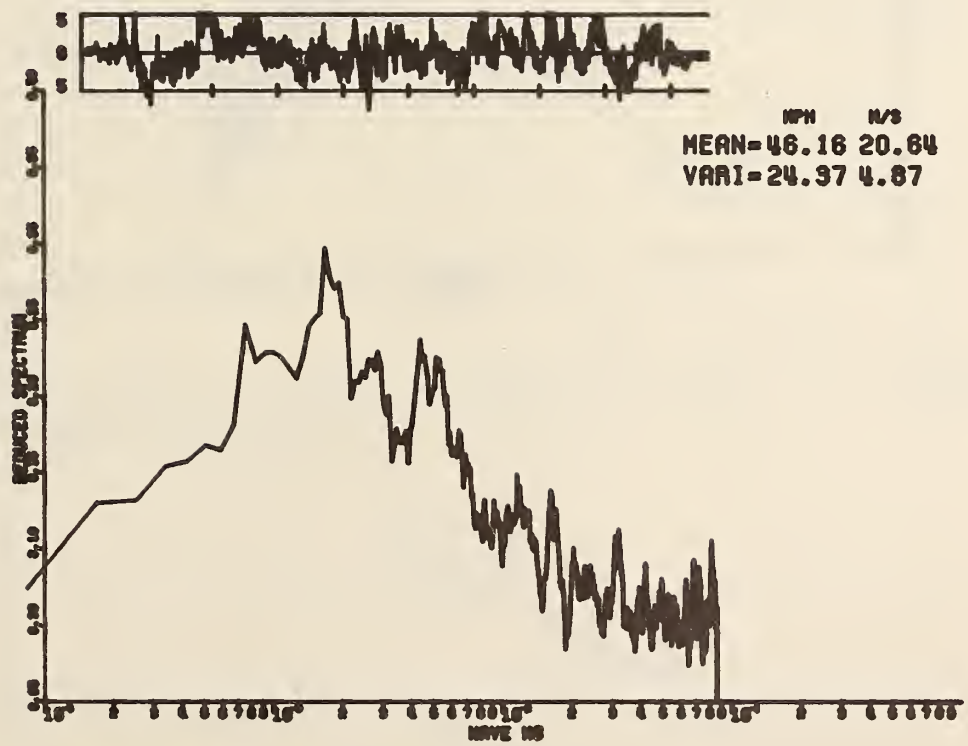

n) Resultant horizontal - 9R.

Figure 33. Individual channel horizontal and vertical wind spectra for 35 mph wind (Newport, August 1971)(continued).

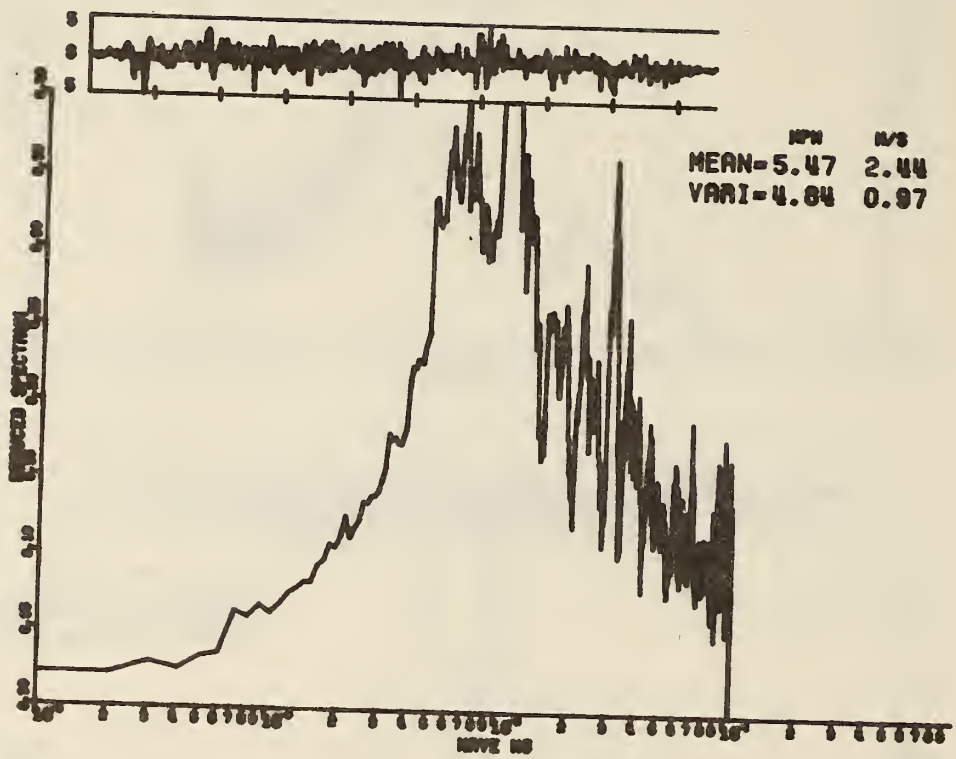

o) Vertical - 9W/U.

Figure 33. Individual channel horizontal and vertical wind spectra for 35 mph wind (Newport, August 1971)(continued).

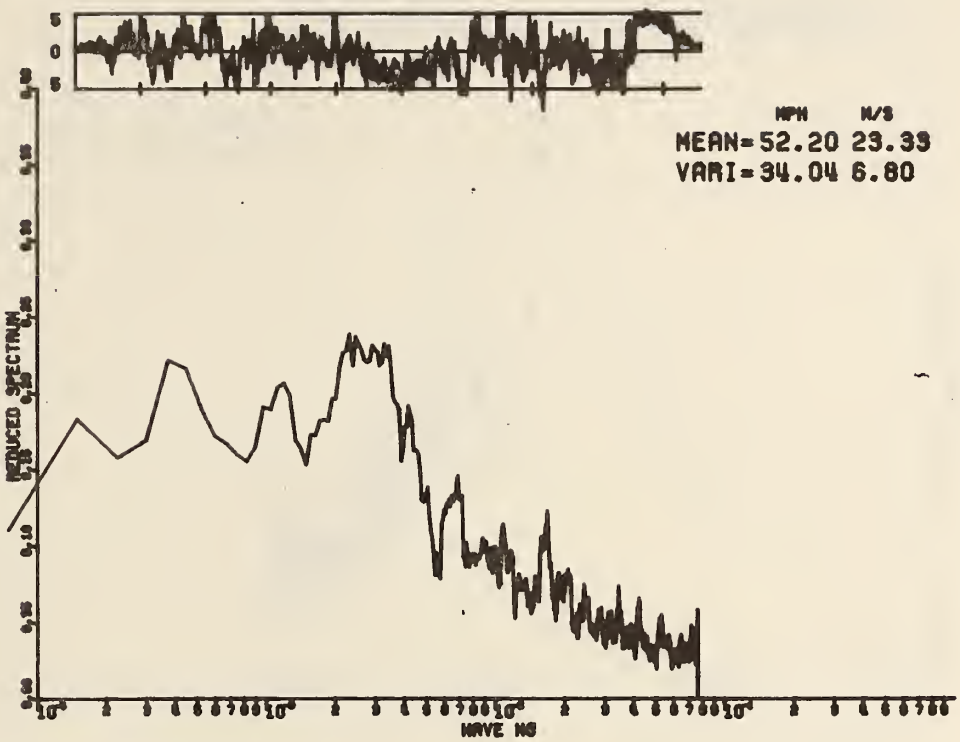

a) U-component - 5U.

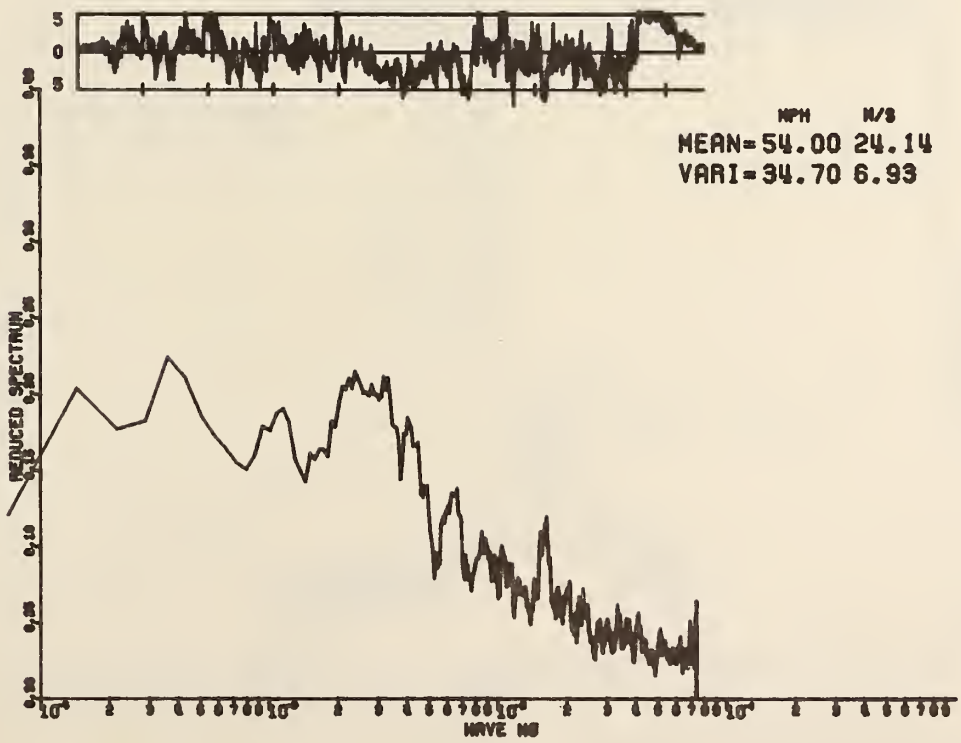

b) Resultant horizontal - 5R.

Figure 34. Individual channel horizontal and vertical wind spectra for 50 mph wind (Newport, August 1971).

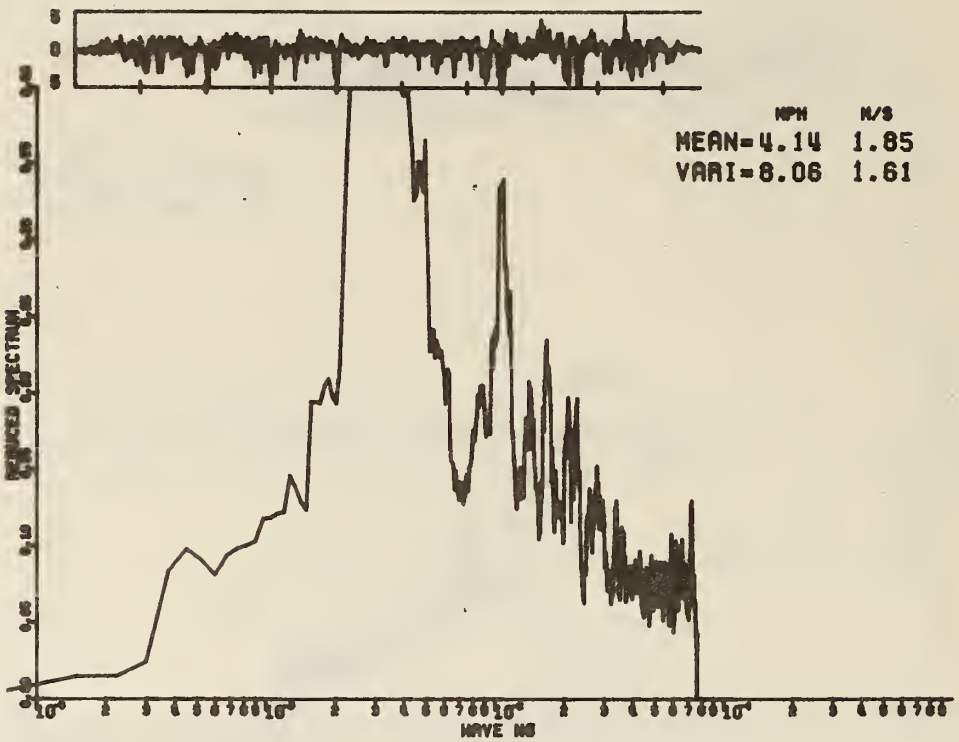

c) Vertical - 5W/U.

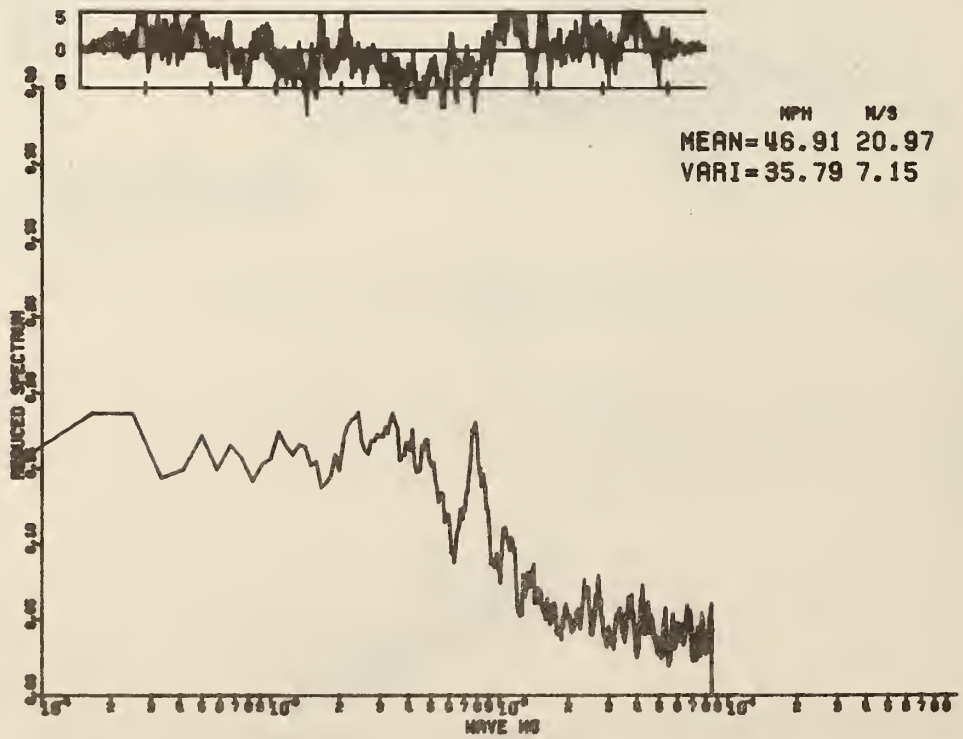

d) U-component - 6U.

Figure 34. Individual channel horizontal and vertical wind spectra for 50 mph wind (Newport, August 1971)(continued).

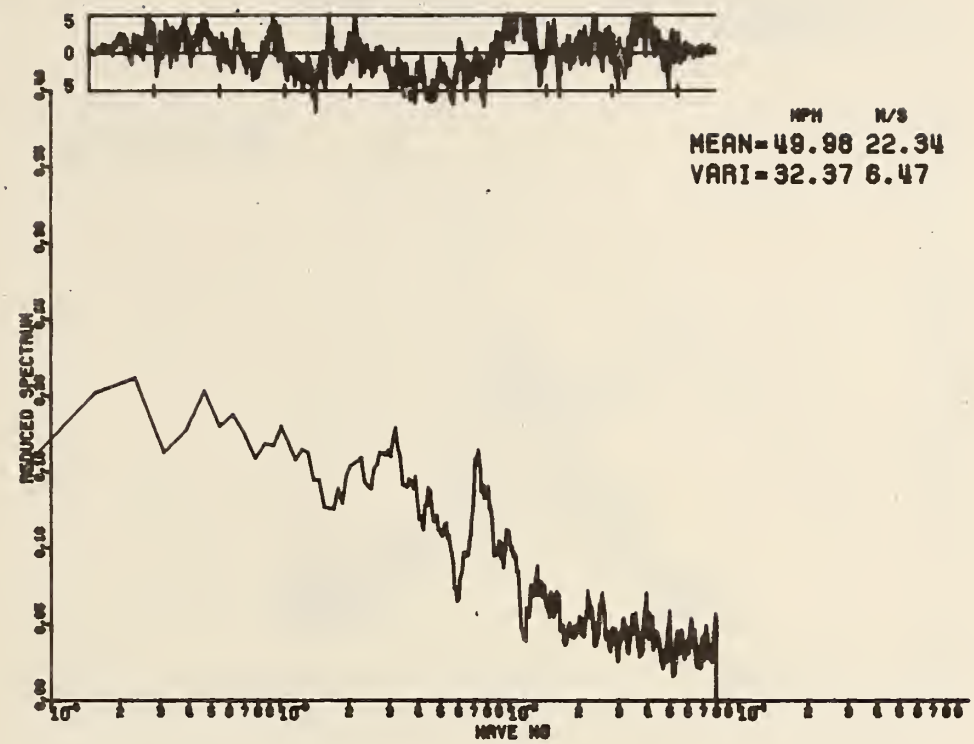

e) Resultant horizontal - 6R.

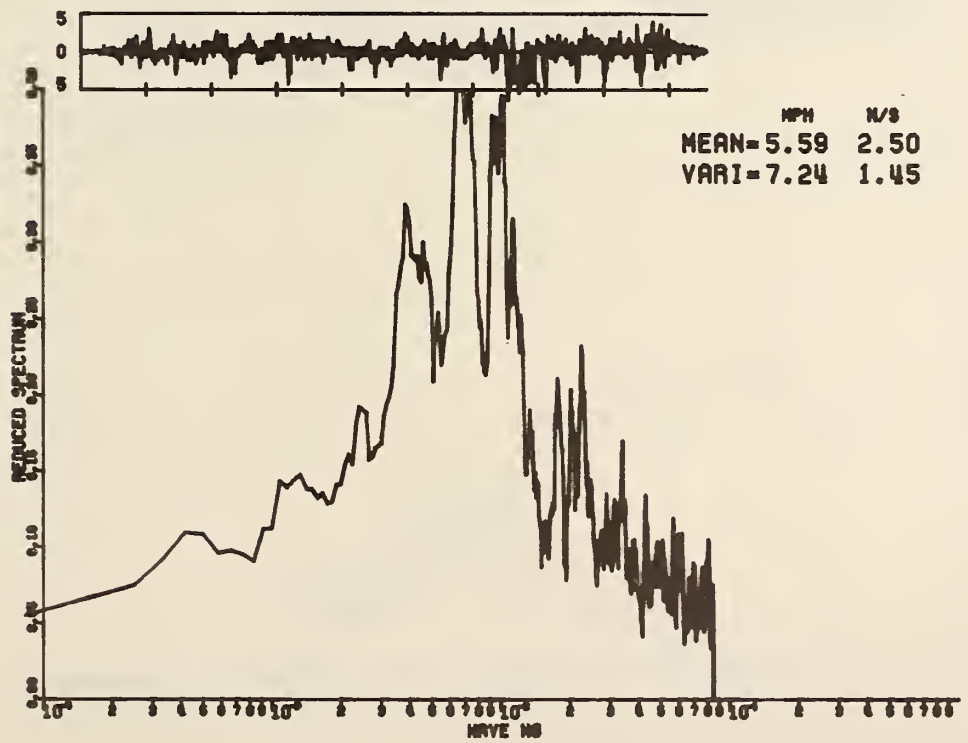

f) Vertical - 6W/U.

Figure 34. Individual channel horizontal and vertical wind spectra for 50 mph wind (Newport, August 1971)(continued).

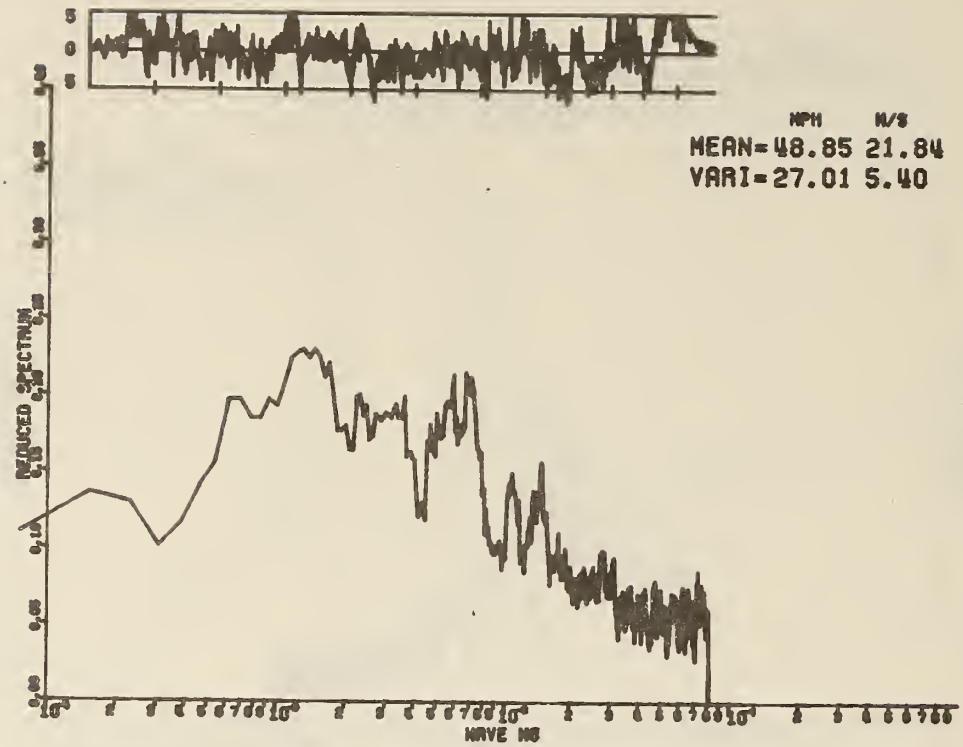

g) U-component - 7U.

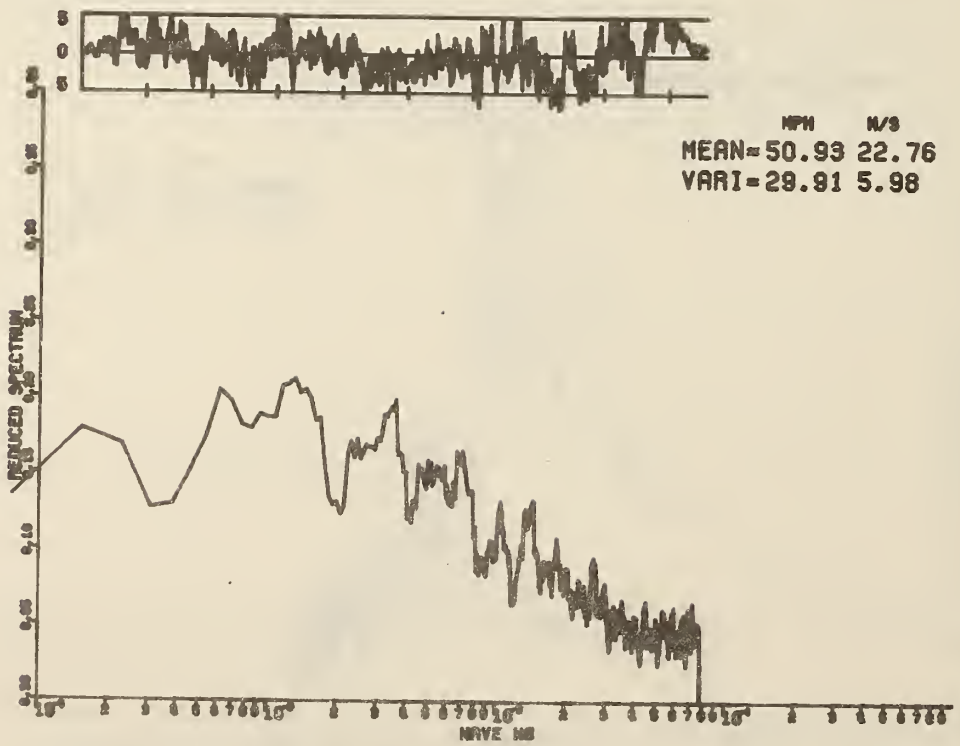

h) Resultant horizontal - 7R.

Figure 34. Individual channel horizontal and vertical wind spectra for 50 mph wind (Newport, August 1971)(continued).

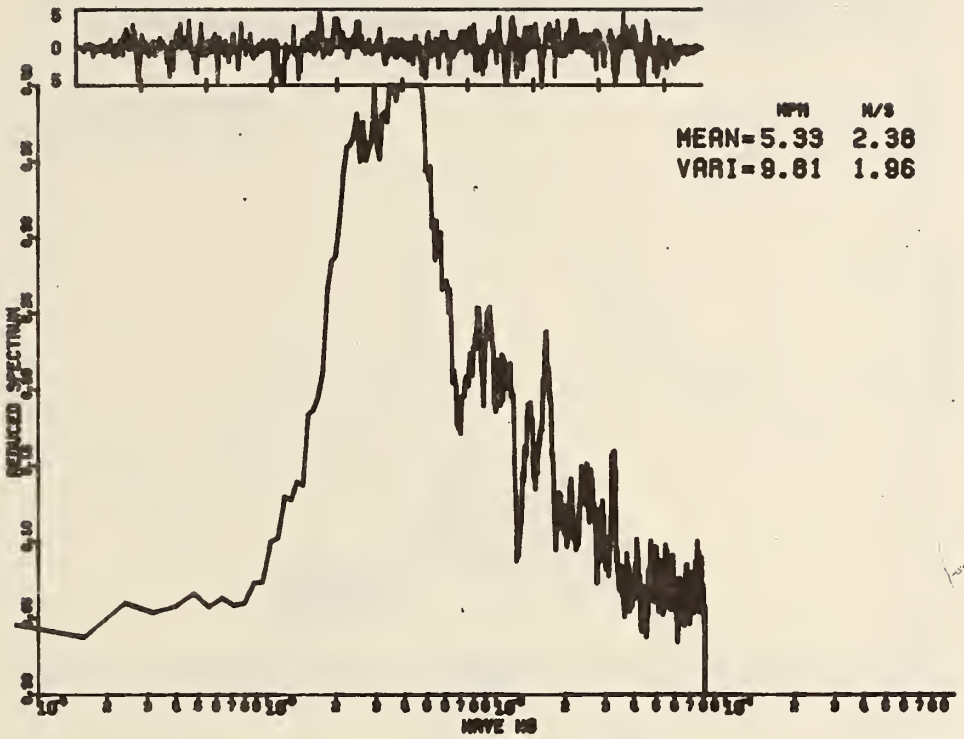

i) Vertical - 7W/U.

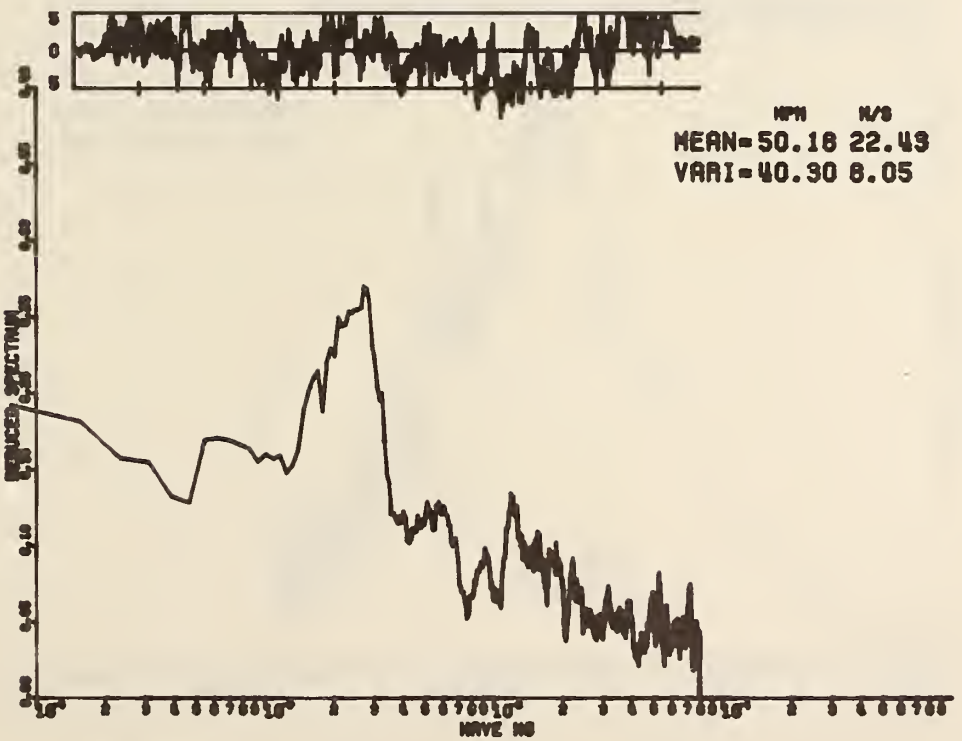

j) U-component - 8U.

Figure 34. Individual channel horizontal and vertical wind spectra for 50 mph wind (Newport, August 1971)(continued).

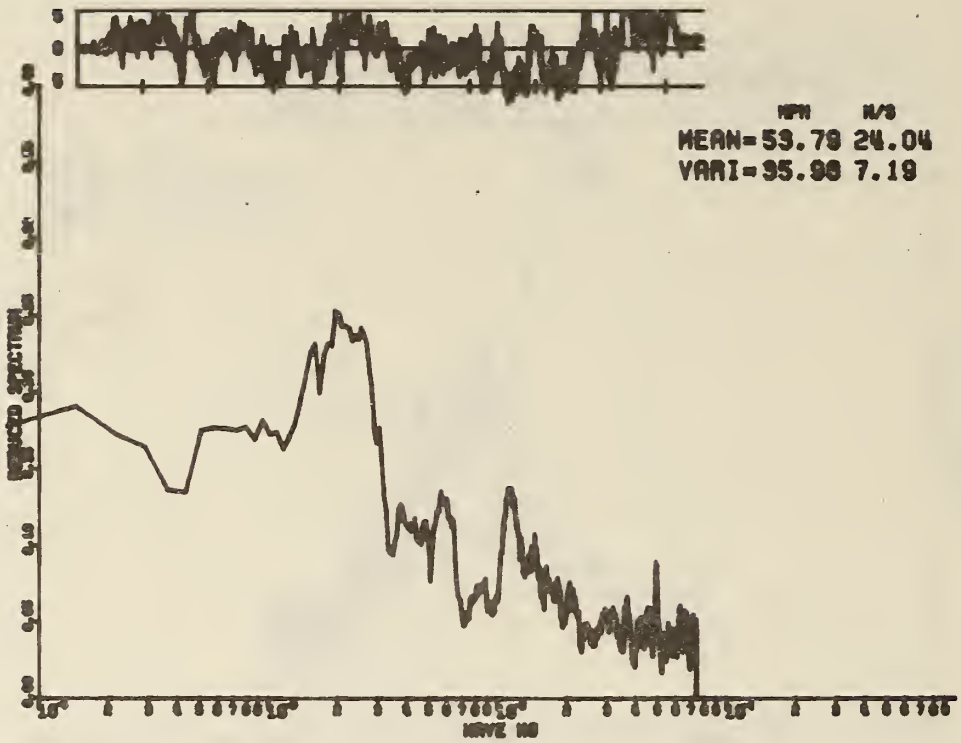

k) Resultant horizontal - 8R.

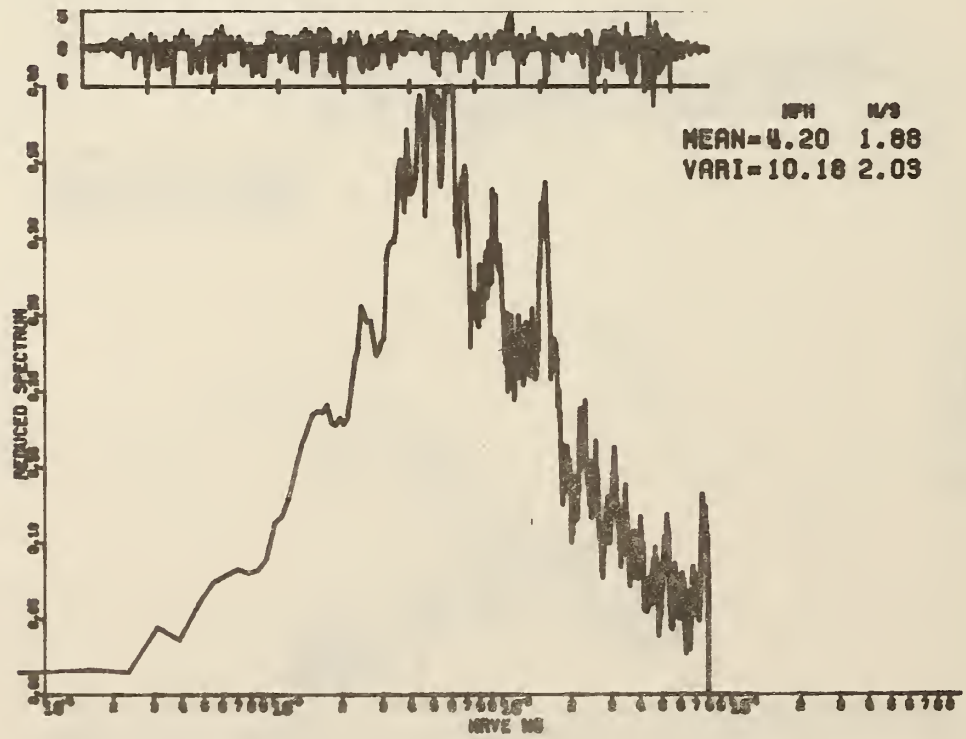

l) Vertical - 8W/U.

Figure 34. Individual channel horizontal and vertical wind spectra for 50 mph wind (Newport, August 1971)(continued).

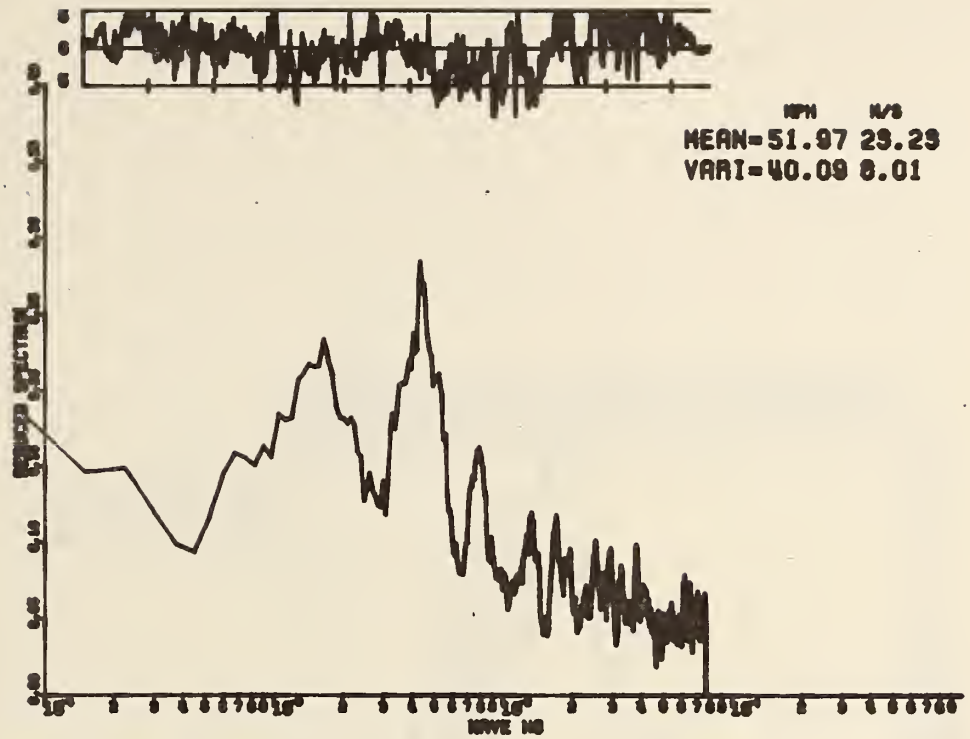

m) U-component - 9U.

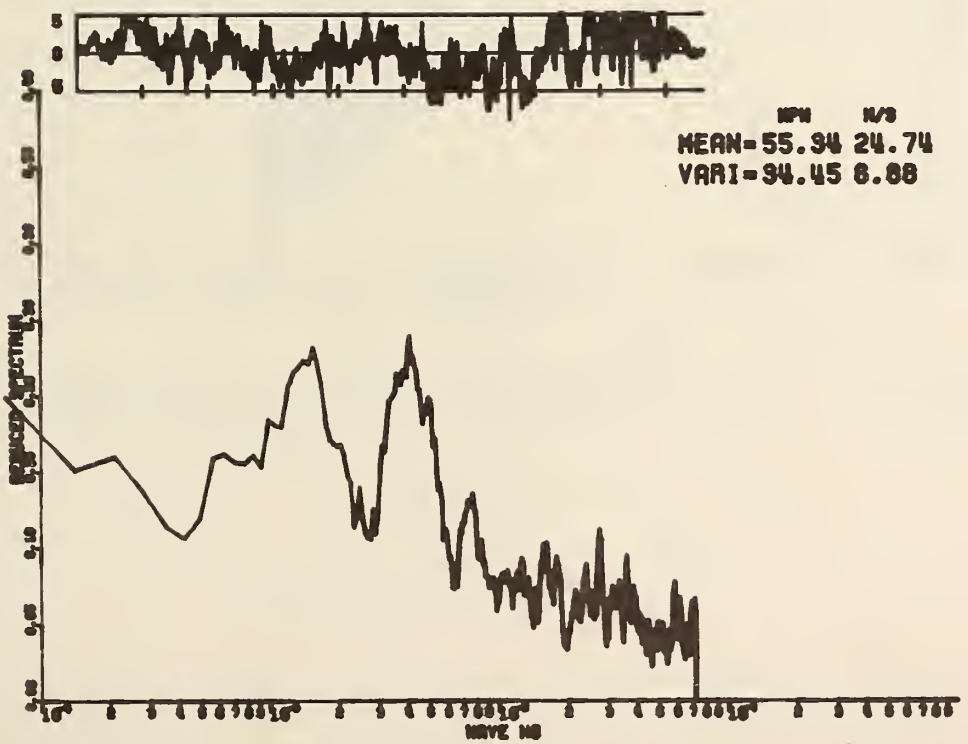

n) Resultant horizontal - 9R.

Figure 34. Individual channel horizontal and vertical wind spectra for 50 mph wind (Newport, August 1971)(continued).

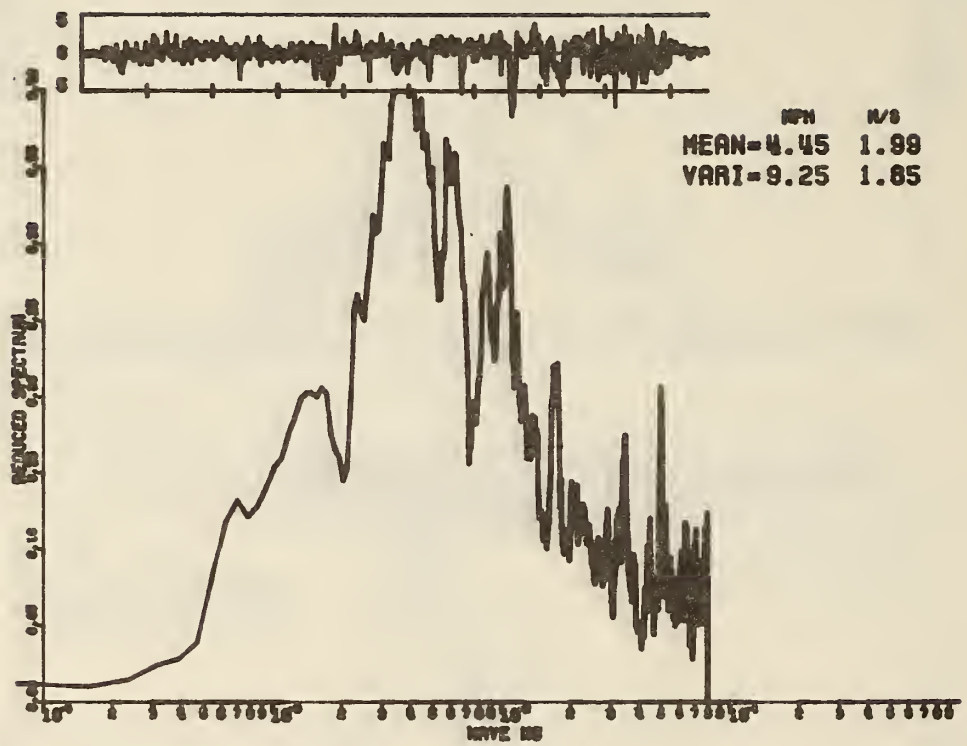

o) Vertical - 9W/U.

Figure 34. Individual channel horizontal and vertical wind spectra for 50 mph wind (Newport, August 1971)(continued).

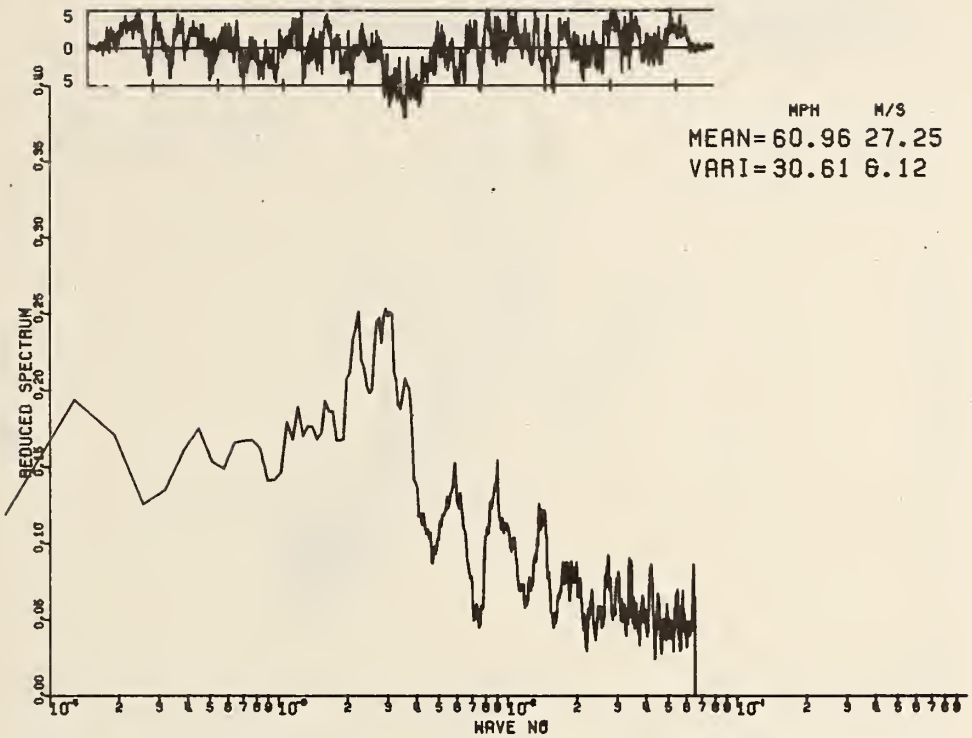

a) U-component - 5U.

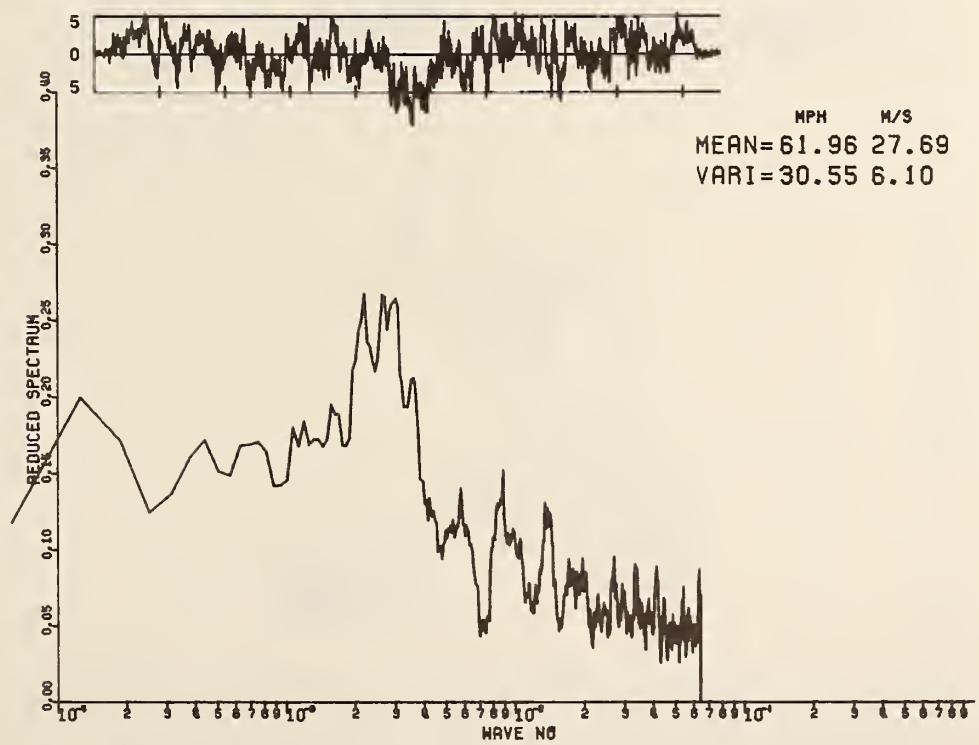

b) Resultant horizontal - 5R.

Figure 35. Individual channel horizontal and vertical wind spectra for 60 mph wind (Newport, August 1971).

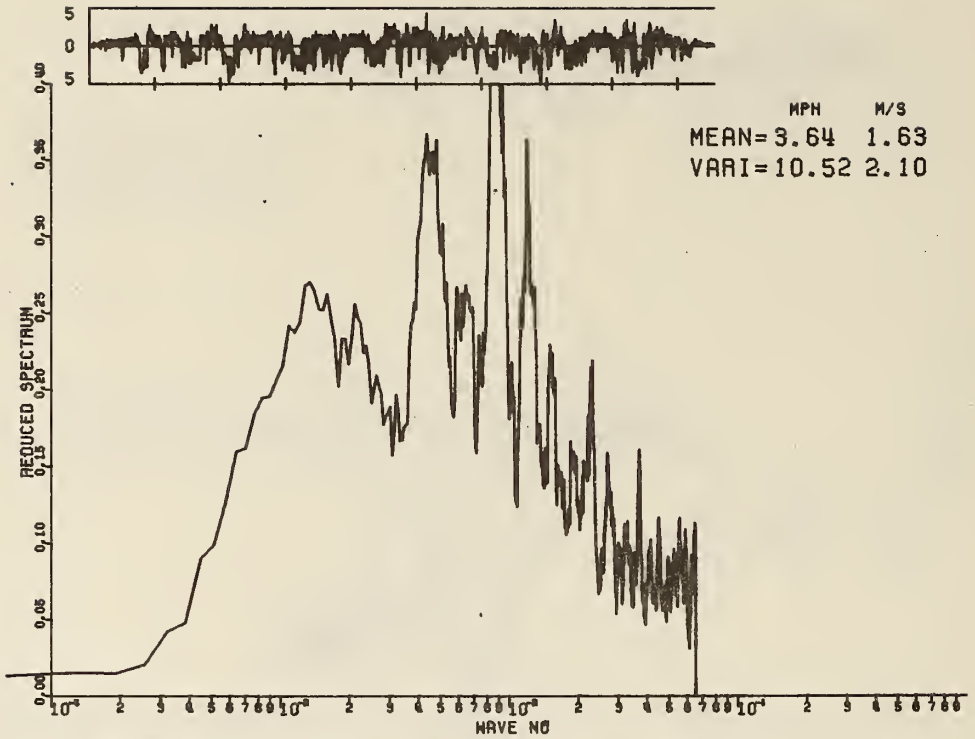

c) Vertical - 5W/U.

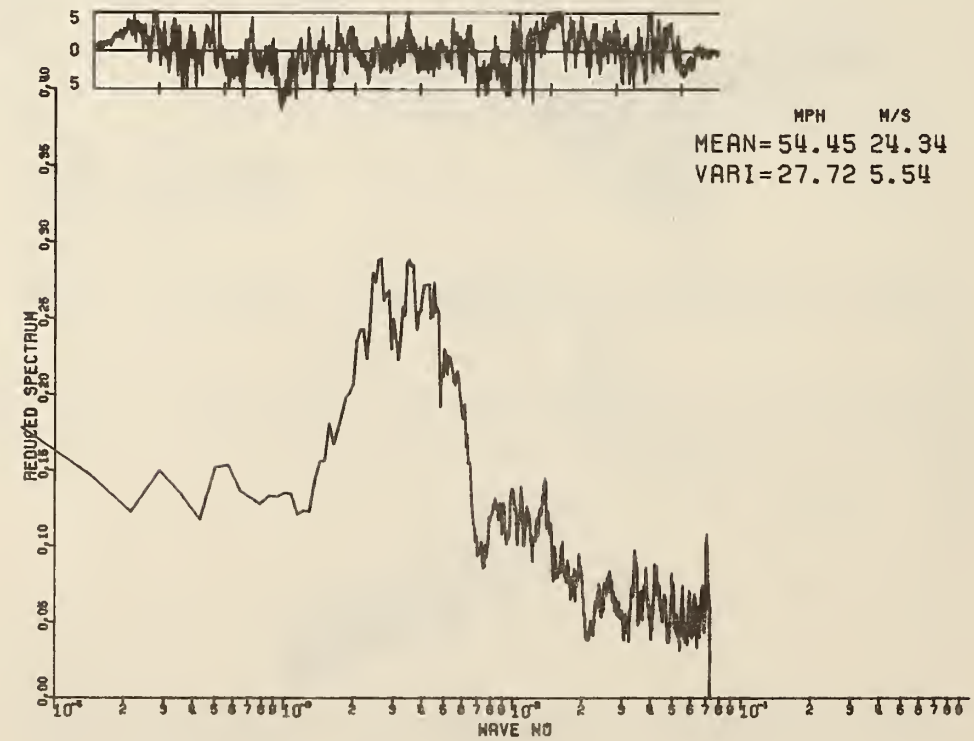

d) U-component - 6U.

Figure 35. Individual channel horizontal and vertical wind spectra for 60 mph wind (Newport, August 1971)(continued).

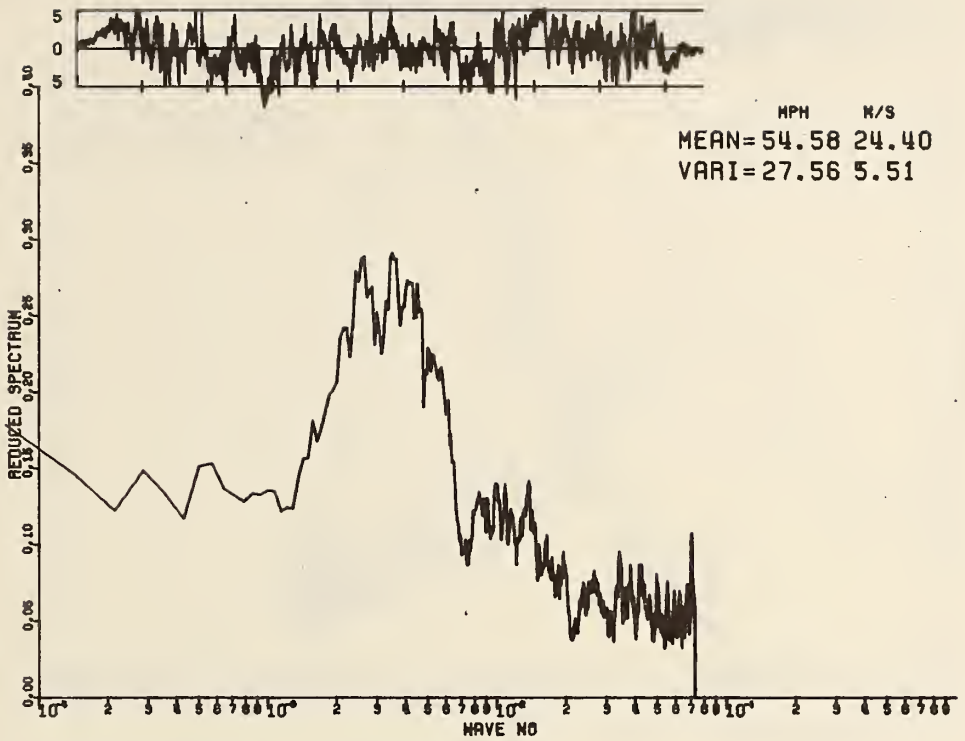

e) Resultant horizontal - 6R.

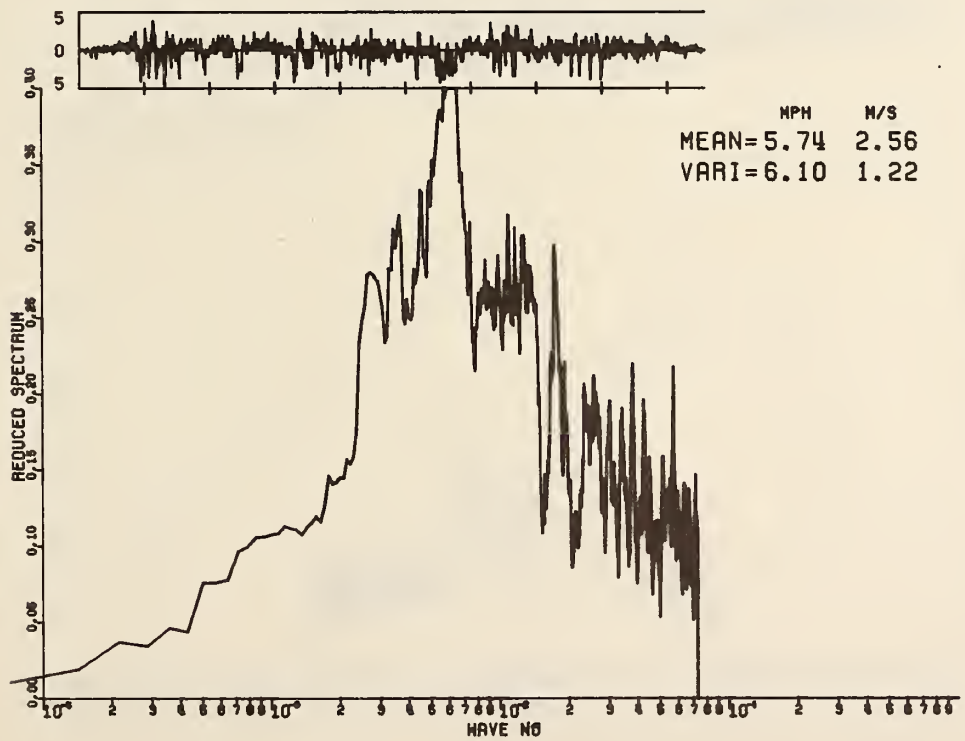

f) Vertical - 6W/U.

Figure 35. Individual channel horizontal and vertical wind spectra for 60 mph wind (Newport, August 1971)(continued).

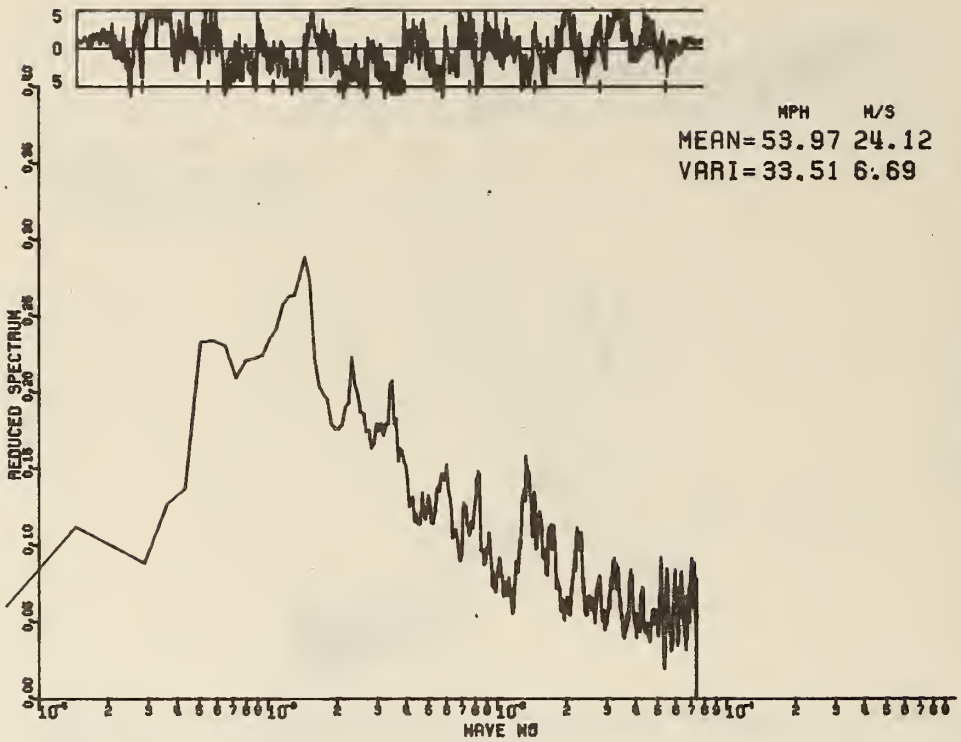

g) U-component - 7U.

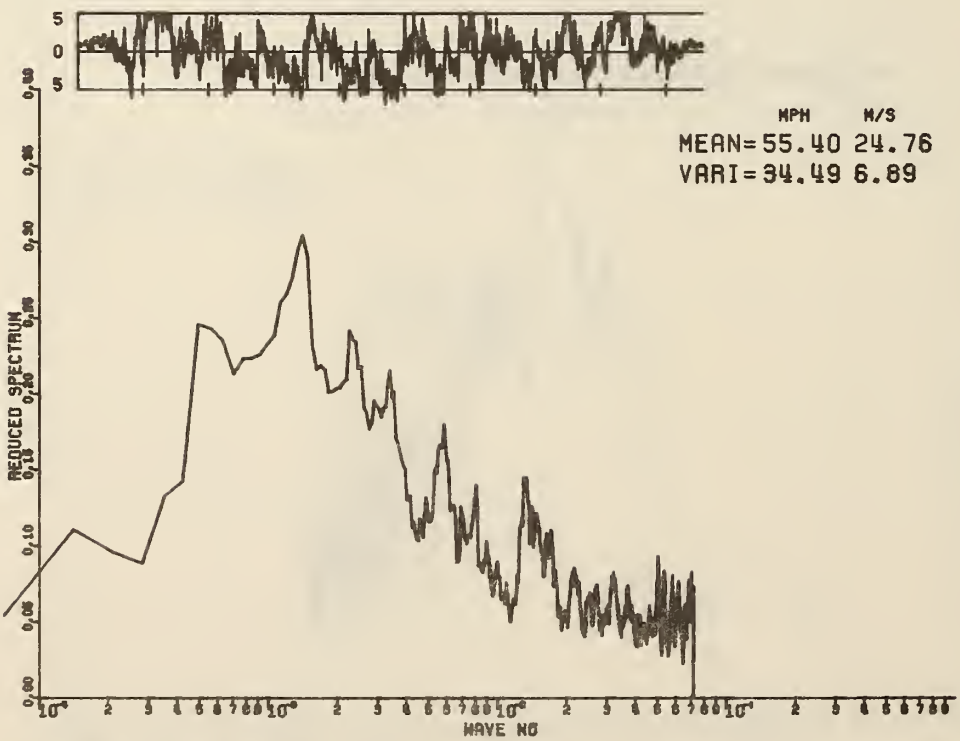

h) Resultant horizontal - 7R.

Figure 35. Individual channel horizontal and vertical wind spectra for 60 mph wind (Newport, August 1971)(continued).

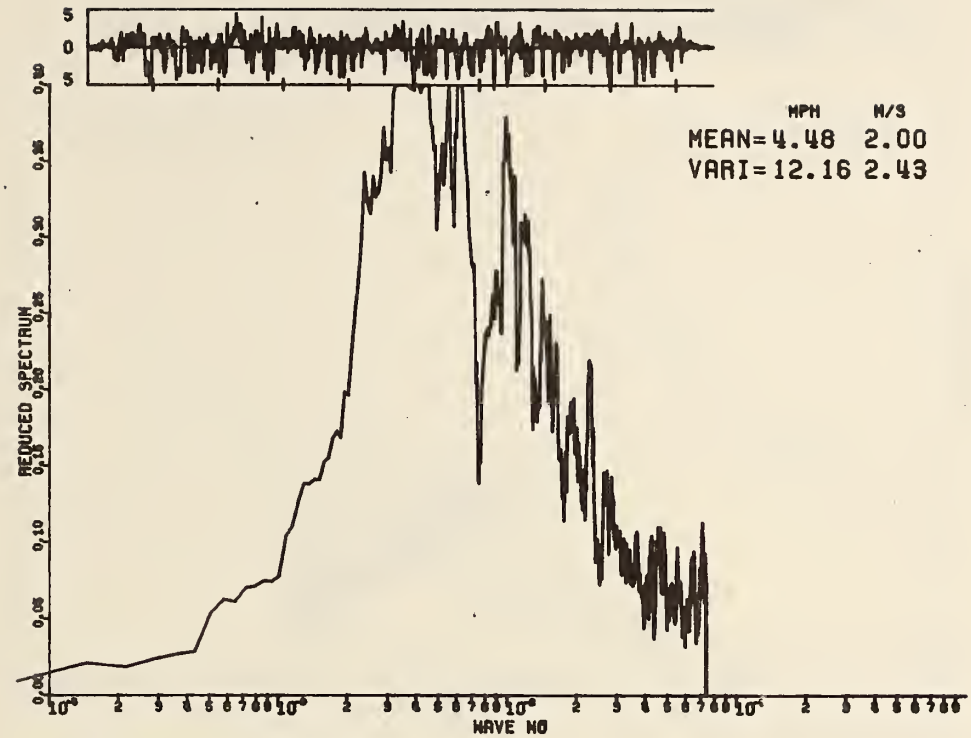

i) Vertical - 7W/U.

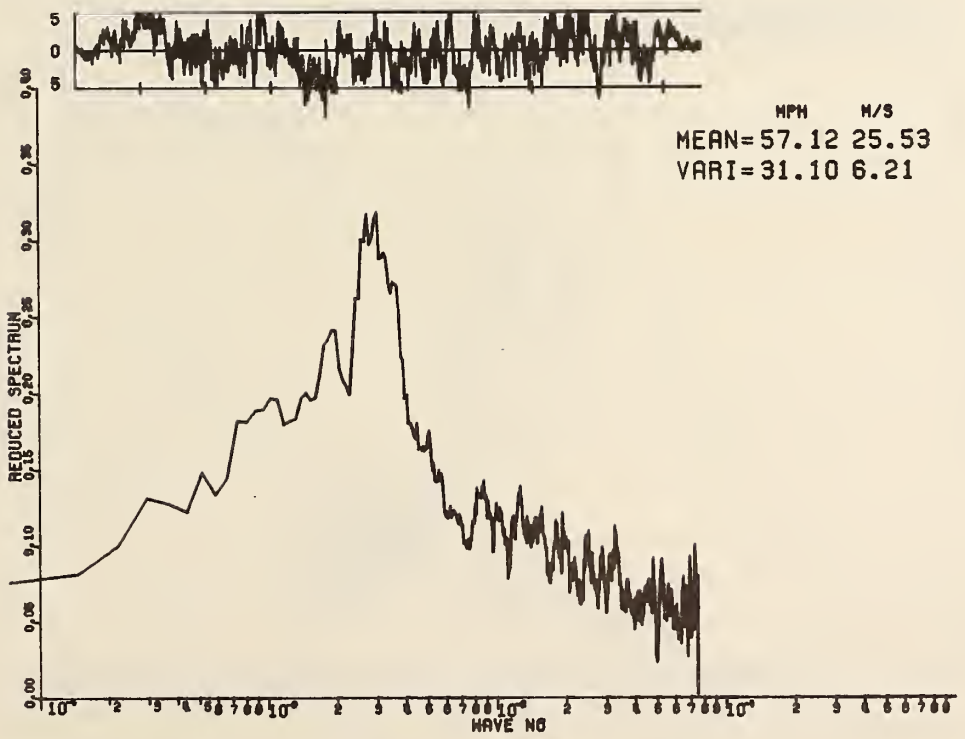

j) U-component - 8U.

Figure 35. Individual channel horizontal and vertical wind spectra for 60 mph wind (Newport, August 1971)(continued).

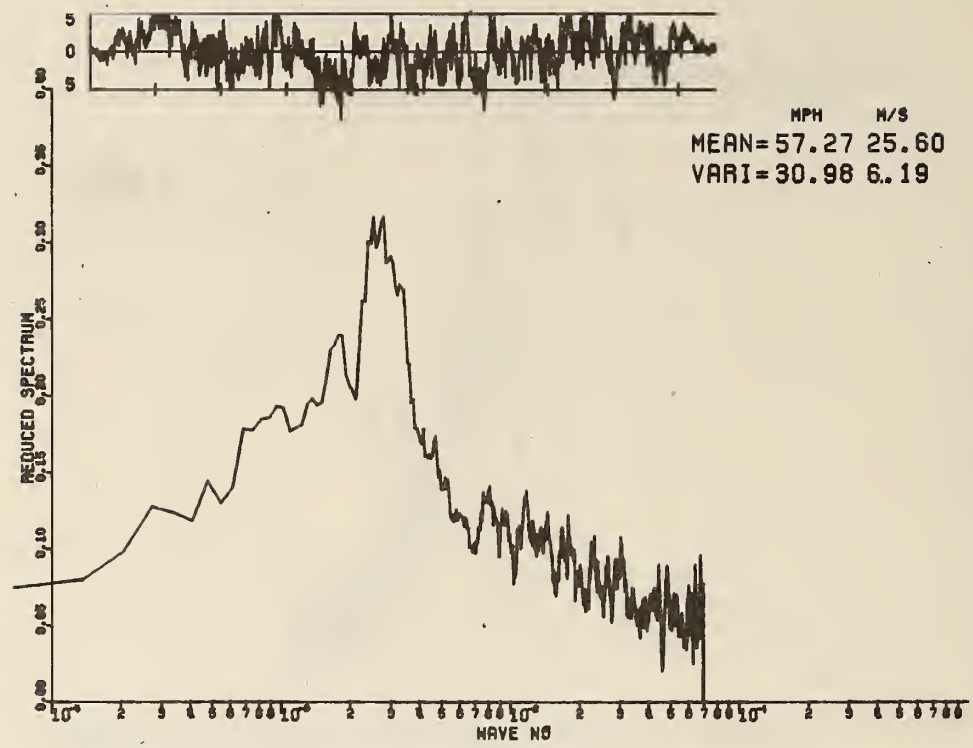

k) Resultant horizontal - 8R.

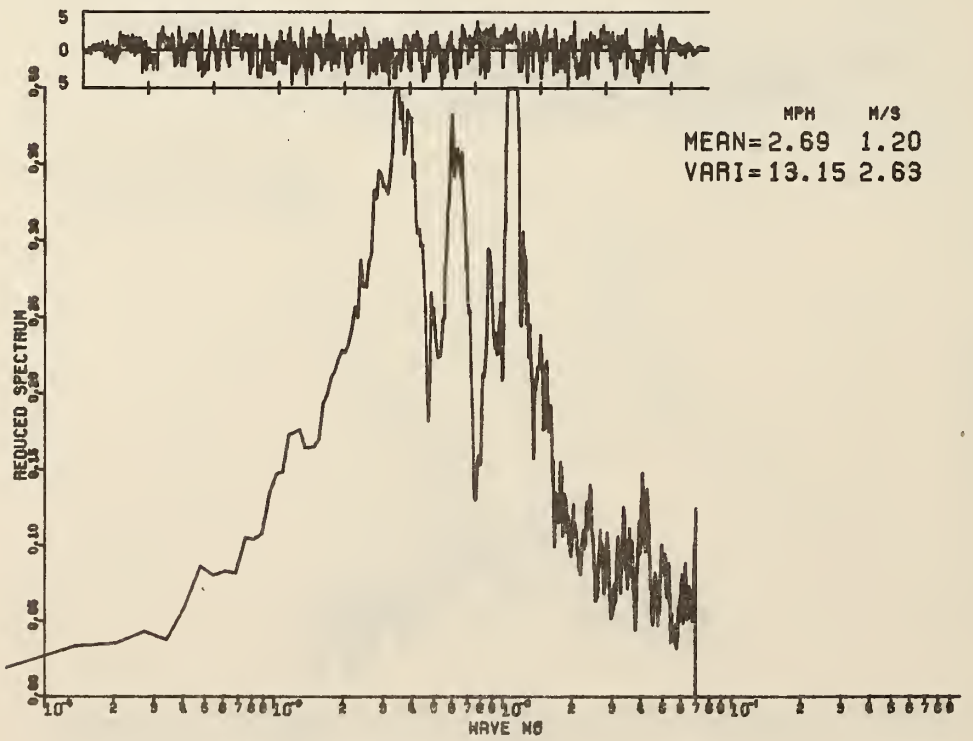

l) Vertical - 8W/U.

Figure 35. Individual channel horizontal and vertical wind spectra for 60 mph wind (Newport, August 1971)(continued).

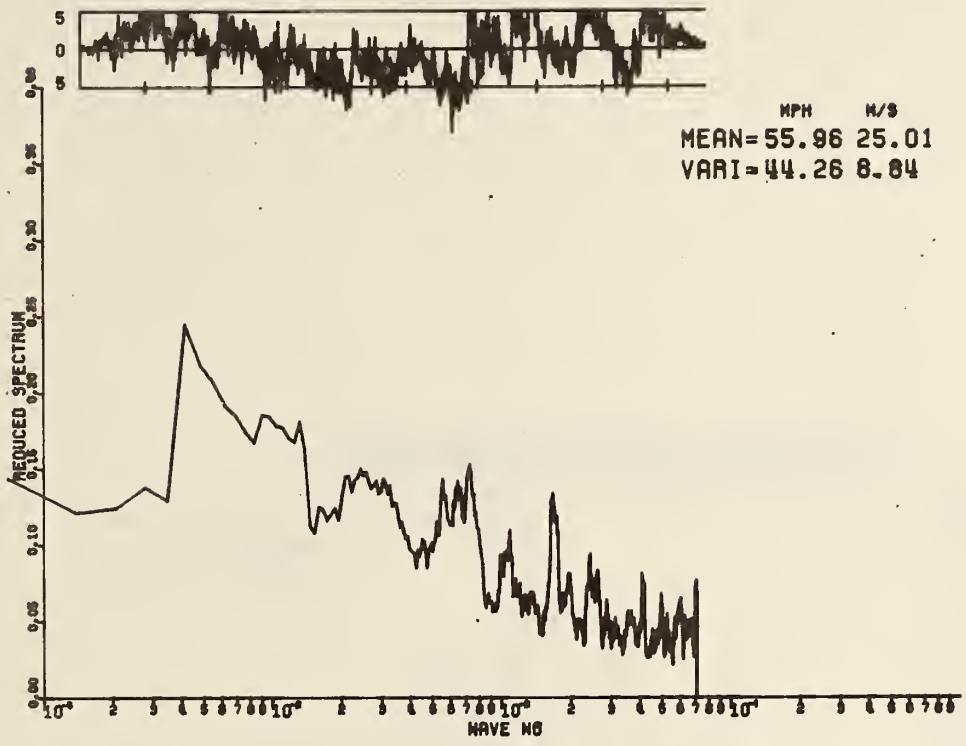

m) U-component - 9U.

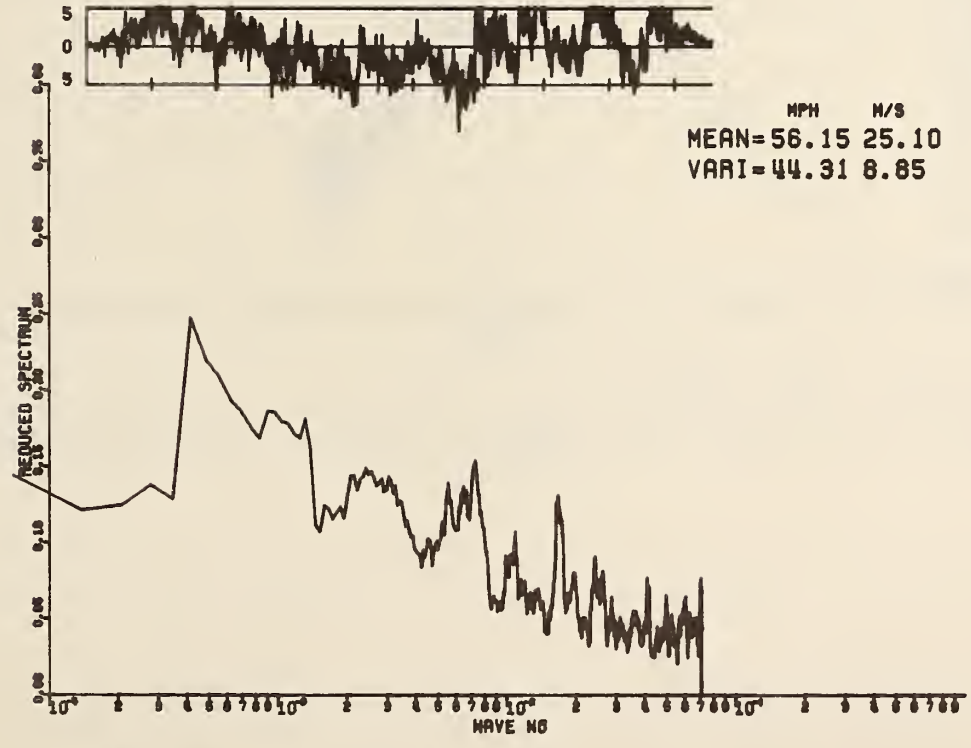

n) Resultant horizontal - 9R.

Figure 35. Individual channel horizontal and vertical wind spectra for 60 mph wind (Newport, August 1971)(continued).

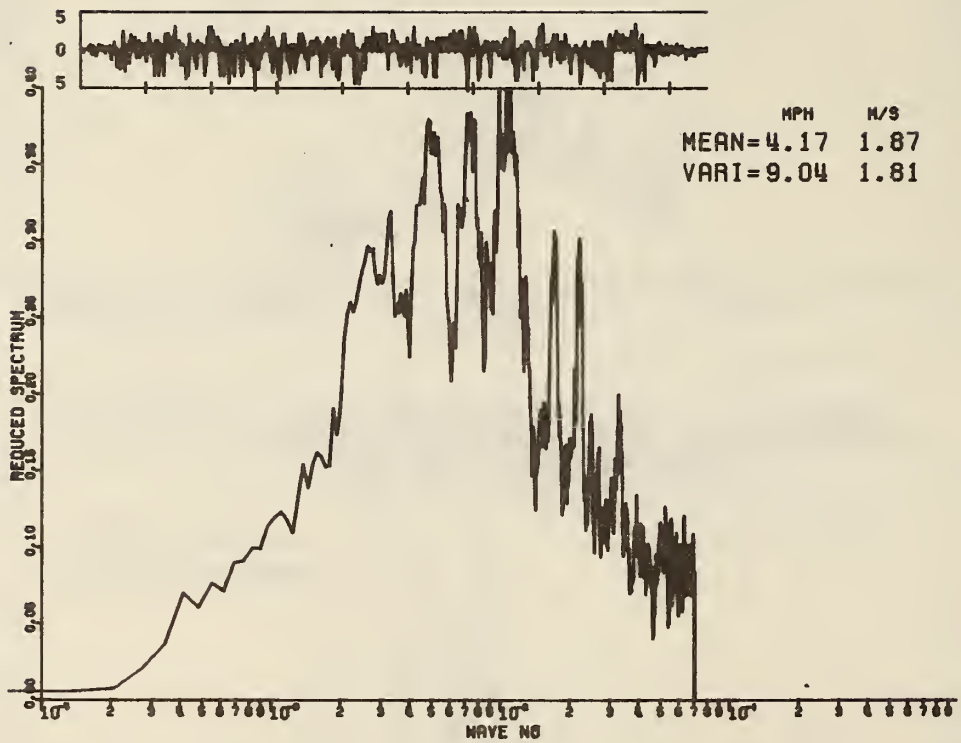

o) Vertical - 9W/U.

Figure 35. Individual channel horizontal and vertical wind spectra for 60 mph wind (Newport, August 1971)(continued).

APPENDIX D

INDIVIDUAL CHANNEL WIND SPECTRA: NEWPORT, JANUARY 1972

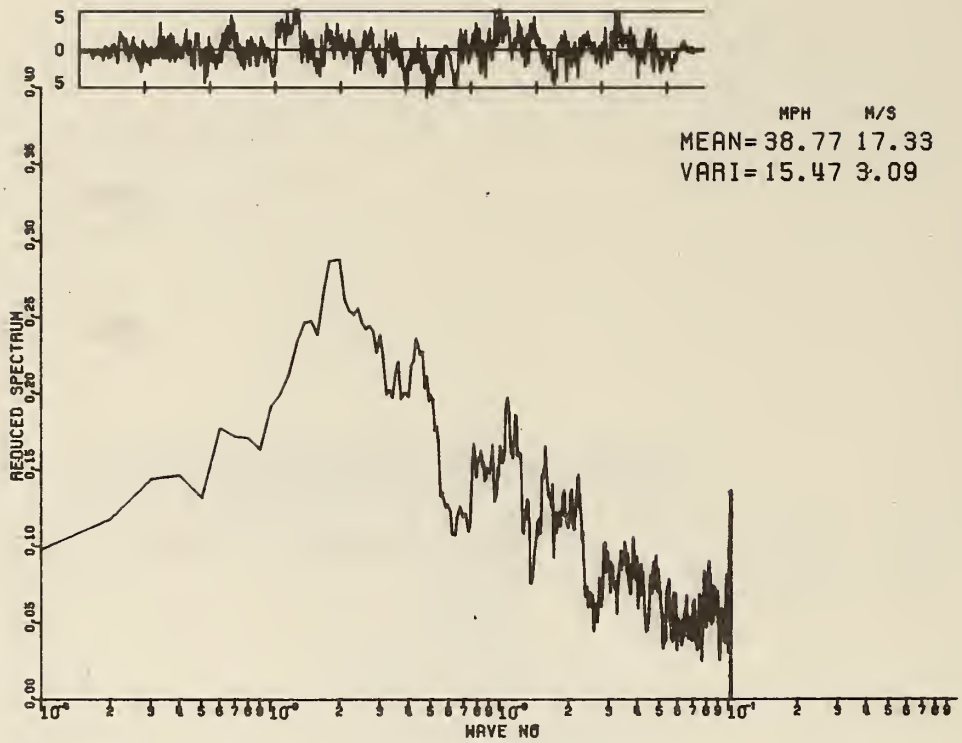

a) U-component - 2U.

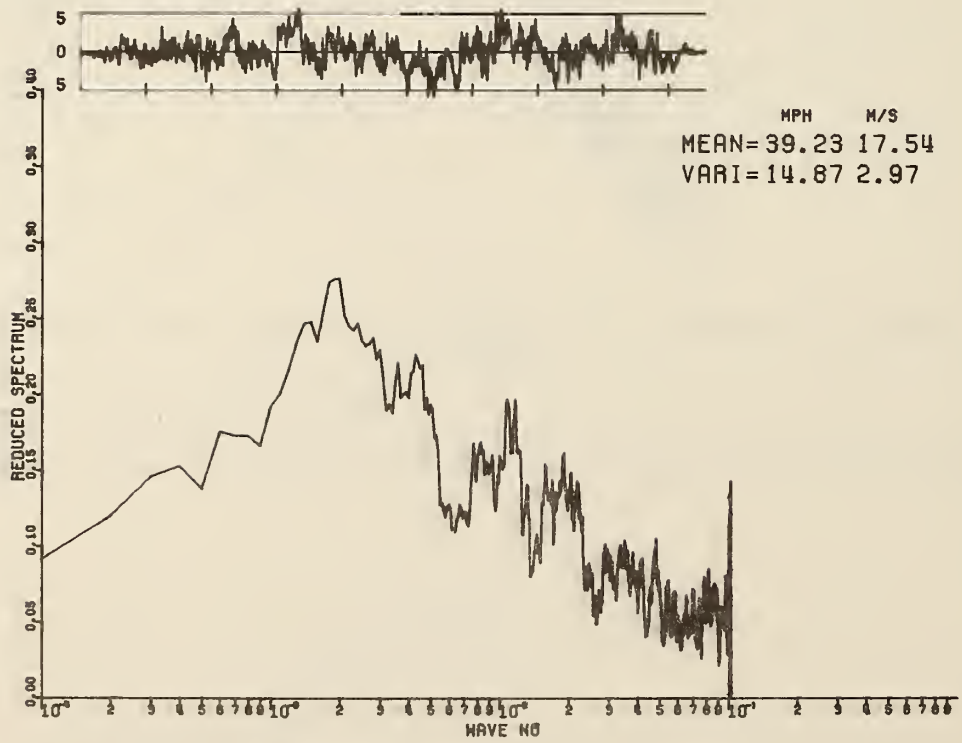

b) Resultant horizontal - 2R.

Figure 36. Individual channel horizontal and vertical wind spectra for 40 mph wind (Newport, January 1972).

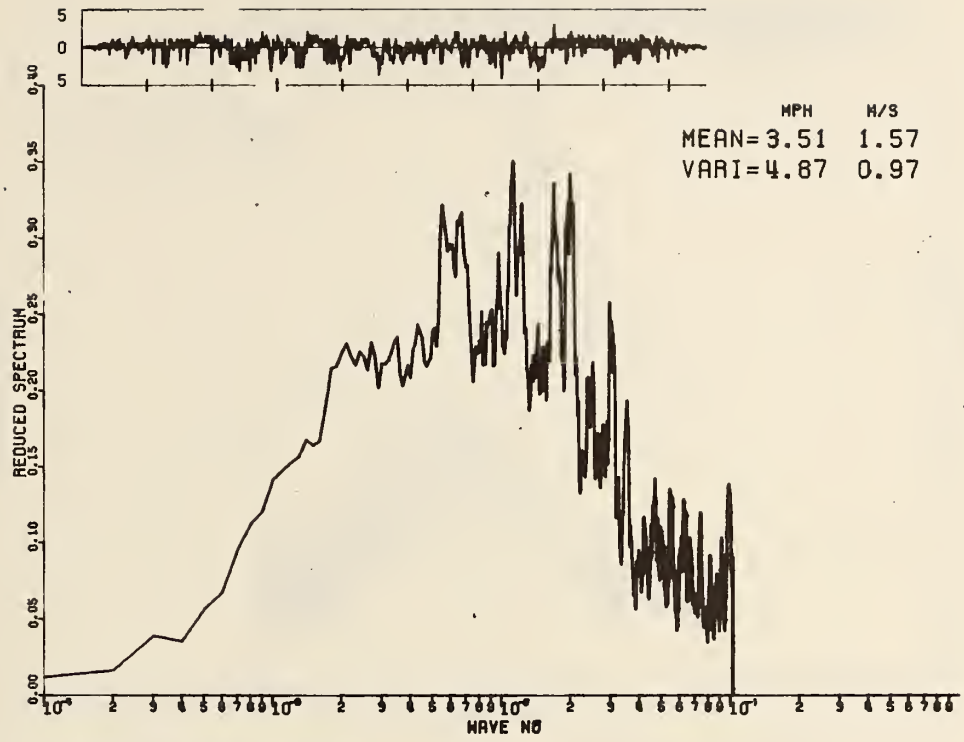

c) Vertical - 2W/U.

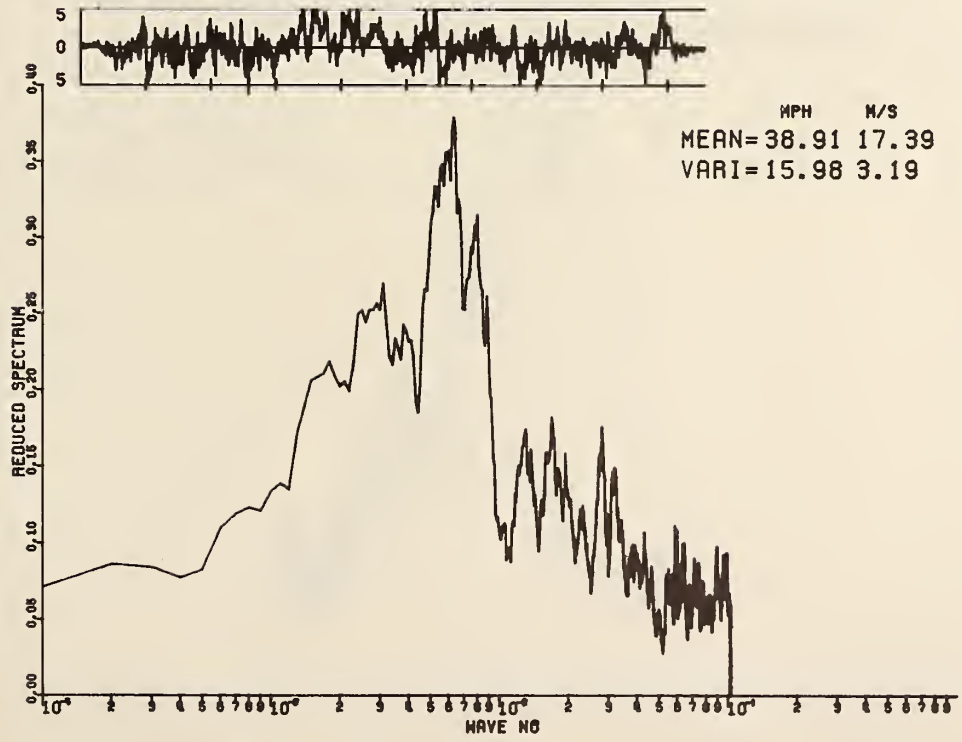

d) U-component - 3U.

Figure 36. Individual channel horizontal and vertical wind spectra for 40 mph wind (Newport, January 1972) (continued).

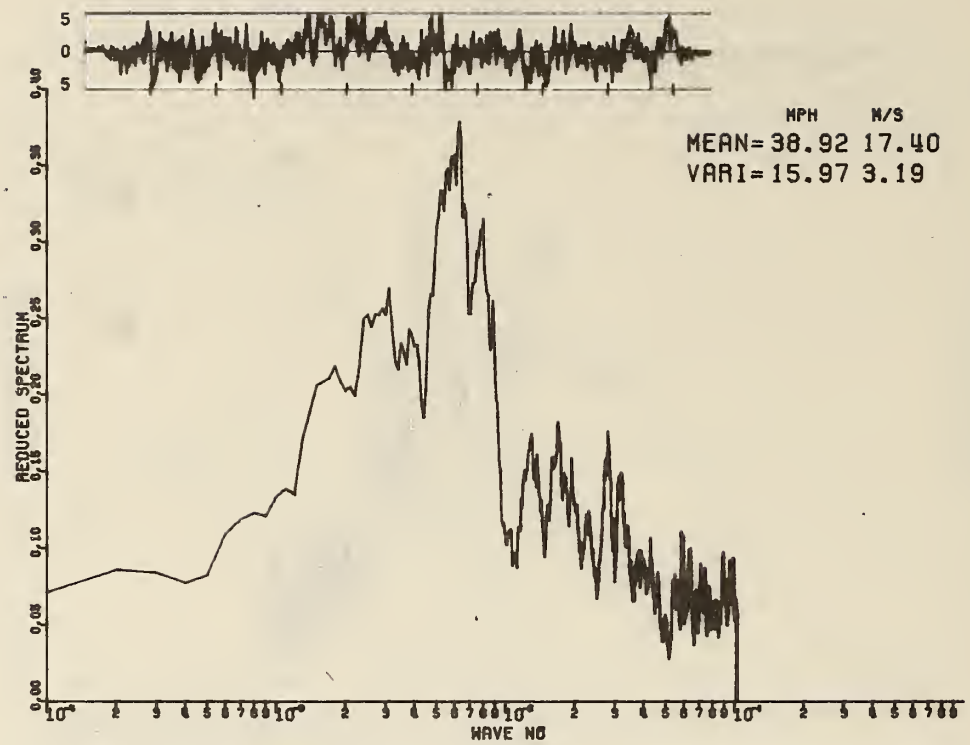

e) Resultant horizontal - 3R.

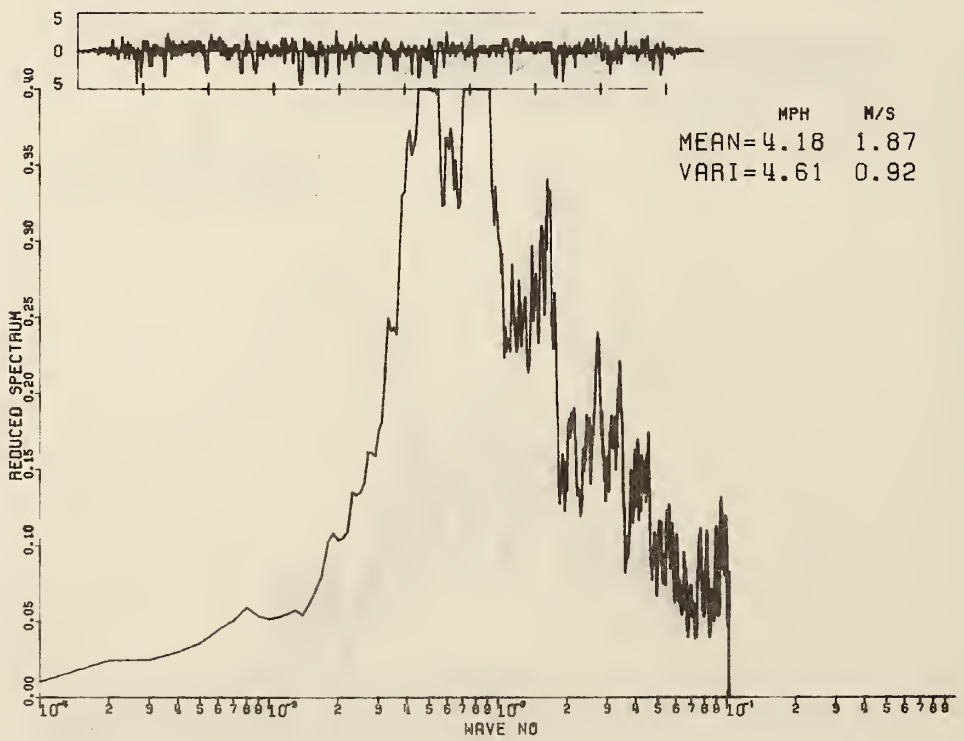

f) Vertical - 3W/U.

Figure 36. Individual channel horizontal and vertical wind spectra for 40 mph wind (Newport, January 1972)(continued).

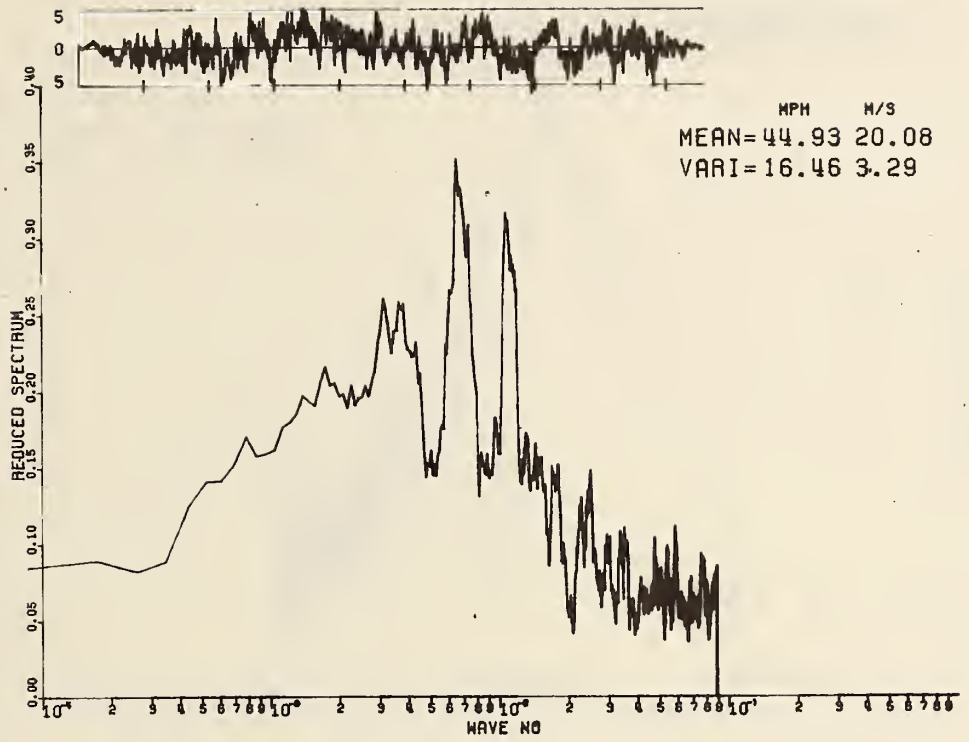

g) U-component - 5U.

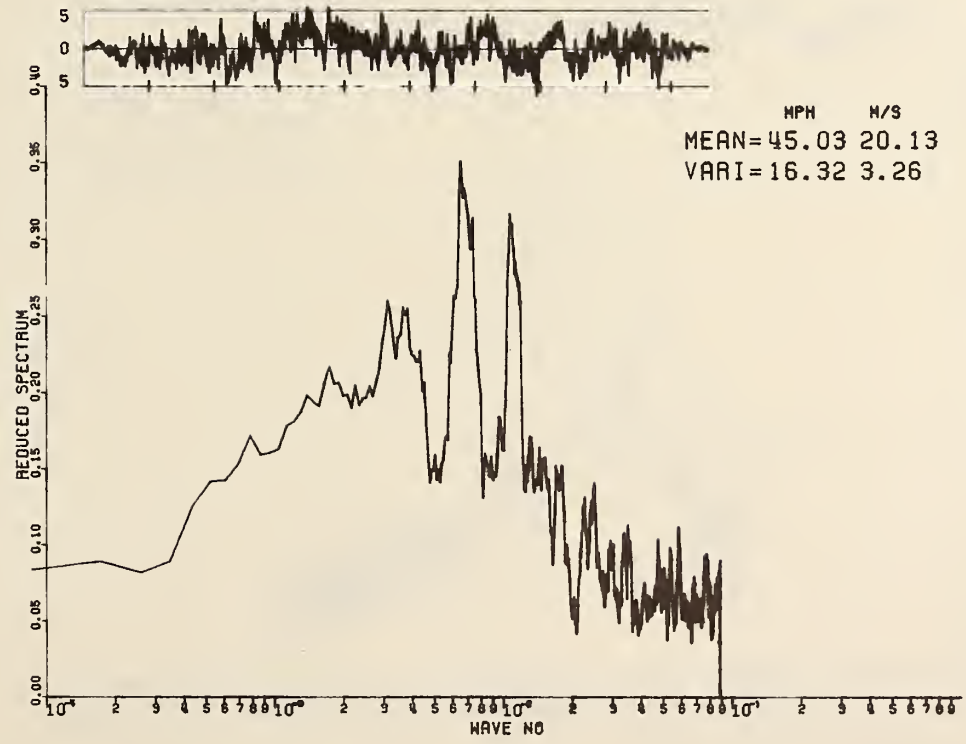

h) Resultant horizontal - 5R.

Figure 36. Individual channel horizontal and vertical wind spectra for 40 mph wind (Newport, January 1972)(continued).

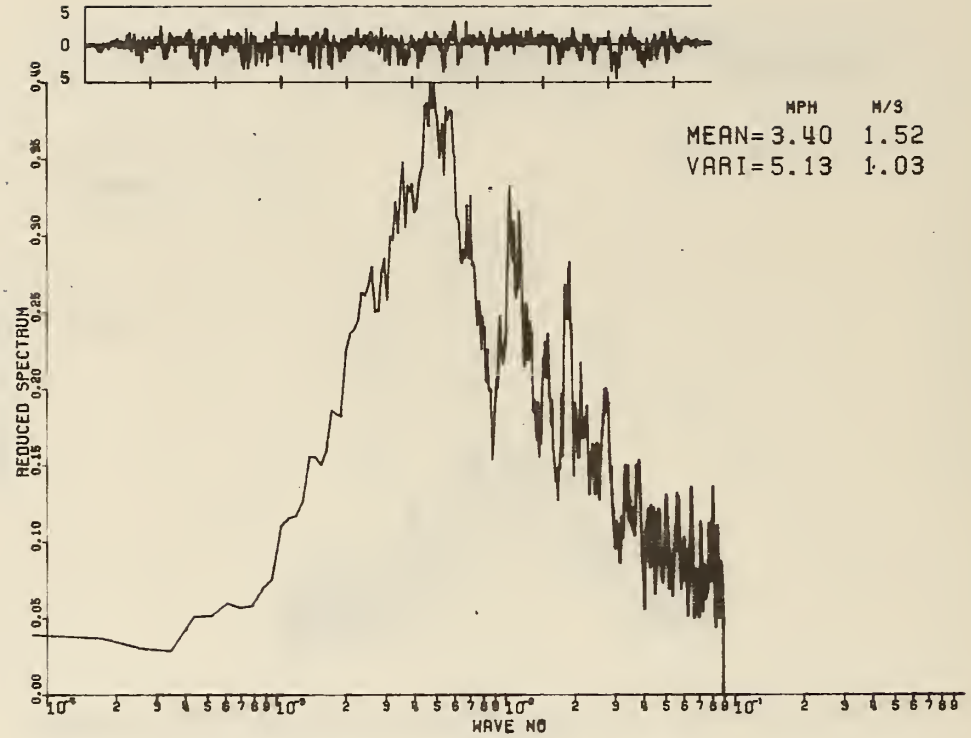

i) Vertical - 5W/U.

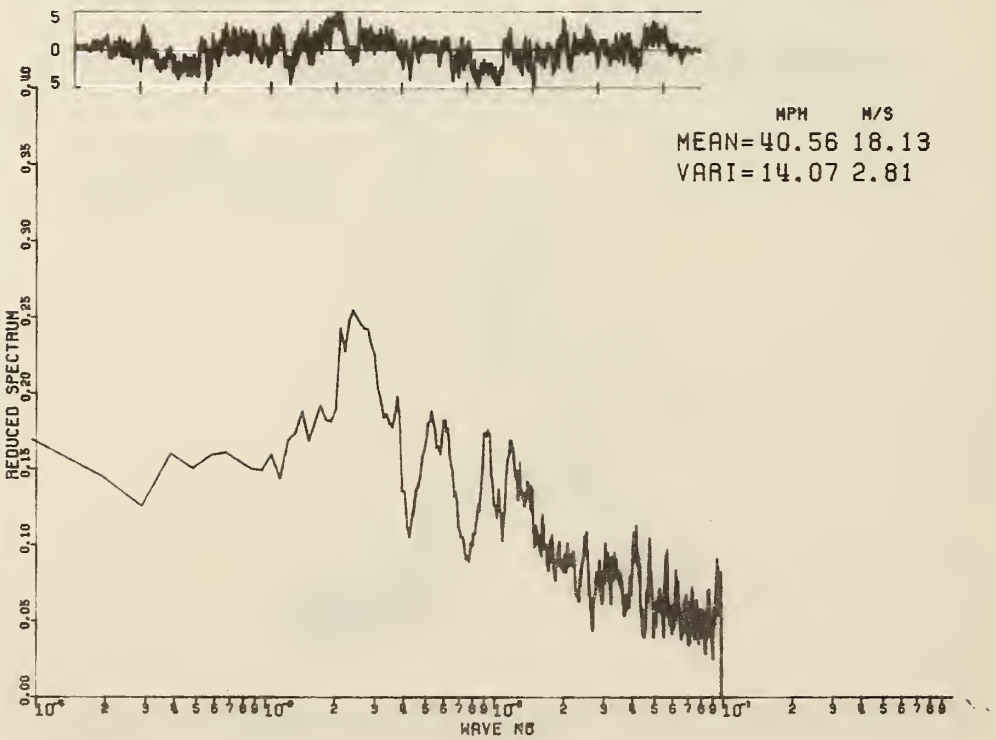

j) U-component - 6U.

Figure 36. Individual channel horizontal and vertical wind spectra for 40 mph wind (Newport, January 1972)(continued).

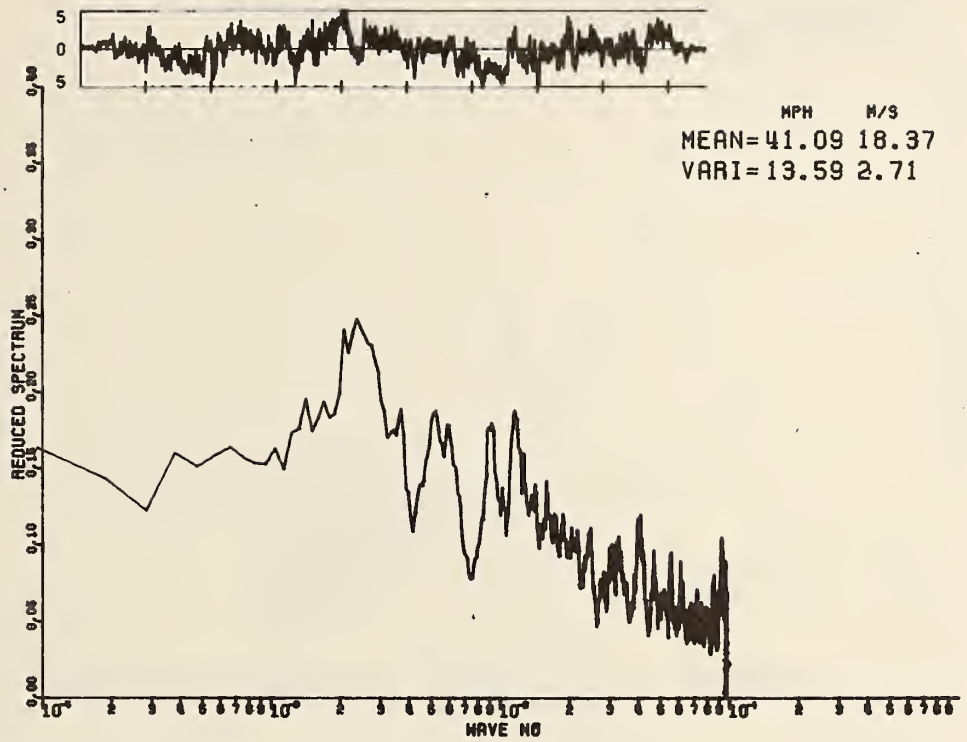

k) Resultant horizontal - 6R.

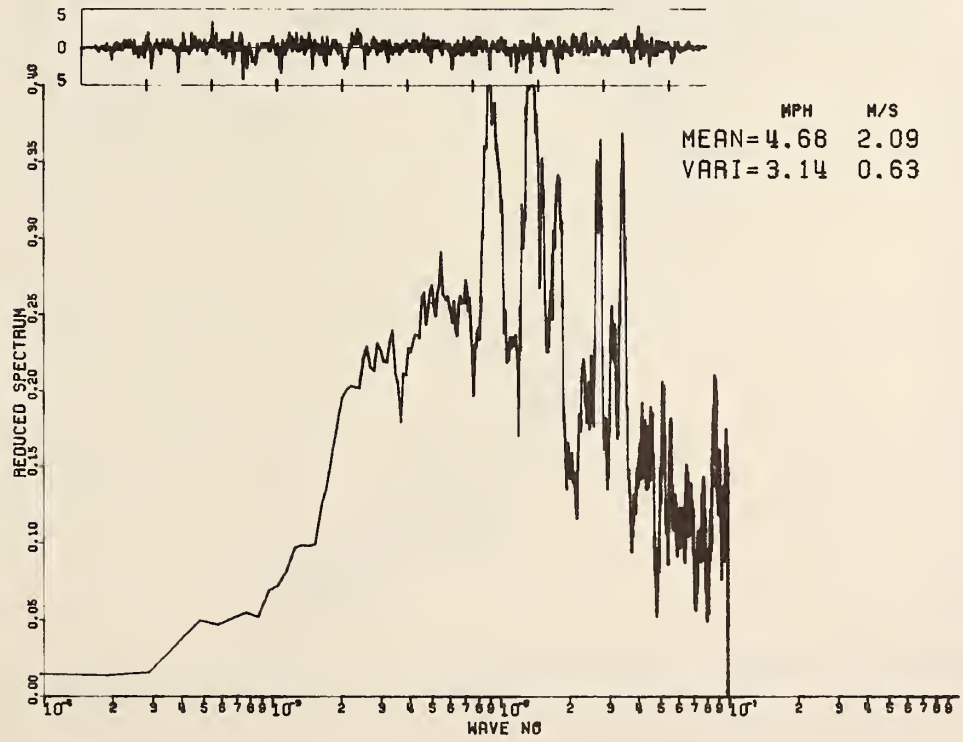

l) Vertical - 6W/U.

Figure 36. Individual channel horizontal and vertical wind spectra for 40 mph wind (Newport, January 1972)(continued).

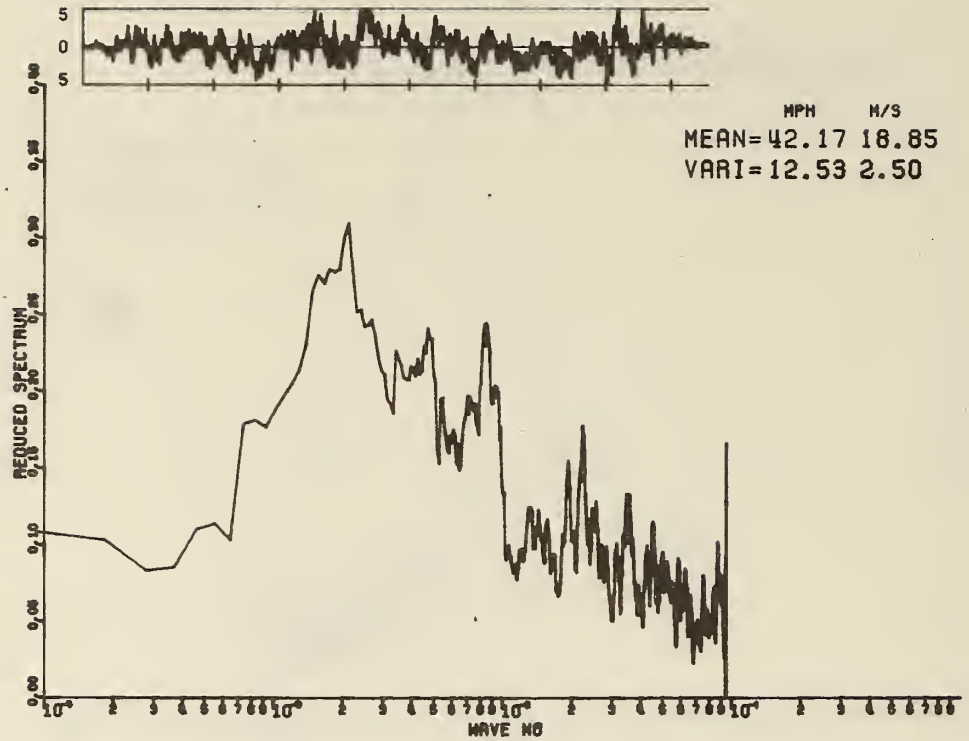

m) U-component - 7U.

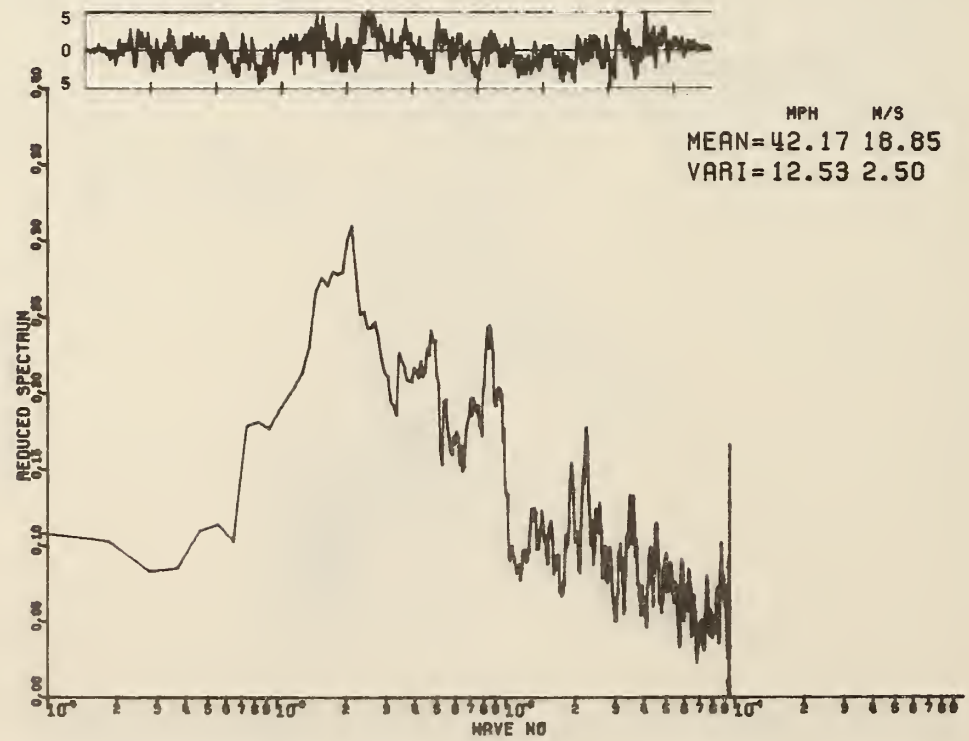

n) Resultant horizontal - 7R.

Figure 36. Individual channel horizontal and vertical wind spectra for 40 mph wind (Newport, January 1972)(continued).

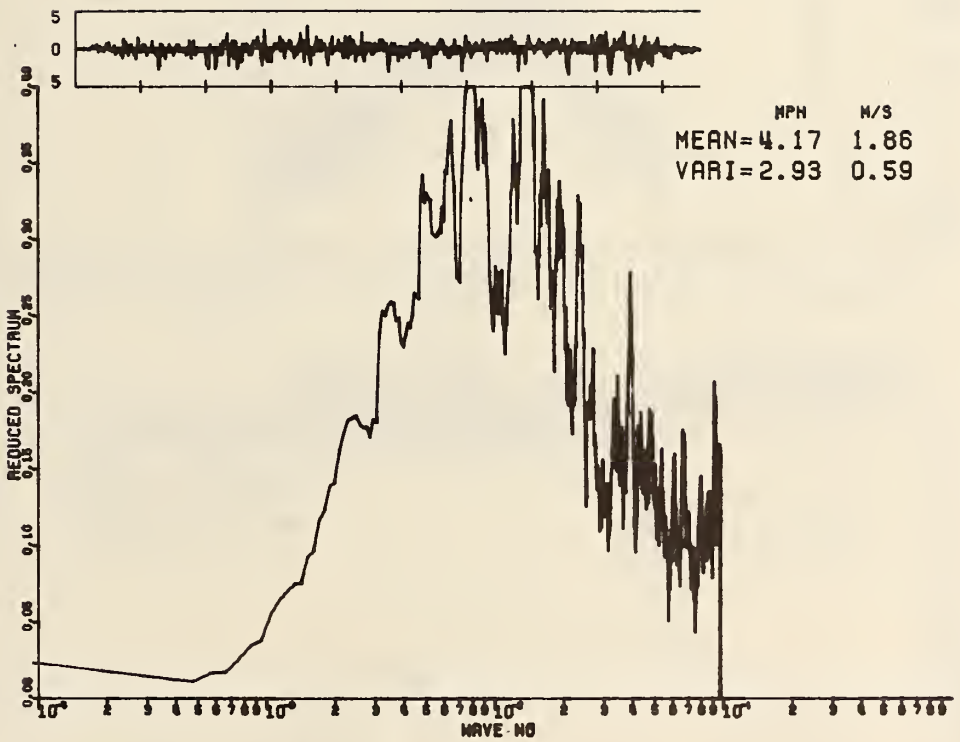

o) Vertical - 7W/U.

Figure 36. Individual channel horizontal and vertical wind spectra for 40 mph wind (Newport, January 1972)(continued).

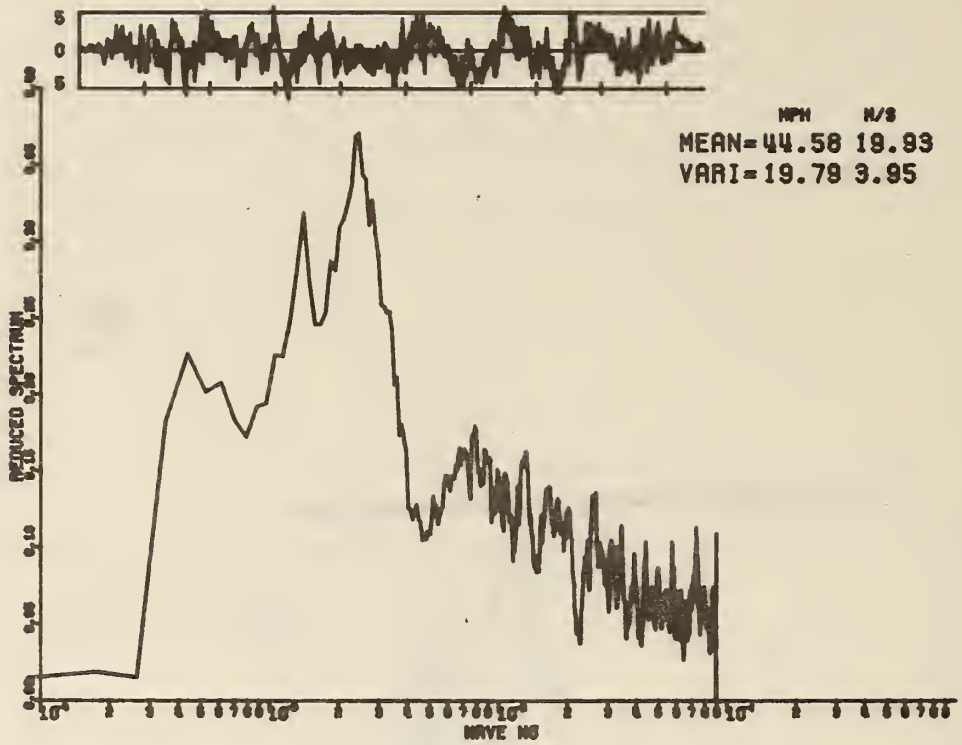

a) U-component - 2U.

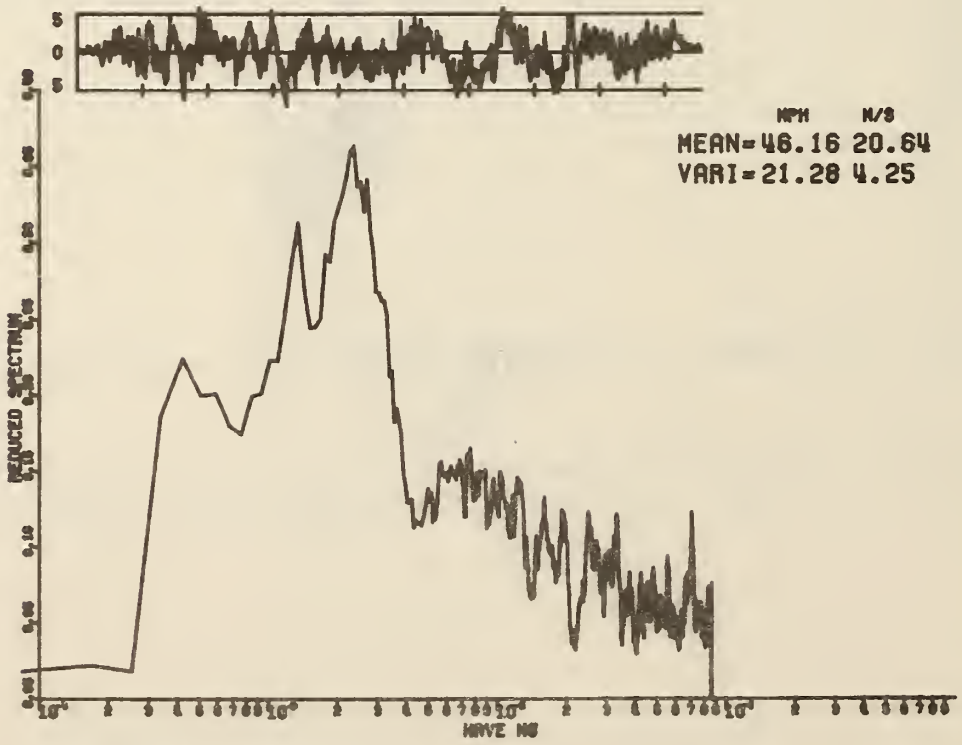

b) Resultant horizontal - 2R.

Figure 37. Individual channel horizontal and vertical wind spectra for 50 mph wind (Newport, January 1972).

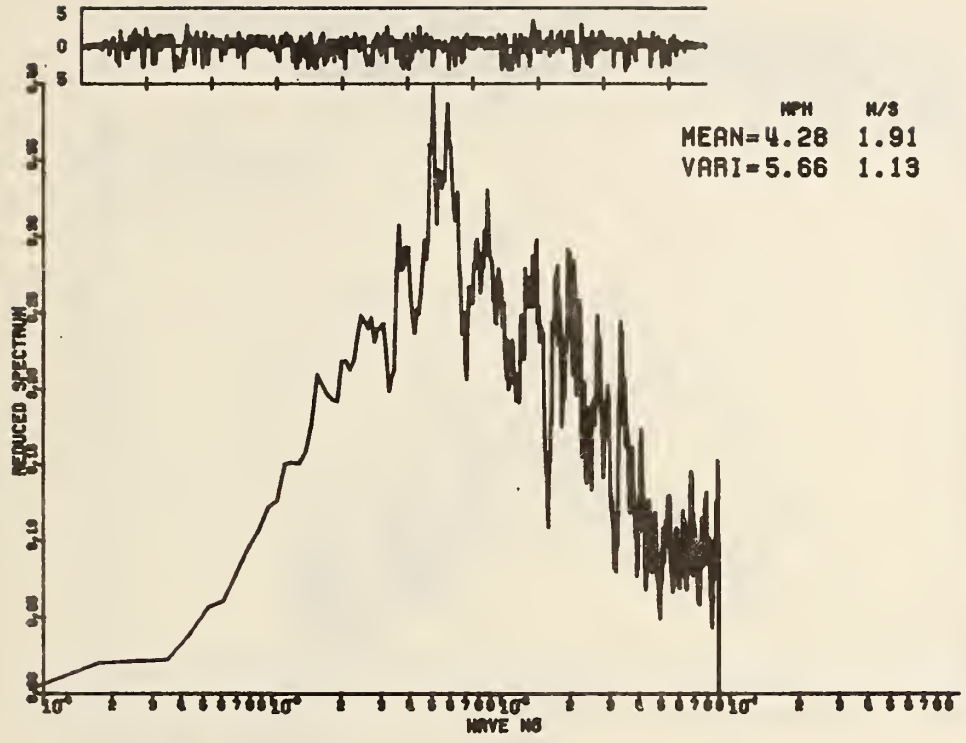

c) Vertical - 2W/U.

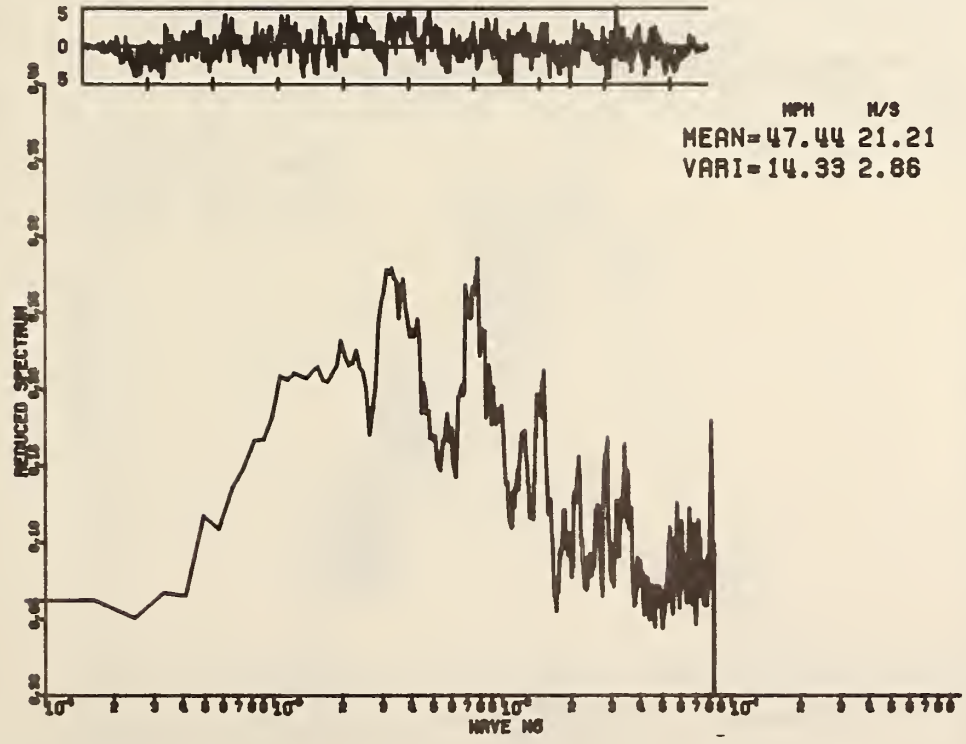

d) U-component - 3U.

Figure 37. Individual channel horizontal and vertical wind spectra for 50 mph wind (Newport, January 1972)(continued).

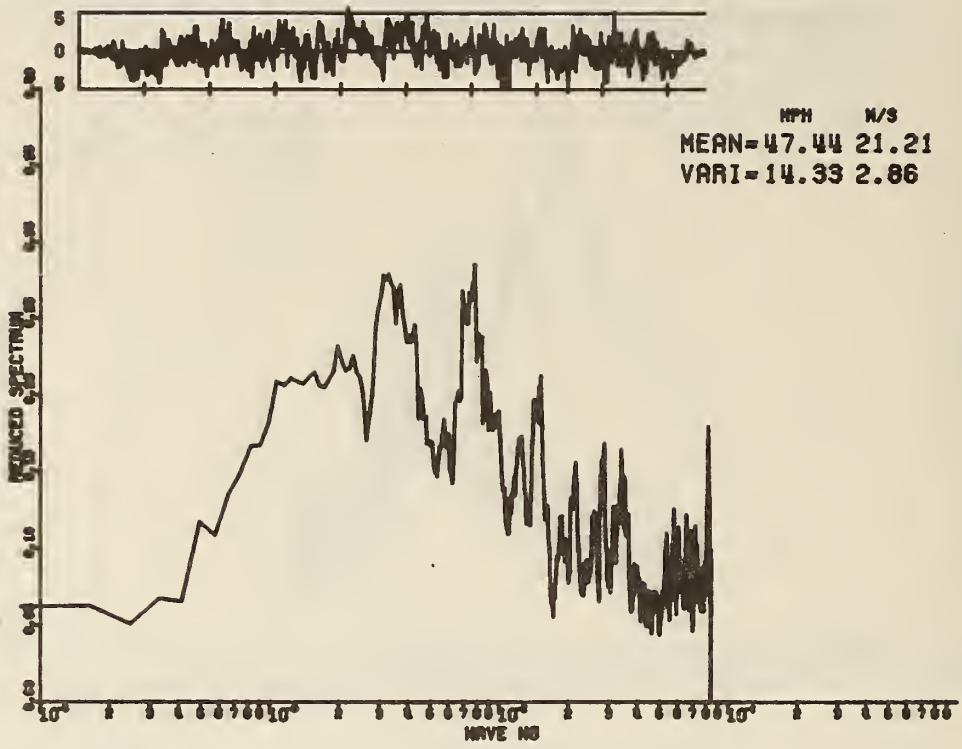

e) Resultant horizontal - 3R.

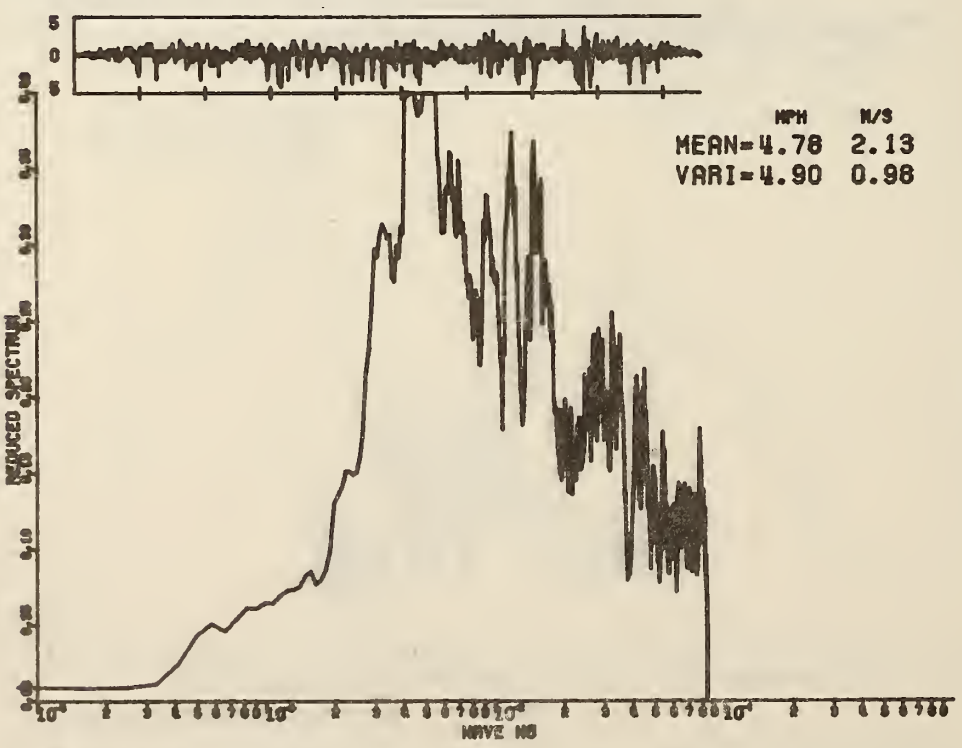

f) Vertical - 3W/U.

Figure 37. Individual channel horizontal and vertical wind spectra for 50 mph wind (Newport, January 1972)(continued).

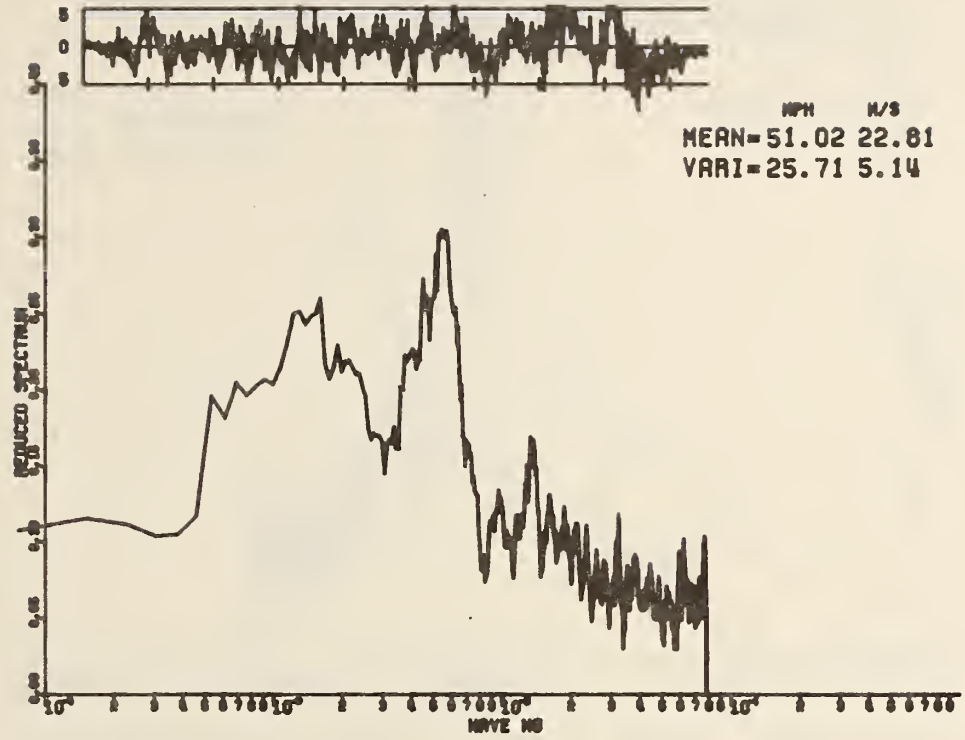

g) U-component - 5U.

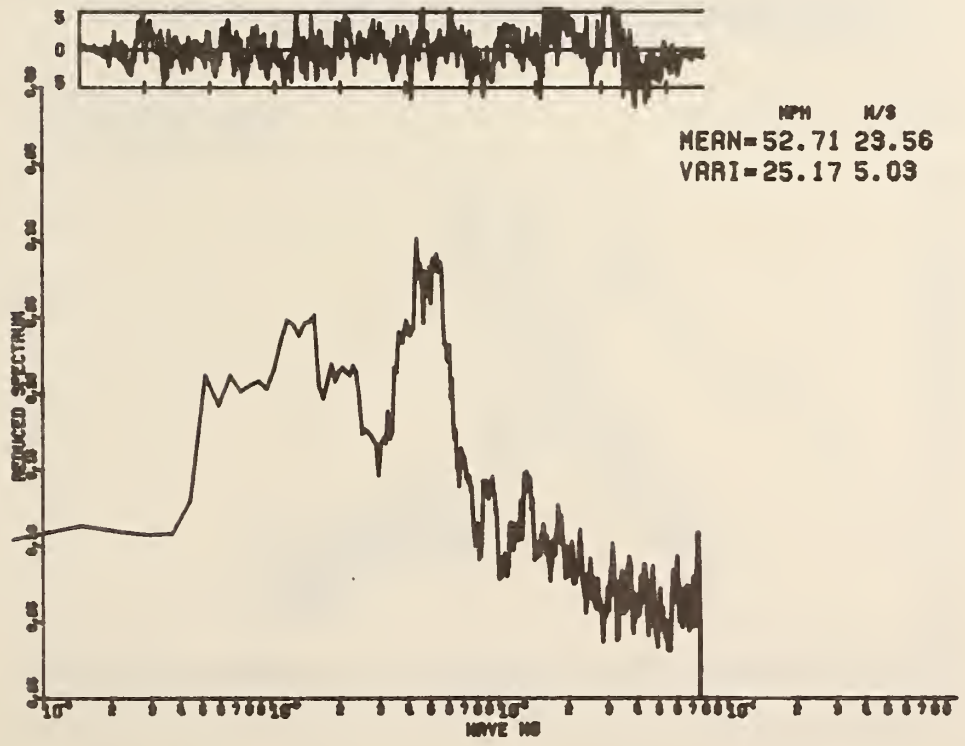

h) Resultant horizontal - 5R.

Figure 37. Individual channel horizontal and vertical wind spectra for 50 mph wind (Newport, January 1972)(continued).

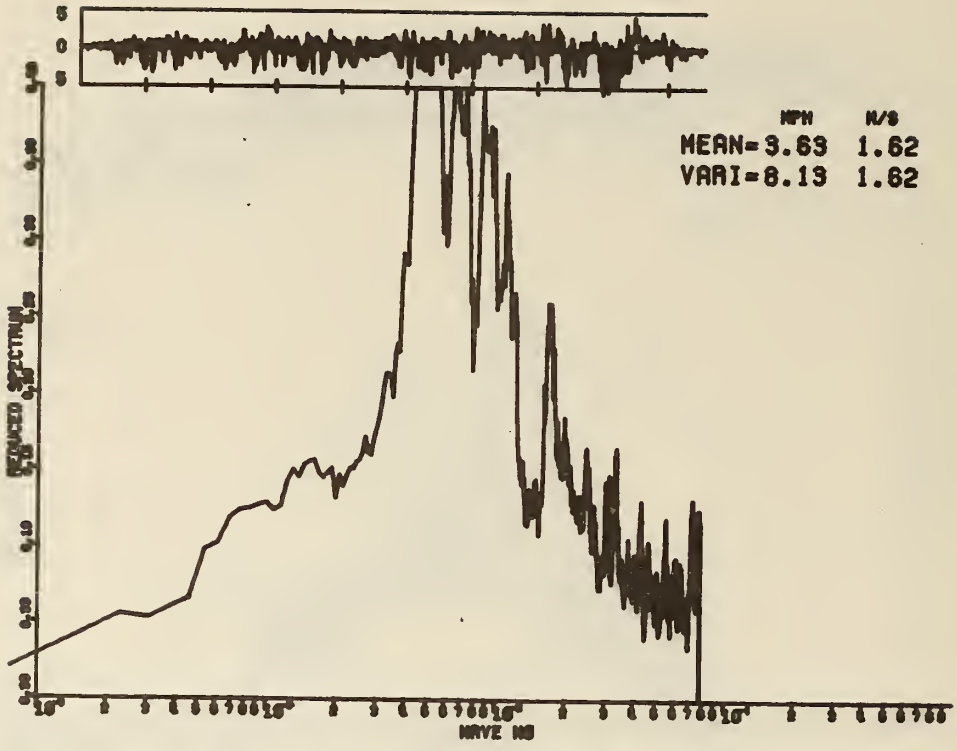

i) Vertical - 5W/U.

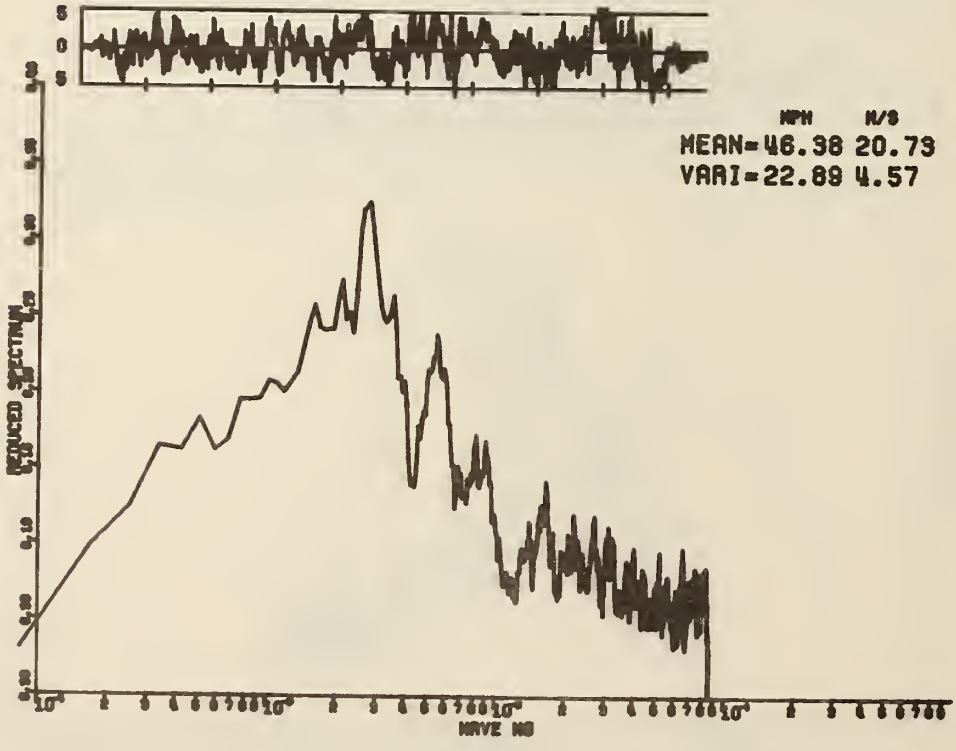

j) U-component - 6U.

Figure 37. Individual channel horizontal and vertical wind spectra for 50 mph wind (Newport, January 1972)(continued).

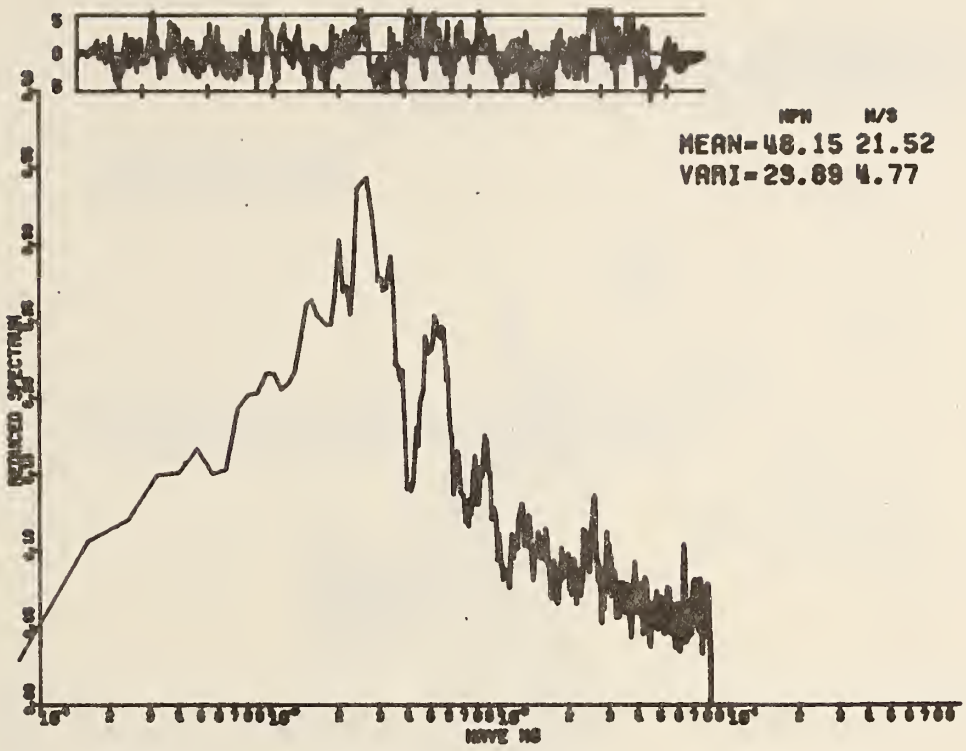

k) Resultant horizontal - 6R.

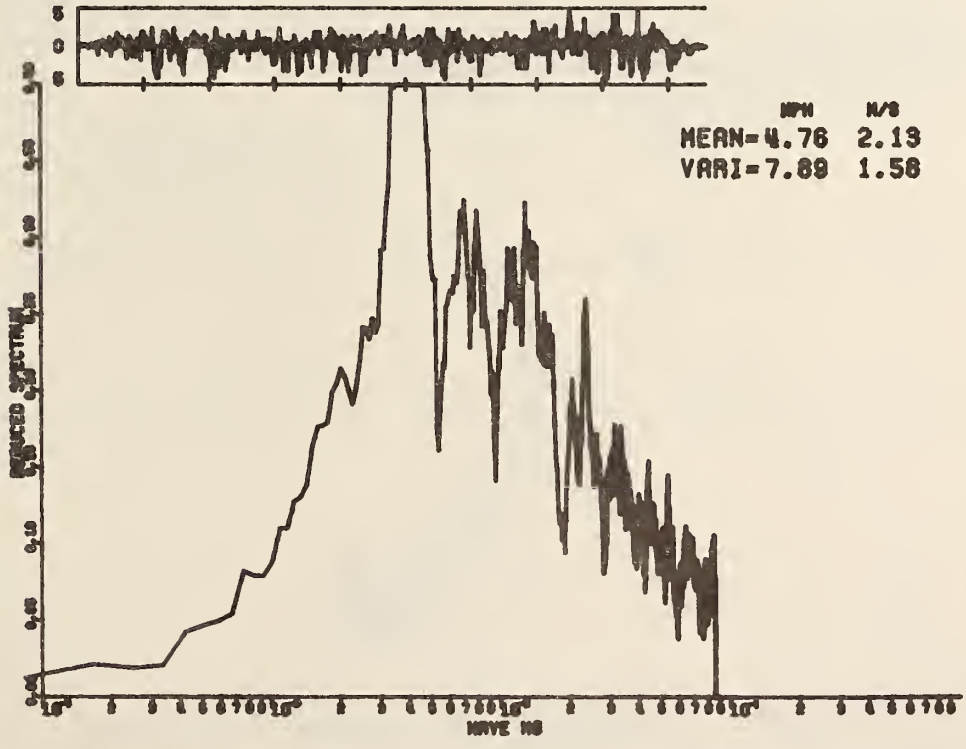

l) Vertical - 6W/U.

Figure 37. Individual channel horizontal and vertical wind spectra for 50 mph wind (Newport, January 1972)(continued).

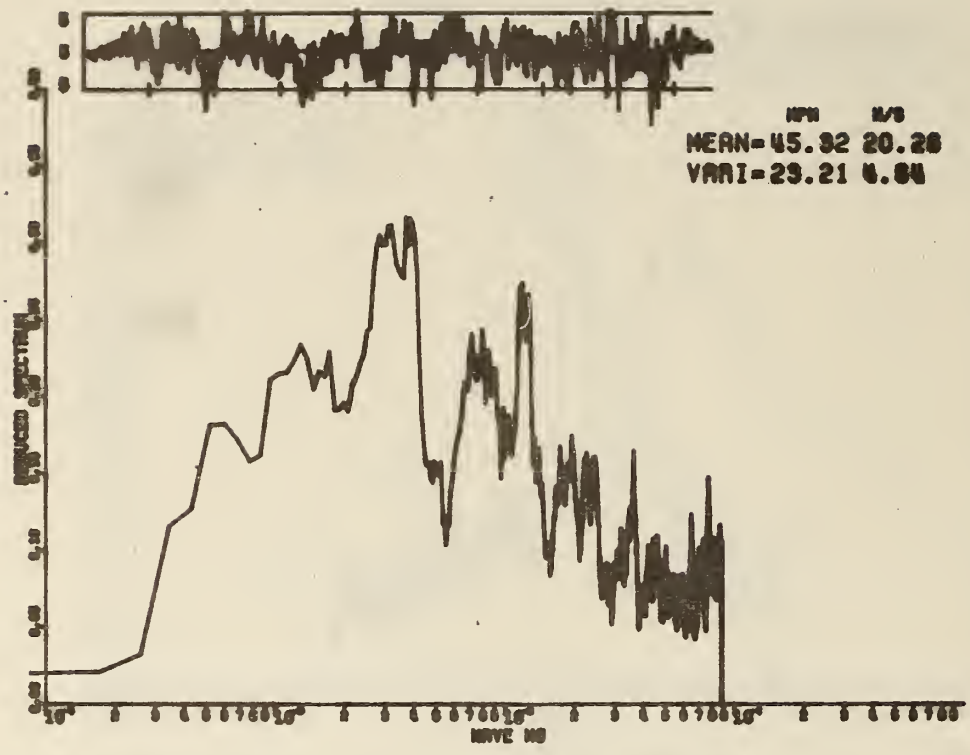

m) U-component - 7U.

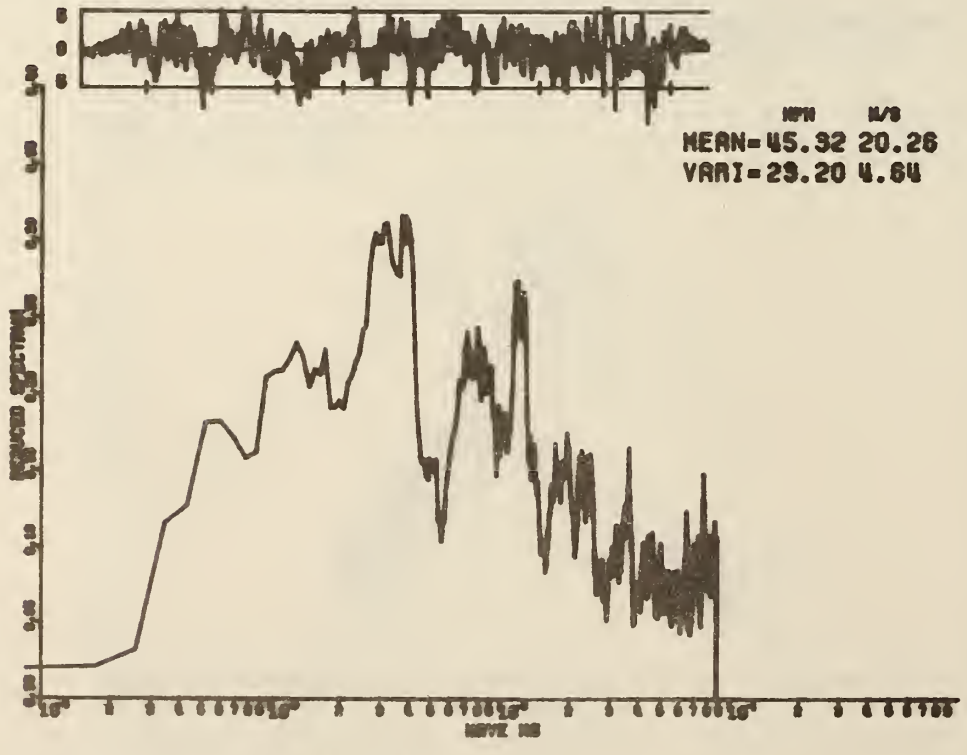

n) Resultant horizontal - 7R.

Figure 37. Individual channel horizontal and vertical wind spectra for 50 mph wind (Newport, January 1972)(continued).

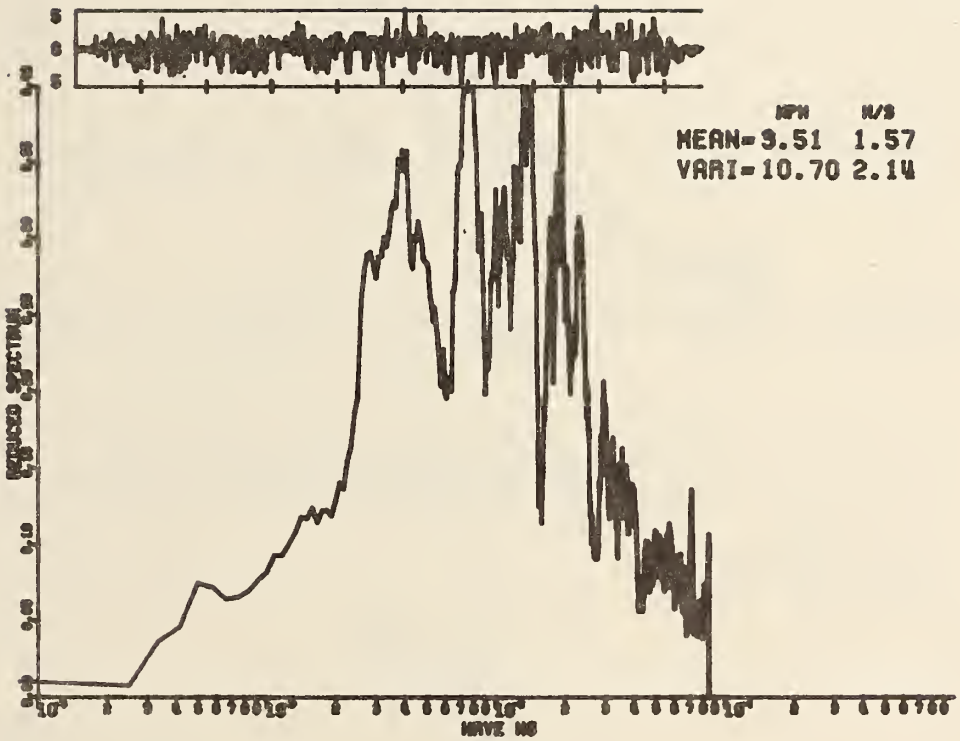

o) Vertical - 7W/U.

Figure 37. Individual channel horizontal and vertical wind spectra for 50 mph wind (Newport, January 1972)(continued).

APPENDIX E

INDIVIDUAL CHANNEL WIND SPECTRA: SITKA, NOVEMBER 1975

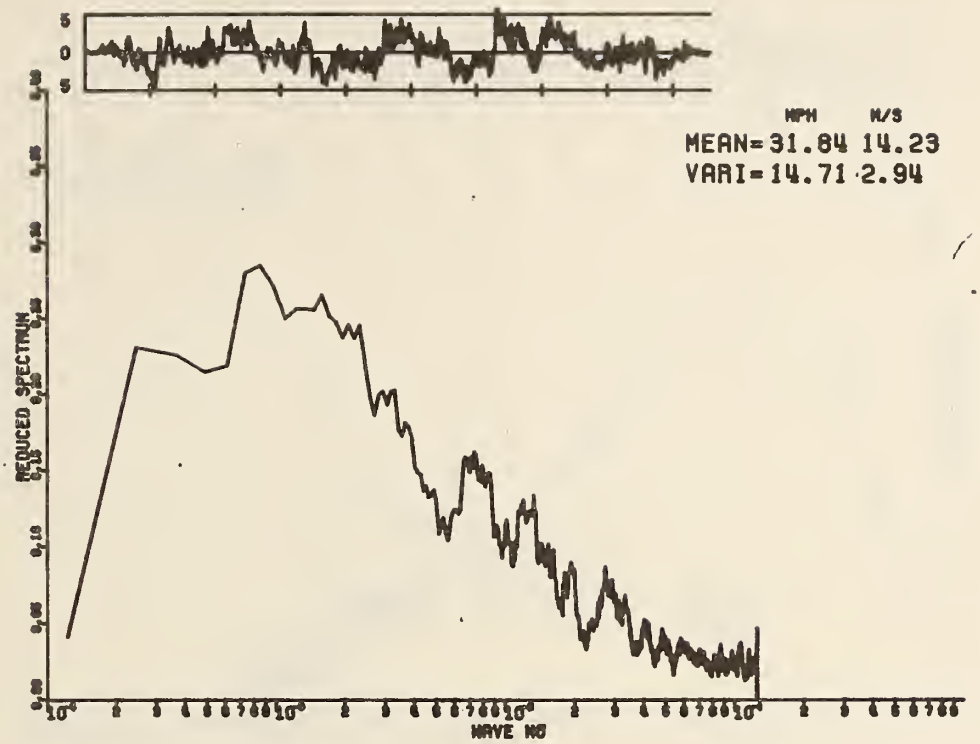

a) Horizontal - 2R.

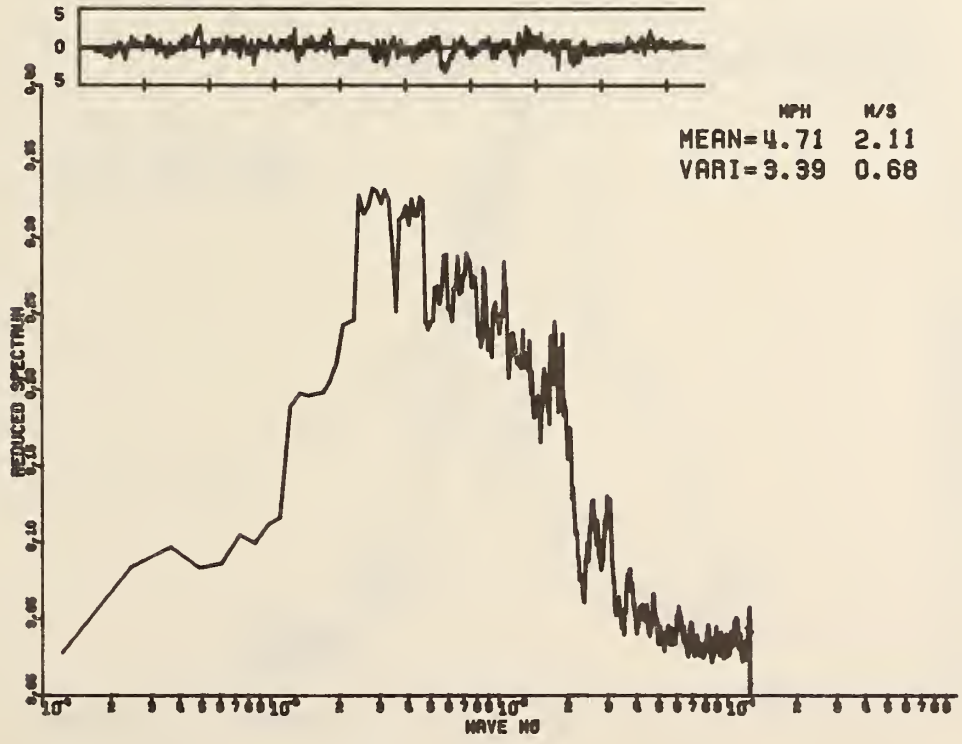

b) Vertical - 2W/R.

Figure 38. Individual channel horizontal resultant and vertical wind spectra for 30 mph wind (Sitka, November 1975).

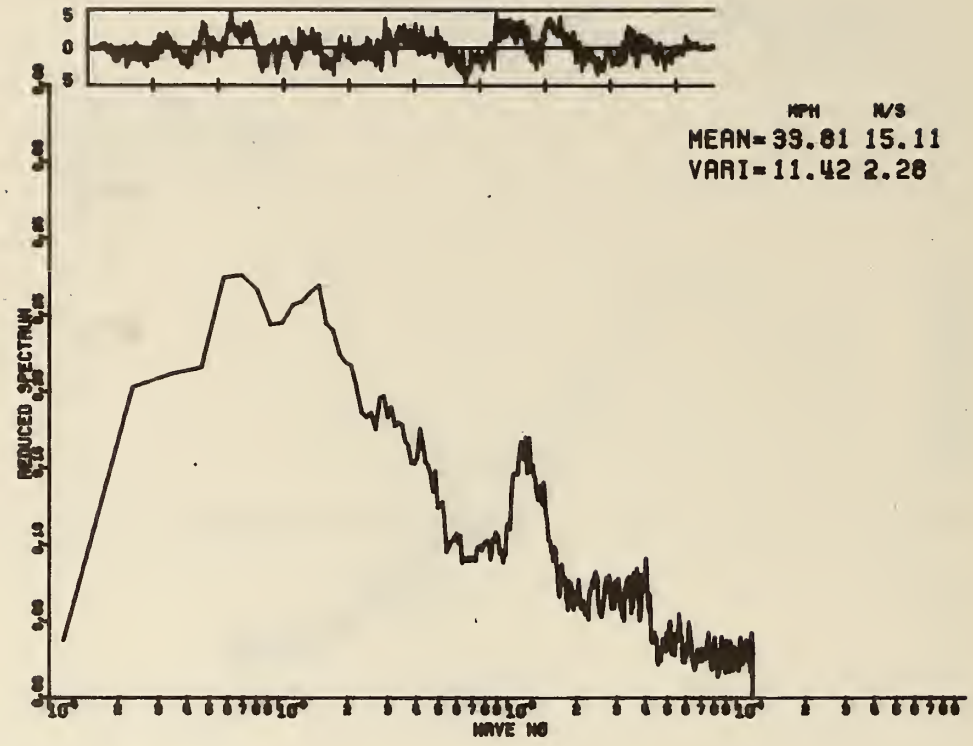

c) Horizontal - 3R.

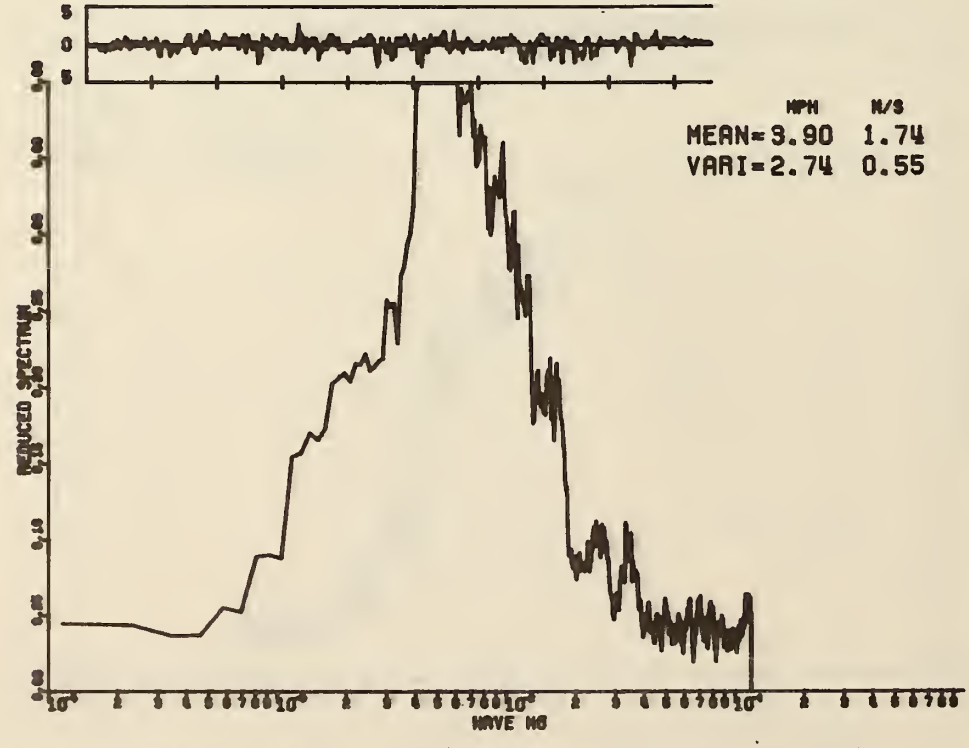

d) Vertical - 3W/R.

Figure 38. Individual channel horizontal resultant and vertical wind spectra for 30 mph wind (Sitka, November 1975)(continued).

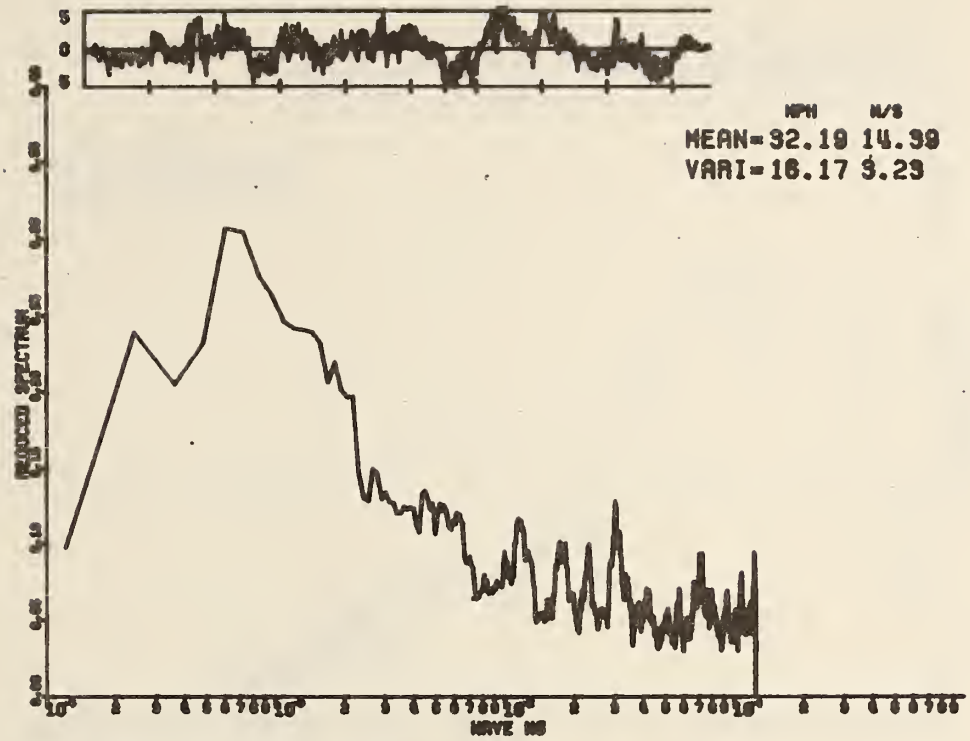

e) Horizontal - 4R.

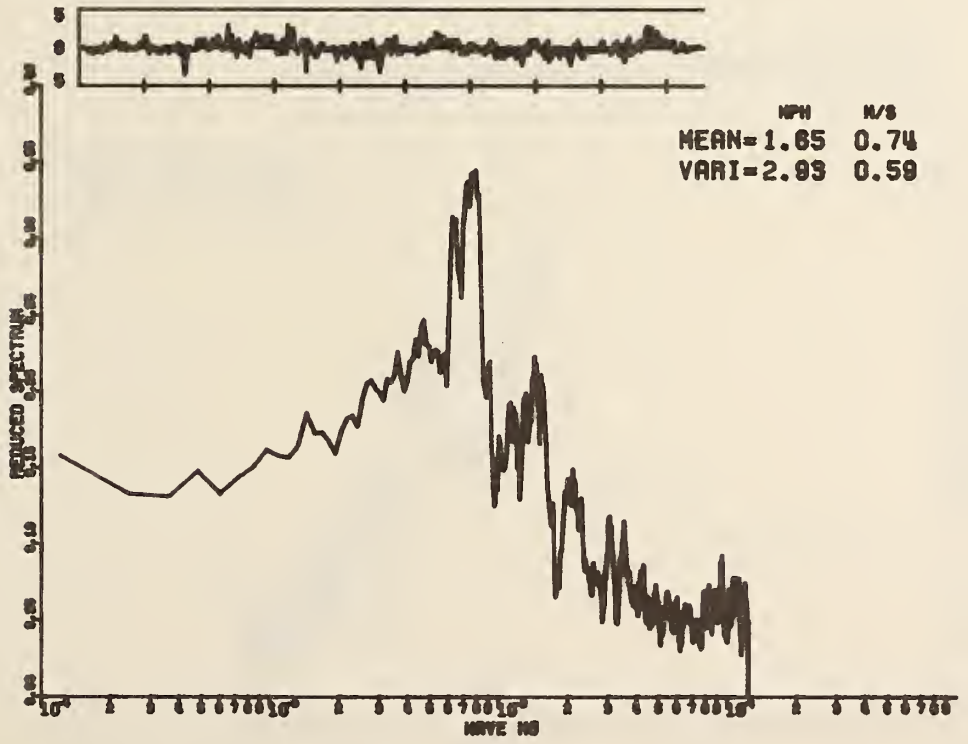

f) Vertical - 4W/R.

Figure 38. Individual channel horizontal resultant and vertical wind spectra for 30 mph wind (Sitka, November 1975)(continued).

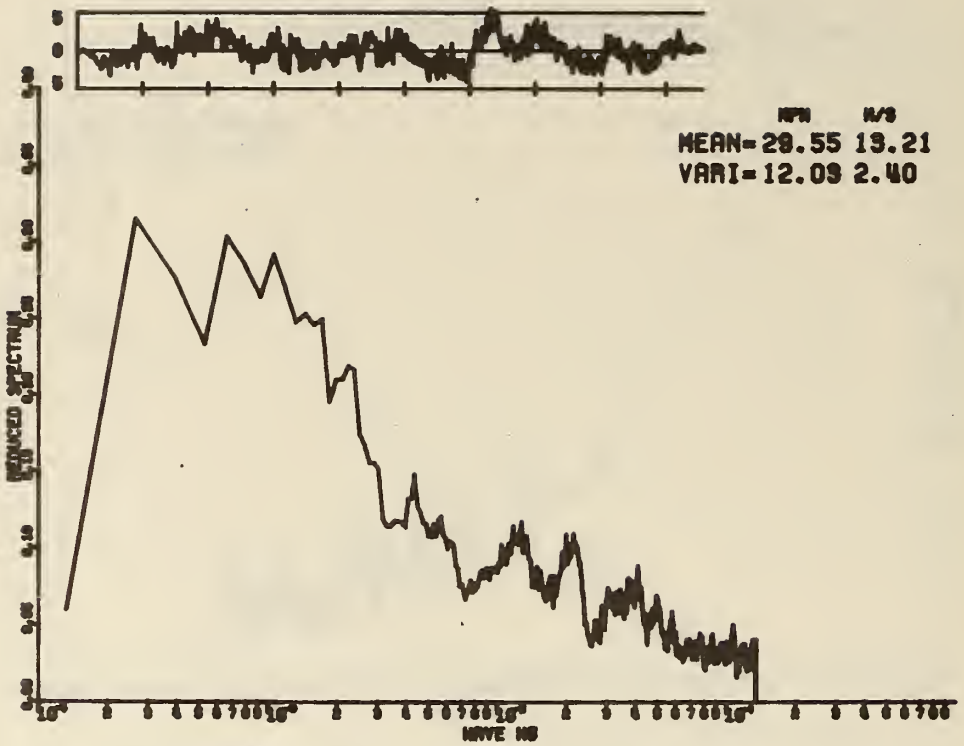

g) Horizontal - 5R.

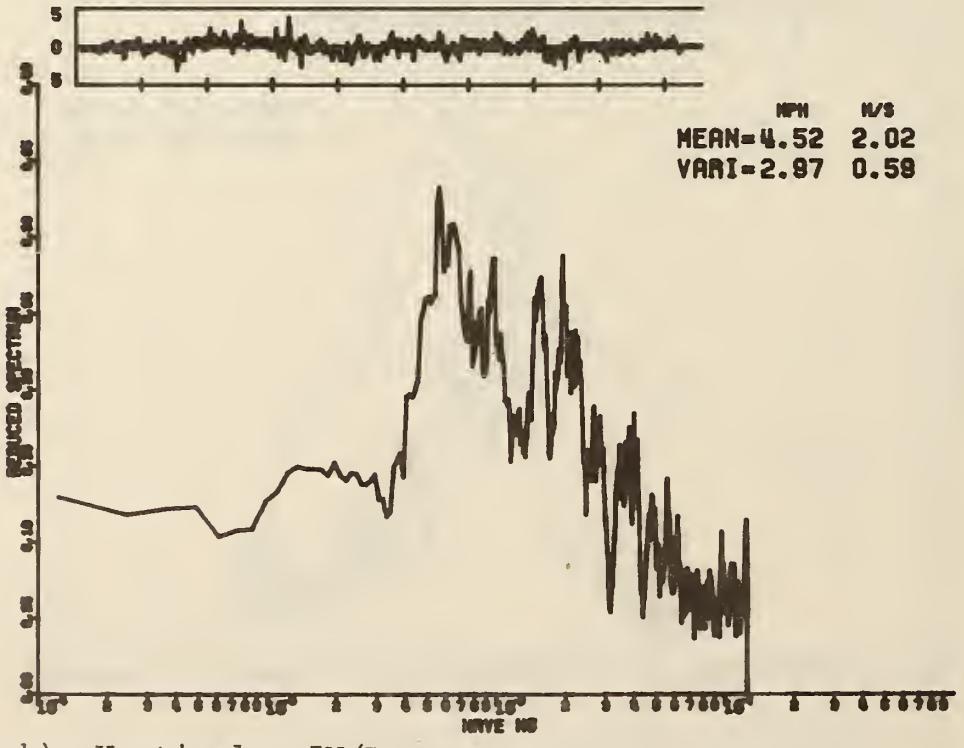

h) Vertical - 5W/R.

Figure 38. Individual channel horizontal resultant and vertical wind spectra for 30 mph wind (Sitka, November 1975)(continued).

APPENDIX F

INDIVIDUAL CHANNEL WIND SPECTRA: SITKA, MAY 1975

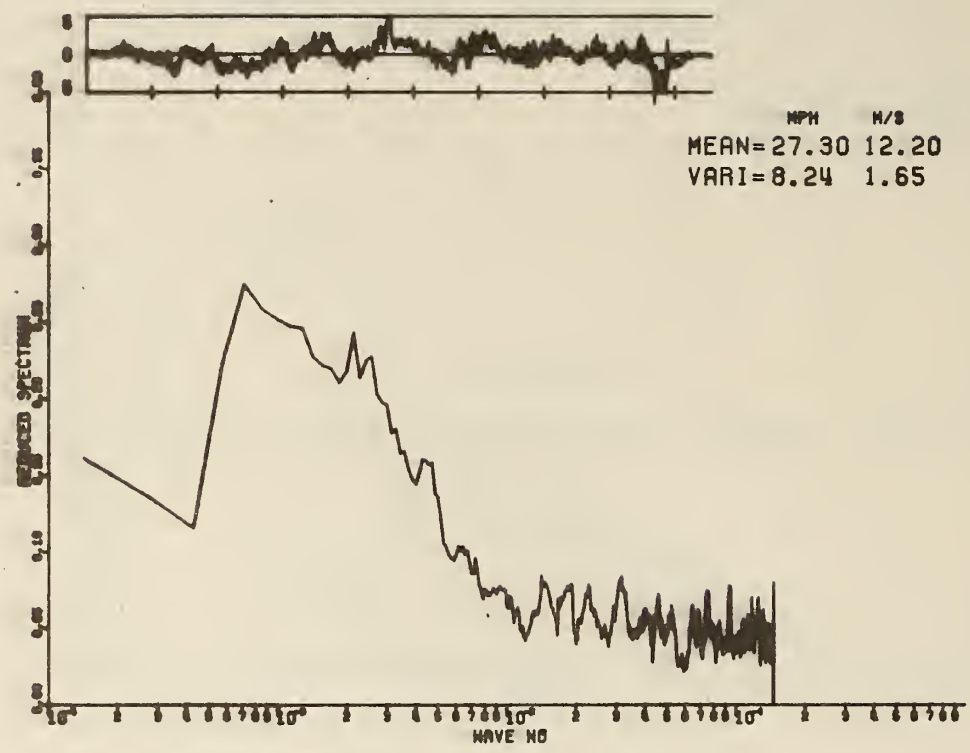

a) Horizontal - 1R.

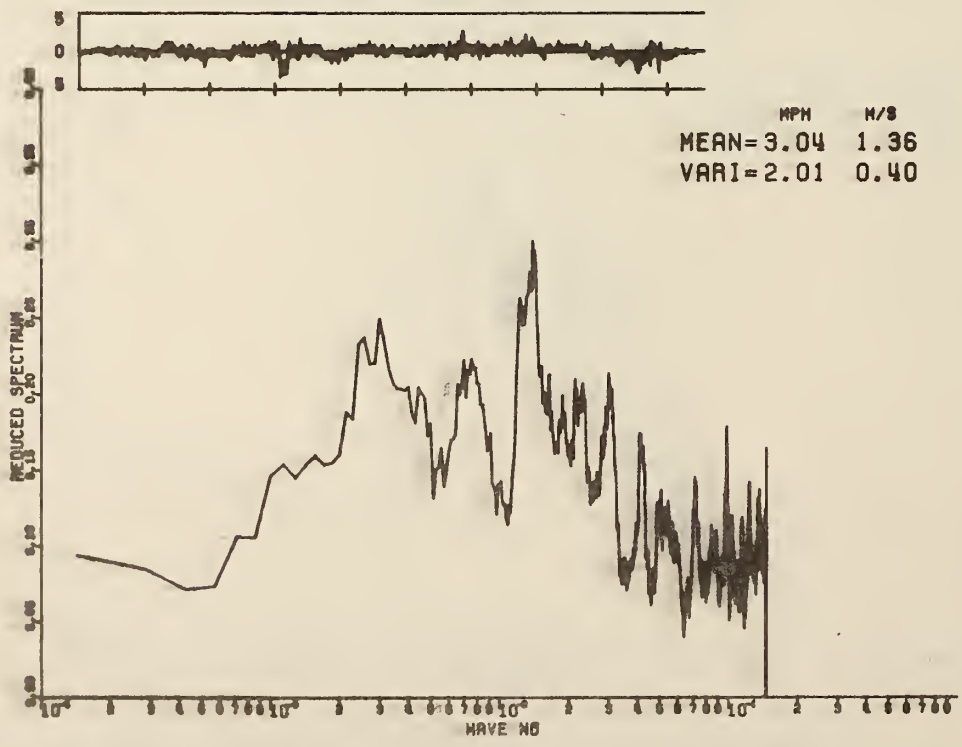

b) Vertical - 1W/R.

Figure 39. Individual channel horizontal resultant and vertical wind spectra for 25 mph wind (Sitka, May 1976).

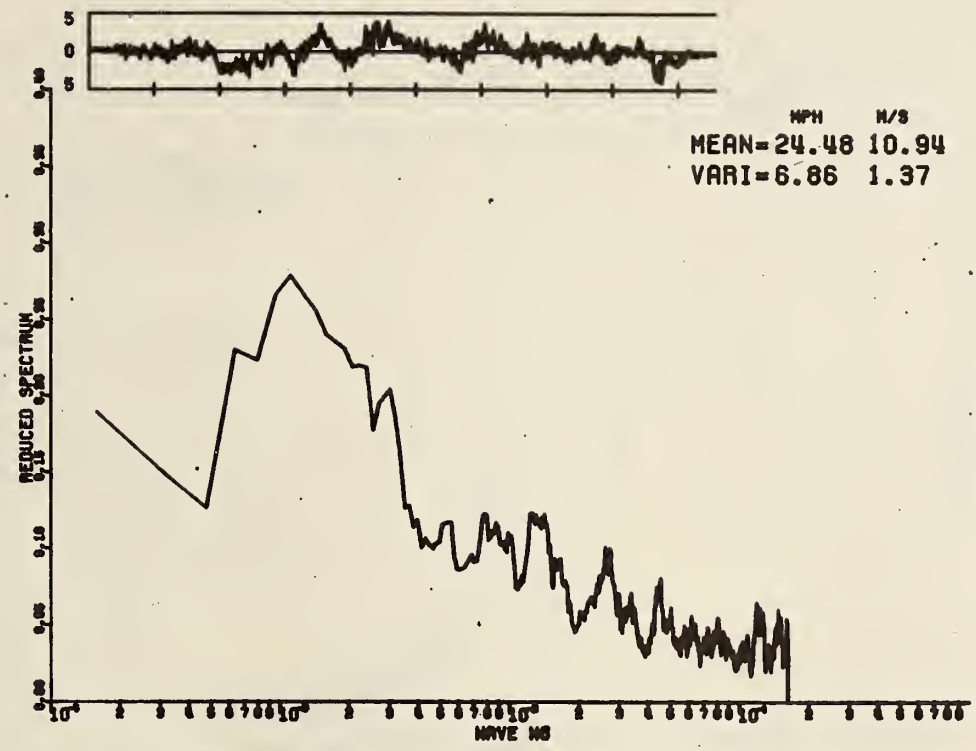

c) Horizontal - 2R.

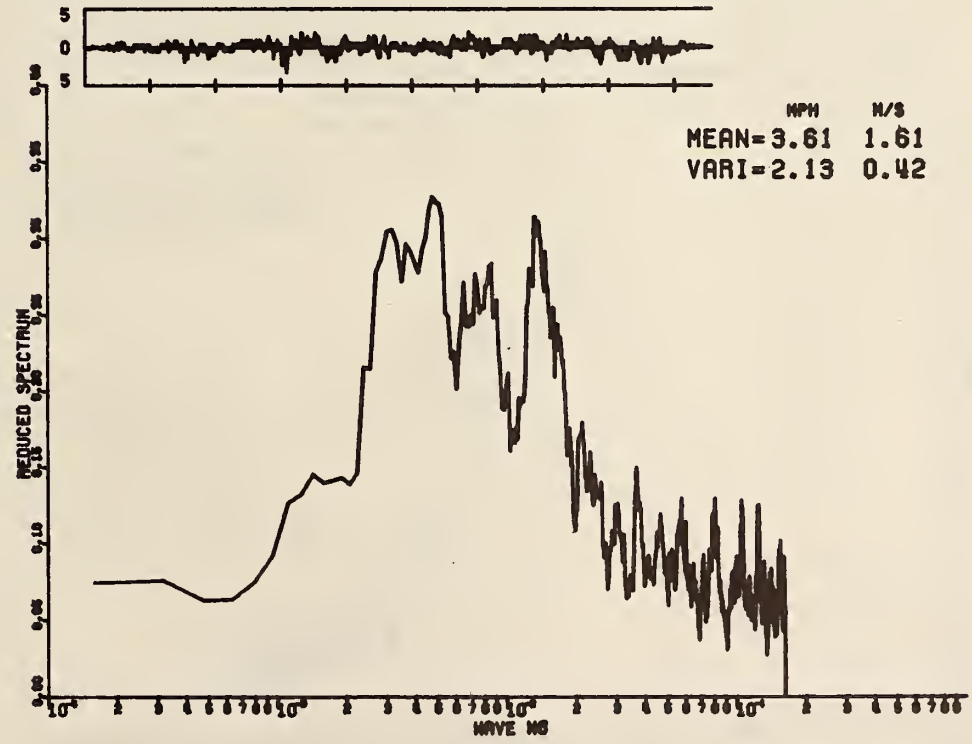

d) Vertical - 2W/R.

Figure 39. Individual channel horizontal resultant and vertical wind spectra for 25 mph wind (Sitka, May 1976) (continued).

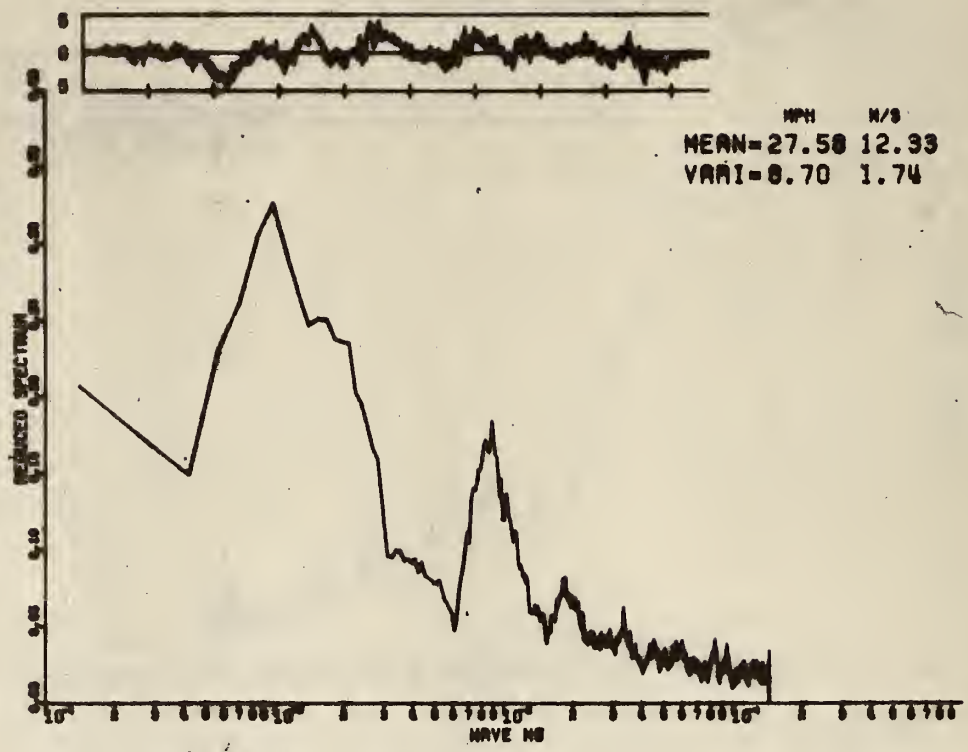

e) Horizontal - 3R.

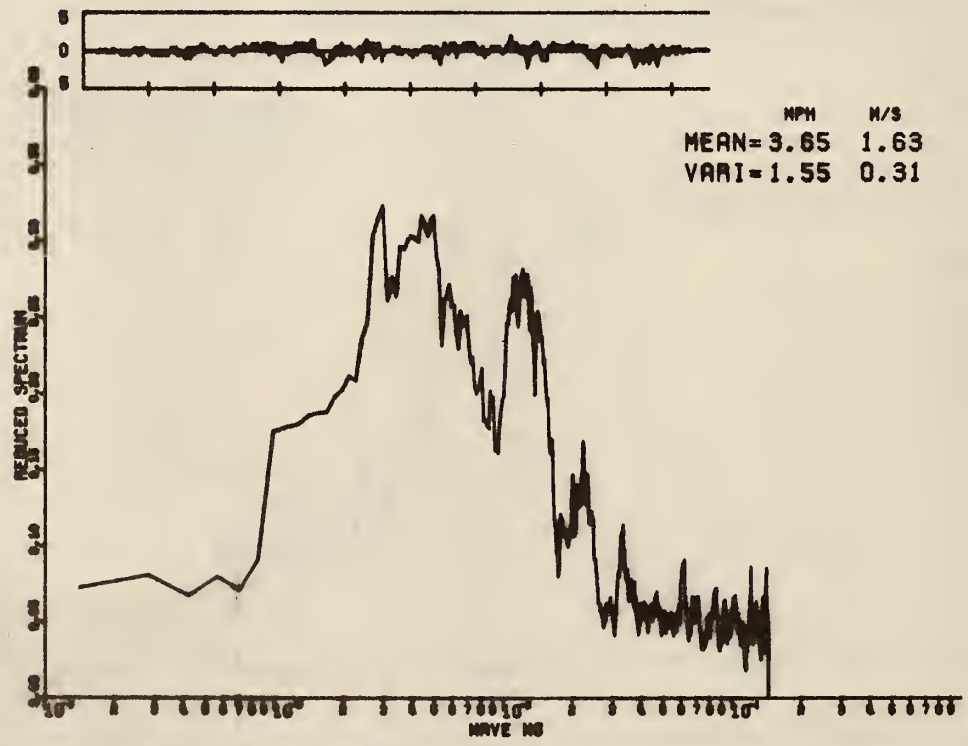

f) Vertical - 3W/R.

Figure 39. Individual channel horizontal resultant and vertical wind spectra for 25 mph wind (Sitka, May 1976) (continued).

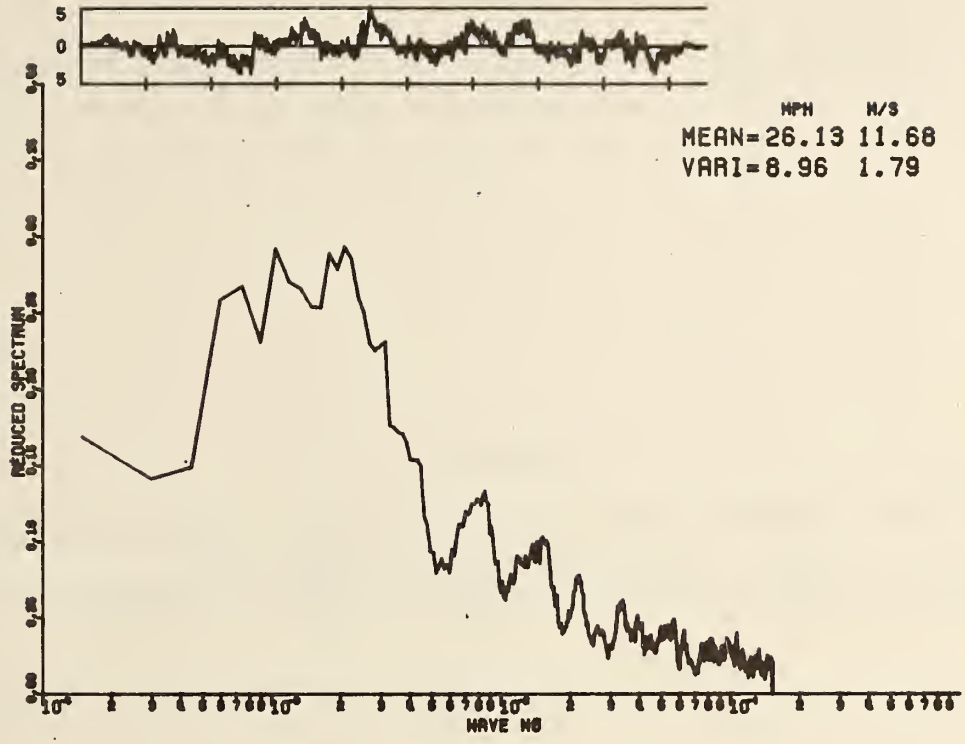

g) Horizontal - 5R.

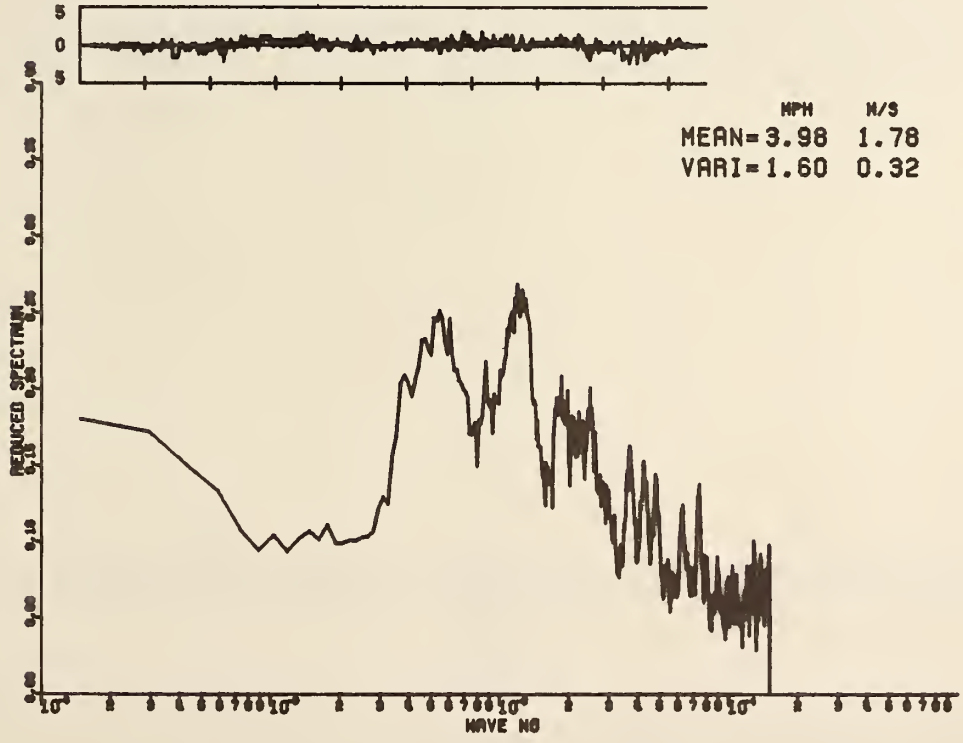

h) Vertical - 5W/R.

Figure 39. Individual channel horizontal resultant and vertical wind spectra for 25 mph wind (Sitka, May 1976) (continued).

APPENDIX G

INDIVIDUAL CHANNEL ACCELERATION SPECTRA: SITKA, DECEMBER 1975

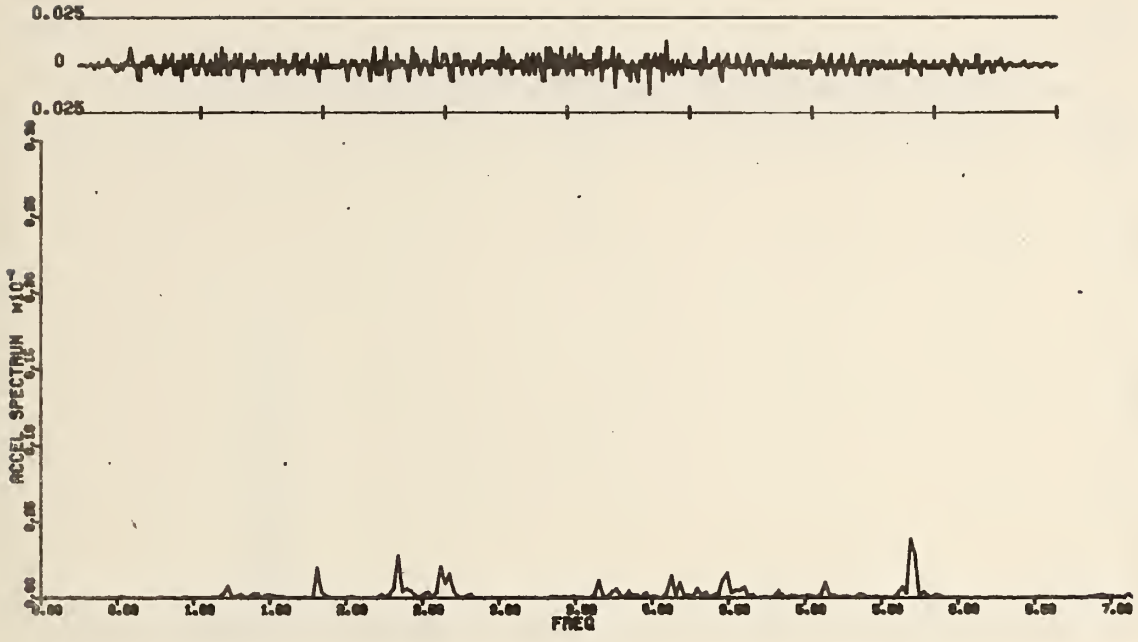

a) A1.

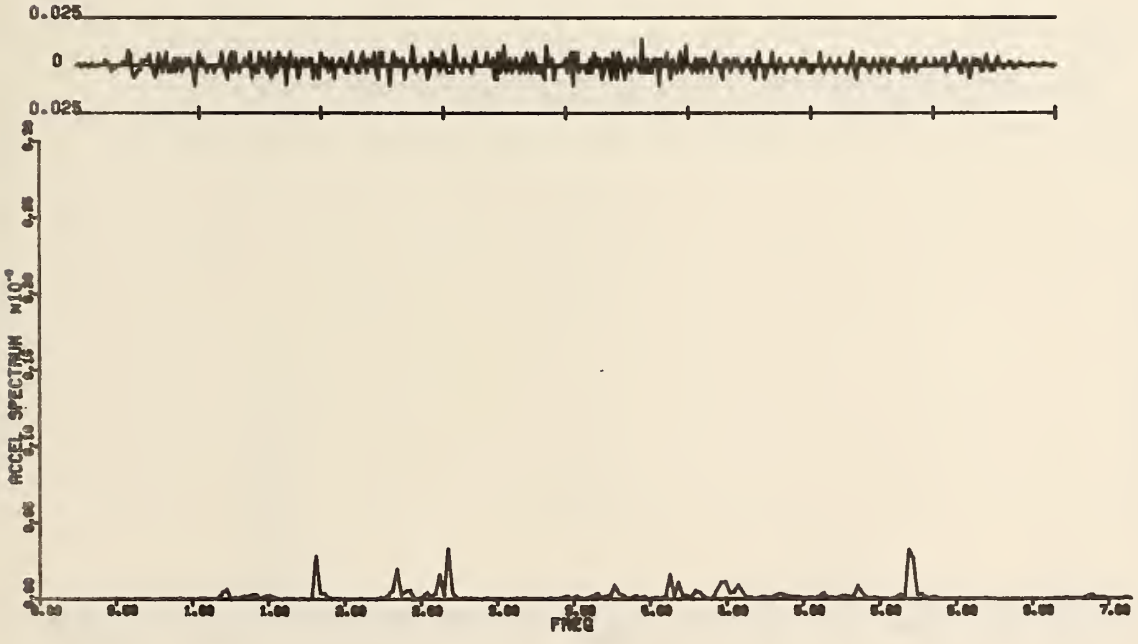

b) A2.

Figure 40. Individual channel acceleration spectra during first bridge motion event.

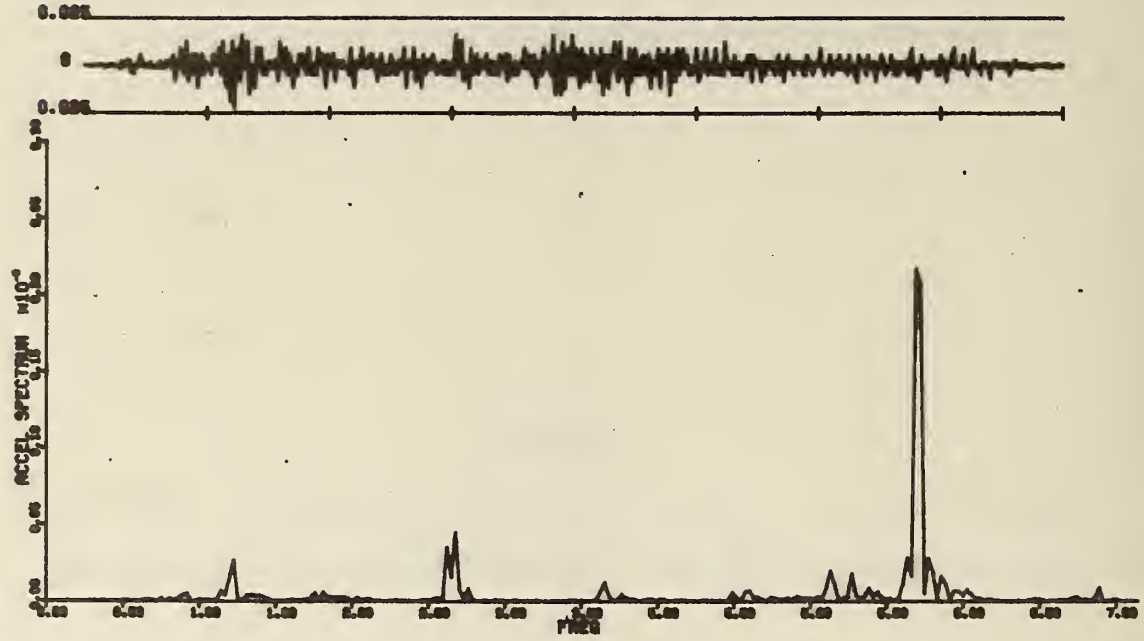

c) A3.

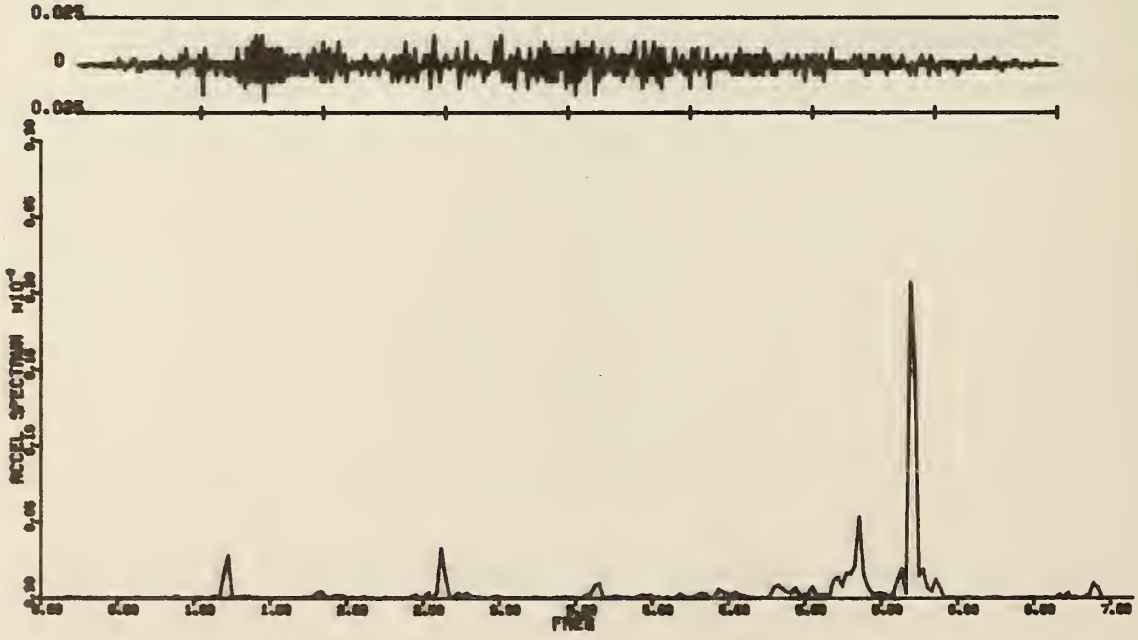

d) A4.

Figure 40. Individual channel acceleration spectra during first bridge motion event (continued).

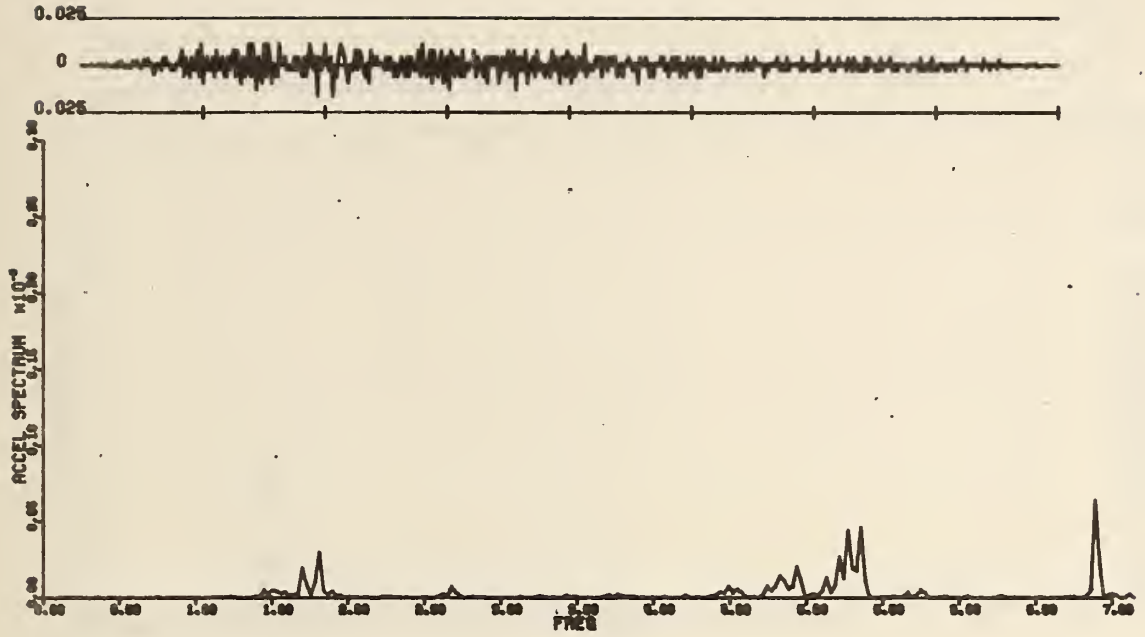

e) A5.

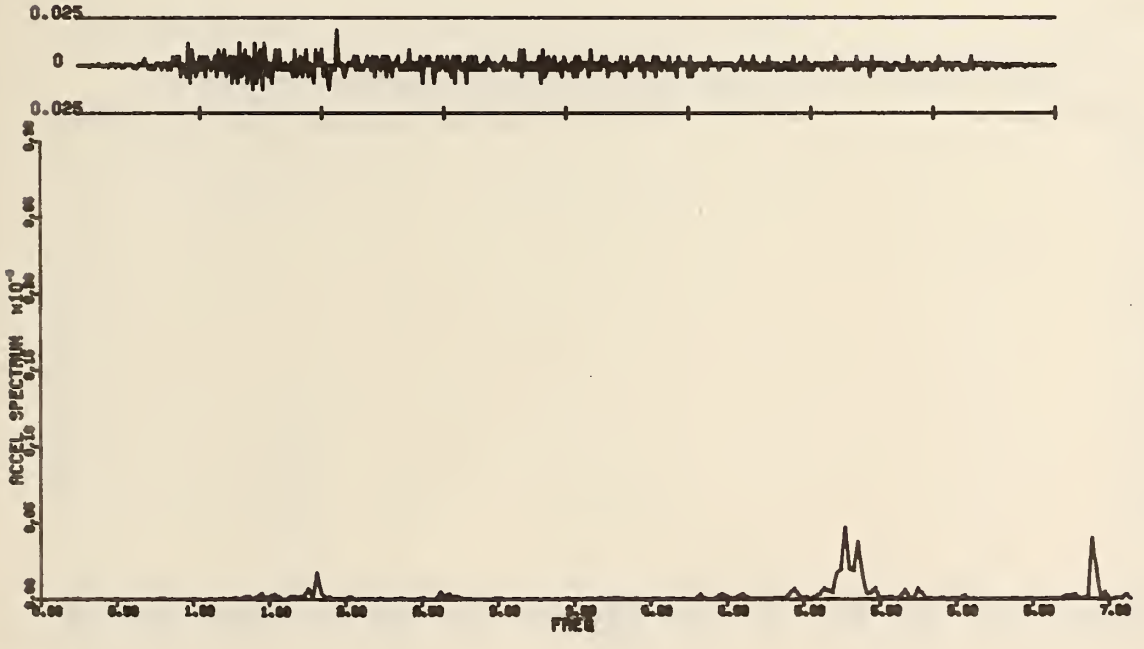

f) A6.

Figure 40. Individual channel acceleration spectra during first bridge motion event (continued).

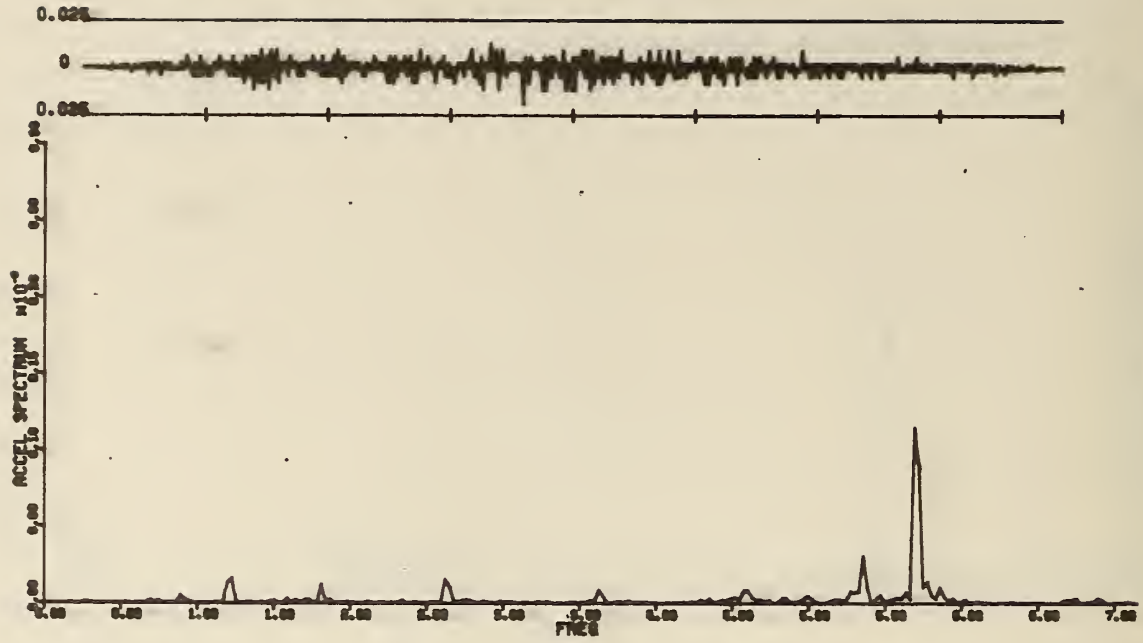

g) A7.

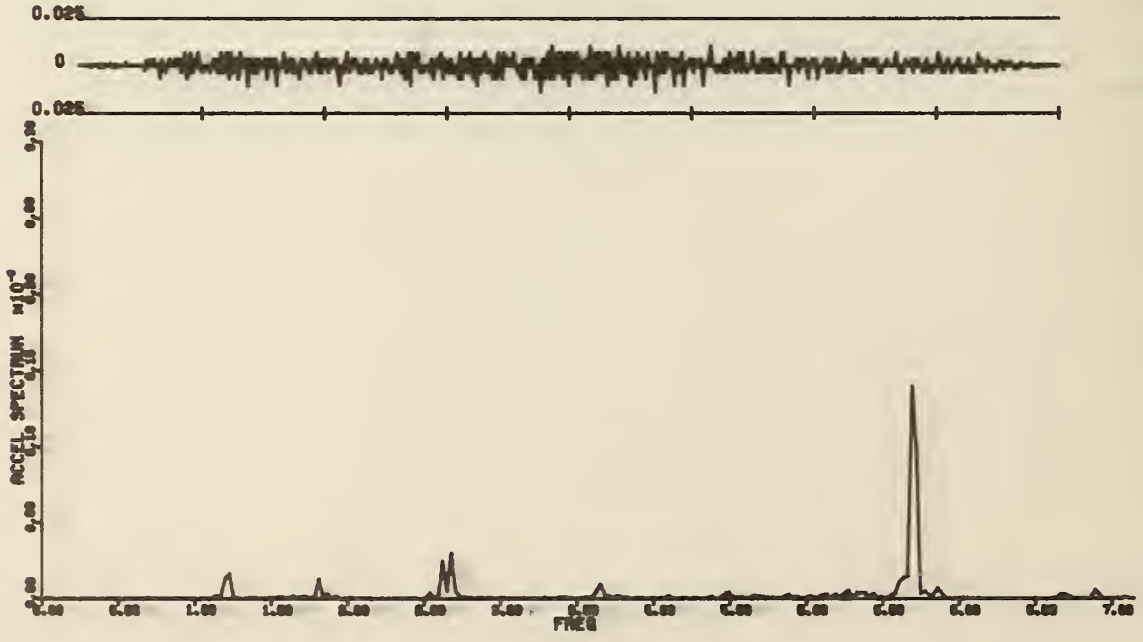

h) A8.

Figure 40. Individual channel acceleration spectra during first bridge motion event (continued).

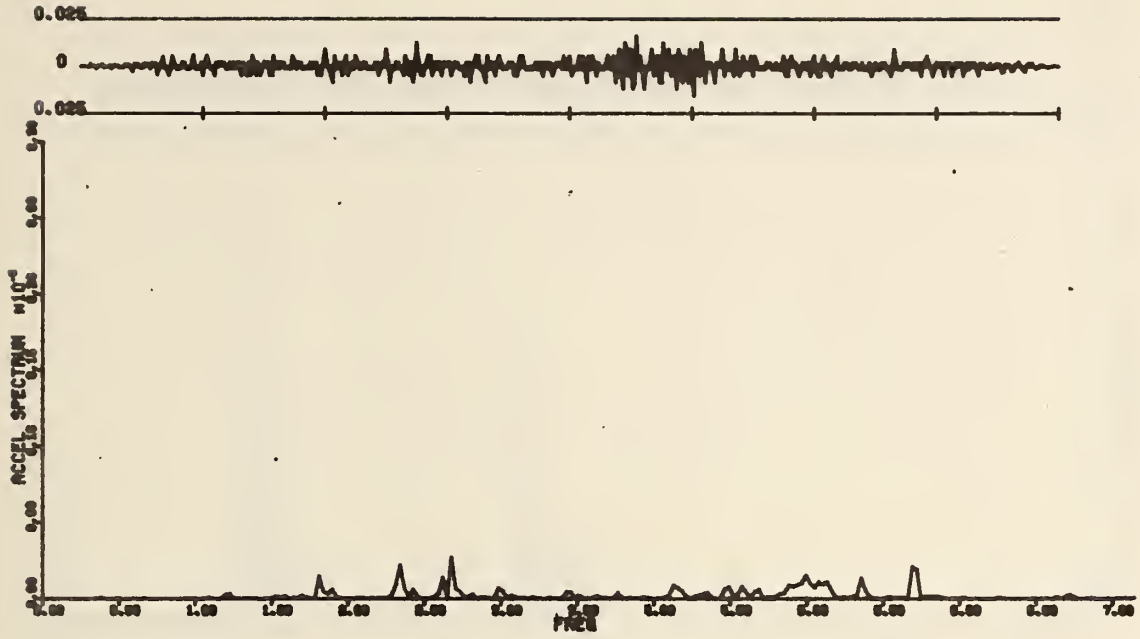

i) A9.

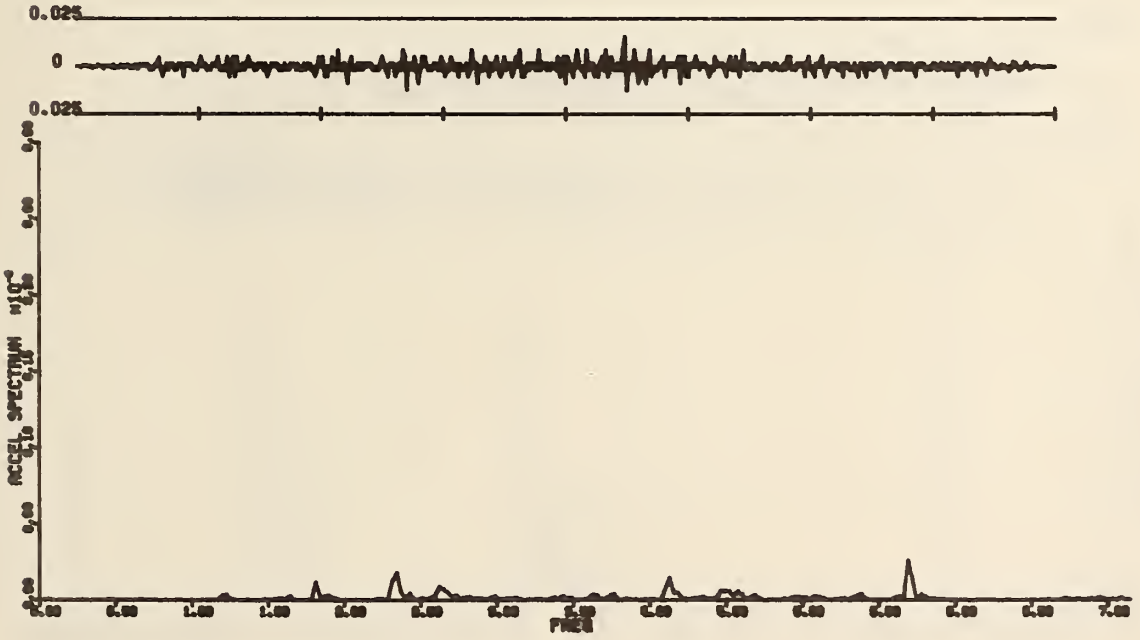

j) A10.

Figure 40. Individual channel acceleration spectra during first bridge motion event (continued).

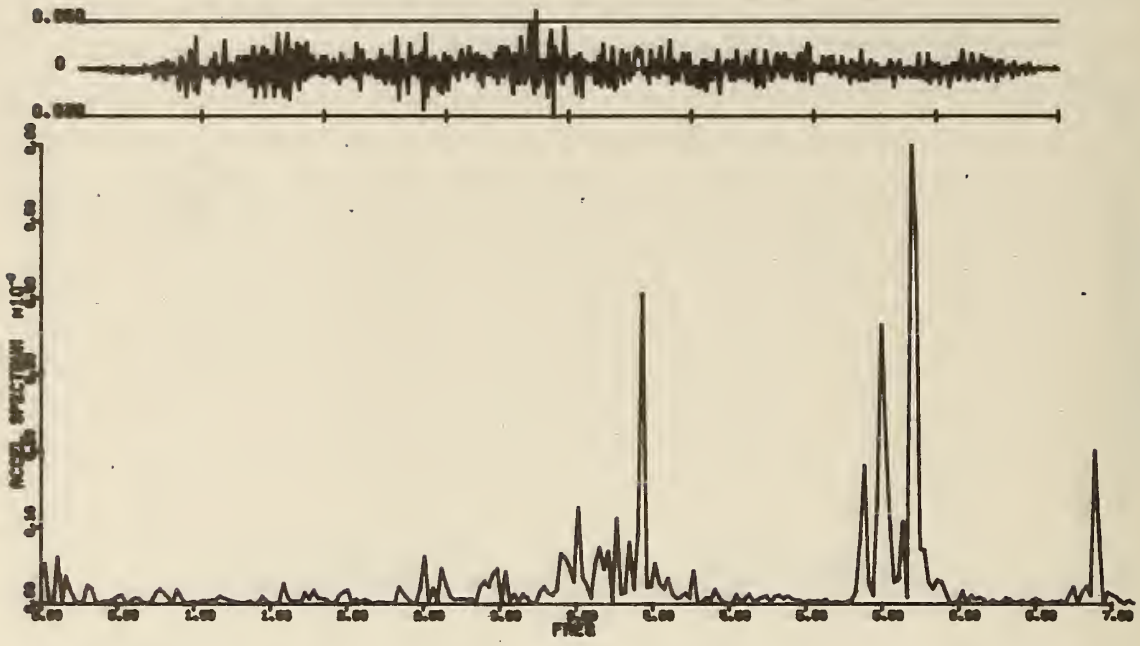

k) A13.

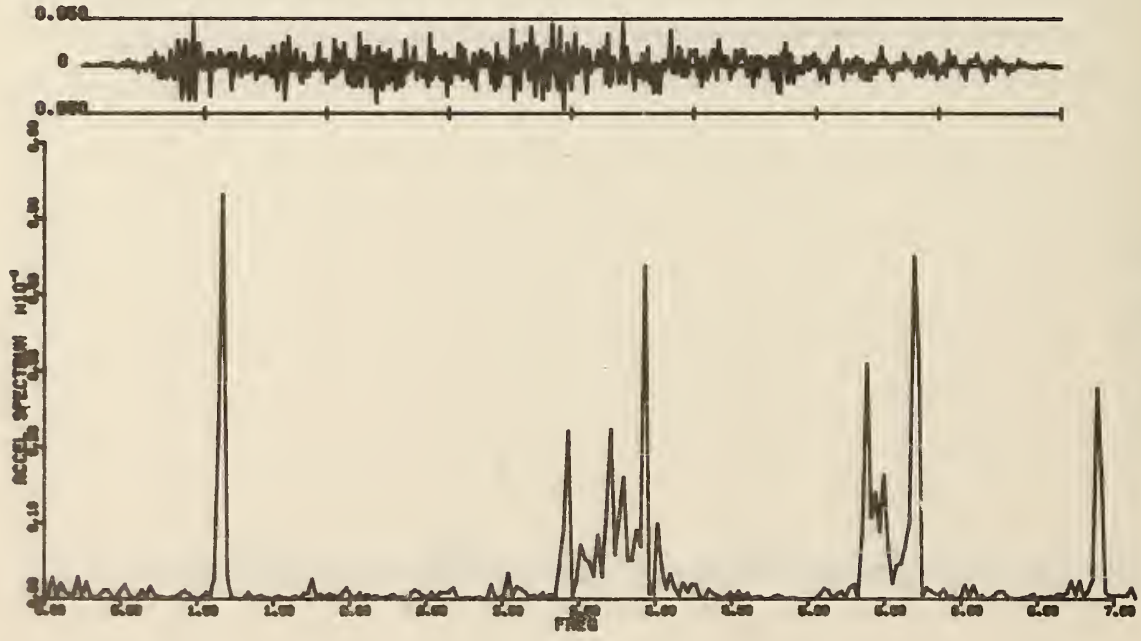

l) A12.

Figure 40. Individual channel acceleration spectra during first bridge motion event (continued).

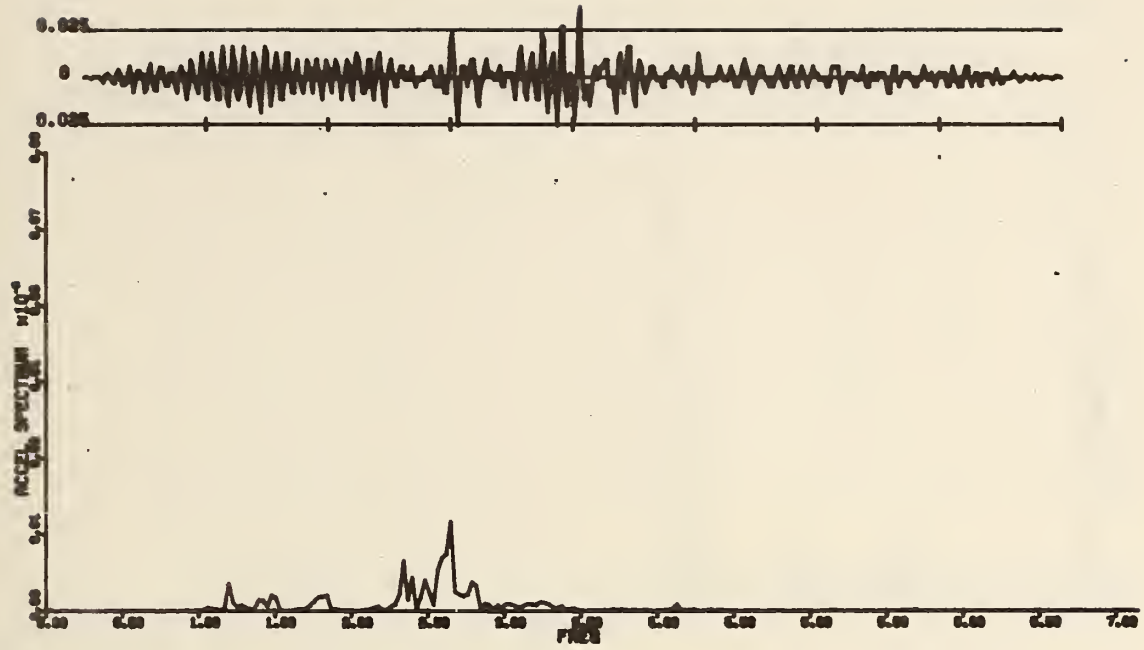

a) A1.

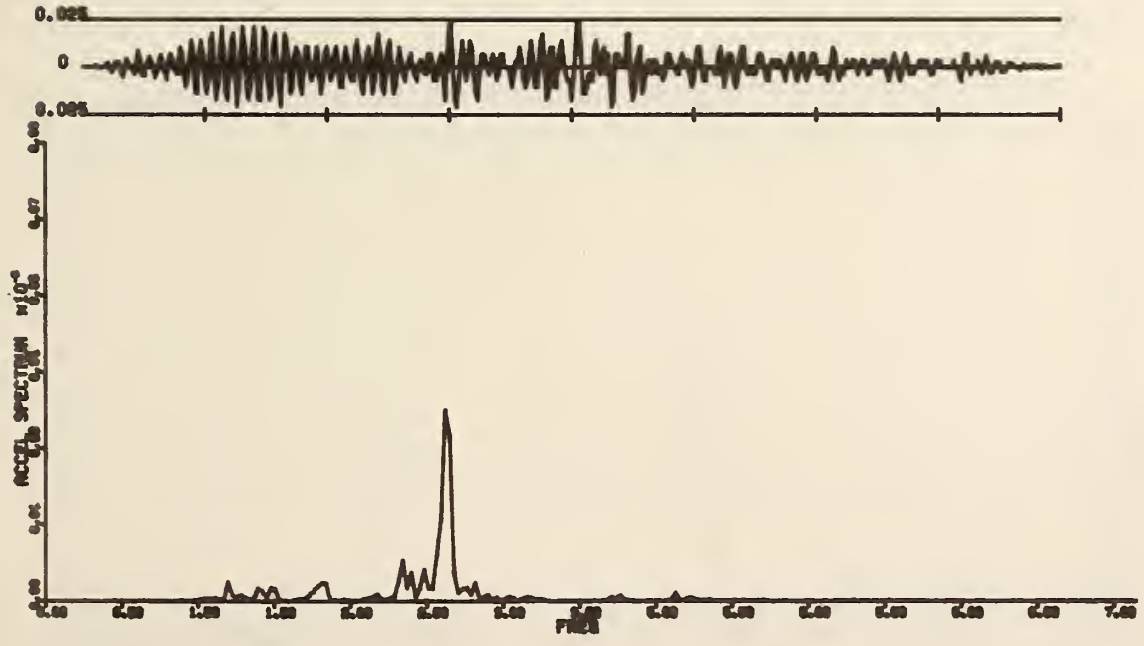

b) A2.

Figure 41. Individual channel acceleration spectra during second bridge motion event.

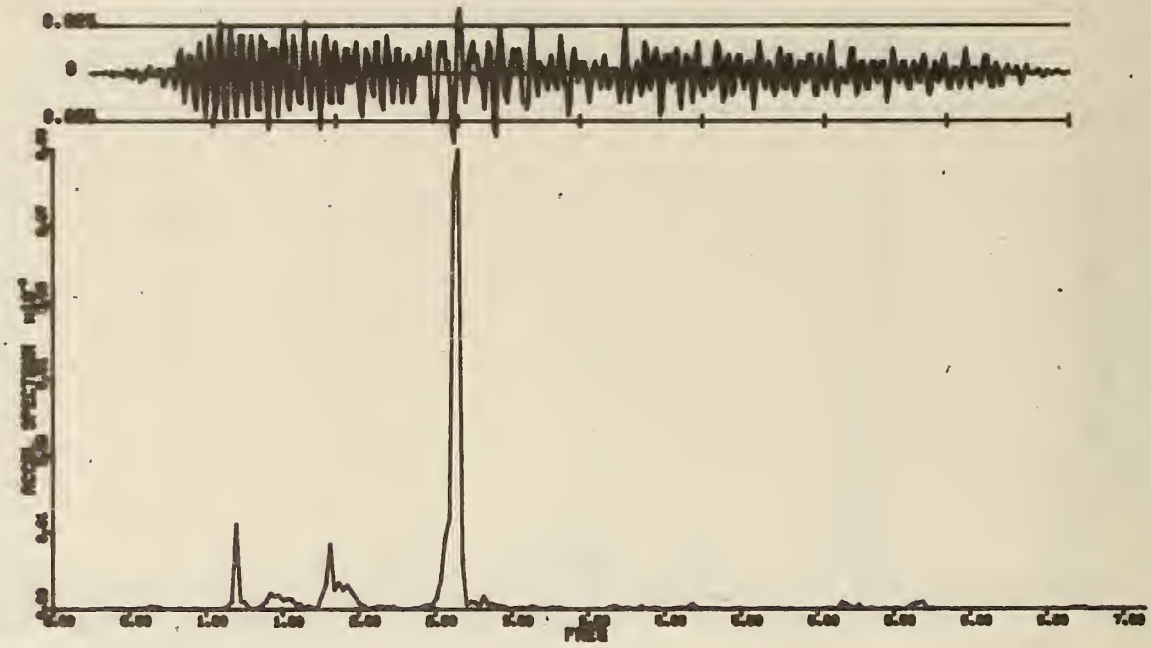

c) A3.

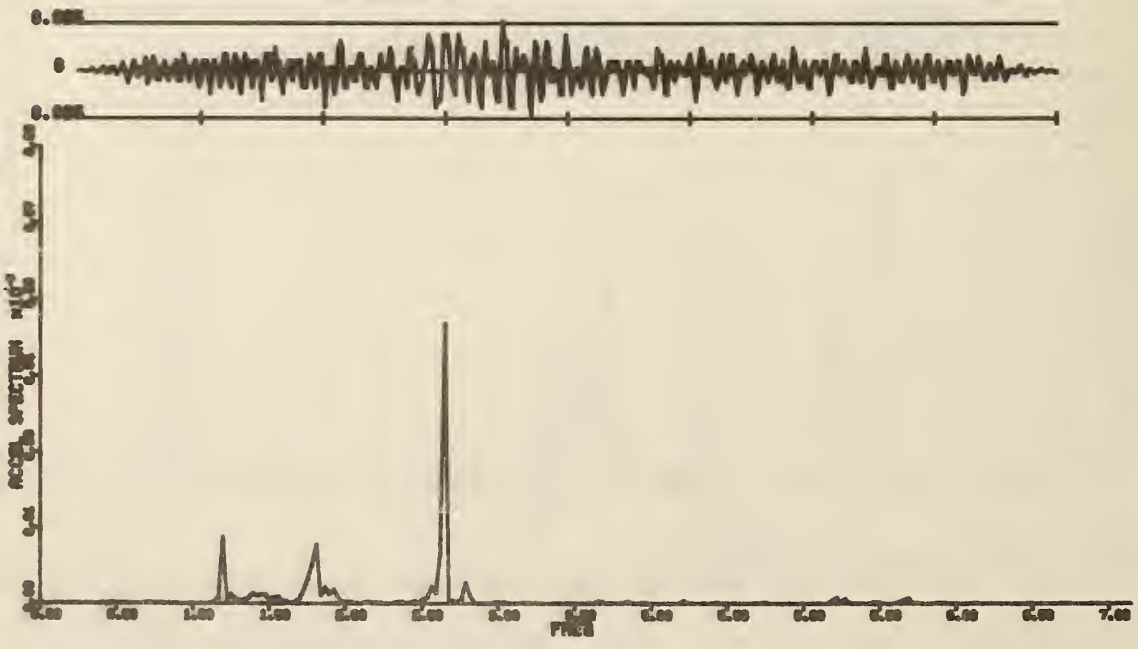

d) A4.

Figure 41. Individual channel acceleration spectra during second bridge motion event (continued).

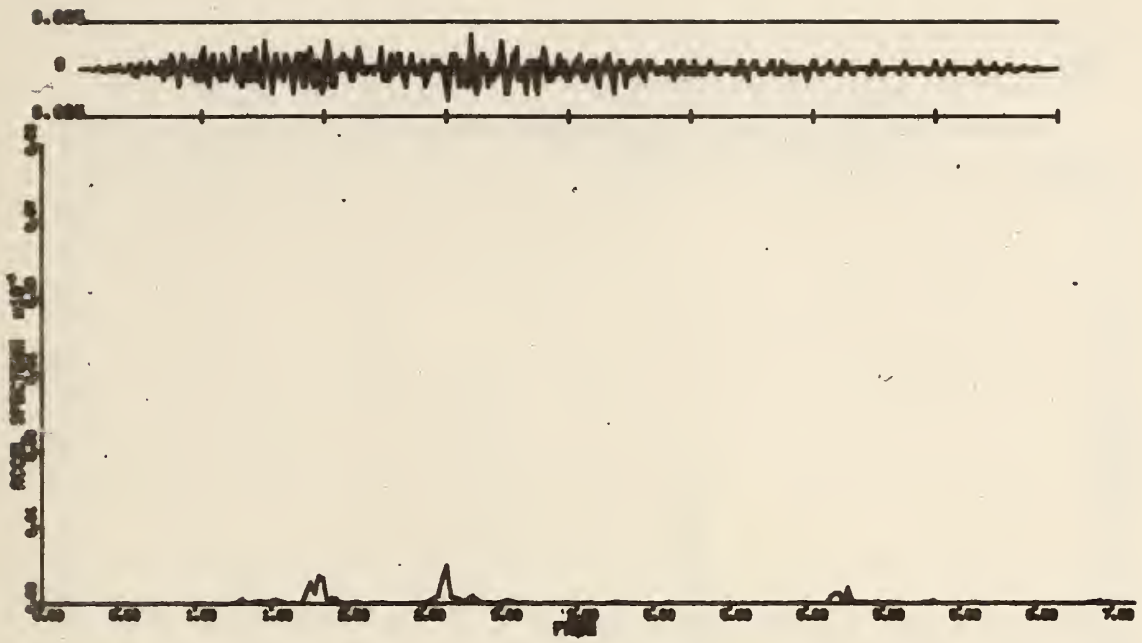

e) A5.

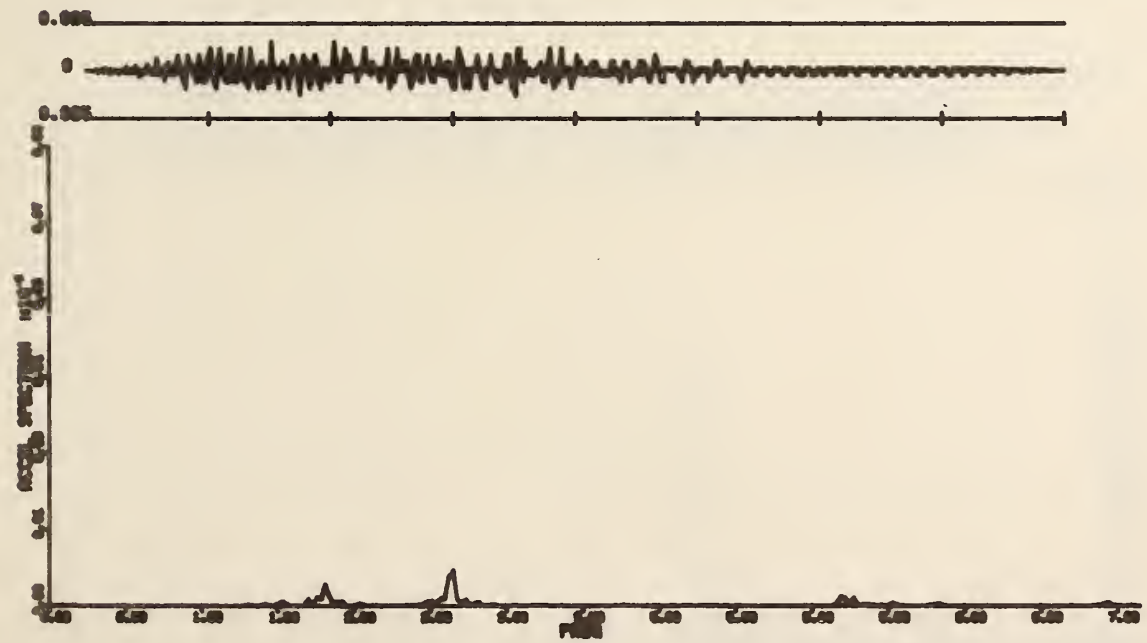

f) A6.

Figure 41. Individual channel acceleration spectra during second bridge motion event (continued).

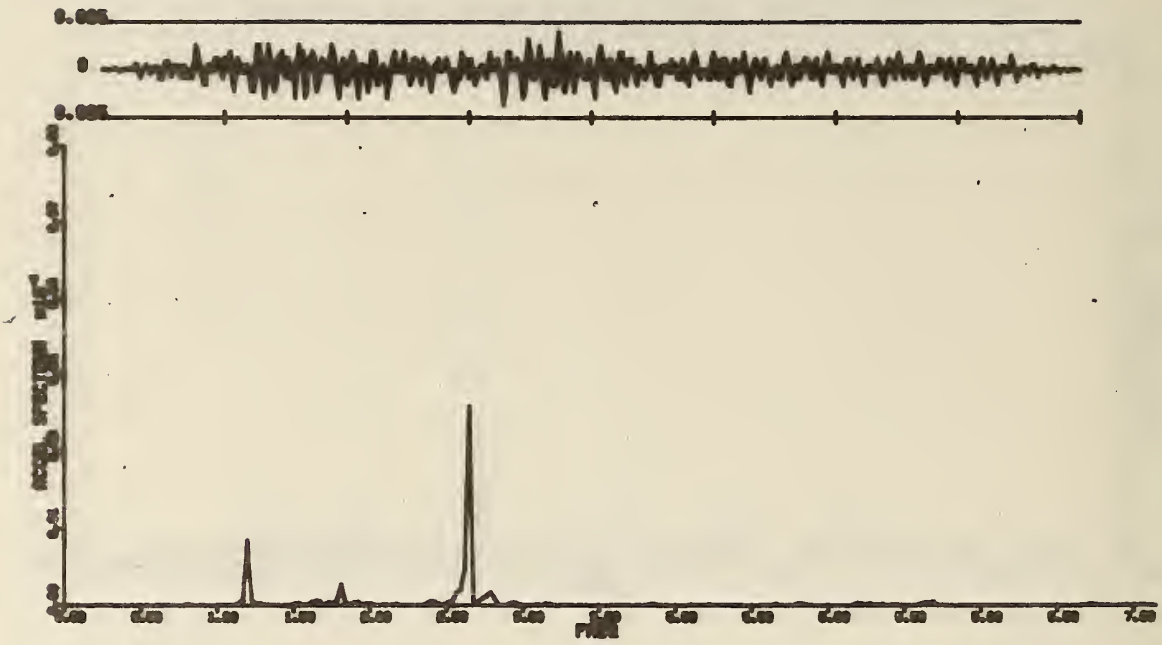

g) A7.

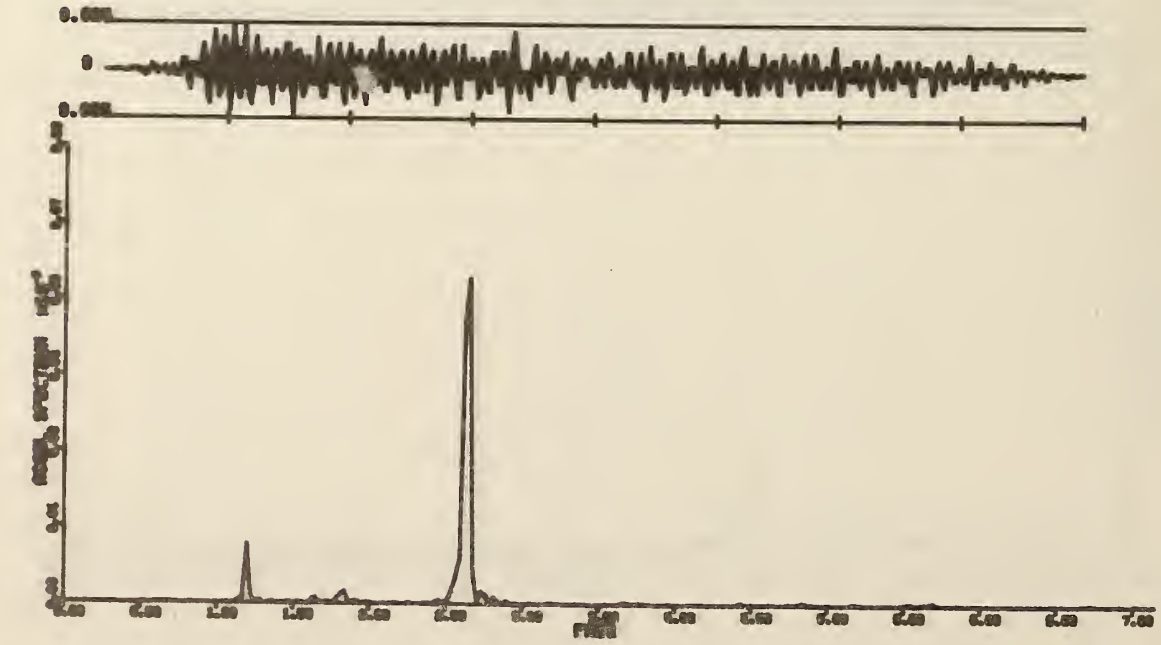

h) A8.

Figure 41. Individual channel acceleration spectra during second bridge motion event (continued).

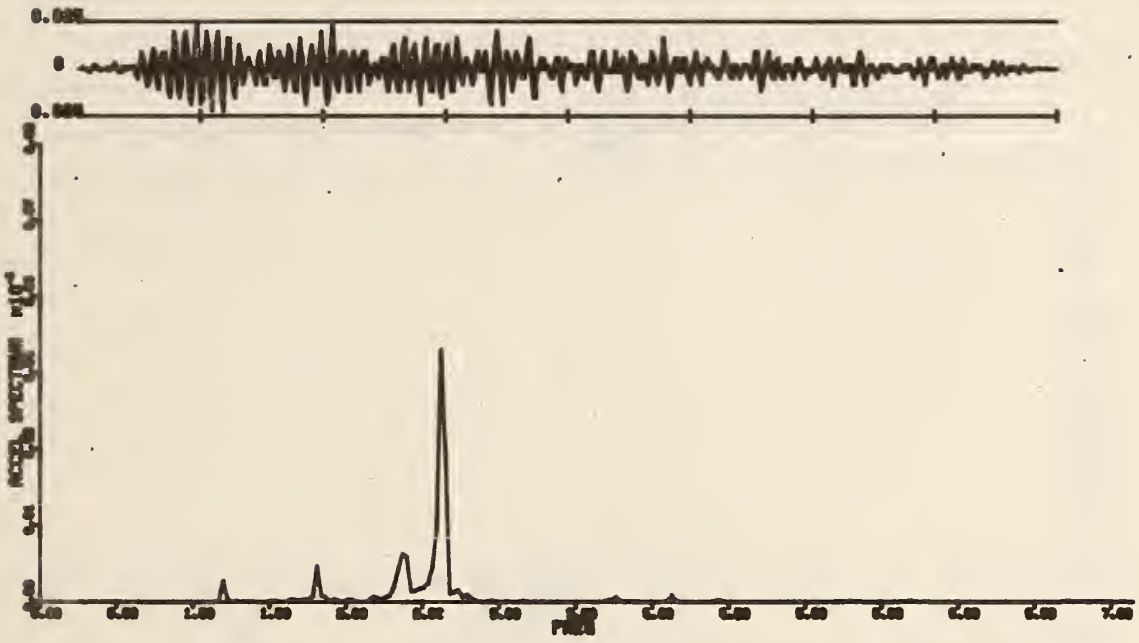

i) A9.

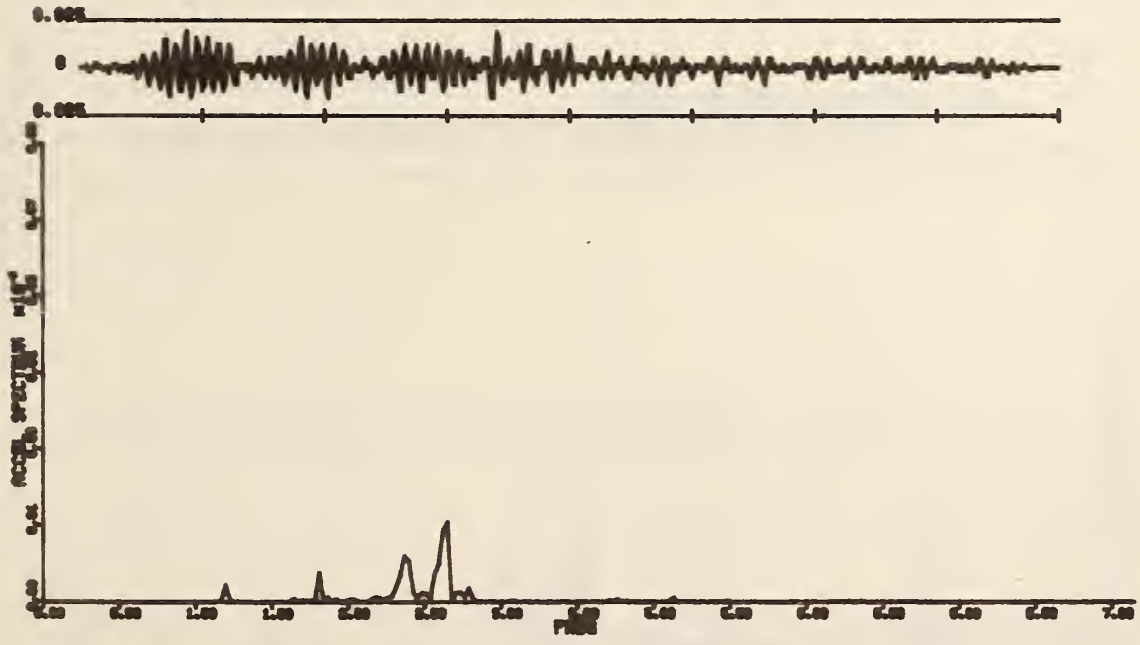

j) A10.

Figure 41. Individual channel acceleration spectra during second bridge motion event (continued).

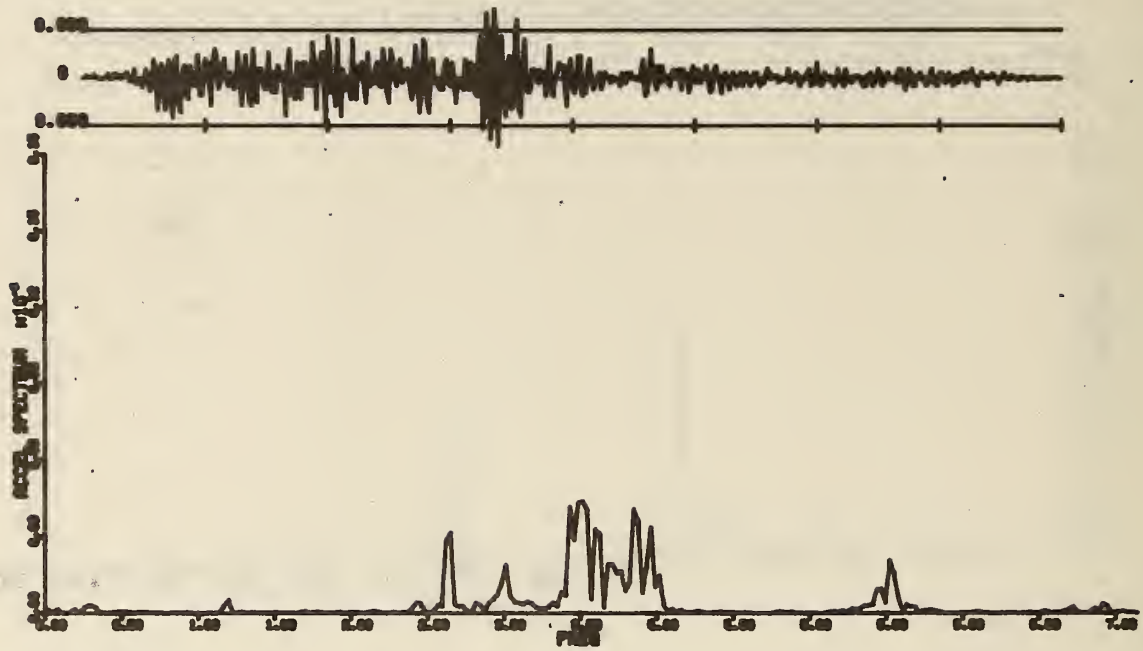

k) A13.

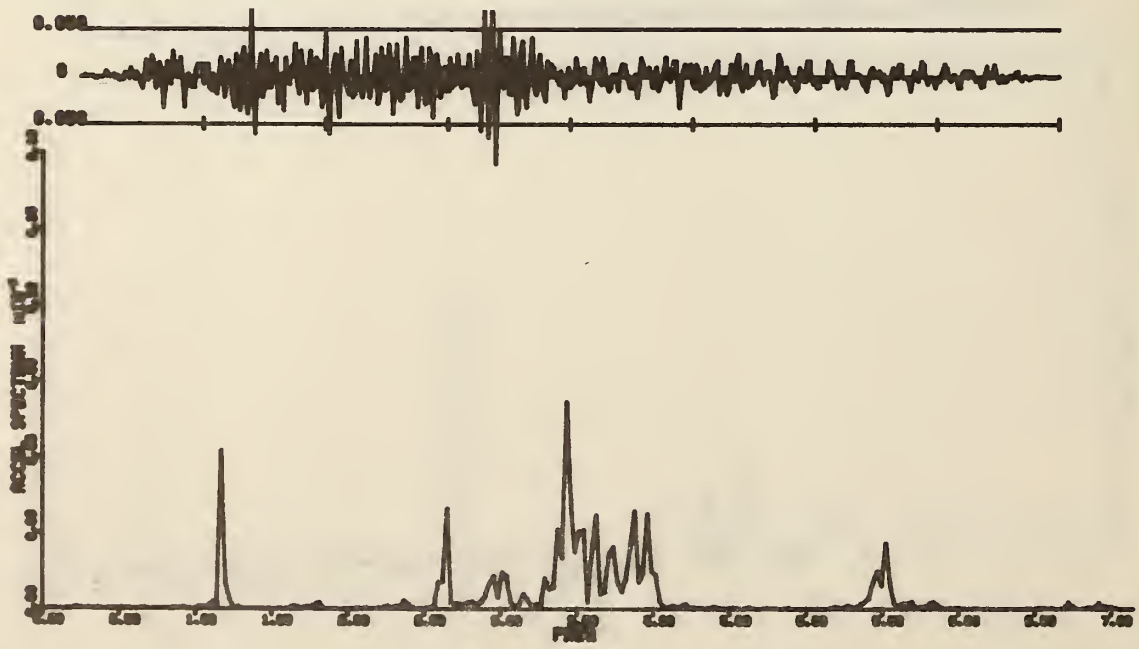

l) A12.

Figure 41. Individual channel acceleration spectra during second bridge motion event (continued).

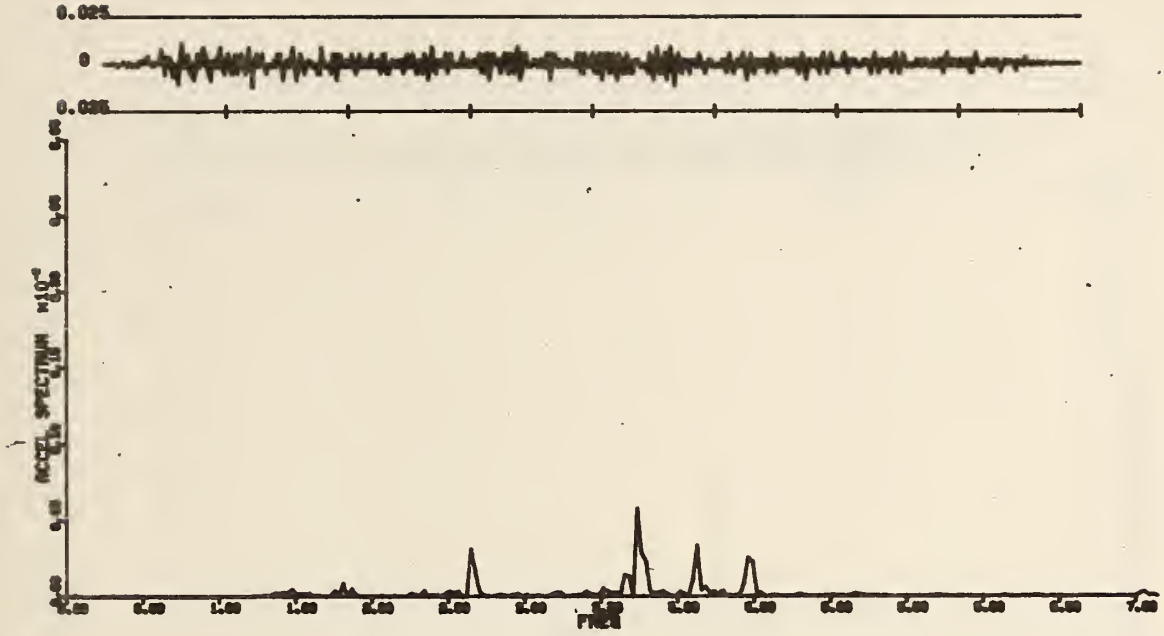

a) A1.

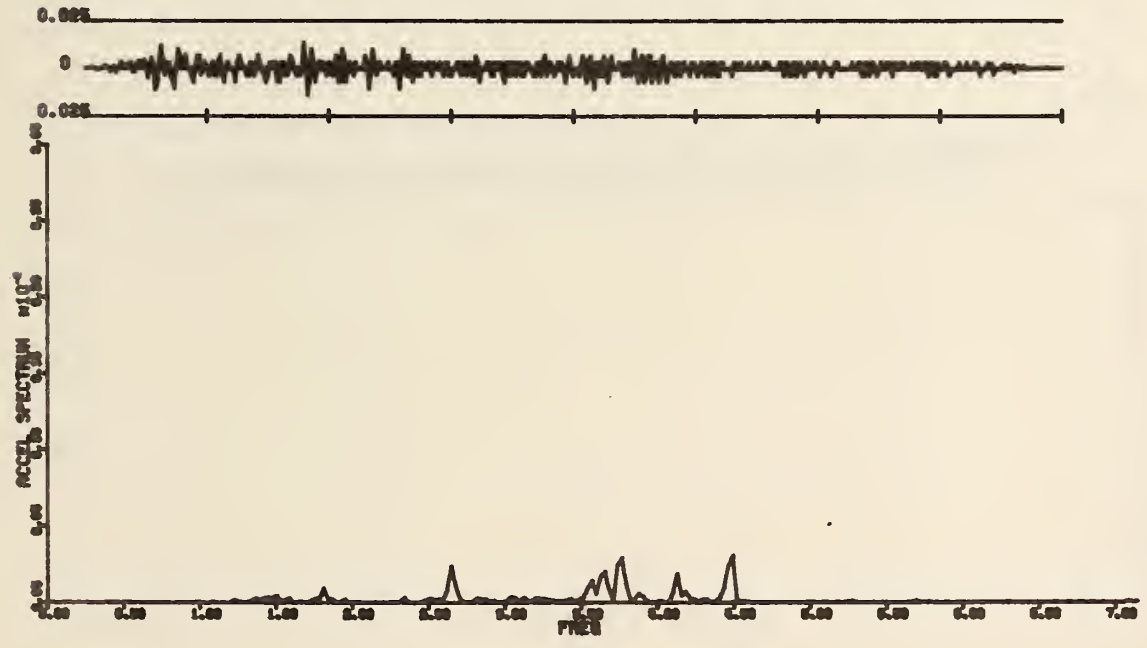

b) A2.

Figure 42. Individual channel acceleration spectra during third bridge motion event.

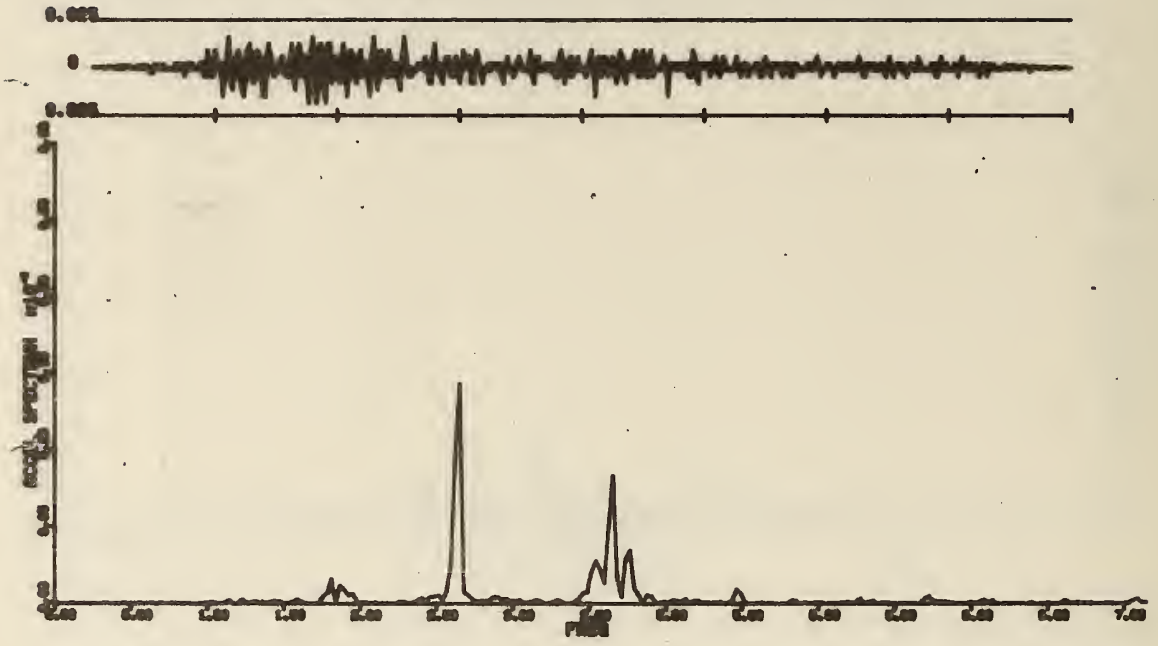

c) A3.

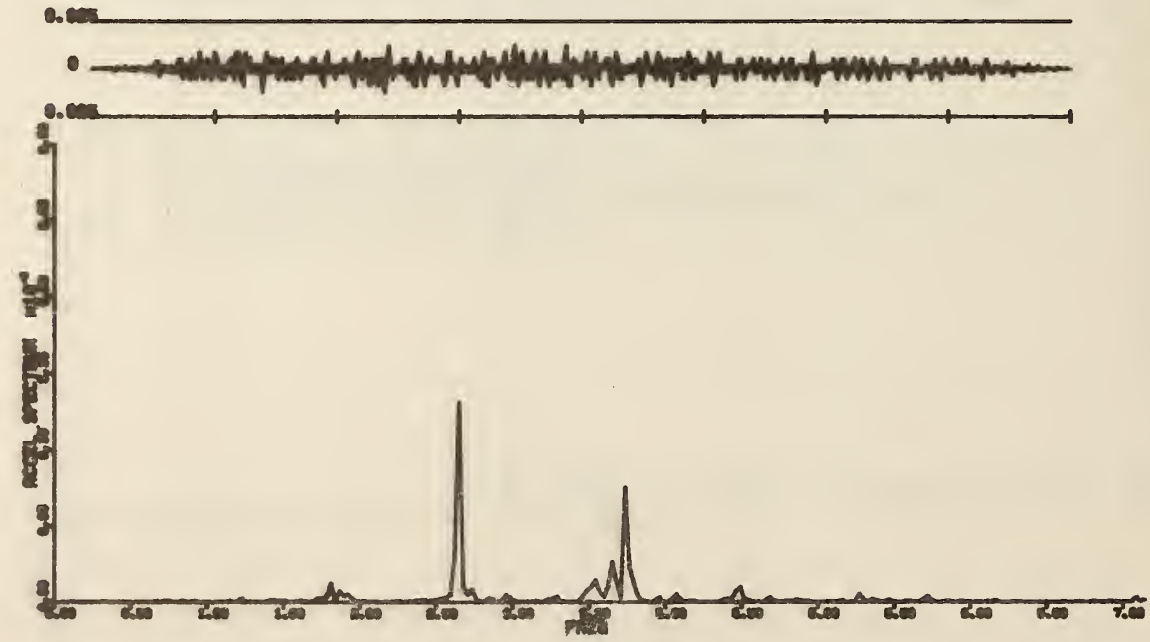

d) A4.

Figure 42. Individual channel acceleration spectra during third bridge motion event (continued).

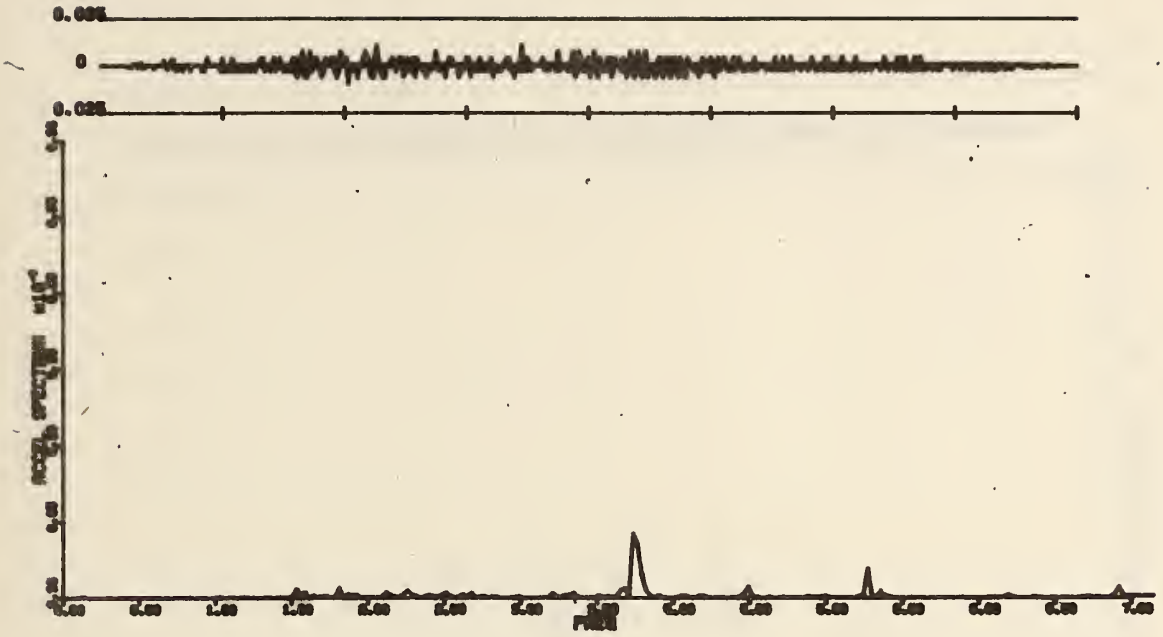

e) A5.

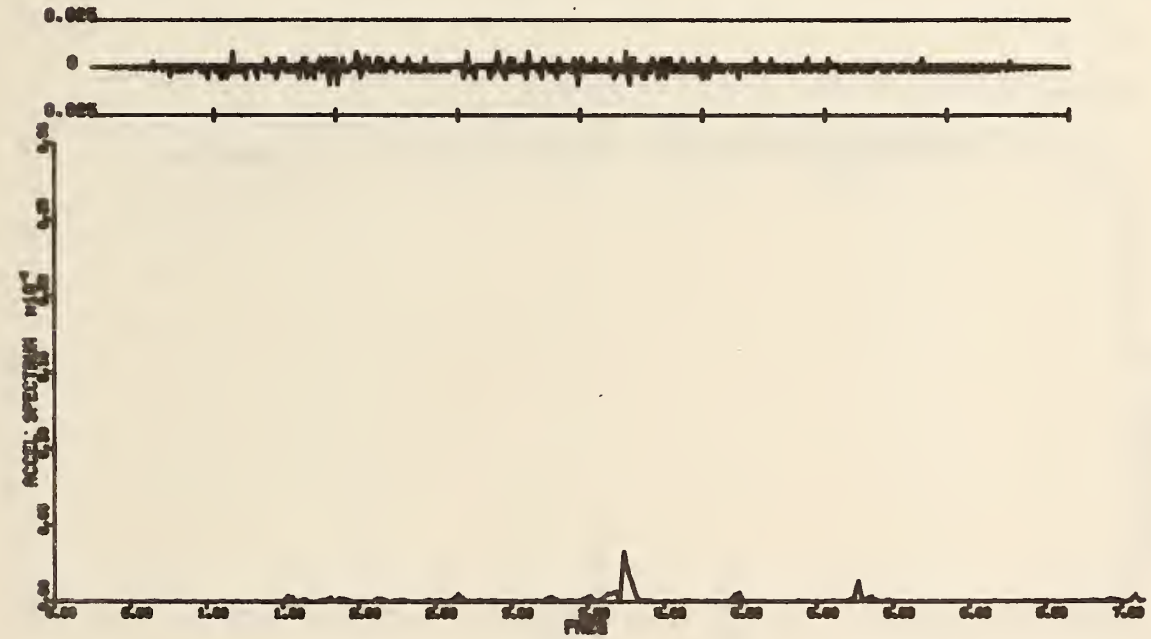

f) A6.

Figure 42. Individual channel acceleration spectra during third bridge motion event (continued).

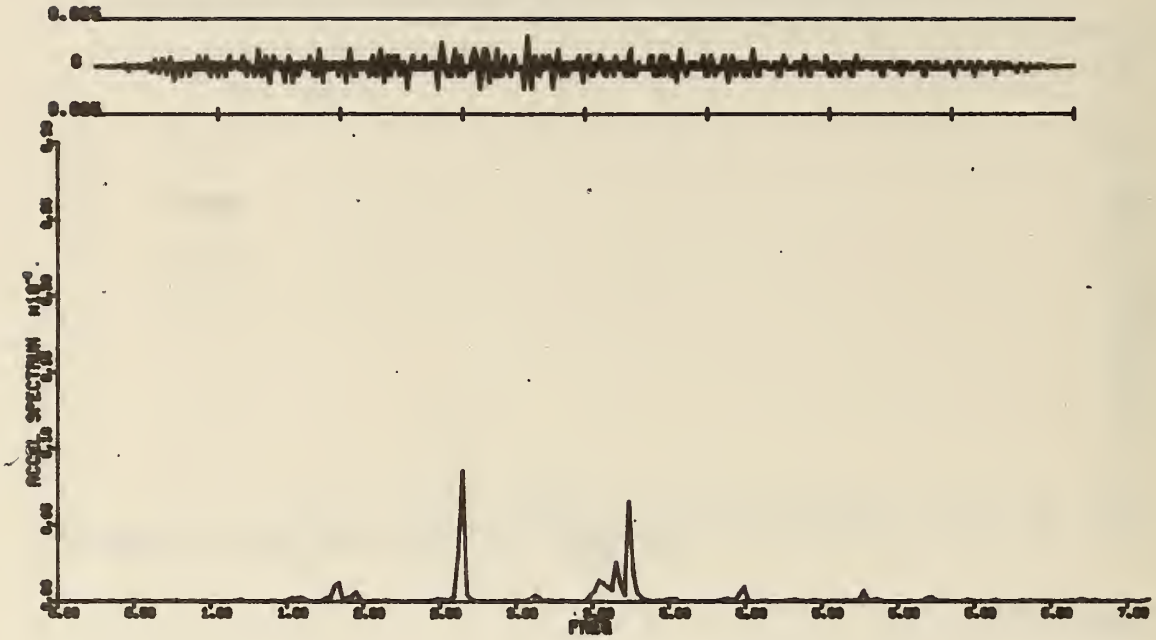

g) A7.

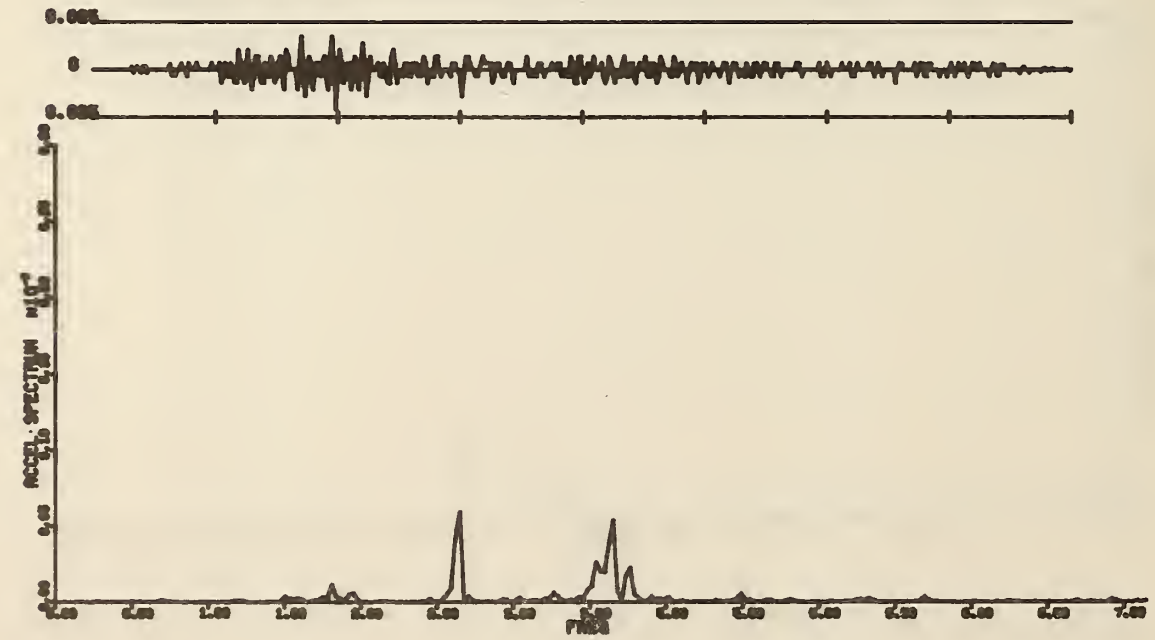

h) A8.

Figure 42. Individual channel acceleration spectra during third bridge motion event (continued).

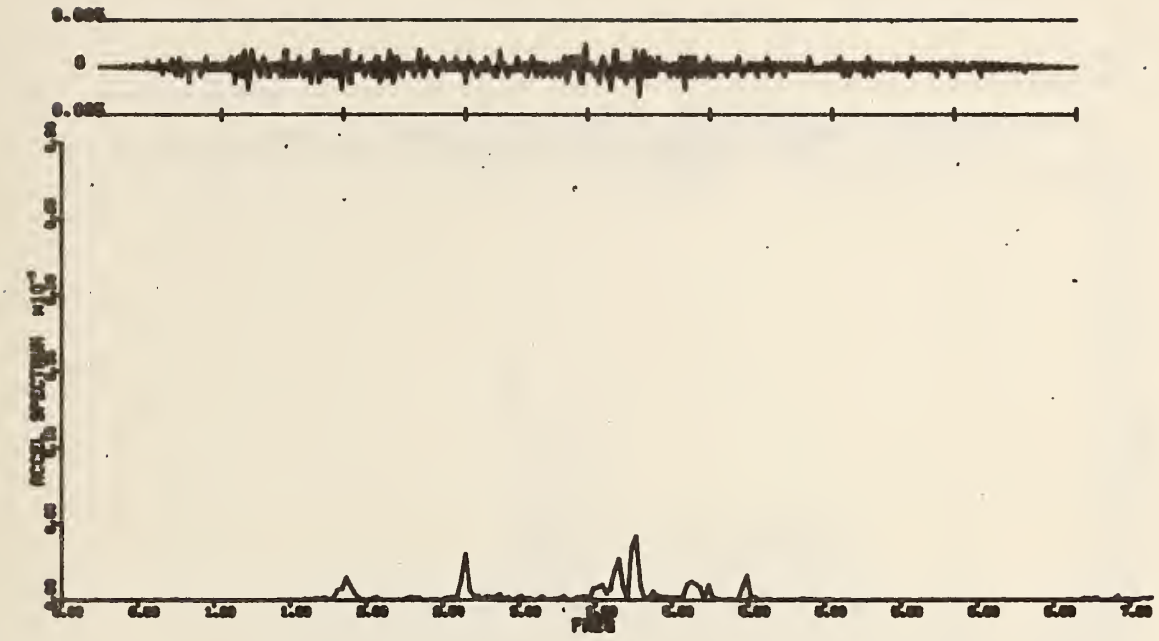

i) A9.

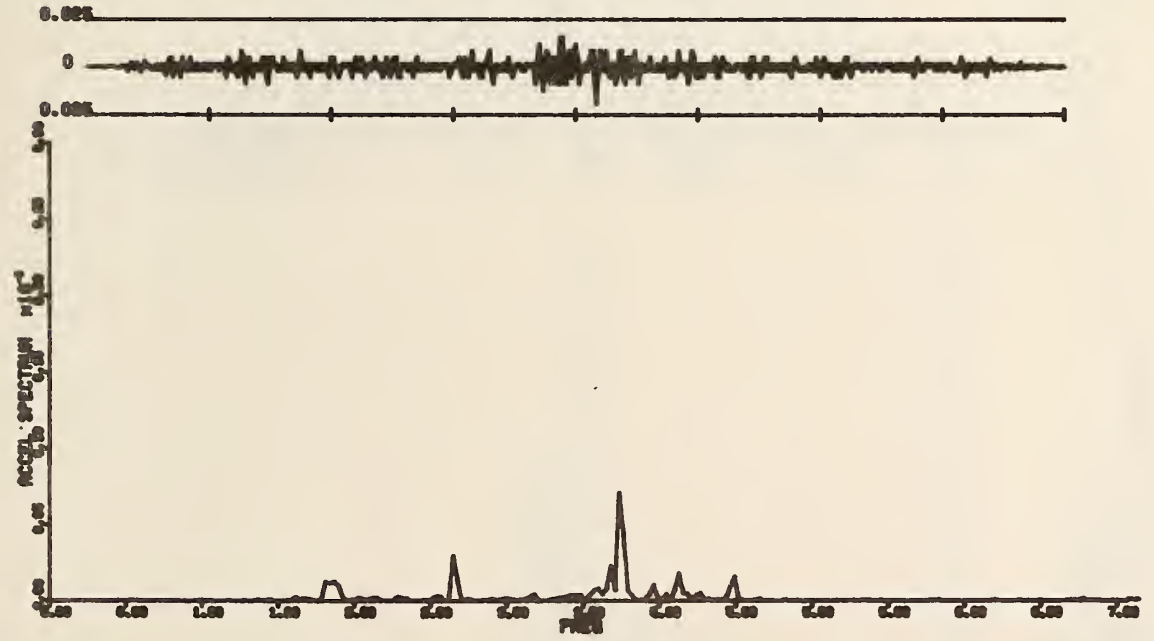

j) A10.

Figure 42. Individual channel acceleration spectra during third bridge motion event (continued).

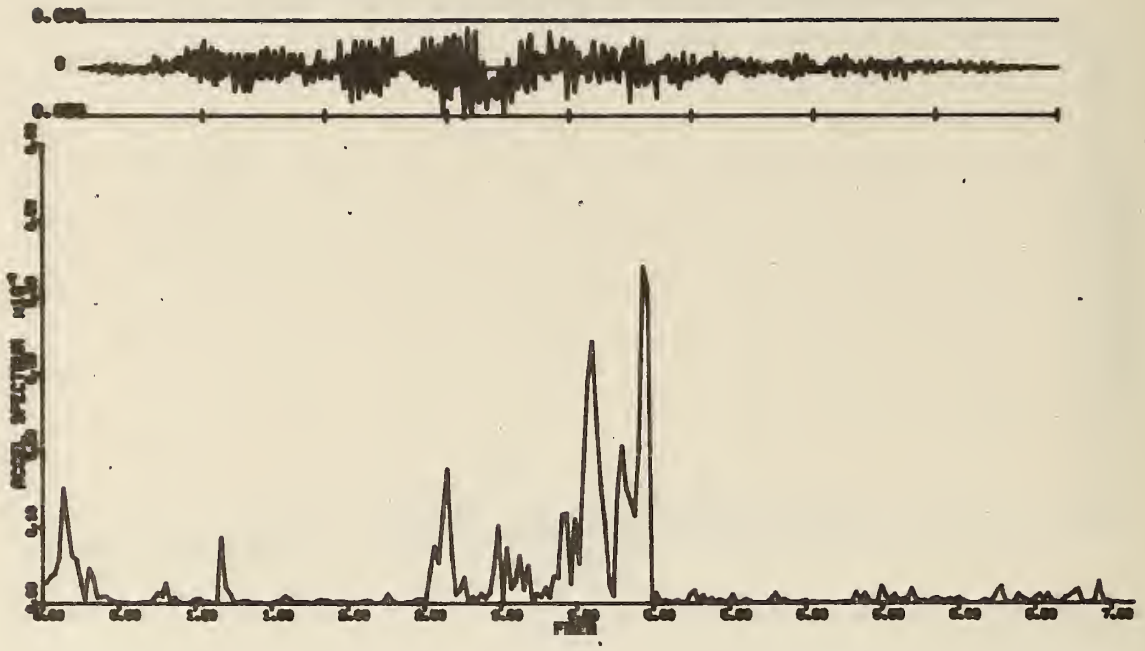

k) A13.

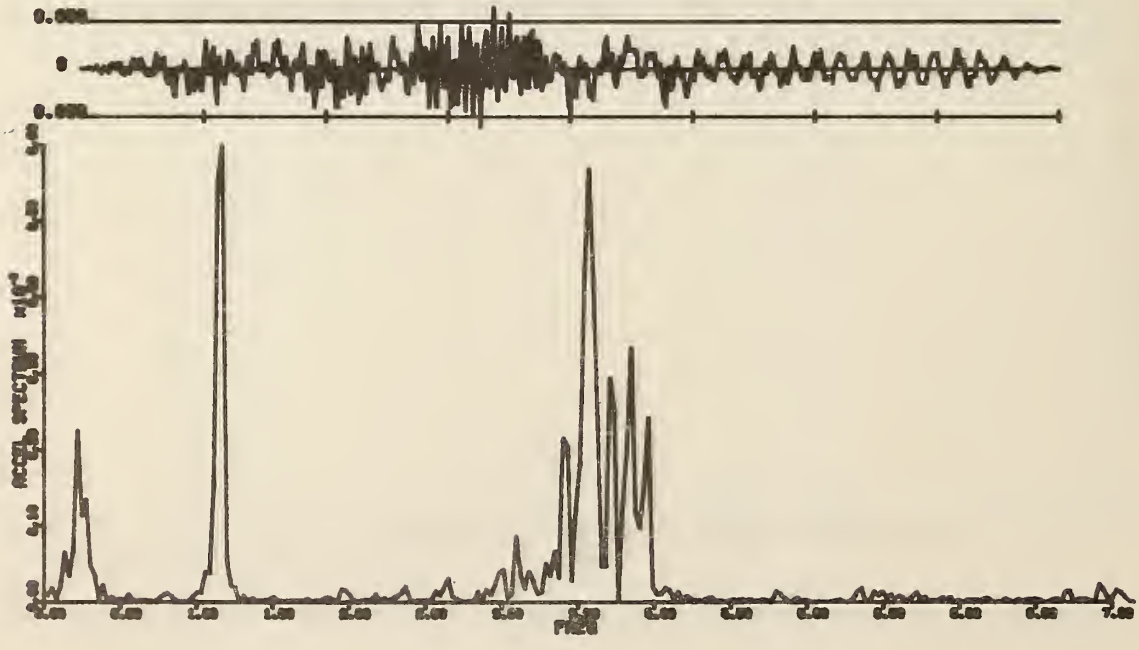

l) A12.

Figure 42. Individual channel acceleration spectra during third bridge motion event (continued).

GPO 912-551

TE 662
.A3
no.FHWA-RD-
76-180 BORROWER

DOT LIBRARY
00057928